JOURNAL of the

Structural

Division

AMERICAN
SOCIETY OF
CIVIL
ENGINEERS
FOUNDED
1852

BASIC REQUIREMENTS FOR MANUSCRIPTS

Original papers and discussions of current papers should be submitted to the Manager of Technical Publications, ASCE. Authors should indicate the technical division to which the paper is referred. The final date on which a discussion should reach the Society is given as a footnote with each paper. Those who are planning to submit material will expedite the review and publication procedures by complying with the following basic requirements:

1. Titles must have a length not exceeding 50 characters and spaces.

2. A summary of approximately 50 words must accompany the paper, a 300-word synopsis must precede it, and a set of conclusions must end it.

3. The manuscript (an original ribbon copy and two duplicate copies) should be double-spaced on one side of $8\frac{1}{2}$-inch by 11-inch paper. Three copies of all illustrations, tables, etc., must be included.

4. The author's full name, Society membership grade, and footnote reference stating present employment must appear on the first page of the paper.

5. Mathematics are recomposed from the copy that is submitted. Because of this, it is necessary that letters be drawn carefully, and that special symbols be properly identified. The letter symbols used should be defined where they first appear, in the illustrations or in the text, and arranged alphabetically in an Appendix.

6. Tables should be typed (an original ribbon copy and two duplicate copies) on one side of $8\frac{1}{2}$-inch by 11-inch paper. Specific illustrations and explanation must be made in the text for each table.

7. Illustrations must be drawn in black ink on one side of $8\frac{1}{2}$-inch by 11-inch paper. Because illustrations will be reproduced with a width of between 3-inches and $4\frac{1}{2}$-inches, the lettering must be large enough to be legible at this width. Photographs should be submitted as glossy prints. Explanations and descriptions must be made within the text for each illustration.

8. The desirable average length of a paper is about 12,000 words and the absolute maximum is 18,000 words. As an approximation, each full page of typed text, table, or illustration is the equivalent of 300 words.

9. Technical papers intended for publication must be written in the third person.

10. The author should distinguish between a list of "Reading References" and a "Bibliography," which would encompass the subject of his paper.

Journal of the

STRUCTURAL DIVISION

Proceedings of the American Society of Civil Engineers

CONTENTS

December, 1961

Papers

(over)

DISCUSSION

Journal of the
STRUCTURAL DIVISION
Proceedings of the American Society of Civil Engineers

ECONOMY OF HIGH STRENGTH STEEL STRUCTURAL MEMBERS

By Geerhard Haaijer,[1] M. ASCE

SYNOPSIS

Several types of structural members are analyzed to determine how higher strength steels can be used to their greatest advantage. The influence of the yield stress, modulus of elasticity, and price on the optimum proportioning of structural members is investigated. By applying the results of the analyses to specific commercially available steels, it is demonstrated that through optimum design, the application of higher strength steels can lead to significant material-cost savings for lighter weight structures.

INTRODUCTION

The continuous development of new steels for structural applications has been in progress ever since the early days of steel construction. As a result, a large family of such steels is presently (1961) available to structural designers. The steels vary in yield stress (stress at the yield point or 0.2% offset yield strength) from 33,000 psi for structural carbon steel to 100,000 psi for heat-treated constructional alloy steel. In contrast with many of the higher strength steels that have been available in the past, the modern higher strength steels show more favorable price-to-strength ratios than structural carbon steel. That is, when the modern higher strength steels are compared with carbon steel in price and in yield stress, the higher strength steels show a relative increase in price that is less than the relative increase

[1] Sect. Supervisor, Applied Research Lab., U. S. Steel Corp., Monroeville, Pa.

in yield stress. As a result, the application of higher strength steels to structures in which the higher strength can be utilized often results in significant material-cost savings.

In an earlier paper[2] it was shown that the application of the higher strength steels to structural members of the type used in automotive and mobile equipment would, in many instances, result in material-cost savings in addition to the weight savings. The weight and material-cost comparisons are extended in the present paper to structural members of the type used in bridges and buildings.

In the present work, different structural members, such as tension members, hot-rolled beams, and built-up welded girders, are first analyzed to determine the effect of yield stress, modulus of elasticity, and price on the optimum proportioning of these members. The results of the analyses are then applied to several commercially available steels so as to obtain realistic material-cost comparison for the different structural members. Special attention is given to the economies of so-called hybrid steel beams—a term used below to refer to beams consisting of higher strength steel flanges connected by lower strength steel webs.

Notation.—The letter symbols adopted for use in this paper are defined where they first appear, in the illustrations or in the text, and are arranged alphabetically, for convenience of reference, in The Appendix.

STRUCTURAL STEELS

Before presenting the analyses of the various structural members, the mechanical properties and typical prices of several commercially available structural steels will be reviewed so as to provide sufficient information for realistic material-cost comparisons of structural members made from different steels.

The structural steels that are widely used at present can be divided into the following three broad categories:

1. Structural carbon steels.
2. High-strength low-alloy steels.
3. Constructional alloy steels.

The pertinent mechanical properties and typical prices of steels that are representative of these three categories are shown in Table 1.

The structural carbon steels are represented by ASTM-A7 and ASTM-A36 steel. A7 steel will be used as the basis for the weight and cost comparisons. The new A36 steel is included because this steel is expected to replace A7 steel in many applications.

ASTM-A440 high-strength steel is a manganese-copper steel used primarily for riveted and bolted construction. ASTM-A441 high-strength low-alloy steel is a manganese-copper-vanadium steel intended for applications requiring cold forming, welding, and improved toughness properties. The resistance to atmospheric corrosion of A440 and A441 steel is twice that of structural carbon steel. USS COR-TEN high-strength low-alloy steel is a chromium-copper-

---

[2] "Higher Strength Steels Mean Reduced Weight With Economy," by G. Haaijer, presented at the March 15, 1961. SAE Natl. Automobile Week, Reprint No. 327B, Soc. of Automotive Engrs., Inc., New York 17, N. Y.

TABLE 1.—MECHANICAL PROPERTIES AND PRICES OF CONSTRUCTIONAL STEELS

Category (1)	Steel (2)	Thickness Range, inches (3)	Yield Point, psi (min.) (4)	Tensile Strength, (psi) (5)	Elongation in 8 Inches (min. per cent) (6)	Typical Price,[a] (cents per lb.) Plates (7)	Shapes (8)
Structural Carbon Steel	ASTM A7 ASTM A36	All thicknesses 4 and under	33,000 36,000	60,000 to 75,000 60,000 to 80,000	21 20	6.4 6.5	6.4 6.5
High-Strength Steel	ASTM A440	3/4 and under Over 3/4 to 1 1/2 incl. Over 1 1/2 to 4 incl.	50,000 46,000 42,000	70,000 min. 67,000 min. 63,000 min.	18 19 19	7.4	7.4
	ASTM A441	3/4 and under Over 3/4 to 1 1/2 incl. Over 1 1/2 to 4 incl.	50,000 46,000 42,000	70,000 min. 67,000 min. 63,000 min.	18 19 19	8.4	8.4
	USS COR-TEN	1/2 and under Over 1/2 to 1 1/2 incl. Over 1 1/2 to 3 incl.	50,000 47,000 43,000	70,000 min. 67,000 min. 63,000 min.	18 19 19	8.7	8.7
Constructional Alloy Steel	USS "T-1" type A	3/16 to 1 incl.	100,000[b]	115,000 to 135,000	18[c]	13.2	15.2
	USS "T-1"	3/16 to 2 1/2 incl. Over 2 1/2 to 4 incl.	100,000[b] 90,000[b]	115,000 to 135,000 105,000 to 135,000	18[c] 17[c]	15.5	17.5

[a] Average mill price including typical extras in effect on September 1, 1961.

[b] Yield Strength, minimum.

[c] Elongation in 2 Inches, minimum.

silicon-phosphorus steel intended for applications involving cold forming and welding (for thicknesses of 1/2 in. and less) in which improved atmospheric corrosion resistance and increased paint life are important. Its resistance to atmospheric corrosion is 4 to 6 times that of structural carbon steel.

USS "T-1" and "T-1" Type A constructional alloy steels are heat-treated (quenched and tempered) alloy steels suitable for welded structures. The resistance to atmospheric corrosion of "T-1" steel is 4 times that of structural carbon steel, and the resistance of "T-1" Type A is twice that of structural carbon steel. Both steels can be furnished specially hardened (321 min Bhn) for maximum resistance to impact abrasion. "T-1" steel can also be furnished to 360 min Bhn in thicknesses not exceeding 1-1/2 in.

STRUCTURAL ANALYSES

Tension Members.—The general method of analysis that will be applied in the present paper can best be illustrated with the simple example of a tension member. For structural purposes the strength of a tension member is equal to the maximum load that the member can sustain without undergoing appreciable plastic deformation. Thus, the useful strength of a tension member is given by the product of the cross-sectional area of the tension member and the yield stress of the material. Or

$$P = A f \dotfill (1)$$

in which P denotes useful strength (load); A is the cross-sectional area; and f is the yield stress (stress at the yield point or 0.2% offset yield strength).

The allowable design load is of course only a fraction of the load given by Eq. 1 and is commonly determined by replacing the yield stress f by an allowable stress. That is, the allowable stress is equal to the yield stress divided by the factor of safety. However, Eq. 1 is satisfactory for the present purpose of comparing two tension members made from different materials and will suffice to identify members that have the same strength.

If the cross section and material properties of the two members are identified by the subscripts a and b, respectively, the condition of equal strength can be expressed as

$$A_a f_a = A_b f_b \dotfill (2)$$

From Eq. 2 it follows immediately that the required cross-sectional areas are inversely proportional to the yield stresses. Hence,

$$\frac{A_b}{A_a} = \frac{f_a}{f_b} \dotfill (3)$$

The ratio of the weights of two tension members made from different steels is identical with the area ratio given by Eq. 3.

The elongation of a tension member may be important because it contributes to the deflections of the structure of which the member is a component; in some instances maximum deflection replaces strength as the design criterion.

The elongation of a tension member is given by the following equation:

$$e = \frac{P L}{A E} \dotfill (4)$$

in which e denotes elongation; L represents the length of the member; E is the modulus of elasticity; and P and A are as previously defined. The relative elongation of two members of equal strength P and equal length L can, therefore, be expressed as follows:

$$\frac{e_b}{e_a} = \frac{A_a \, E_a}{A_b \, E_b} \quad \dots\dots\dots\dots\dots\dots \quad (5)$$

Substitution of Eq. 3 in Eq. 5 gives the following expression for the relative elongation:

$$\frac{e_b}{e_a} = \frac{f_b \, E_a}{f_a \, E_b} \quad \dots\dots\dots\dots\dots\dots \quad (6)$$

Although the modulus of elasticity is the same for all structural steels (about 30,000,000 psi) and, therefore, $E_b/E_a = 1$, Eq. 6 and the subsequent equations for the deflections of beams and girders will be used in the form given so as not to limit the applicability of the results of the analyses.

Beams and Girders.—The analysis of beams and girders proceeds in the same way as that outlined previously for tension members. The elastic bending strength is given by the product of the section modulus and the yield stress. Thus,

$$M_e = Sf \quad \dots\dots\dots\dots\dots\dots \quad (7)$$

in which M_e denotes elastic bending strength; S is the section modulus; and f is the yield stress. From the condition of equal bending strength

$$S_a \, f_a = S_b \, f_b \dots\dots\dots\dots\dots\dots \quad (8)$$

it follows that the required section moduli are related as follows:

$$\frac{S_b}{S_a} = \frac{f_a}{f_b} \quad \dots\dots\dots\dots\dots\dots \quad (9)$$

The deflection of a beam is inversely proportional to the product of the modulus of elasticity of the material and the moment of inertia, I, of the cross section. The relation between the deflections, d_a and d_b, of two beams made from different materials can, therefore, be expressed as follows:

$$\frac{d_b}{d_a} = \frac{E_a \, I_a}{E_b \, I_b} \quad \dots\dots\dots\dots\dots\dots \quad (10)$$

Eq. 9 shows that a higher strength requires a smaller section modulus, and this usually means less weight and a smaller moment of inertia. For equal modulus of elasticity, a smaller moment of inertia results in greater deflections as shown by Eq. 10.

In all the analyses that follow, the optimum relationship between section modulus and cross-sectional area will be determined for different types of beams so as to determine the minimum material cost. (Cost of the material to

ACTUAL   SCHEMATIC
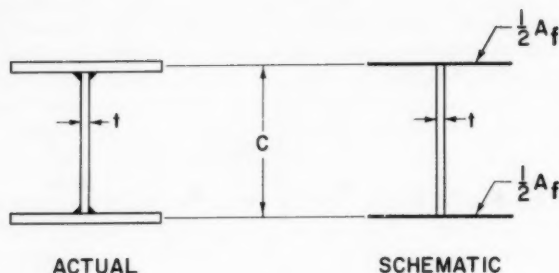
FIG. 1.—I – SHAPED BEAM

the fabricator). Although the following analysis concerns I-shaped members, it can be readily extended to other members, such as box girders.

For the present purposes, it is sufficient to consider the schematic cross section shown in Fig. 1 in which the areas of the flanges are concentrated along their center. The section modulus is then given by:

$$S = \frac{1}{6} t\, c^2 + \frac{1}{2} A_f\, c \quad\ldots\ldots\ldots\ldots\ldots\ldots \quad (11)$$

in which t is the thickness of web; c represents the depth of web (distance between centers of flanges); and A_f is the area of both flanges. Noting that

$$A_f = A - c\, t \quad\ldots\ldots\ldots\ldots\ldots\ldots\ldots \quad (12)$$

the following expression for the area can be derived from Eq. 11:

$$A = \frac{2\,S}{c} + \frac{2}{3}\, c\, t \quad\ldots\ldots\ldots\ldots\ldots\ldots \quad (13)$$

If the web depth-to-thickness ratio c/t equals α, then Eq. 13 becomes

$$A = \frac{2\,S}{c} + \frac{2\,c^2}{3\,\alpha} \quad\ldots\ldots\ldots\ldots\ldots\ldots \quad (14)$$

For a given value of α the depth that is required for minimum area is found by equating to zero the derivative of A with respect to c. Hence,

$$\frac{dA}{dc} = -\frac{2\,S}{c^2} + \frac{4\,c}{3\,\alpha} = 0 \quad\ldots\ldots\ldots\ldots\ldots \quad (15)$$

and, therefore,

$$c_{opt} = \left(\frac{3\,S\,\alpha}{2}\right)^{1/3} \quad\ldots\ldots\ldots\ldots\ldots \quad (16)$$

Substitution of Eq. 16 in Eq. 14 gives the following minimum area of the cross section:

$$A_{min} = \left(\frac{18 \, S^2}{\alpha} \right)^{1/3} \quad \dots\dots\dots\dots\dots \quad (17)$$

From these equations, it can be shown that the moment of inertia of the minimum-area section is as follows:

$$I = \frac{\alpha \, A_{min}^2}{12} \quad \dots\dots\dots\dots\dots\dots \quad (18)$$

The web depth-to-thickness ratio, α, has a major influence on the required minimum area. Eq. 14 shows that the area decreases as α increases.

There are, of course, limitations that determine the maximum values of α. For example, the rolling process imposes a maximum value of 55 on the lightest weight hot-rolled shapes and even smaller values on heavier shapes. Also, the web depth-to-thickness ratio for welded built-up shapes is often limited by buckling. These examples will be examined subsequently.

Rolled Beams with Equal Web Depth-to-Thickness Ratios.— The comparison of two rolled beams or other I-shaped beams made from different materials, but with equal web depth-to-thickness ratios, can be obtained by substituting Eq. 17 in Eq. 9. The minimum areas are related as follows:

$$\frac{A_b}{A_a} = \left(\frac{f_a}{f_b} \right)^{2/3} \quad \dots\dots\dots\dots\dots \quad (19)$$

Eq. 16 then gives the following comparison of the optimum depths of the two beams:

$$\frac{c_b}{c_a} = \left(\frac{f_a}{f_b} \right)^{1/3} \quad \dots\dots\dots\dots\dots \quad (20)$$

By substituting the value of the moment of inertia given by Eq. 18 in Eq. 10, it is found that the ratio of the deflections is as follows:

$$\frac{d_b}{d_a} = \frac{E_a}{E_b} \left(\frac{f_b}{f_a} \right)^{4/3} \quad \dots\dots\dots\dots\dots \quad (21)$$

Built-up Girders with Web Depth-to-Thickness Ratio Limited by Buckling.— For built-up girders the web depth-to-thickness ratio is often limited by buckling considerations. Buckling may be caused by shear stresses, by compressive stresses due to bending, or by combinations of these.

As shown in the pertinent literature,[3] the elastic buckling stress of a plate element is given by the following equation:

$$f_{cr} = \frac{\pi^2 E k}{12(1 - \nu^2)} \left(\frac{1}{\alpha}\right)^2 \dots\dots\dots\dots\dots \quad (22)$$

in which f_{cr} is the buckling stress; ν denotes Poisson's ratio; and k is the plate buckling coefficient. The plate buckling coefficient, k, depends on the stress and boundary conditions of the plate element. For example, k equals 23.9 for webs subjected to pure bending. In the plastic range the behavior of plates subjected to compressive stresses is more complicated.[4] However, because the present paper is concerned with relative behavior only, Eq. 22 will suffice for the comparative analysis.

Eq. 22 shows the important effect of the modulus of elasticity; that is, the buckling stress is directly proportional to the modulus of elasticity. Therefore, the modulus of elasticity affects the economy of girders.

Obviously, the higher strength steels will show their full potential advantage only if the buckling stress given by Eq. 22 is increased in the same proportion as the yield stress. When this is done, Eq. 22 shows that the maximum values of α for two different materials are related as follows:

$$\frac{\alpha_b}{\alpha_a} = \left(\frac{E_b f_a}{E_a f_b}\right)^{1/2} \dots\dots\dots\dots\dots \quad (23)$$

The corresponding minimum areas for girders of equal strength can then be found from Eq. 17 with the following result·

$$\frac{A_b}{A_a} = \left(\frac{E_a}{E_b}\right)^{1/6} \left(\frac{f_a}{f_b}\right)^{1/2} \dots\dots\dots\dots \quad (24)$$

Eq. 16 shows that the optimum depths of the two beams are related as follows:

$$\frac{c_b}{c_a} = \left(\frac{E_b}{E_a}\right)^{1/6} \left(\frac{f_a}{f_b}\right)^{1/2} \dots\dots\dots\dots \quad (25)$$

Finally, from Eq. 10, 18, 23, and 24, it can be shown that the relative deflections are as follows:

$$\frac{d_b}{d_a} = \left(\frac{E_a}{E_b}\right)^{7/6} \left(\frac{f_b}{f_a}\right)^{3/2} \dots\dots\dots\dots \quad (26)$$

---

[3] "Buckling Strength of Metal Structures," by Friedrich Bleich, McGraw-Hill Book Co., Inc., New York, 1952, p. 320.

[4] "Inelastic Buckling in Steel," by G. Haaijer and B. Thurlimann, Transactions, ASCE, Vol. 125, Part I, 1960, p. 308.

All the preceding analyses concerned structural members of equal strength but made from different materials. Thus far it has been assumed that the weight reduction obtained with higher strength has no effect on the applied loads. The resulting comparisons are therefore valid for short-span structures in which the dead weight is small compared with the live load. However, for long-span structures the dead weight becomes a significant part of the total load. Thus, the results of the preceding analyses will represent the lower limit of the scale for comparing the weight and material cost required for different materials. To determine the upper limit of this scale, "long" girders that are required to support only their own weight will be analyzed next.

"Long" Girders.—The maximum moment in a girder subjected to its own weight is given by

$$M = \frac{1}{8} w A L^2 \quad \ldots \ldots \ldots \ldots \ldots \quad (27)$$

in which M is the moment; w denotes weight per unit volume; A is the cross-sectional area; and L represents the equivalent simply supported span.

The required section modulus is, therefore,

$$S = \frac{w A L^2}{8 f} \quad \ldots \ldots \ldots \ldots \ldots \ldots \quad (28)$$

It follows from Eq. 17 that the minimum cross-sectional area is then given by

$$A_{min} = \frac{9 w^2 L^4}{32 f^2 \alpha} \quad \ldots \ldots \ldots \ldots \ldots \ldots \quad (29)$$

The comparison of two "long" girders of equal span L but made from different materials gives the following result:

$$\frac{A_b}{A_a} = \left(\frac{w_b}{w_a}\right)^2 \left(\frac{f_a}{f_b}\right)^2 \left(\frac{\alpha_a}{\alpha_b}\right) \ldots \ldots \ldots \ldots \quad (30)$$

If the web depth-to-thickness ratios of the girders are limited by buckling, it follows from a substitution of Eq. 23 in Eq. 30 that the cross-sectional areas are related as follows:

$$\frac{A_b}{A_a} = \left(\frac{w_b}{w_a}\right)^2 \left(\frac{E_a}{E_b}\right)^{1/2} \left(\frac{f_a}{f_b}\right)^{3/2} \ldots \ldots \ldots \quad (31)$$

Eq. 16 gives the following relationship between the optimum depths of the section:

$$\frac{c_b}{c_a} = \left(\frac{w_b}{w_a}\right)\left(\frac{f_a}{f_b}\right) \quad \ldots \ldots \ldots \ldots \ldots \quad (32)$$

In this instance, relative deflections are of no interest because of the absence of live loads.

The improved effectiveness of higher strength steels for longer span girders can be illustrated by contrasting Eq. 24 and 31, which give the relative cross-sectional areas for "short" and "long" girders, respectively. For "short" girders the cross-sectional areas are proportional to the inverse ratio of the yield stresses to the 1/2 power; this exponent increases to 3/2 for "long" girders.

Hybrid Steel Beams.—All preceding analyses were concerned with beams of uniform strength throughout their cross sections, that is, with beams constructed of the same material in the webs and flanges. It is intuitively obvious, however, that the higher strength steels will be more effective in the flanges than in the webs. Hybrid steel beams constructed by welding higher strength steel flanges to lower strength steel webs should therefore be more economical. The term "composite beams" has also been used for this type of construction. To avoid confusion with composite steel and concrete beams, the term "hybrid beams" is suggested for the all-steel beams.
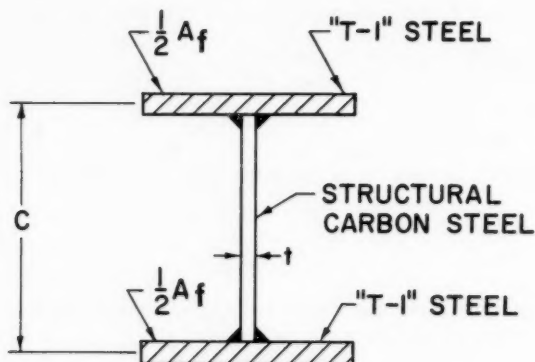
FIG. 2.—HYBRID STEEL BEAM

Because of the different yield stresses of the elements of hybrid beams, the previously used elastic analyses do not apply. Plastic design methods[5] must be used to assess the true strength of such beams. To illustrate the structural behavior of hybrid beams, a plastic analysis of a hybrid beam consisting of a web of structural carbon steel (yield point 33,000 psi) and flanges of "T-1" steel (yield strength 100,000 psi), as shown in Fig. 2, will now be presented.

Bending Behavior.—Fig. 3 shows a schematic moment-versus-curvature curve and the distribution of strains and stresses across the section for three stages of loading. During Stage I all stresses are smaller than the yield stresses of the respective parts; thus, the behavior of the beam is completely elastic. The end of Stage I is reached when the maximum stress in the web equals the yield stress of the web (in this example, 33 ksi). During Stage II,

5 "Plastic Design of Steel Frames," by Lynn S. Beedle, John Wiley and Sons, Inc., New York, 1958.

part of the web is yielding but the flanges are still elastic. Stage III is reached when the flanges also start to yield. The fully plastic moment, M_p, is determined from the condition that the entire section has yielded. Therefore, M_p is the true measure of the bending strength of the beam.

It is of interest to analyze the behavior of a hybrid steel beam subjected to repeated loads when the design load causes a moment corresponding to Stage II. Fig. 4 illustrates this behavior when the design moment is equal to 60% of the

STRAIN
DISTRIBUTIONS
(all stages)

STAGE I   STAGE II   STAGE III

STRESS DISTRIBUTIONS (stress in ksi)
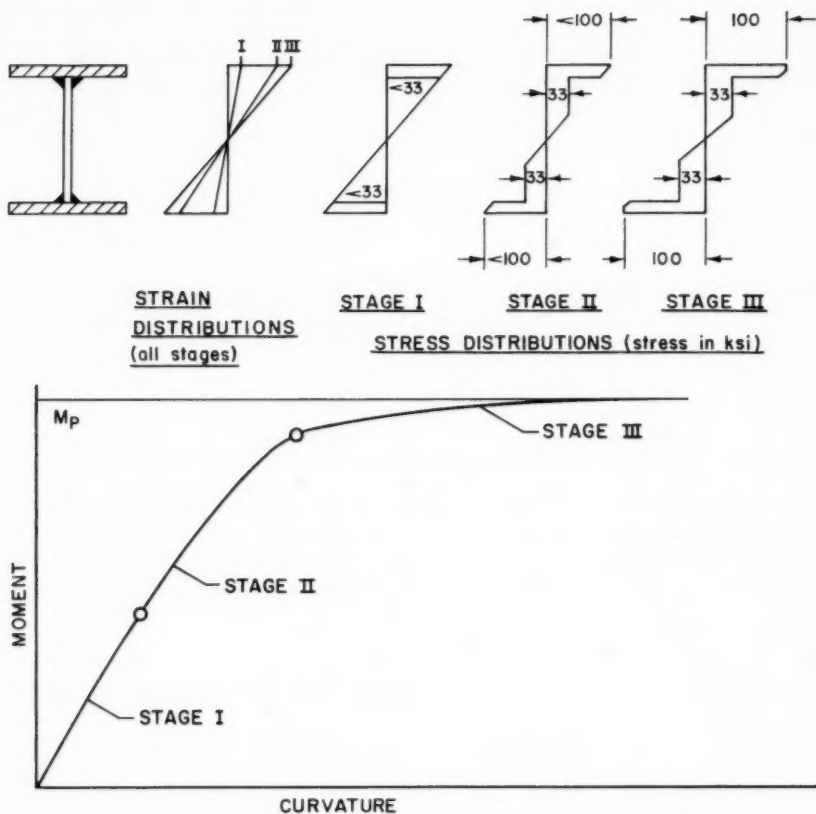
FIG. 3.—STRUCTURAL BEHAVIOR OF A HYBRID STEEL BEAM

plastic moment. When the maximum moment is reached the first time, the stress in the outer fibers of the flanges is about 50 ksi and part of the web has yielded, as shown in Fig. 4(a). This stress value applies to a hybrid steel beam in which the web constitutes 70% of the total area. When the beam is subsequently unloaded, the stress pattern shown in Fig. 4(b) must be subtracted from the loading pattern. Because unloading stresses are elastic, this pattern is linear and the magnitude of the unloading stresses can be deter-

mined by the conventional elastic method. In the present example, the maximum unloading stress is about 47 ksi.

Although the moments corresponding to the loading pattern and the unloading pattern are of equal magnitude, the differences between the patterns cause residual stresses to remain in the section after the beam has been unloaded. The residual stress pattern is shown schematically in Fig. 4(c).

The moment-versus-curvature curve shown in Fig. 4 indicates that after unloading, a permanent residual curvature remains in addition to the residual

(A) LOADING   (B) UNLOADING   (C) RESIDUAL

STRESS DISTRIBUTION (stress in ksi)
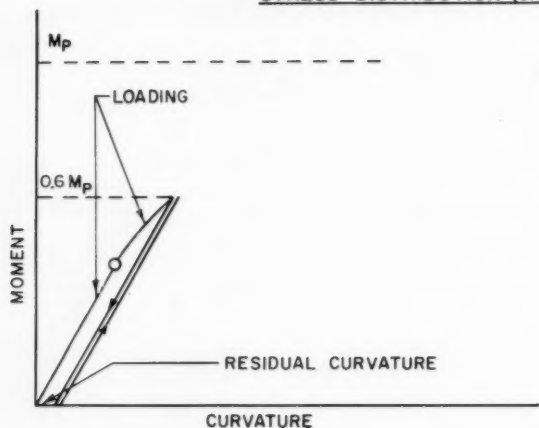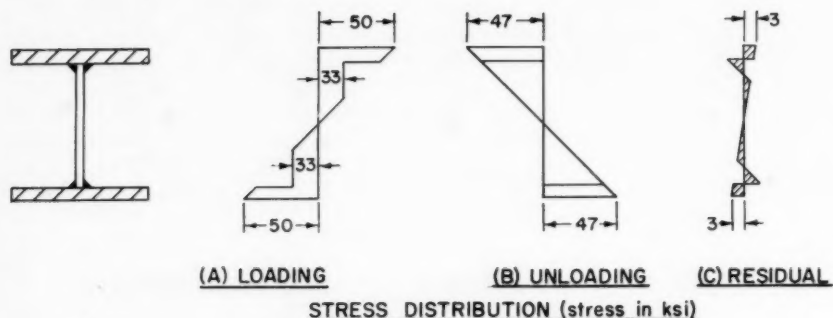
FIG. 4.—REPEATED LOADING OF A HYBRID BEAM

stresses. Integrated along the length of the beam, the residual curvatures result in residual deflections. It should be pointed out that the residual deflections are quite small for the following two reasons: (1) the residual curvatures are only a fraction of the elastic curvature of a beam of uniform strength, and (2) residual curvatures occur only in the region near the maximum moment.

Furthermore, any reloading occurs in a completely elastic manner provided that (1) the reloading moment does not exceed the original maximum moment and (2) the residual stresses do not exceed the respective yield

stresses. This is readily seen because adding the elastic stress pattern caused by the reapplied moment to the residual stress pattern simply restores the stress pattern created by the first loading. However, it should be pointed out that the yield stress of the plastically deformed material will be lower than that of the virgin material if reversal of stress has occurred. This phenomenon is known as the Bauschinger effect.

Bending Strength.—On the basis of the preceding examination of the bending behavior of hybrid beams, it is now possible to analyze the bending strength of such beams and establish the optimum proportions for minimum material cost.

Let the yield stress of the web material be f and that of the flange material $(1 + \beta)$ f; then the bending strength (plastic moment), M_p, is given by the following equation:

$$M_p = \frac{1}{4} t c^2 f + \frac{1}{2} A_f c (1 + \beta) f \quad \dots \dots \dots \dots \quad (33)$$

Again $c/t = \alpha$ and $A_f = A - c t$.

Thus,

$$M_p = \left[\frac{1}{2} A c (1 + \beta) - \frac{1}{4} \frac{c^3}{\alpha} (2 \beta + 1) \right] f \quad \dots \dots \quad (34)$$

The cross-sectional area, A, can, therefore, be expressed as follows:

$$A = \frac{2 M_p}{f (1 + \beta)} \frac{1}{c} + \frac{2 \beta + 1}{2(\beta + 1) \alpha} c^2 \quad \dots \dots \dots \dots \quad (35)$$

Because the cross section consists of materials that differ not only in strength but also in price, minimizing the cross-section area, as was done for beams of uniform strength, does not necessarily give the lowest material cost.

Minimum Material Cost.—It is therefore necessary to establish an expression for the total material cost. Let the price of the web material be p and that of the flange material $(1 + \gamma)$ p. Then the total material cost, C, is given by

$$C = A_w p + A_f (1 + \gamma) p \quad \dots \dots \dots \dots \quad (36)$$

In terms of the previously selected parameters, Eq. 36 reduces as follows:

$$C = p \left[(1 + \gamma) A - \gamma \frac{c^2}{\alpha} \right] \quad \dots \dots \dots \dots \quad (37)$$

By substituting A as given by Eq. 35 in Eq. 37 and then differentiating the total material cost, C, with respect to the depth c, it is possible to determine the value of the depth that gives the minimum material cost. The result is as follows:

$$c = \left(\frac{2 \alpha M_p q}{f} \right)^{1/3} \quad \dots \dots \dots \dots \quad (38)$$

in which q is given by

$$q = \frac{\gamma + 1}{2 \beta - \gamma + 1} \quad \dots \dots \dots \dots \quad (39)$$

The corresponding cross-sectional area is then determined by substituting Eq. 38 in Eq. 35 with the following result:

$$A_{opt} = \left(\frac{M_p}{f}\right)^{2/3} \left(\frac{1}{2\alpha}\right)^{1/3} \frac{2 + 2\beta q + q}{(\beta + 1) q^{1/3}} \quad \dots \dots \quad (40)$$

It is of interest to note which portion of the cross-sectional area as given by Eq. 40 constitutes the web of the section. The ratio, R, of web area to total area is found from Eq. 38 and 40 to be as follows:

$$R = \frac{A_w}{A} = \frac{2(\beta + 1) q}{2 + (2\beta + 1) q} \quad \dots \dots \dots \dots \quad (41)$$

Finally, the minimum material cost can be found by substituting in Eq. 37 the optimum values of c and A given by Eq. 38 and 40.

Comparison of Hybrid Beam with Beam of Uniform Yield Stress.—The previously-derived information for optimum hybrid steel beams makes it possible to establish the relative weight, cost, depth of section, and deflection of a hybrid steel beam as compared with those of an optimum beam of uniform yield stress (equal to the yield stress of the web of the hybrid beam). If the properties of the beam of uniform yield stress are identified by the subscript 1 and those of the hybrid steel beam by the subscript 2, the relative cross-sectional area (which is equal to the relative weight) is found to be

$$\frac{A_2}{A_1} = \frac{2}{3 R_2} q_2^{2/3} \quad \dots \dots \dots \dots \dots \quad (42)$$

The relative material cost is

$$\frac{C_2}{C_1} = \frac{A_2}{A_1} \left(1 + \gamma_2 - R_2 \gamma_2\right) \quad \dots \dots \dots \dots \quad (43)$$

The depths of the sections are related as follows:

$$\frac{c_2}{c_1} = q_2^{1/3} \quad \dots \dots \dots \dots \dots \dots \quad (44)$$

From a straightforward calculation of the moments of inertia it can be shown that the relative elastic deflections are related as follows:

$$\frac{d_2}{d_1} = \left(\frac{A_1}{A_2}\right)^2 \frac{5}{27 R_2 \left(\frac{1}{2} - \frac{1}{3} R_2\right)} \quad \dots \dots \dots \dots \quad (45)$$

It should be noted that these deflections do not include the initial permanent set.

RESULTS

Weight and material-cost comparisons can now be obtained by substituting the pertinent material properties in the general formulas that resulted from the preceding analyses. In drawing conclusions from the results, it should be kept in mind that the optimum designs, on which the comparisons are based, must in many instances be tempered by practical design considerations. For example, the exact rolled structural shape required for the design may not be available and the next larger shape must be specified. Or, the greater deflection of a high-strength steel member may be objectionable and, thus, the theoretically optimum shape cannot be used. With limitations such as these in mind, the results will be examined in the following paragraphs.

TABLE 2.—TENSION MEMBERS OF EQUAL STRENGTH (Built Up From Plates)

Steel (1)	Yield Point (psi) (2)	Relative Weight (3)	Relative Material Cost (4)	Relative Elongation (5)
ASTM A7	33,000	1.00	1.00	1.00
ASTM A36	36,000	0.92	0.93	1.09
ASTM A441	50,000	0.66	0.87	1.52
USS COR-TEN	50,000	0.66	0.90	1.52
USS "T-1" type A	100,000[a]	0.33	0.68	3.03
USS "T-1"	100,000[a]	0.33	0.80	3.03

[a]Yield Strength.

Tension Members.—The preceding analysis of tension members leads to the comparisons of tension members of equal strength shown in Tables 2 and 3. Table 2 applies to tension members built up from plates, whereas Table 3 applies to rolled shapes. In both tables, when the high-strength steels and the "T-1" steels are compared in relative weight with A7 steel, the weight savings of the high-strength steels and "T-1" steels are 34% and 67%, respectively. The maximum material-cost saving for members built up from plates is obtained with "T-1" Type A steel (32%). For rolled shapes the maximum material-cost saving is obtained with A440 steel.

The high-strength-steel members elongate 1.52 times as much as the corresponding structural-carbon-steel members, whereas the "T-1" steels elongate 3.03 times as much. Because greater elongations mean greater deflections for the structure of which the tension member is a component, this may impose a limitation on the applicability of the higher strength steels.

It should be noted that the weight and material-cost savings for "short" columns (that is, columns with small slenderness ratios) approach those given for tension members in Tables 2 and 3.

Beams and Girders.—The analysis of I-shaped beams and girders showed that the web depth-to-thickness ratio, α, has a major influence on the efficiency of such beams. In fact, the minimum cross-section area that is required to support a given moment is proportional to the inverse of the cube root α. It is obvious that significant weight savings can be obtained by constructing beams with large web depth-to-thickness ratios. For example, replacing a hot-rolled wide-flange beam by a welded built-up girder (both made from structural carbon steel) would allow an increase in α from about 55 to 170 and thus afford a 31% weight savings. In this instance, however, a comparison of material cost would not be indicative of economic advantages because the hot-rolled shape would require little or no fabrication, whereas the cost of fabricating the

TABLE 3.—TENSION MEMBERS OF EQUAL STRENGTH (Hot-Rolled[a] Shapes)

Steel (1)	Yield Point (psi) (2)	Relative Weight (3)	Relative Material Cost (4)	Relative Elongation (5)
ASTM A7	33,000	1.00	1.00	1.00
ASTM A36	36,000	0.92	0.93	1.09
ASTM A440	50,000	0.66	0.76	1.52
ASTM A441	50,000	0.66	0.87	1.52
USS COR-TEN	50,000	0.66	0.90	1.52
USS "T-1" type A	100,000[b]	0.33	0.78	3.03
USS "T-1"	100,000[b]	0.33	0.90	3.03

[a] Except for the "T-1" steels, which are heat-treated.

[b] Yield Strength.

welded built-up girder, which would also require vertical web stiffeners, might be significant.

The results presented in the following sections will, therefore, be limited to comparisons of beams that require about the same amount of fabrication so as to truly assess the economies of higher strength steels.

Rolled Beams with Equal Web Depth-to-Thickness Ratios.—Rolled beams of equal bending strength and with equal web depth-to-thickness ratios are compared in Table 4. It will be noted that two yield points are used for the high-strength low-alloy steels; the higher yield-point values apply to shapes with thin webs (1/2 in. or less for COR-TEN steel and 3/4 in. or less for A440 and A441 steel), and the lower values apply to thicker webs (up to a maximum thickness of 1-1/2 in.).

TABLE 4.—HOT-ROLLED[a] BEAMS OF EQUAL STRENGTH
(Equal Web Depth-to-Thickness Ratios)

Steel (1)	Yield Point, psi (2)	Relative Weight (3)	Relative Material Cost (4)	Relative Depth of Section (5)	Relative Deflection (6)
ASTM A7	33,000	1.00	1.00	1.00	1.00
ASTM A36	36,000	0.94	0.95	0.97	1.12
ASTM A440	50,000	0.76	0.88	0.87	1.74
	46,000	0.80	0.92	0.90	1.56
ASTM A441	50,000	0.76	1.00	0.87	1.74
	46,000	0.80	1.05	0.90	1.56
USS COR-TEN	50,000	0.76	1.03	0.87	1.74
	47,000	0.79	1.08	0.89	1.59
USS "T-1" type A	100,000[b]	0.48	1.12	0.69	4.38
USS "T-1"	100,000[b]	0.48	1.31	0.69	4.38

[a] Except for the "T-1" steels, which are heat-treated.

[b] Yield Strength.

TABLE 5.—"SHORT" GIRDERS OF EQUAL STRENGTH (Web Depth-to-Thickness Ratios Limited by Buckling)

Steel (1)	Yield Point, (psi) (2)	Relative Weight (3)	Relative Material Cost (4)	Relative Depth of Section (5)	Relative Deflection (6)
ASTM A7	33,000	1.00	1.00	1.00	1.00
ASTM A36	36,000	0.96	0.97	0.96	1.14
ASTM A441	50,000	0.81	1.07	0.81	1.86
USS COR-TEN	50,000	0.81	1.10	0.81	1.86
USS "T-1" type A	100,000[a]	0.57	1.18	0.57	5.27
USS "T-1"	100,000[a]	0.57	1.39	0.57	5.27

[a] Yield Strength.

The results show that the weight savings obtainable with the higher strength steels are in some instances accompanied by material-cost savings, but in other instances by an increase in material cost. A440 steel shows the greatest material-cost saving (12%), whereas "T-1" steel demands the greatest increase in material cost (31%). The "T-1" steels show the greatest weight saving (52%).

As indicated in the next to the last column, the optimum designs, on which the comparison is based, require shallower sections for the higher strength steels. For example, if a 20-in.-deep beam would be required for A7 steel, the depth of the required high-strength low-alloy steel beam would be about 18 in. For "T-1" steel a 14-in-deep section would be required.

Built-up Girders with Web Depth-to-Thickness Ratios Limited by Buckling.— In the analysis of girders of equal strength for which the web depth-to-thickness ratios are limited by buckling, the distinction was made between "short" and

TABLE 6.—"LONG" GIRDERS OF EQUAL SPAN (Web Depth-to-Thickness Ratios Limited by Buckling)

Steel (1)	Yield Point (psi) (2)	Relative Weight (3)	Relative Material Cost (4)	Relative Depth of Section (5)
ASTM A7	33,000	1.00	1.00	1.00
ASTM A36	36,000	0.88	0.89	0.92
ASTM A441	50,000	0.54	0.71	0.66
USS COR-TEN	50,000	0.54	0.74	0.66
USS "T-1" type A	100,000[a]	0.19	0.39	0.33
USS "T-1"	100,000[a]	0.19	0.46	0.33

[a]Yield Strength.

"long" girders. "Short" girders are those for which the dead weight is negligible compared with the live load, whereas the reverse is true for "long" girders.

The comparison of "short" girders is shown in Table 5. Because the maximum web depth-to-thickness ratio of a girder decreases as the yield stress increases (in proportion to the square root of the yield stress), the effectiveness of the higher strength steels is somewhat reduced in this application.

As a result, most higher strength steels demand an increase in material cost. However, A36 steel still shows a material-cost saving of 3%. The weight savings for "short" girders are 19% for the high-strength low-alloy steels and 43% for the "T-1" steels.

"Long" Girders.—"Long" girders of equal span that are required to carry only their own weight are compared in Table 6. The results are the opposite of those for "short" girders. For "long" girders the greatest material-cost
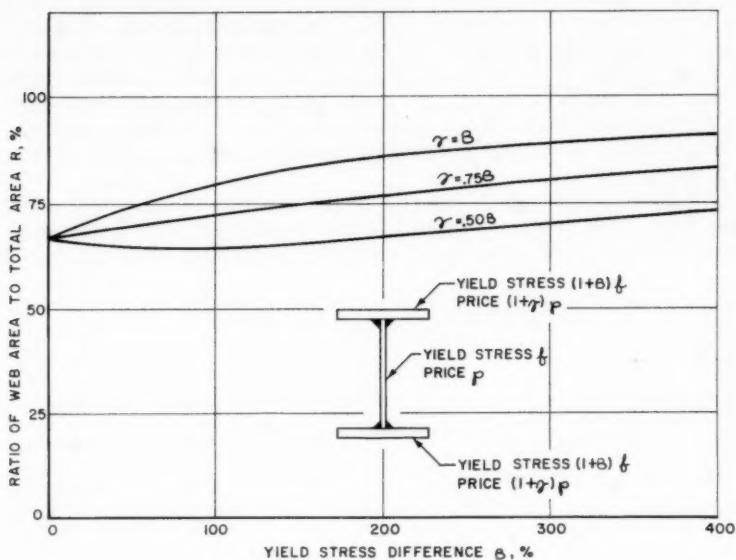
FIG. 5.—EFFECT OF THE RELATIVE DIFFERENCE IN YIELD STRESS, β, AND THE RELATIVE DIFFERENCE IN PRICE, γ, ON THE RATIO R
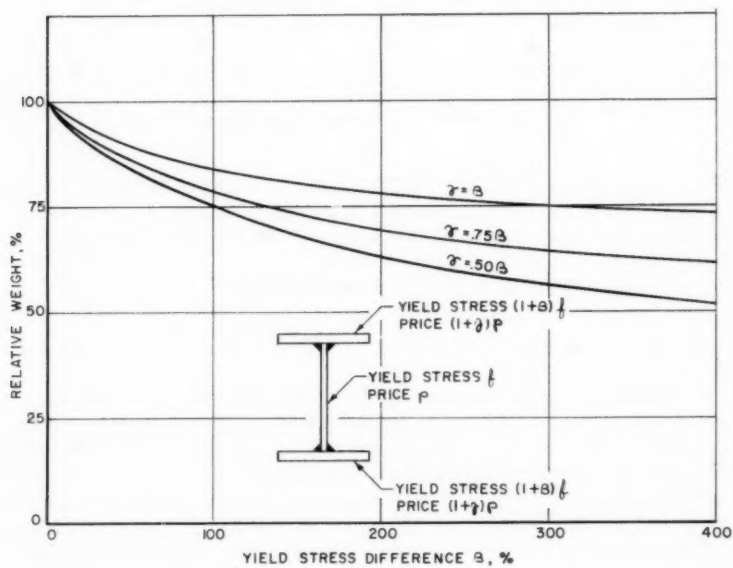
FIG. 6.—RELATIVE WEIGHTS OF BEAMS DESIGNED FOR MINIMUM MATE-RIAL COST

savings are obtained with the strongest steels; the maximum material-cost saving is 61% for "T-1" Type A steel. The weight savings are 46% and 81% for the high-strength low-alloy steels and the "T-1" steels, respectively.

As was mentioned in the analysis, "short" and "long" girders represent the lower and upper limit of the scale for measuring the effectiveness of higher strength steels in girder applications. Thus, the weight and material-cost comparisons of actural girders will show values between those given in ·Table 5 and 6.

Hybrid Steel Beams.—The results of the analysis of hybrid steel beams indicate how such beams of equal strength and with equal web depth-to-thickness ratios should be proportioned to minimize the total material cost.
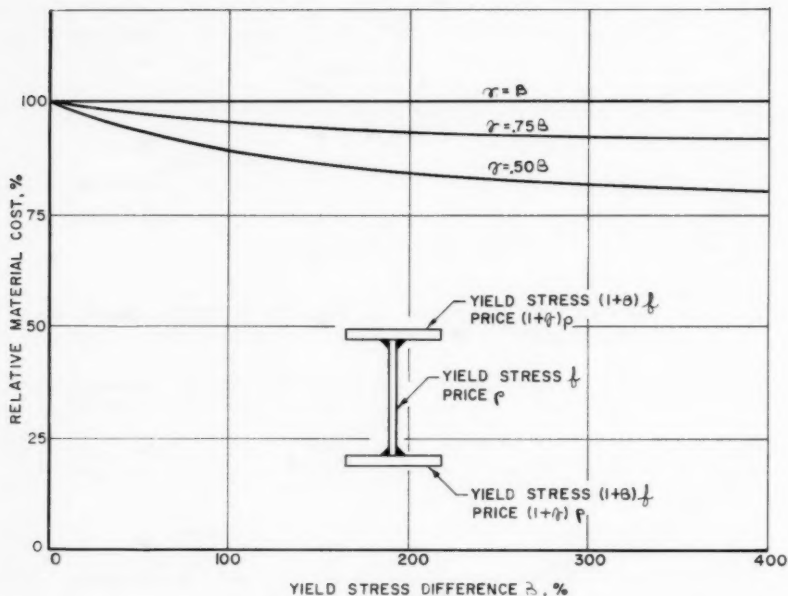
FIG. 7.—COST OF OPTIMUM HYBRID STEEL BEAMS

The significant parameter influencing the total material cost is the ratio, R, of web area to total area.

Fig. 5 shows the effect of the relative difference in yield stress, β, and the relative difference in price, γ, on the ratio R. Three curves are plotted corresponding to $\gamma = \beta$, $\gamma = 0.75\beta$ and $\gamma = 0.50\beta$. The curves show that if relatively expensive steels are used for the flanges ($\gamma = \beta$), a greater portion of the area should be in the web than when flanges are made from a relative cheap steel ($\gamma < \beta$). The ratio of web area to total area, R, is 2/3 for beams of uniform strength ($\gamma = \beta = 0$). From the analysis it will be clear that this value of R = 2/3 applies only to plastically designed beams. Elastically designed

beams require a value of $R = 1/2$ for optimum elastic section modulus. Optimum stiffness (moment of inertia) is obtained for $R = 3/4$.

The relative weights of beams designed for minimum material cost are shown in Fig. 6. The smallest weights are obtained with the cheapest highest strength steels. The cost comparison for these beams is shown in Fig. 7. The results indicate that if the relative increase in price equals the relative increase in yield stress ($\gamma = \beta$), no change in total material cost occurs. If the relative increase in price is less than the relative increase in yield stress (which is true of virtually all higher strength steels), the material cost of a hybrid steel beam is less than the material cost of a beam of uniform strength.

TABLE 7.—HYBRID STEEL BEAMS OF EQUAL STRENGTH
(Equal Web Depth-to-Thickness Ratios)

Steel		R^a	Relative Depth of Beam	Relative Weight	Relative Material Cost	Relative Elastic Deflection
Web (1)	Flanges (2)	(3)	(4)	(5)	(6)	(7)
A7	A7	0.67	1.00	1.00	1.00	1.00
A7	A441	0.65	0.91	0.85	0.95	1.38
A7	"T-1" type A	0.68	0.80	0.63	0.85	2.49
A7	"T-1"	0.75	0.87	0.68	0.92	2.16
A441	"T-1" type A	0.65	0.75	0.58	0.90	3.17
COR-TEN	"T-1"	0.73	0.81	0.60	0.99	2.74

^{a}R = ratio of web area to total area.

The latter point is illustrated for specific steels in Table 7. All hybrid steel beams show less material cost than the A7 steel beam of equal strength. Most remarkable are the cost savings obtained for the hybrid steel beam with an A7 steel web and "T-1" Type A steel flanges (15%) and for hybrid steel beam with an A441 steel web and "T-1" Type A steel flanges (10%). The weight savings for these two low-cost beams are 37% and 42%, respectively.

SUMMARY

A large family of structural steels with yield stresses varying from about 33,000 psi to 100,000 psi is presently available to designers. Because the relative increase in price of higher strength steels (compared with the price of structural carbon steel) is less than the relative increase in yield point, the application of higher strength steels results in lighter weight structures accompanied in many instances by material-cost savings.

Tension members show weight savings up to 67% (for the "T-1" steels). Material-cost savings are as high as 32% for members built-up from "T-1"

Type A steel plates, whereas for rolled shapes the maximum material-cost savings is 24% for A440 steel shapes.

Special attention is given to the optimum design of I-shaped beams and girders. For rolled beams with equal web depth-to-thickness ratios, the maximum weight savings are obtained for the "T-1" steels (52%). Material-cost savings are shown by A440 steel (12%). For girders in which the web depth-to-thickness ratios are limited by buckling, weight savings are accompanied by an increase in material cost for short spans. However, for longer span girders the material-cost savings become again significant.

Hybrid steel beams that are built up by welding higher strength steel flanges to lower strength steel webs show both weight and material-cost savings in all combinations investigated. For example, a hybrid steel beam with an A7 steel web (33,000-psi yield point) and "T-1" Type A steel flanges (100,000-psi yield strength) shows a 15% material-cost saving in addition to a 37% weight saving.

From the results of the studies presented in this paper, it can be concluded that through the optimum design of structural members the application of higher strength steels can lead to lighter weight structures and often to significant material-cost savings as well.

APPENDIX—NOTATION

The following symbols, adopted for use in the paper conform essentially with "American Standard Letter Symbols for Structural Analysis" (ASA 210.8 - 1949), prepared by a committee of the American Standards Association with Society representation, and approved by the Association in 1949.

A = cross sectional area;

A_f = total flange area (two flanges);

A_{min} = minimum cross sectional area;

A_{opt} = optimum cross sectional area;

A_w = web area;

a, b = subscripts to indentify cross section and material properties of structural members being compared;

C = total material cost;

c = depth (distance between centers of flanges) of I-section;

c_{opt} = optimum depth of I-section;

d = deflection of beam or girder;

E = modulus of elasticity;

e = elongation of tension member;

f = yield stress (stress at the yield point or 0.2% offset yield strength);

f_{cr} = buckling stress;

I = moment of inertia;

k = plate buckling coefficient;

L = length of structural member;

M = bending moment;

M_e = elastic bending strength;

M_p = plastic bending strength;

P = useful strength (load) of tension member;

p = material price;

q = parameter defined by Eq. 39;

R = ratio of web area to total area;

S = section modulus;

t = web thickness;

w = weight per unit volume;

α = web depth-to-thickness ratio;

β = relative difference in yield stress;

γ = relative difference in price; and
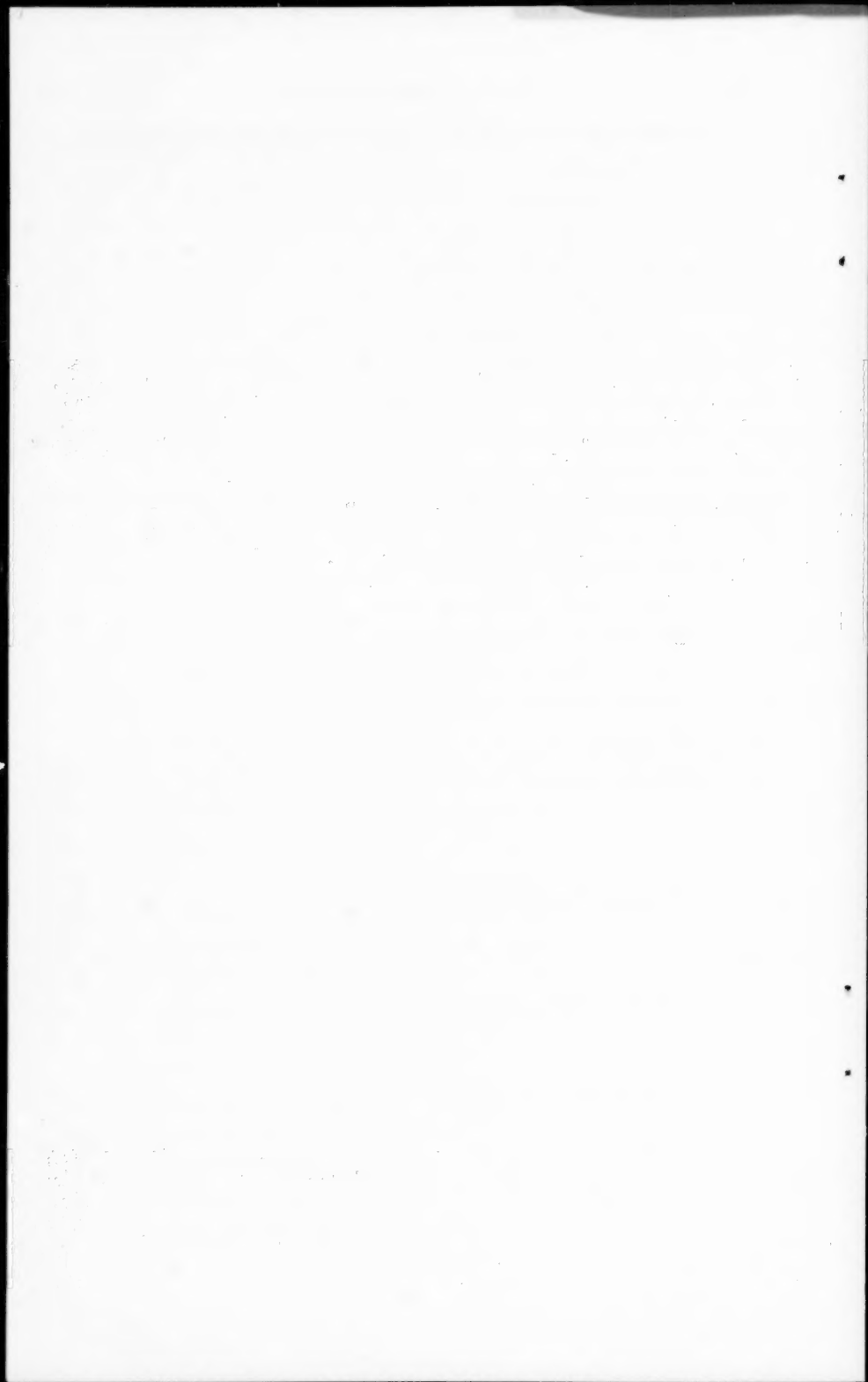
ν = Poisson's ratio.

Journal of the
STRUCTURAL DIVISION

Proceedings of the American Society of Civil Engineers

RESTRAINT OF STRUCTURES ATTACHED TO MASS CONCRETE

By Keith Jones,[1] F. ASCE

SYNOPSIS

On some massive concrete structures such as dams, comparatively light structural frames such as trashracks or control appurtenances are extended and built as integral parts of the massive structures. Those structural frames are, in general, exposed to widely varying temperatures imposed by climatic conditions. The varying temperatures induce length changes in the frames. Similarly induced length changes at the surface of the mass concrete between any two points of attachment of the frame must be restrained by the mass, whose range of temperature variation becomes smaller at increasing distances from the surface into the mass.

This paper presents measurements of length and temperature changes occuring at depths of up to 5 ft into the masses of three concrete dams in actual service. The measurements were made, periodically, by means of elastic-wire strainmeters that were embedded in the concrete during construction, and extend over periods of several years after embedment. Based on those measurements, a rational method of calculating the effects of the restraint by the mass concrete is deduced and presented. The method is applicable in de-

sign of reinforcement at junctures of massive concrete with comparatively
light structural frames where temperature variations are significant.

INTRODUCTION

The major portion of the data presented in this paper was obtained from
strainmeters embedded, in sets of three, in the Bureau of Reclamation's Hun-
gry Horse Dam in northern Montana. Figs. 1 and 2 show the locations and ori-
entations of those trios of strainmeters. On Figs. 3, 4, and 5 are the curves
of strains and temperatures, varying with time, derived from data obtained
from the strainmeters shown in Figs. 1 and 2. Fig. 5 also includes curves of
construction progress, reservoir elevation, and air temperature at Hungry
Horse Dam. Additional data were obtained from less complete strainmeter
installations in the Bureau of Reclamation's Shasta and Canyon Ferry Dams.
Details of those two strainmeter installations together with the corresponding
time curves of strain and temperature are shown in Figs. 6 and 7, respectively.
Figs. 1 through 7 comprise the basic information from which the analysis of
the restraint effect developed in this paper has been deduced.

ANALYSIS OF DATA

Figs. 8, 9, and 10 compare, graphically, the range of strains and tempera-
tures measured by the strainmeters shown in details "U" and "T" in Fig. 1.
The directions in which the strainmeters are oriented and, hence, in which the
strain measurements are made, are designated in Figs. 8, 9, and 10 as "Nor-
mal," that is, normal to the nearest face of the dam; "Parallel," that is, paral-
lel to the slope of the nearest face of the dam; and "Axial," that is, parallel
to the axis of the dam. The graphs on those three figures show the relations
among the total length changes, for each seasonal increase and decrease of
temperature, in those three directions at each of the distances of the strain-
meters, 1 ft, 2 ft, and 5 ft from the nearest face of the dam. The values used
in plotting those graphs were taken directly from the curves of Figs. 3 and 4.
Strainmeter SM433 yields clearly inconsistent results not used in plotting the
"Normal" curve, but those results are included, for the sake of completeness,
on Figs. 8, 9, and 10.

Details "U" and "T" of Fig. 1 describe the only strainmeter installations
that were made in which the meters are located at different distances from
the face of the dam. Details "O," "P," "Q," and "R" in Fig. 2 and all groups
in Shasta and Canyon Ferry Dams, Figs. 6 and 7, show that the strainmeters
in those locations are all about 2 ft from the faces of the respective dams. It
is, therefore, impossible to compare the values represented by the curves in
Figs. 5, 6, and 7 by the use of the same method as that used to plot Figs. 8, 9,
and 10. Figs. 11 and 12 are bar diagrams comparing the strain changes and
temperatures from Figs. 5, 6, and 7 in the same three directions as used on
Figs. 8, 9, and 10. The values represented in Figs. 11 and 12 are for all strain-
meters in those three directions and which are located about 24 in. from the
faces of all three dams. The first two seasonal temperature cycles after in-
stallation of each such strainmeter group are used in the comparisons in Figs.
11 and 12.
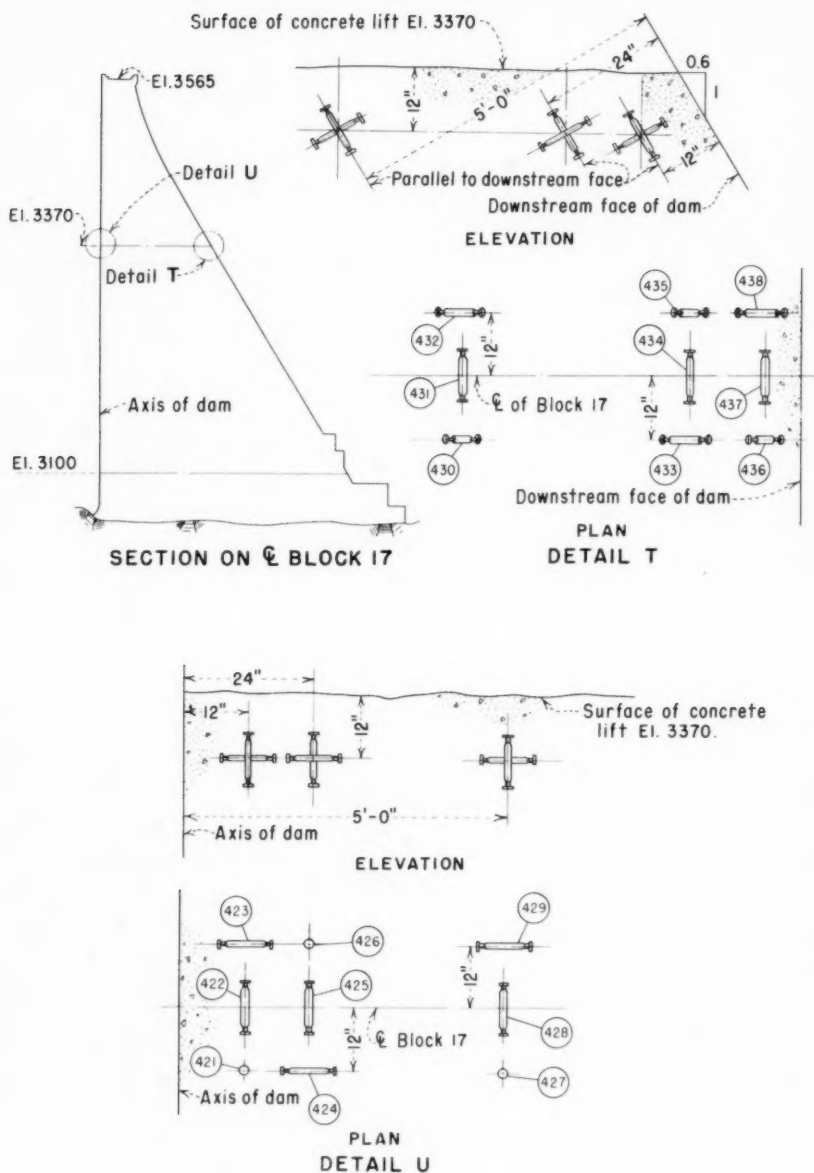
FIG. 1.—LOCATIONS AND ORIENTATIONS OF STRAINMETERS IN HUNGRY HORSE DAM
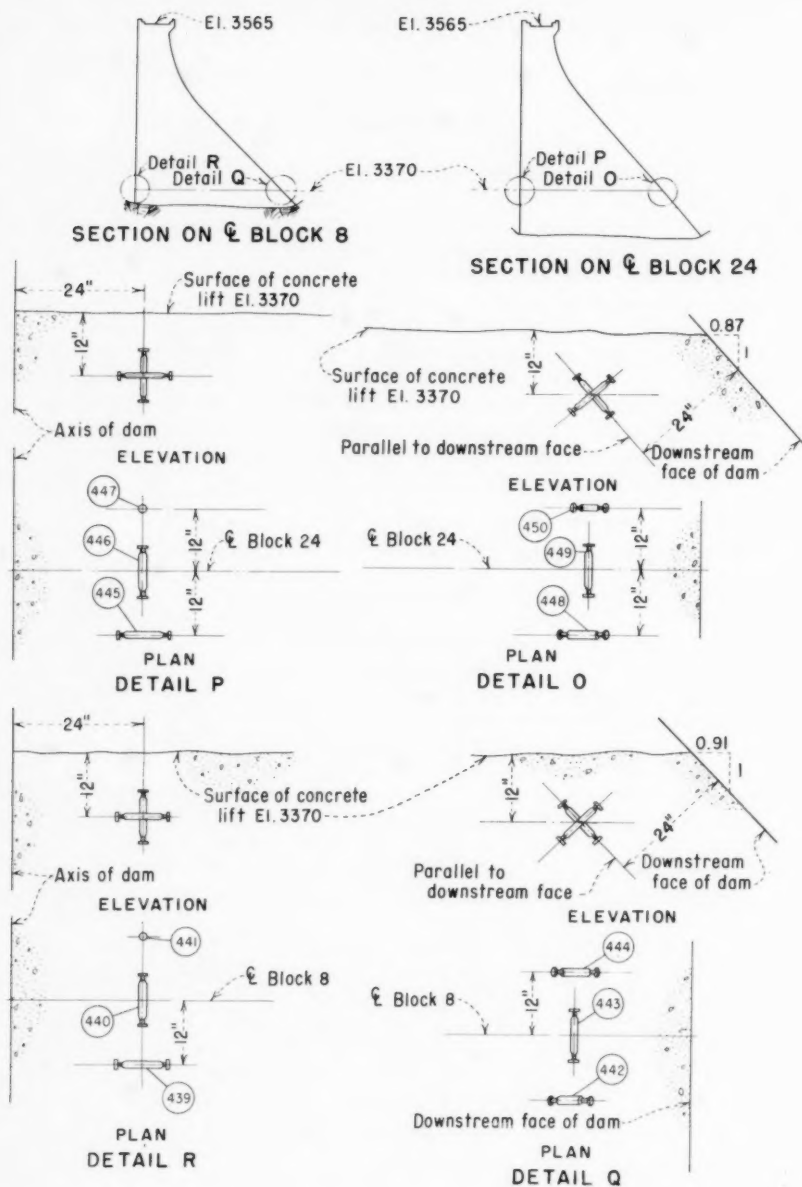
FIG. 2.—LOCATIONS AND ORIENTATIONS OF STRAINMETERS IN HUNGRY HORSE DAM
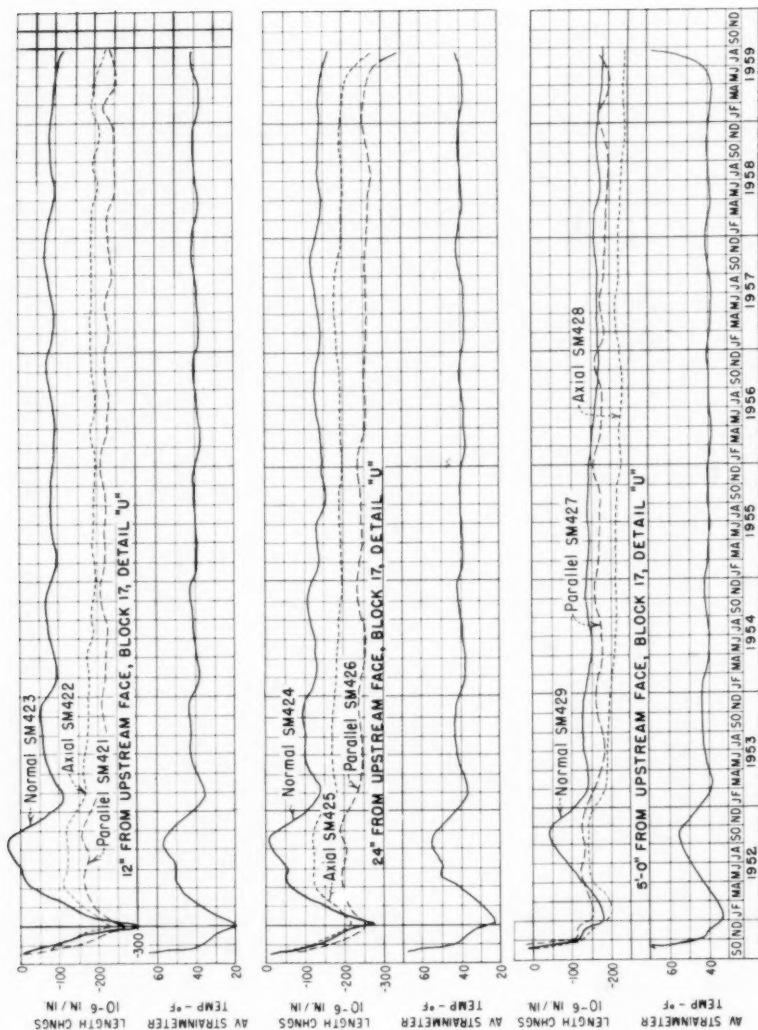
FIG. 3.—LENGTH AND TEMPERATURE CHANGES OF STRAINMETERS SHOWN ON FIG. 1
HUNGRY HORSE DAM
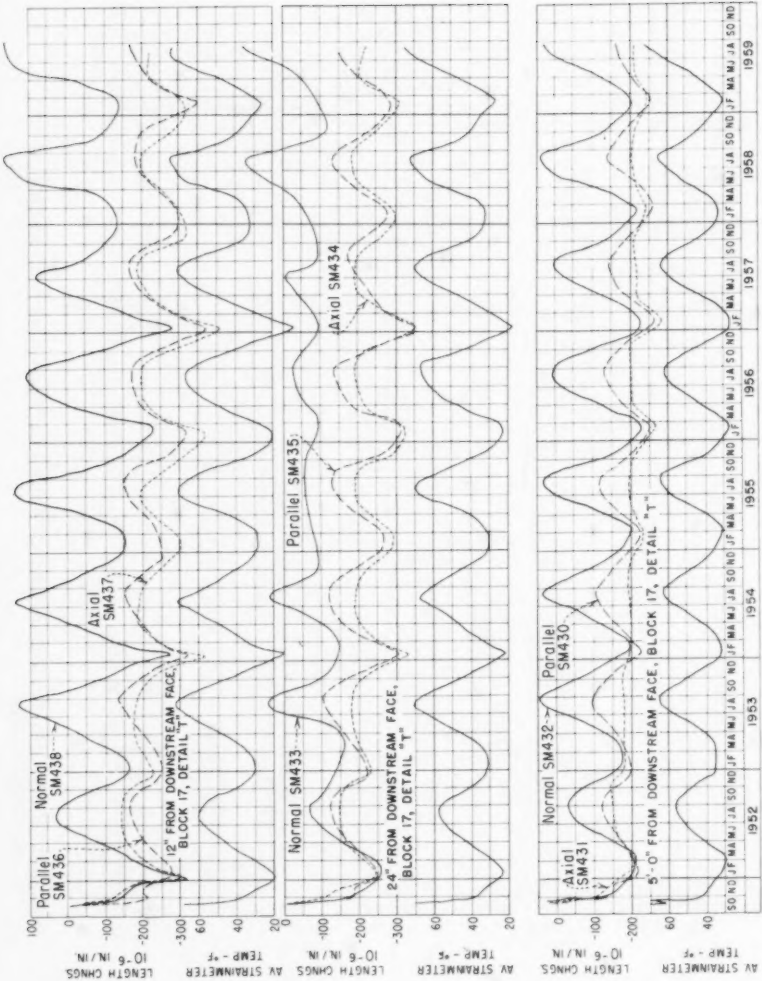
FIG. 4.—LENGTH AND TEMPERATURE CHANGES OF STRAINMETERS SHOWN ON FIG. 1
HUNGRY HORSE DAM
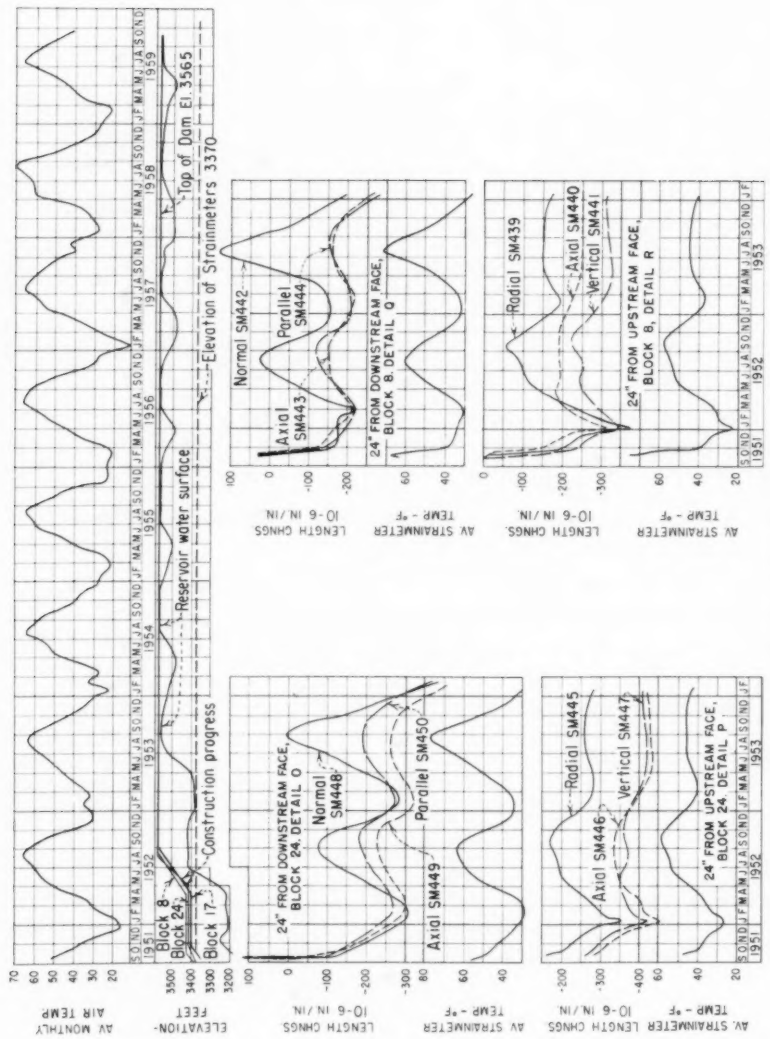
FIG. 5.—CONSTRUCTION, AIR TEMPERATURE AND RESERVOIR ELEVATION RECORD AND LENGTH AND TEMPERATURE CHANGES OF STRAINMETERS SHOWN ON FIG. 2 HUNGRY HORSE DAM
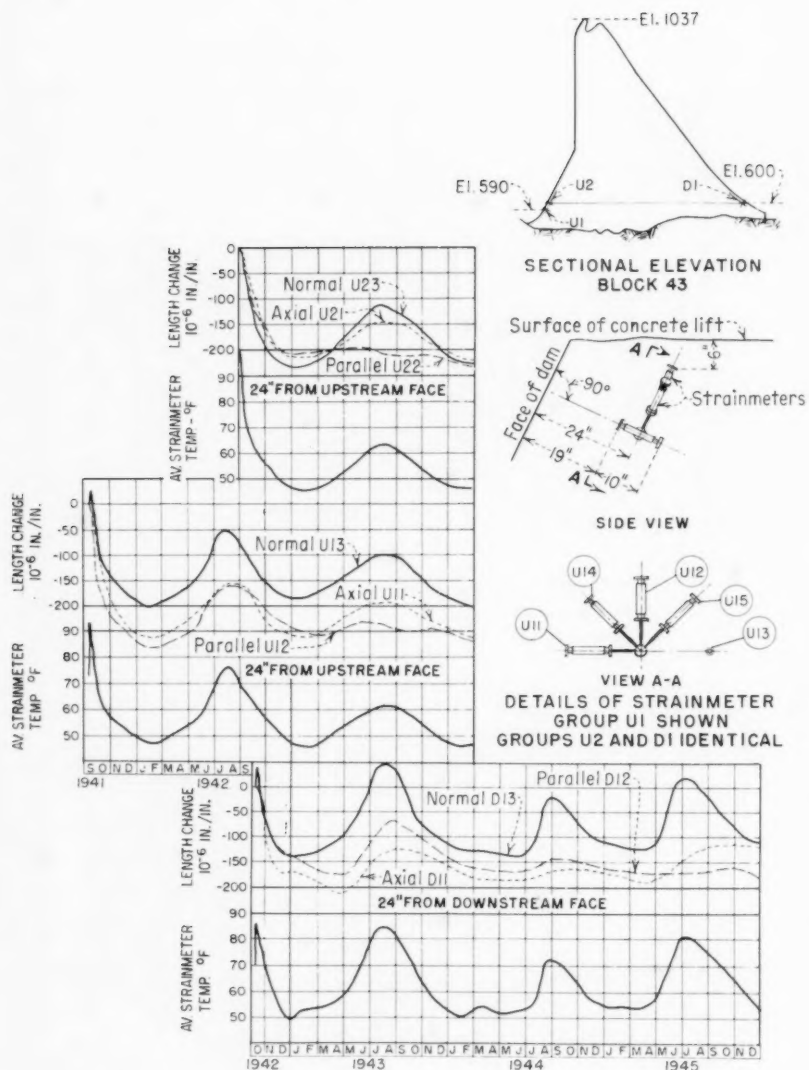
FIG. 6.—LOCATIONS AND LENGTH AND TEMPERATURE CHANGES OF STRAIN-
METERS SHASTA DAM
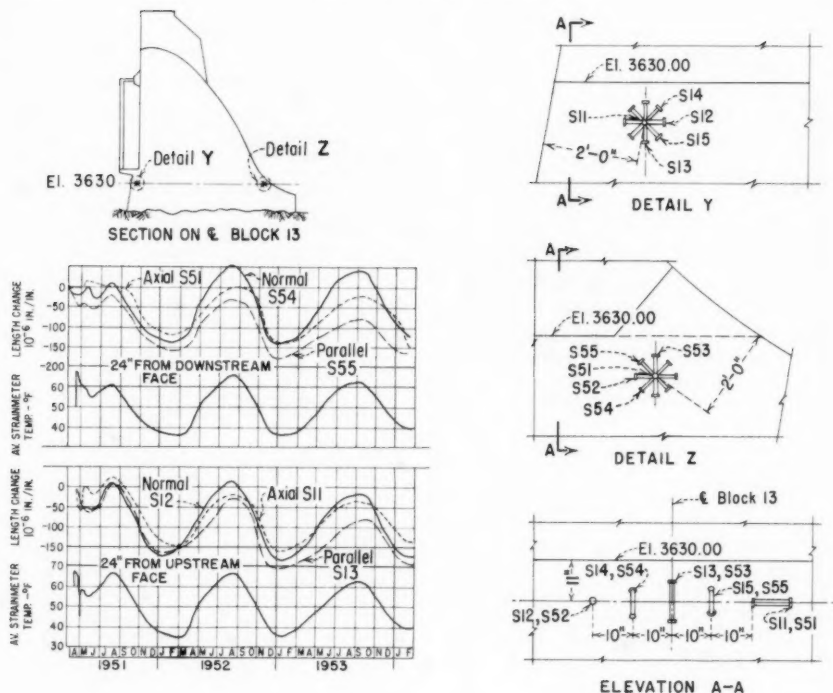
FIG. 7.—LOCATIONS AND LENGTH AND TEMPERATURE CHANGES OF STRAIN-
METERS CANYON FERRY DAM

Figs. 8 through 12 show, consistently, that greater length changes occur in
the direction normal to the face of any of the dams than in the other measured
directions. The smaller length changes are attributable to the restraint af-
forded by the rigidity of the mass concrete.

ELASTICITY CONSIDERATIONS

If the assumption is made that length changes, due to temperature changes,
which take place in the mass concrete near a face, are not restrained in a di-
rection normal to the face, but are restrained in the other perpendicular direc-
tions, the following equation applies:

$$\epsilon_N = \alpha T + \mu\left(\epsilon_A + \epsilon_P\right) \dotfill (1)$$

in which ϵ indicates length change with subscripts N, A, and P denoting direc-
tions as normal to face, parallel to axis, and parallel to face, respectively;
α represents the thermal coefficient of expansion of the concrete, T, the tem-
perature change; and μ represents Poisson's ratio.
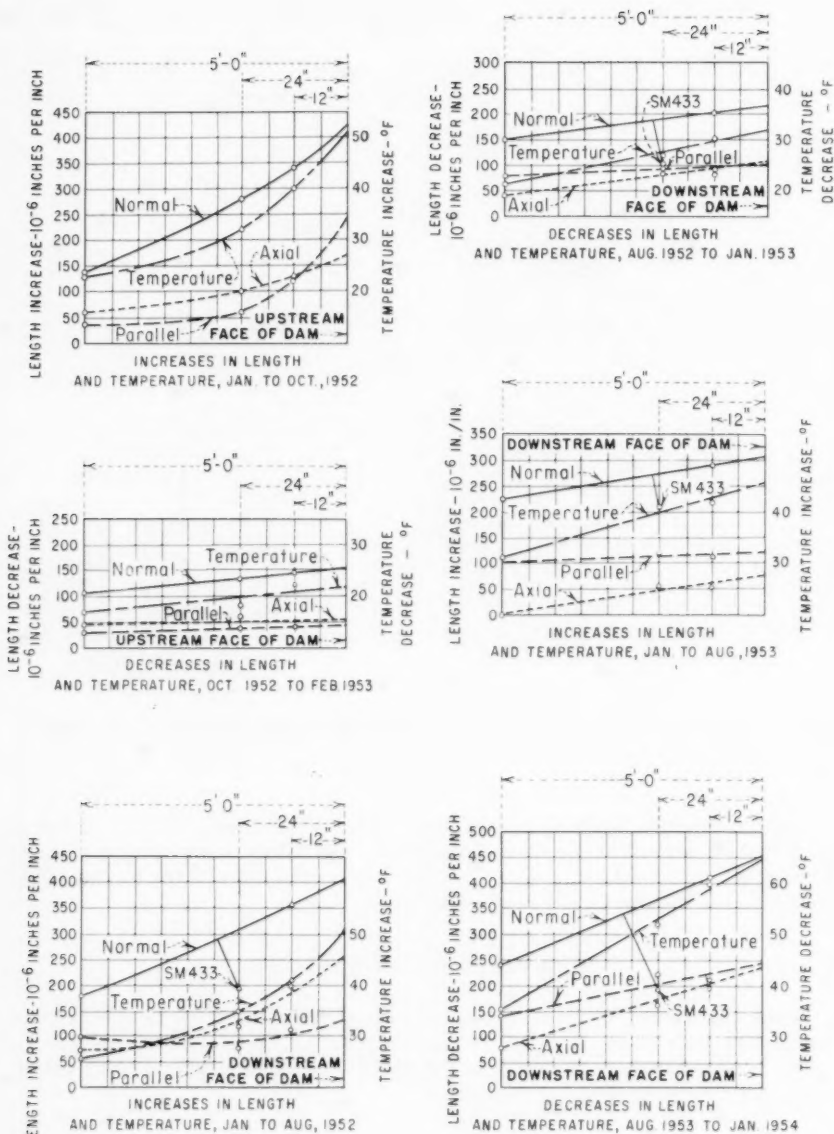
FIG. 8.—TOTAL LENGTH AND TEMPERATURE CHANGES OF STRAINMETERS DUR-
ING ENTIRE PERIODS OF SEASONAL TEMPERATURE INCREASES AND DE-
CREASES HUNGRY HORSE DAM
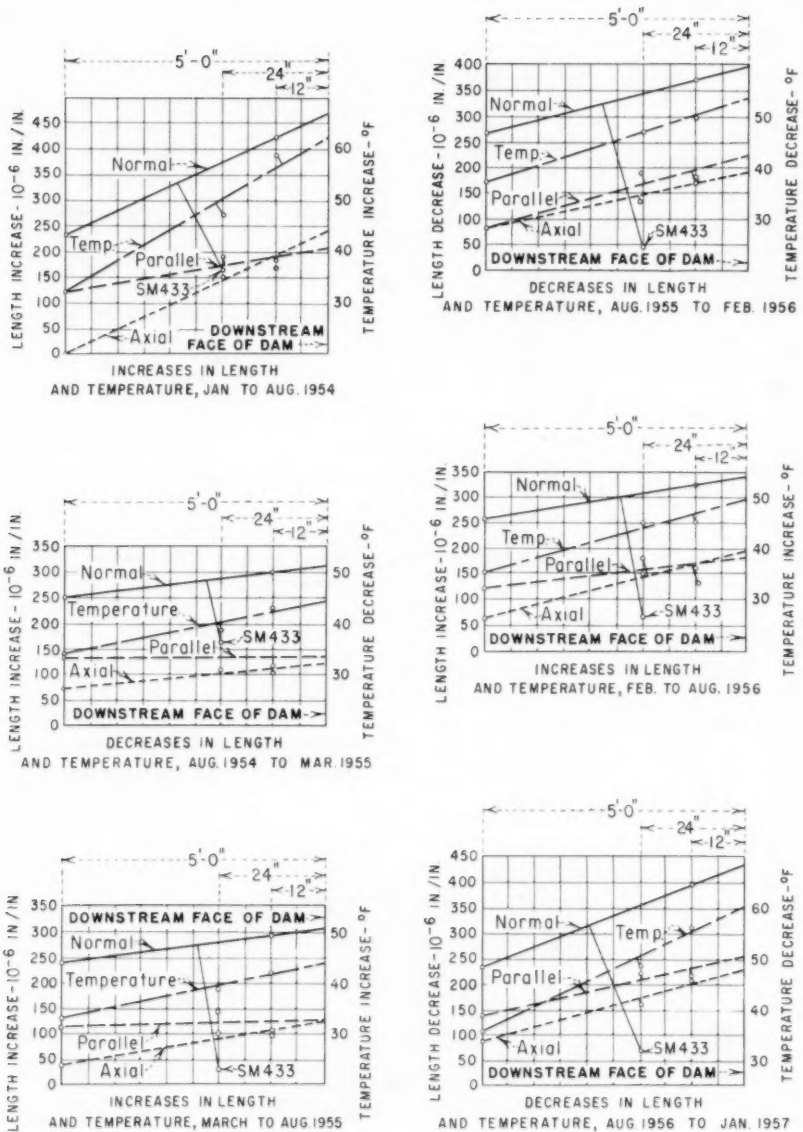
FIG. 9.—TOTAL LENGTH AND TEMPERATURE CHANGES OF STRAINMETERS DUR-
ING ENTIRE PERIODS OF SEASONAL TEMPERATURE INCREASES AND DE-
CREASES HUNGRY HORSE DAM

FIG. 10.—TOTAL LENGTH AND TEMPERATURE CHANGES OF STRAINMETERS DUR-
ING ENTIRE PERIODS OF SEASONAL TEMPERATURE INCREASES AND DE-
CREASES HUNGRY HORSE DAM

FIG. 11.—COMPARISONS OF TOTAL LENGTH AND TEMPERATURE CHANGES OF STRAINMETERS DURING ENTIRE PERIODS OF SEASONAL TEMPERATURE INCREASES AND DECREASES HUNGRY HORSE, SHASTA, AND CANYON FERRY DAMS
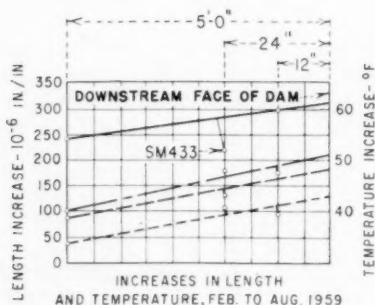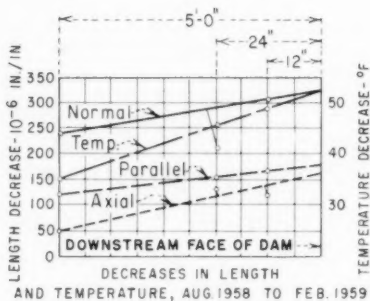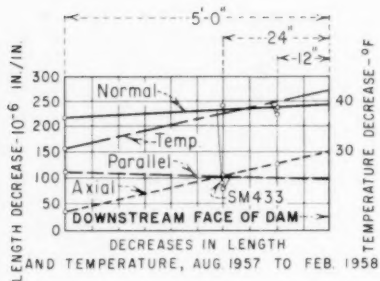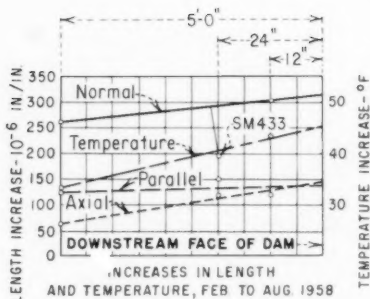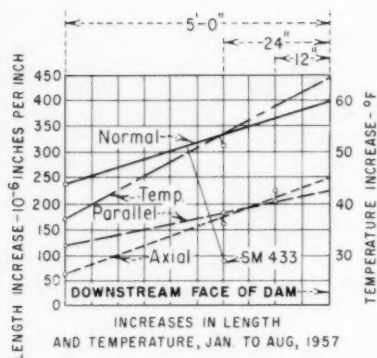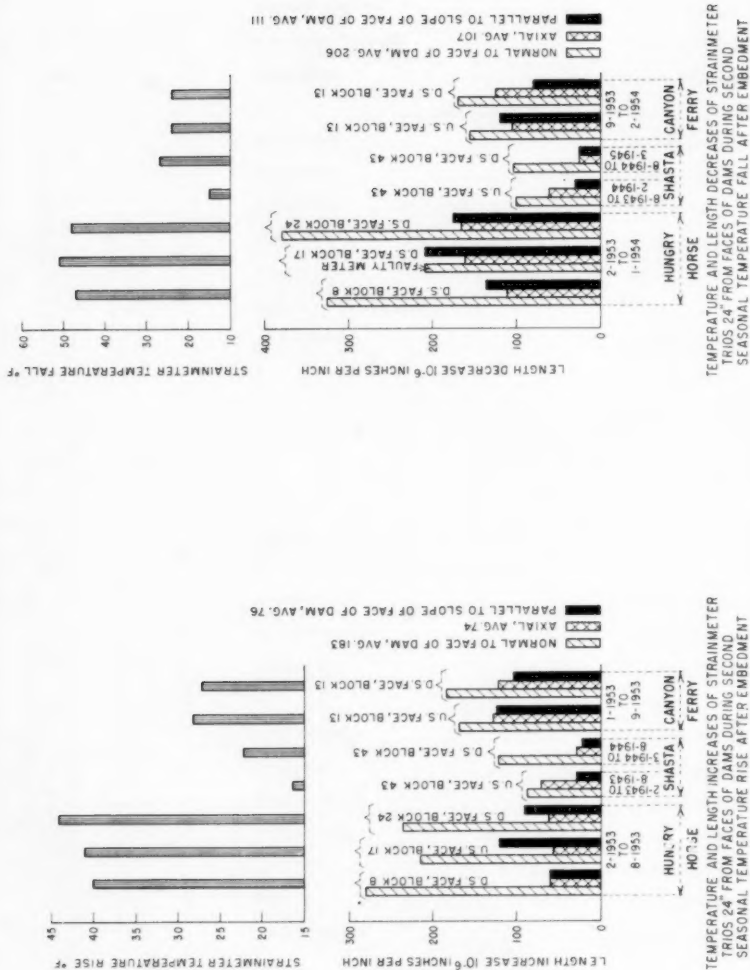
FIG. 12.—COMPARISONS OF TOTAL LENGTH AND TEMPERATURE CHANGES OF STRAINMETERS DURING ENTIRE PERIODS OF SEASONAL TEMPERATURE INCREASES AND DECREASES HUNGRY HORSE, SHASTA, AND CANYON FERRY DAMS

Laboratory tests of the concrete in Hungry Horse Dam have determined that

$$\alpha = 6 \times 10^{-6} \text{ in. per in. per } °F$$
$$\mu = 0.17.$$

If those values are substituted into Eq. 1 together with values of ϵ_A, ϵ_P, and T, at a face of the dam, from Figs. 8, 9, and 10, a value of ϵ_N may be calculated which agrees, with reasonable experimental accuracy, with the appropriate measured values from those figures.

For example, the curves on Fig. 8 for the seasonal temperature drop from August, 1952, to January, 1953, may be chosen, and values at the downstream face of the dam, from those curves, substituted into Eq. 1 are

$$\epsilon_N = 6 \times 32 + 0.17(110 + 100) = 228$$

and from the normal curve of the same set, $\epsilon_N = 215$.

Another example from the curves of August, 1957, to February, 1958, appear in Fig. 10:

$$\epsilon_N = 6 \times 42 + 0.17(155 + 100) = 295$$

from the normal curve of the same set, $\epsilon_N = 245$.

A study of Figs. 8 through 12 leads to the following approximations:

$$\epsilon_N = \epsilon_A + \epsilon_P \text{ (approximately)} \dots\dots\dots\dots\dots (2)$$

and

$$\epsilon_A = \epsilon_P \text{ (approximately)} \dots\dots\dots\dots\dots\dots (3)$$

Acceptance of the empirical relationships of Eqs. 2 and 3 enables, by use of Eq. 1, calculation of the values of the restrained length changes in the axial direction and in the direction parallel to the slope of the face; that is, values of ϵ_A and ϵ_P may be calculated as follows:

Substituting Eq. 2 in Eq. 1:

$$\epsilon_N = \alpha T + \mu \epsilon_N = \frac{\alpha T}{1 - \mu} \dots\dots\dots\dots\dots (4)$$

from Eqs. 2 and 3:

$$\epsilon_A = \epsilon_P = \frac{\epsilon_N}{2}$$

and substituting that value in Eq. 4:

$$\epsilon_A = \epsilon_P = \frac{\alpha T}{2(1-\mu)} \dots\dots\dots\dots\dots\dots (5)$$

Eq. 5 enables calculations of restrained length changes to be made and applied. Fig. 13 illustrates the application of Eq. 5 to a typical problem of designing reinforcement in a frame attached to a massive concrete structure.

The evidence presented herein shows that only partial restraint of change in distance between A and D, as shown by Fig. 13, is effective, and that the net change is approximately evaluated by use of Eq. 5.

The accepted practice has been to design the reinforcement at the junctures of the frame with the mass concrete, that is at A and D, by assuming that no change in distance between those two points occurs or, equivalently, that A' D' = AD. A reduction in temperature-induced moment at A and D results from the reduction of restraint and a corresponding saving of reinforcement if justified.

Engineers generally recognize that great accuracy in, and agreement among, measurements of length changes in concrete is not to be expected, because of the variations in the elastic properties of the concrete itself. Those variations occur not only between different structures but also between different places in the same structure and are attributable to the heterogeneity of concrete.
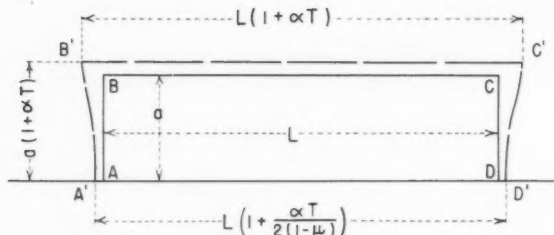
FIG. 13.— Let the line, AD, produced, represent the plan view of a part of a vertical face of a concrete mass. Let ABCD represent the center line of a rectangular concrete frame fixed to the face of the mass at A and D.

If a temperature rise, T, be imposed on the entire system the three sides of the frame, AB, BC and CD lengthen, relatively unrestrained, by the amounts shown in the above diagram. The side AD, being also part of the mass concrete and therefore restrained will lengthen less than will BC according to Equation (5) in the text. The condition accompanying a temperature decrease is analogous.

A designer, having calculated the new shape A' B'C'D', has sufficient information to enable the determination of the amount of reinforcement required.

Neither the variations nor their effects are predictable. Where a large number of measurements are made, such as during the time of seasonal rise or fall of temperature, observational and instrumental errors tend to vary at random, and their effects are minimized when curves of the observed values are smoothed; some obviously incompatible values can be omitted from consideration.

CONCLUSIONS

Climatic temperature changes induce partially restrained length changes in concrete near the exposed surfaces of massive structures. Restraint of

length change by the rigidity of the massive structure is not complete. Evidence obtained from embedded strainmeters and presented herein indicates that the rigidity of the massive structure permits about one-half of the unrestrained value of temperature-induced length changes to occur near exposed surfaces.

That reduction of restraint may be used to advantage in the design of reinforcement in frames or structures attached to the faces of massive concrete structures.
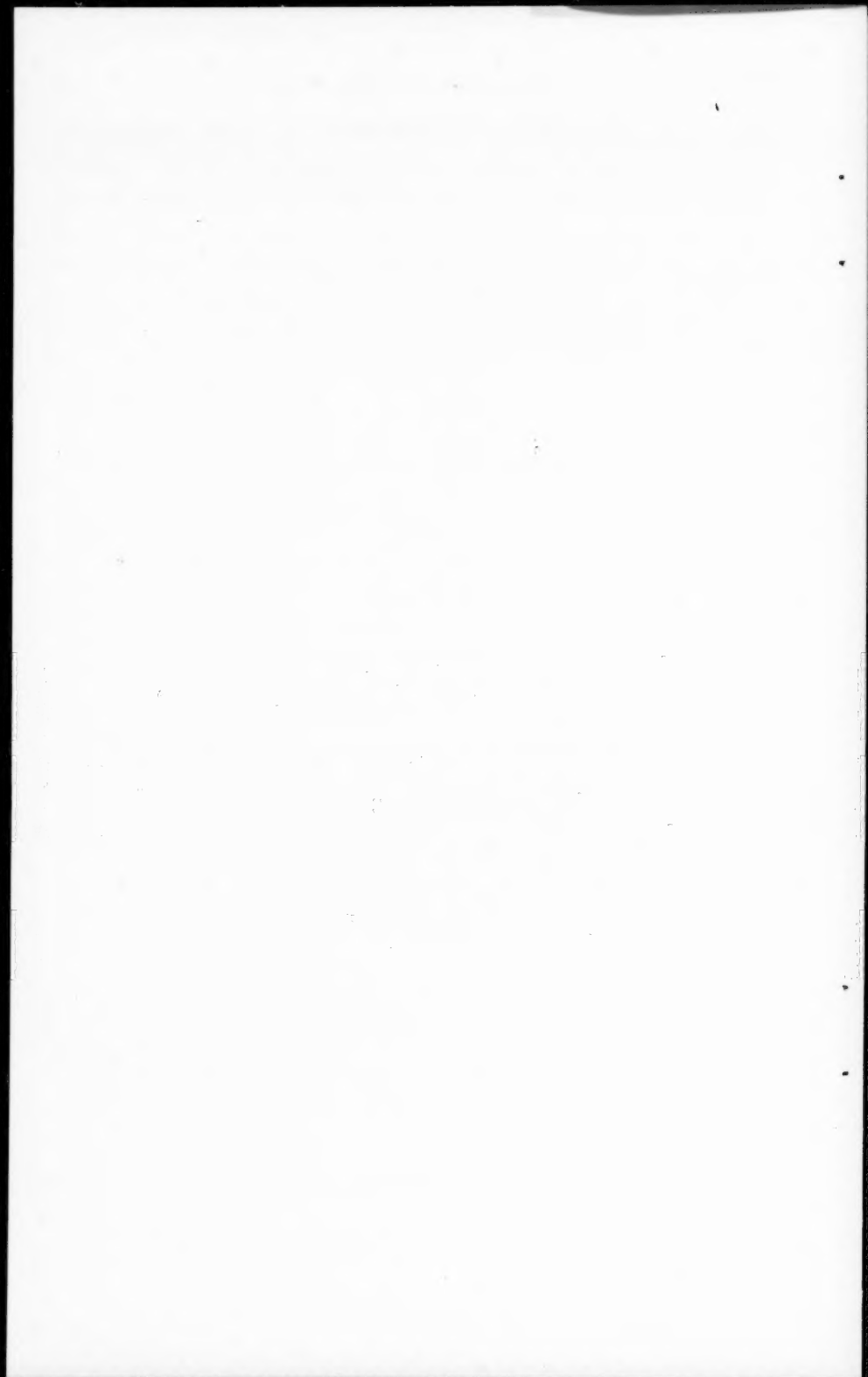
Journal of the
STRUCTURAL DIVISION
Proceedings of the American Society of Civil Engineers

POST-ELASTIC BEHAVIOR OF WIDE-FLANGE STEEL BEAMS

By Herbert A. Sawyer, Jr.,[1] F. ASCE

SYNOPSIS

Strain hardening tends to cause the flexural strength of a wide-flange steel section to be higher than its fully plastic strength, and instability tends to make the flexural strength lower than the fully plastic strength.

By means of tests on twenty-one simple beams of various cross-sectional dimensions and moment gradients, these deviations in strength with the corresponding flexural deformations are evaluated experimentally, and semi-empirical expressions for the strengths and deformations are established. From these data, expressions for the effective moment-curvature relationships for any rolled steel section are obtained.

The behavior predicted by these expressions of a simple and a continuous beam tested by others is compared with test results and with the behavior assumed by the rigid-plastic and elastic theories.

INTRODUCTION

The elastic behavior of flexural structures is determined from an assumed linear relationship between bending moment and curvature. Because rolled steel flexural members are elastic for a relatively small range of curvature, it is generally recognized that a non-linear moment-curvature relationship must be used to even approximate the true behavior of steel flexural structures. A two-segment approximation consisting of the elastic line and an infinitely

---

long, horizontal, plastic line has been increasingly used, and this approximation gives results much nearer to true behavior than elastic theory.

However, this approximation neglects four important factors that affect the strength and deformations of steel flexural members: Strain hardening, that tends to increase strength; instability or buckling, that tends to reduce strength; and the inseparable shear and moment-gradient, the former of which tends to reduce strength, and the latter to increase strength. Because these are opposing factors, the plastic theory may, by coincidence, give close results for. certain structures, but precise prediction or explanation of the strength and deformations of any structure must consider these factors; that is, a more accurate moment-curvature relationship must be used. (This is not to say that the existing method of plastic design[2] is unreliable. For the ordinary building this method is conservative, because it: (1) excludes use of the least stable sections, (2) neglects strain hardening, (3) contains many built-in safeguards against premature buckling, and (4) assumes the conservative yield stress of 33 ksi.)

Purpose of Tests.—The purpose of this investigation is to establish a semiempirical basis for determination of more accurate moment-curvature (M-ϕ) relationships for rolled steel wide-flange or I selections with moment applied about the strong axis and with insignificant axial loading. Any typical moment-curvature relationship will be determined as a function of the following parameters: The cross-sectional dimensions of the shape; the moment graident (shear); and the tensile stress-strain relationship of the steel. This investigation is not concerned with the actual moment-curvature relationship at any single cross section (which could vary significantly along the length of a member) but with the single, effective M-ϕ relationship that defines the behavior of a considerable length of member with linearly-varying moment.

To achieve this purpose, the behavior of various simple steel beams with various constant moment-gradients was determined experimentally after measurement of the previously noted parameters for these beams. Then, moment-curvature relationships that would agree with this behavior were determined, using, in the pre-buckling range, rational methods based on the measured parameters, and using, for the ultimate moment and curvature, empirically determined coefficients.

It is believed that this investigation provides much basic data for the analytical prediction of the behavior of any flexural rolled-steel structure subjected to a proportional loading, provided the structural dimensions and the tensile stress-strain relationships are known.

Previous Work.—There have been several experimental studies[3-10] of the post-elastic flexural behavior of wide-flange sections subjected to uniform moment (zero shear). However, there seem to have been only four limited ex-

2 "Plastic Design in Steel," American Inst. of Steel Constr., New York, N. Y., 1958.

3 "Behavior of Rolled-Steel Joists in the Plastic Range," by J. W. Roderick and H. H. L. Pratley, British Welding Journal, Vol. 1, 1954.

4 "The Plastic Behavior of Structural Members and Frames," G. C. Driscoll, Jr. and L. S. Beedle, Welding Journal, Vol. 36, No. 6, June, 1957, p. 275s.

5 "Plastic Behavior of Wide-Flange Beams," by W. W. Luxion and B. G. Johnston, Welding Journal, Vol. 27, No. 11, November, 1948, p. 538s.

6 "Residual Stress and the Yield Strength of Steel Beams," by C. H. Yang, L. S. Beedle, and B. G. Johnston, Progress Report No. 5, Welding Journal, Vol. 31, No. 4, April, 1952, p. 205s.

7 "Plate Buckling in the Strain-Hardening Range," by G. Haaijer, Proc. Paper No. 1212, ASCE, Vol. 83, No. EM2, April, 1957, p. 46.

perimental studies[3,4,10,11] of the more general case of wide-flange sections subjected to a moment of constant gradient (shear) and no axial load, and because determination of effective moment-curvature relationships was not within the intent of these studies, the flexural angles necessary to such a determination were not measured. (T. Kusuda and Bruno Thürlimann, M. ASCE, have performed[12] three tests on wide-flange section subjected to moment, shear, and axial tension in which the flexural angles were measured).

For a summary and comprehensive bibliography of the theoretical work done on this problem reference should be made to a paper[13] by C. G. Lee. Impressive theoretical work has been done by M. W. White.[9]

As a beam approaches its ultimate moment, buckling of indefinite mode involving large displacements is always present. None of these purely theoretical approaches can even approximately predict behavior at this stage, because no theory yet presented accounts for the following factors, all of which would seem to be important:

1. The amount of purely plastic strain of the stress-strain diagram and the reduction in strain-hardening modulus after the initiation of strain-hardening. (Present theory only accounts for the initial strain-hardening modulus). Also, the difference in stress-strain relationship for tension and compression.

2. The non-linear distribution of normal strains at a section caused by relative reduction in compressive strain of fibers which buckle.

3. The change in shape of cross section area caused by buckling. Also, the post-elastic shift of the shear center with respect to the area of a cross section (insignificant for sections with two axes of symmetry).

4. Initial imperfections and eccentricities.

These would be of minor importance for moments approaching the ultimate were it not for their effect on the timing and even sequence of the successive modes of buckling; that is, the configuration achieved from one mode may drastically affect the initiation-load and the severity of the next mode. Thus, there is, unfortunately, an inherent uncertainty in post-elastic flexural behavior that obviously applies to both theoretical and experimental results. For example, a typical (not universal) sequence of buckling modes is as follows: (a) local buckling of the two edges of the compression flange, (b) buckling by rotation as a unit of the compression flange and the compressed half of the web about the flange-web junction, (c) a somewhat local lateral buckling of the compression flange, (d) an "S" type overall lateral buckling continuous across lateral supports. For the transition from mode (a) to (b) of this sequence, imperfections that cause an initial local upward buckling of both edges of the compres-

8 "On Inelastic Buckling in Steel," by G. Haaijer and B. Thürlimann, Report No. 205 E. 9, Fritz Engrg. Lab., Lehigh Univ., Bethlehem, Pa., May, 1957.

9 "The Lateral-Torsional Buckling of Yielded Structural Steel Members," by M. W. White, Report No. 205 E. 8, Fritz Engrg. Lab., Lehigh Univ., Bethlehem, Pa.. October, 1956.

10 "Shear Deflection of Wide Flange Steel Beams in the Plastic Range," by W. J. Hall and N. M. Newmark, Proc. Paper No. 814, ASCE, Vol. 81, October, 1955.

11 "Theory and Practice in Steel Construction," by F. Stussi, Acier, Vol. 23, No. 2, Brussels, Belgium, February, 1958, p. 84.

12 "Strength of Wide Flange Beams under Combined Influence of Moment, Shear and Axial Force," by T. Kusuda and B. Thürlimann, Report No. 248.1, Fritz Engrg. Lab., Lehigh Univ., Bethlehem, Pa., May, 1958.

13 "A Survey of Literature on the Lateral Instability of Beams," by C. G. Lee, Bulletin No. 63, Welding Research Council, August, 1960, p. 50.

sion flange at a section will tend to suppress mode (b), whereas an initial buck-
ling of these edges in opposite directions would encourage mode (b). (Because
similar considerations hold for the transitions to subsequent modes, the ulti-
mate strength may be realized during any mode.)

5. Residual stresses.
6. Shear. The usual treatment of shear[14] neglects strain-hardening.

It would seem that even if a theory should be developed in the future that
would account for these factors, it would be so complex as to be of little prac-
tical use. Because tests automatically account for such factors, extremely
useful engineering solutions to highly complex problems in other fields—for
example, flexure and diagonal tension of reinforced concrete, flow in fluid me-
chanics, and bolted or riveted connections of steel—have been obtained by
semi-empirical analytical methods. The purpose of this investigation is to ob-
tain the test results that are a necessary basis for applying any such methods
to the post-elastic flexure of steel, and also to interpret these results using
one such method.
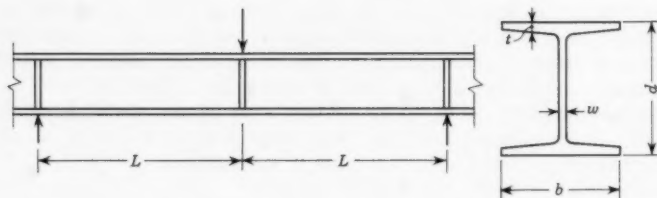
FIG. 1.—DIMENSIONS OF BEAMS

Notation.—Letter symbols adopted for use in this paper are defined where
they first appear and are arranged alphabetically, for convenience of reference,
in the Appendix.

METHOD AND RESULTS OF TESTS

Plan of Tests.—The tests were planned under the assumption that the post-
elastic strength and deformation of rolled steel sections under flexure were
governed primarily by instability, and that instability depended primarily on
the flange proportions expressible by the two parameters L/b and b/t, and sec-
ondarily on the web proportions expressed by d/w, all as defined by Fig. 1.
Therefore, it was decided to test six different shapes, one with a b/t ratio of
approximately 11, three of approximately 14, and two of approximately 18. For
each of these shapes, three specimens with values of L/b of approximately 4.25,
5.75, and 8, all cut from one length, were tested. Values of d/w ranged from
21.1 to 57.7. Relative lateral translation of the compressive flange at the three
loading points was prevented with the arrangement shown in Fig. 3. (The
flanges were removed from the center portion of the channel to make its flex-

---

14 "The Full Plastic Moments of Sections Subjected to Shear Force and Axial Load,"
by M. R. Horne, British Welding Journal, Vol. 5, No. 4, April, 1958.
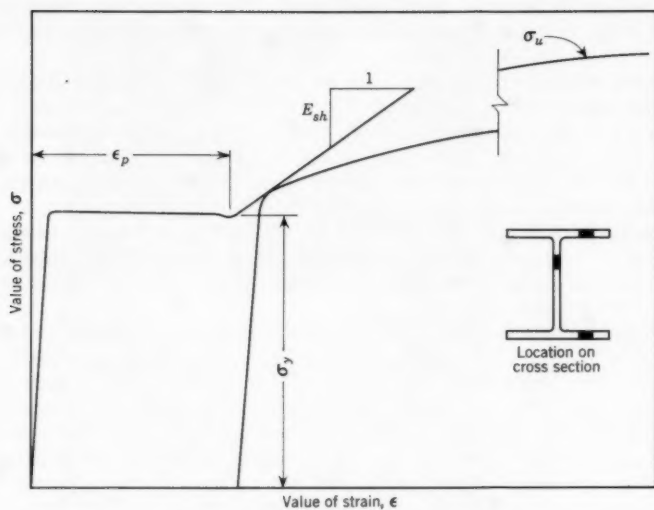
FIG. 2.—TENSILE TEST COUPONS
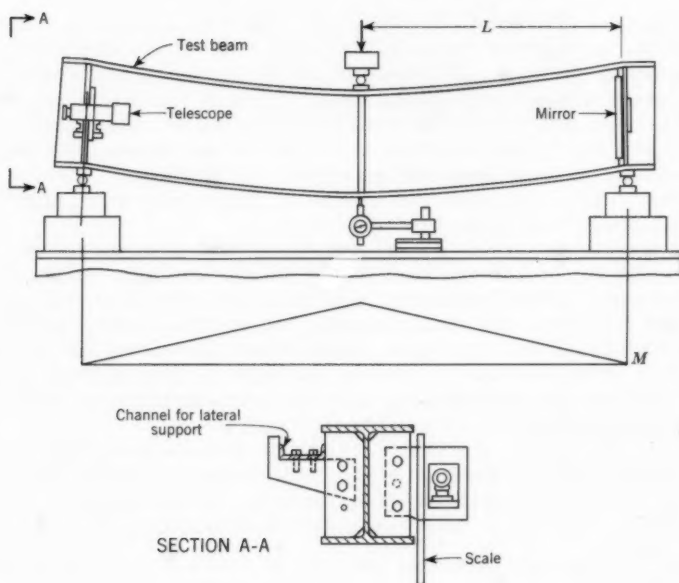
FIG. 3.—TEST ASSEMBLY

ural resistance to vertical loads negligible). No attempt was made to prevent rotation of the cross-section at the central load about any axis (for example, Fig. 17).

Thus, the main test program involved the testing of eighteen flexural specimens, specimens numbered "4" to "21." Three specimens, numbered "1" to "3," with a b/t ratio of approximately 17 and with a limited amount of lateral support, were also tested. Because of the uncertainty of the degree of lateral support, test results for specimens 1 to 3, although presented herein, should not be considered to have great significance.

For each specimen, all dimensions shown in Fig. 1 were measured. For each shape, two coupons taken from the quarter points of the flanges and one from the quarter point of the web (as shown in Fig. 2) were tested in tension to obtain stress-strain curves.

Each specimen was tested in flexure with the apparatus shown in Figs. 3 and 4 with loads, or, more precisely, deflections, applied by a universal hydraulic testing machine. Deflections were applied at a continuous rate, slow below the elastic limit and faster above the elastic limit so that the total time of loading was from $\frac{1}{2}$ hr to $1\frac{1}{2}$ hr per specimen. For each of a series of pre-determined values of load, essentially simultaneous reading of Δ, the center-line deflections, and 2θ, the angle of rotation of one end-stiffener with respect to the corresponding stiffener at the other end, were taken (Figs. 3 and 5). For the more shallow beams tested, θ attained values exceeding the range of the telescope-mirror apparatus. These values were obtained with acceptable accuracy by extrapolations of the plots of $L\theta$ versus center-deflections [(Figs. 8(b) through 13(b)].

Note that the values of θ obtained by the apparatus of Fig. 3 do not include any possible relative rotation of the flanges from shear deformations (and shear deformations were quite large for the shorter members). The apparatus was designed for this exclusion because the rotations of sections initially normal to the beam axis have primary and special significance for analytical purposes. If shear deformations should be desired for any reason, their magnitude may be calculated from these test results, as will be shown.

Results of Tests.—Quantitative results of these tests were presented in Tables 1 through 5 and Figs. 8 through 13.

Table 1 shows deviations in measured dimensions in inches for each specimen from the nominal dimensions listed in the standard manual.[15] Each value of t was obtained as the average of eight measurements, b of four measurements, and d and w of two measurements, half of these measurements being taken at each end of each specimen. Actual values of the first and second moments of the cross-sectional areas about the major bending axis were computed for each section, and the deviations and percentage deviations of these values from the nominal values are also shown in Table 1.

Table 2 shows values of yield stress, plastic strain, initial strain-hardening modulus, E_{sh}, rate of reduction of E_{sh} with respect to strain, and ultimate stress, as defined by Fig. 2, for each specimen, as determined from coupon tensile tests. The rate of reduction in the initial strain-hardening modulus, $\dfrac{\partial E_{sh}}{\partial \epsilon}$ or $\dfrac{\partial^2 \sigma}{\partial \epsilon^2}$, was determined as the average over a strain of 0.02 after initiation of strain-hardening. Values of the thicknesses of the rolled metal are

---

[15] "Steel Construction," American Inst. of Steel Constr., New York, N. Y., 1958.
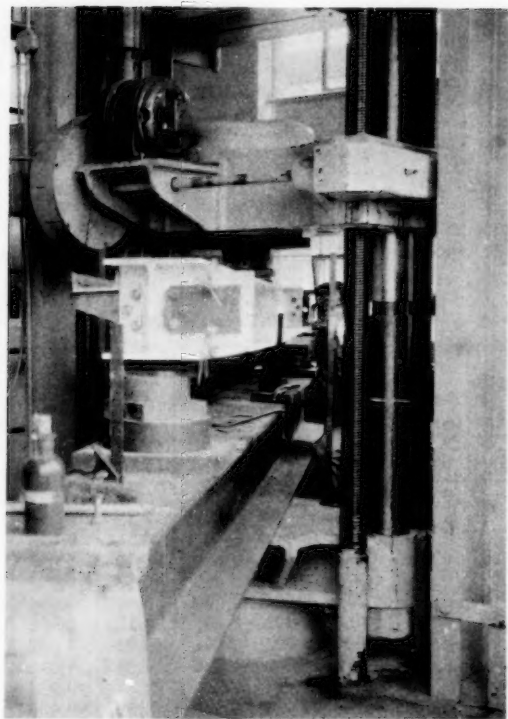
FIG. 4.—A TEST IN PROGRESS
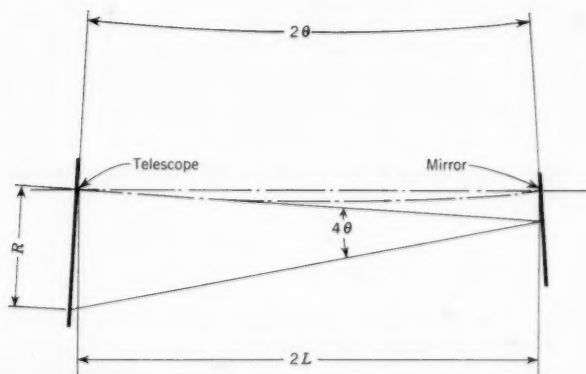
FIG. 5.—GEOMETRY OF ROTATION MEASUREMENT

also given in order that any correlation between thickness and yield point may be observed.

Table 3 shows three values of the fully plastic moment, the first, M_{po}, being the handbook[15] values based on nominal dimensions and a σ_y of 33 ksi, and the second a value based on the actual dimensions and actual flange yield stress

$$M_p = \int_{-d/2}^{+d/2} \sigma_{yf}\, dA \quad \ldots\ldots\ldots\ldots\ldots \quad (1)$$

in which σ_y is the tensile yield stress of the flange steel, A is the area, and d denotes the depth of the beam. The third value is a more accurate value, found

TABLE 1.—MEASURED VERSUS NOMINAL DIMENSIONS

Specimen Number (1)	Shape (2)	Length, L, in inches (3)	Δd, in inches (4)	Δb, in inches (5)	Δt, in inches (6)	$2\Delta w$, in inches (7)	ΔI_{xx} in.^{4} (8)	$\dfrac{\Delta I_{xx}}{I_{xx}}$ (9)	ΔZ cu in. (10)	$\dfrac{\Delta Z}{Z}$ (11)
1	12 B 14	–	0.080	−0.01	0.011	−0.008	3.01	0.034	0.18	0.010
2	12 B 14	–	0.095	−0.03	0.012	−0.008	3.14	0.036	0.70	0.040
3	12 B 14	–	0.075	−0.03	0.013	−0.0075	3.11	0.035	0.60	0.034
4	8 WF 20	22.36	−0.095	0.082	0.022	−0.010	1.70	0.025	0.51	0.027
5	8 WF 20	30.27	−0.110	0.042	0.026	−0.010	1.56	0.023	0.47	0.025
6	8 WF 20	42.10	−0.120	0.042	0.020	−0.009	0.60	0.009	0.24	0.013
7	5 WF 16	21.23	0.045	0.000	−0.003	−0.001	0.17	0.008	0.08	0.008
8	5 WF 16	28.73	0.040	−0.020	−0.003	−0.004	0.04	0.002	0.01	0.001
9	5 WF 16	39.96	0.055	0.000	−0.003	−0.003	0.26	0.012	0.10	0.010
10	10 B 19	17.06	0.030	−0.013	−0.019	0.005	−2.41	−0.025	−0.45	−0.021
11	10 B 19	23.07	0.000	−0.005	0.021	0.003	−3.38	−0.035	−0.65	−0.030
12	10 B 19	32.25	−0.020	−0.040	−0.021	0.001	−4.62	−0.048	−0.91	−0.042
13	12WF31	27.72	0.000	0.047	−0.011	0.020	−0.45	−0.002	0.14	0.003
14	12WF31	37.47	−0.015	0.040	−0.014	0.022	−2.26	−0.011	−0.12	−0.003
15	12WF31	52.21	−0.010	0.030	−0.009	0.015	−1.24	−0.005	−0.04	−0.001
16	12 B 14	16.96	0.060	0.065	0.009	0.018	6.54	0.074	0.93	0.053
17	12 B 14	22.82	0.045	0.085	0.006	0.014	5.31	0.060	0.81	0.046
18	12 B 14	31.72	0.020	0.077	0.000	0.007	2.40	0.027	0.49	0.028
19	8 WF 31	33.87	0.125	0.031	−0.001	0.007	4.18	0.038	0.83	0.027
20	8 WF 31	45.91	0 100	0.052	−0.002	0.005	3.44	0.031	0.69	0.023
21	8 WF 31	64.00	0.115	0.062	0.000	0.003	4.38	0.040	0.89	0.029

necessary for interpretation of these tests, which takes into account the actual yield stresses of both flange and web

$$M_p = \overset{\text{flange}}{\int \sigma_{yf}\, y\, dA} + \overset{\text{web}}{\int \sigma_{yw}\, dA} \quad \ldots\ldots\ldots\ldots \quad (2)$$

in which y refers to the vertical distance from the centroid of cross-sectional area. Table 3 then shows observed values of maximum moment, M_u, and a comparison of M_u with the three values of fully plastic moment defined by Figs. 1, 2 and 3.

TABLE 2.—COUPON TENSILE - TEST RESULTS

Specimen Number	Shape	Average t, in inches	Top Bottom } Flange					Web					
			σ_{yf}, in ksi	ϵ_p	E_{sh}, in ksi	$\dfrac{\partial E_{sh}}{\partial \epsilon}$, in ksi	σ_u, in ksi	w, in inches	σ_{yw}, in ksi	ϵ_p	E_{sh}, in ksi	$\dfrac{\partial E_{sh}}{\partial \epsilon}$, in ksi	σ_u, in ksi
(1)	(2)	(3)	(4)	(5)	(6)	(7)	(8)	(9)	(10)	(11)	(12)	(13)	(14)
1-3	12 B 14	0.236	44.5 / 44.2	0.0308 / 0.0278	470 / 450	-14,000 / -11,000	61.2 / 61.2	0.192	59.8	0.030	-	-	68.0
4-6	8 WF 20	0.401	42.25 / 39.75	0.0082 / 0.0042	750 / 650	-18,000 / -17,000	71.5 / 63.1	0.238	46.0	0.014	820	-25,000	67.8
7-9	5 WF 16	0.357	41.3 / 41.8	0.0193 / 0.0138	800 / 830	-23,000 / -23,000	65.8 / 66.9	0.237	56.5	0.0109	560	-15,000	71.8
10-12	10 B 19	0.374	38.3 / 37.7	0.0245 / 0.0196	610 / 580	18,000 / -15,000	57.7 / 58.4	0.253	40.5	0.0232	520	-12,000	59.4
13-15	12 WF 31	0.454	37.95 / 39.7	0.0099 / 0.0168	570 / 670	- 8,000 / -16,000	63.8 / 64.5	0.284	47.25	0.0175	680	-18,000	67.0
16-18	12 B 14	0.229	47.6 / 40.5	0.0198 / 0.0204	580 / 520	-20,000 / -14,000	62.4 / 57.7	0.213	54.3	0.0190	440	-13,000	65.0
19-21	8 WF 31	0.431	40.6 / 41.8	0.0174 / 0.0186	760 / 750	-21,000 / -21,000	67.5 / 67.5	0.292	44.6	0.0220	790	-24,000	68.0

TABLE 3.—PLASTIC MOMENTS AND TEST ULTIMATE MOMENT

Specimen Number	Shape	M_{po} (y = 33 ksi), in kip-in.	Average y_f, in ksi	Z, in cu in.	M_{pl} (Eq. 1), in kip-in.	Web y_w, in ksi	M_p (Eq. 2), in kip-in.	$\frac{M_p}{M_{po}}$	$\frac{M_p}{M_{pl}}$	Test M_u, in kip-in.	Test $\frac{M_u}{M_p}$	Test $\frac{M_u}{M_{po}}$	Test $\frac{M_u}{M_{pl}}$
(1)	(2)	(3)	(4)	(5)	(6)	(7)	(8)	(9)	(10)	(11)	(12)	(13)	(14)
1	12 B 14	577	44.35	17.7	784	59.8	891	1.544	1.137	904	1.015	1.153	1.568
2	12 B 14	577	44.35	18.2	807	59.8	912	1.581	1.130	901	0.988	1.117	1.562
3	12 B 14	577	44.35	18.1	802	59.8	909	1.576	1.135	902	0.992	1.125	1.563
4	8 WF 20	630	41.0	19.6	804	46.0	820	1.302	1.020	1125	1.372	1.400	1.785
5	8 WF 20	630	41.0	19.6	804	46.0	820	1.302	1.020	1094	1.336	1.362	1.737
6	8 WF 20	630	41.0	19.3	792	46.0	806	1.279	1.018	1053	1.308	1.331	1.671
7	5 B 16	317	41.6	9.7	404	56.5	420	1.326	1.040	618	1.470	1.528	1.960
8	5 B 16	317	41.6	9.6	400	56.5	416	1.314	1.042	593	1.425	1.483	1.880
9	5 B 16	317	41.6	9.7	404	56.5	420	1.326	1.040	588	1.398	1.455	1.864
10	10 B 19	712	38.0	21.2	805	40.5	819	1.150	1.018	1035	1.263	1.285	1.455
11	10 B 19	712	38.0	20.95	796	40.5	810	1.138	1.019	1088	1.344	1.367	1.529
12	10 B 19	712	38.0	20.7	786	40.5	800	1.124	1.019	1030	1.287	1.310	1.447
13	12 WF 31	1450	38.8	44.0	1709	47.2	1783	1.230	1.044	2197	1.288	1.345	1.515
14	12 WF 31	1450	38.8	43.8	1700	47.2	1774	1.223	1.045	2205	1.242	1.297	1.521
15	12 WF 31	1450	38.8	43.9	1705	47.2	1779	1.227	1.044	2246	1.263	1.318	1.549
16	12 B 14	577	44.0	18.4	810	54.3	882	1.529	1.089	911	1.033	1.125	1.580
17	12 B 14	577	44.0	18.3	805	54.3	876	1.518	1.089	861	0.984	1.070	1.490
18	12 B 14	577	44.0	18.0	793	54.3	864	1.497	1.090	872	1.009	1.100	1.514
19	8 WF 31	1002	41.2	31.2	1284	44.6	1297	1.294	1.009	1520	1.172	1.183	1.517
20	8 WF 31	1002	41.2	31.0	1280	44.6	1293	1.290	1.010	1446	1.118	1.129	1.443
21	8 WF 31	1002	41.2	41.2	1288	44.6	1301	1.298	1.009	1366	1.049	1.060	1.363

Table 4 presents values of the dimensional parameters L/b, b/t, and d/w, as measured for each specimen, as well as the observed value of θ, θ_u, at the instant of attainment of maximum moment. The observed average outer-fiber strain in length L at this same instant, ϵ_{avg}, was then calculated by the geometric relationship

$$\epsilon_{avg} = \frac{\theta_u\, d}{2\, L} \quad \dots\dots\dots\dots\dots\dots \quad (3)$$

Table 4 next presents the results of a solution to the problem of the computation of values of M_u values observed in the flexural tests, using only dimensional and stress-strain curve data. For this solution it was first found that the observed values ϵ_{avg} were approximated by values calculated by the expression

$$\text{calculated } \epsilon_{avg} = \frac{256}{\left(\frac{b}{t}\right)^2 \left(\frac{L}{b}\right)^{3/4} \frac{d}{w}} \quad \dots\dots\dots\dots \quad (4)$$

in which w is the thickness of the web. The maximum moment was then calculated by assuming a value of uniform stress in the flange, $\sigma_{f5\epsilon}$, obtained from the flange tensile stress-strain curves for a strain of $5\epsilon_{avg}$ (using calculated values of ϵ_{avg}) and assuming a value of uniform stress in the web of σ_{yw}

$$M_u = \overset{\text{flange}}{\int \sigma_{f5\epsilon}\, y\, dA} + \overset{\text{web}}{\int \sigma_{yw}\, y\, dA} \quad \dots\dots\dots\dots \quad (5)$$

Values of experimental and calculated M_u are given and compared in Table 4.

A reasonable moment-curvature diagram for a steel rolled section is shown in Fig. 6, in which the known quantities, besides the values of M_p and M_u of Eqs. (2) and (5), are:

$$M_e = \sigma_{yf} \frac{I}{c} \quad \dots\dots\dots\dots\dots\dots \quad (6a)$$

$$\phi_e = \frac{2\, \epsilon_e}{d} = \frac{2\, \sigma_{yf}}{d\, E} \quad \dots\dots\dots\dots\dots \quad (6b)$$

and

$$\phi_p = \frac{2\, \epsilon_p}{d} \quad \dots\dots\dots\dots\dots\dots \quad (6c)$$

The unknown quantity, ϕ_u, was assumed to be given by an expression of the form

$$\phi_u = \frac{2\, v\, \epsilon_{avg}}{d} \quad \dots\dots\dots\dots\dots\dots \quad (7)$$

The maximum other fiber strain of this expression, $v\, \epsilon_{avg}$, was determined

TABLE 4.—CALCULATION OF MAXIMUM MOMENT

| Specimen Number	Size	Length, L, in inches	$\frac{L}{b}$	$\frac{b}{t}$	$\frac{d}{w}$	Test Q_u x 10^{-3}	Test avg. x 10^{-3}	Calc. ϵ avg. Eq. 4	Calc. $\frac{\epsilon \text{ avg.}}{\epsilon \text{ avg. Test}}$	Test M_u kip-in.	Calc. M_u kip-in.	Calc. $\frac{M_u}{M_u \text{ Test}}$
(1)	(2)	(3)	(4)	(5)	(6)	(7)	(8)	(9)	(10)	(11)	(12)	(13)
1	12 B 14	—	5.75	16.85	62.5	8.45	2.23	3.88	1.74	904	893	0.99
2	12 B 14	—	4.27	16.68	62.5	20.17	7.19	4.92	0.69	901	914	1.02
3	12 B 14	—	8.05	16.60	62.5	18.72	4.06	3.09	0.76	902	910	1.01
4	8 WF 20	22.36	4.17	13.36	33.8	95.15	16.05	14.60	0.91	1125.0	1140	1.01
5	8 WF 20	30.27	5.70	13.16	33.8	86.9	11.50	11.84	1.03	1094.0	1124	1.03
6	8 WF 20	42.10	7.92	13.35	33.6	92.0	8.78	9.07	1.04	1053.5	1067	1.01
7	5 WF 16	21.23	4.24	14.00	21.1	192.1	22.81	20.85	0.91	617.7	591	0.96
8	5 WF 16	28.73	5.75	13.97	21.3	162.5	14.25	16.54	1.09	593.0	572	0.97
9	5 WF 16	39.96	7.99	14.00	21.3	198.5	12.58	12.82	1.02	588.0	570	0.97
10	10 B 19	17.06	4.25	10.70	40.3	56.8	16.40	18.62	1.13	1034.7	1037	1.00
11	10 B 19	23.07	5.75	10.78	40.5	68.2	15.13	14.60	0.96	1088.5	1012	0.93
12	10 B 19	32.25	8.10	10.67	40.7	54.4	9.01	11.52	1.28	1030.0	969	0.94
13	12 WF 31	27.72	4.21	14.48	42.4	44.7	9.74	9.76	1.00	2196.8	2271	1.04
14	12 WF 31	37.47	5.70	14.58	42.1	45.7	7.36	7.75	1.05	2205.0	2171	0.99
15	12 WF 31	52.21	7.95	14.40	43.1	69.5	8.03	6.01	0.75	2246.0	2061	0.92
16	12 B 14	16.96	4.19	17.30	54.9	20.5	7.25	5.28	0.73	911.0	914	1.00
17	12 B 14	22.82	5.62	17.62	55.9	14.14	3.70	4.02	1.08	861.5	877	1.02
18	12 B 14	31.72	7.84	18.05	57.7	13.58	2.56	2.89	1.13	872.3	864	0.99
19	8 WF 31	33.87	4.21	18.60	27.55	67.25	8.05	9.10	1.13	1520.5	1657	1.09
20	8 WF 31	45.91	5.20	18.68	27.62	56.0	6.57	7.17	1.09	1446.0	1560	1.08
21	8 WF 31	64.00	7.93	18.60	27.87	90.2	6.31	5.57	0.83	1366.0	1466	1.07
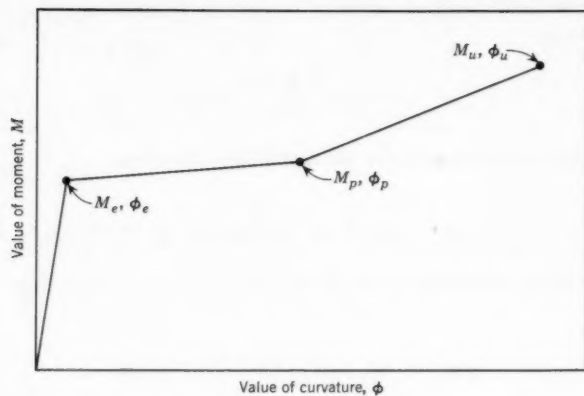
FIG. 6.—ASSUMED MOMENT CURVATURE DIAGRAM
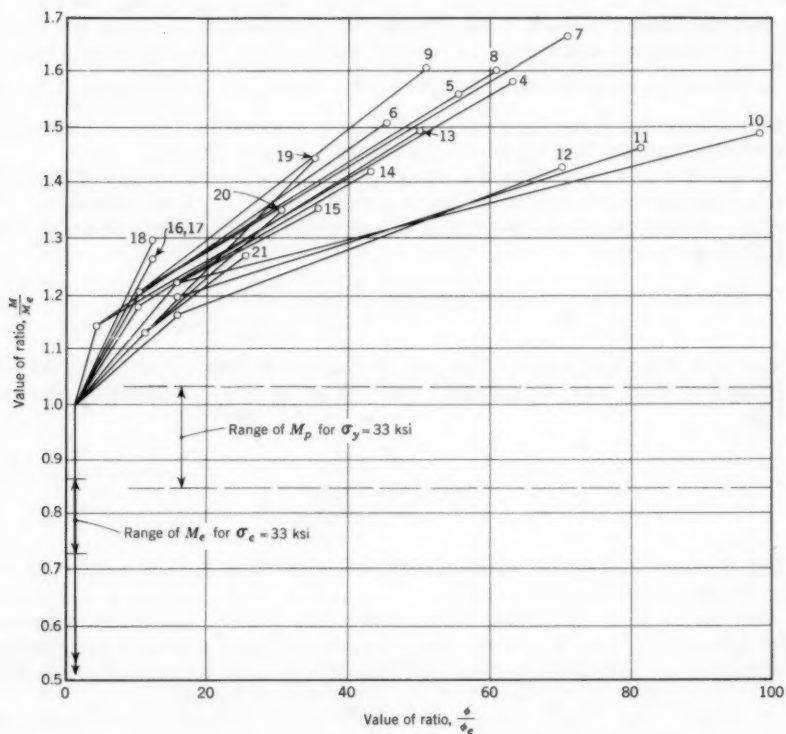
FIG. 7.—CALCULATED MOMENT CURVATURE RELATIONSHIPS

by equating the total bending angle at maximum moment given by previously determined ϵ_{avg}

$$\theta_u = \frac{2 \, L \, \epsilon_{avg}}{d} \quad \ldots\ldots\ldots\ldots\ldots \quad (8)$$

to the same angle as given by the assumed M-ϕ diagram.

$$\theta_u = A_m \frac{L}{M_u} \quad \ldots\ldots\ldots\ldots\ldots \quad (9)$$

in which A_m is the abscissal area of the M-ϕ diagram. Equating and solving for v yields

$$v = \frac{2 \, M_u - \left(M_p - M_e\right) \dfrac{\epsilon_p + \epsilon_e}{\epsilon_{avg}} - M_e \dfrac{\epsilon_p}{\epsilon_{avg}}}{M_u - M_p} - \frac{\epsilon_p}{\epsilon_{avg}} \quad \ldots \quad (10)$$

It should be noted that the $5\epsilon_{avg}$ used to obtain M_u is merely an effective strain that gives the effective value of a tensile stress to give M_u. Because of the buckling always present at M_u, the actual compressive stresses are higher but their effect is lessened by their axial inclinations. Furthermore, even if the actual strain were known at M_u, it would not be equal to $\dfrac{\phi_u \, d}{2}$ because of the further shortening of the compression flange from buckling. Both of these considerations indicate that v should be a variable greater than 5.

Values of v as computed by Eq. 10 are given in the fourth column of Table 5. (Values for specimens for which M_u is nearly equal to M_p are omitted as being trivial). It was then found that these values could be approximated by the empirical expression

$$v = 0.772 \left(\frac{L}{b}\right)^{1/4} \left(\frac{d}{w}\right)^{1/2} \quad \ldots\ldots\ldots\ldots \quad (11)$$

Values of v from this expression are shown in the fifth column of Table 5.

It follows from Eqs. 4, 7, and 11 that the value of ϕ_u for the M-ϕ diagram will be

$$\phi_u = \frac{396}{\left(\dfrac{b}{t}\right)^2 \left(\dfrac{L}{b}\right)^{1/2} \left(\dfrac{d}{w}\right)^{1/2} d} \quad \ldots\ldots\ldots\ldots \quad (12)$$

The moment-curvature relationships defined by Eqs. 2, 5, 6, and 12 for the test specimens are shown in Fig. 7.

With the moment-curvature relationship thus defined, the moment versus angle relationship for any rolled steel flexural specimen may now be predicted theoretically. Theoretical curves calculated for all test specimens are plotted on Figs. 8 through 13, together with the experimental curves.

Of course, θ for these curves was obtained by integrating curvatures as given by the M-ϕ relationship of Fig. 5 along the length L, resulting in the fol-

lowing expressions:

(a) for $M_e < M_m < M_p$:

$$\theta = \frac{L}{d}\left[\epsilon_e + \frac{1}{2\,M_m}\left\{-\,M_e\,\epsilon_e + \left(M_m - M_e\right)^2 \frac{\epsilon_p - \epsilon_e}{M_p - M_e}\right\}\right] \quad \ldots \ldots (13)$$

(b) for $M_p < M_m < M_u$:

$$\theta = \frac{L}{d}\left[\epsilon_p + \frac{1}{2\,M_m}\left\{M_p\,\epsilon_e - \left(M_e + M_p\right)\epsilon_p + \left(M_m - M_p\right)^2 \frac{\epsilon_u - \epsilon_p}{M_u - M_p}\right\}\right] \ldots (14)$$

in which ϵ_u is a (fictitious) strain defined as

$$\epsilon_u = \frac{\phi_u\,d}{2} \quad \ldots \ldots \ldots \ldots \ldots \ldots (15)$$

An unexpected characteristic of the moment-curvature relationships shown in Fig. 7 is that the two lines defining the post-elastic portion are concave

TABLE 5.—CALCULATION OF ϕ_m

Specimen Number (1)	Size (2)	$M_{E.\ L.}$ (3)	v Eq. 10 (4)	v Eq. 11 (5)	ϕ_u Eq. 12 (6)
1	12 B 14	674			
2	12 B 14	675			
3	12 B 14	675			
4	8 WF 20	721	6.32	6.43	23.35
5	8 WF 20	723	6.27	6.96	20.55
6	8 WF 20	714	6.76	7.55	17.05
7	5 WF 16	354	5.65	5.11	42.2
8	5 WF 16	351	5.71	5.53	36.4
9	5 WF 16	356	5.48	6.01	31.0
10	10 B 19	694	7.40	7.08	25.7
11	10 B 19	689	7.26	7.63	21.75
12	10 B 19	681	7.68	8.36	18.80
13	12 WF 31	1528	6.74	7.25	11.80
14	12 WF 31	1519	7.34	7.78	10.00
15	12 WF 31	1525	9.02	8.55	8.16
16	12 B 14	696		8.18	
17	12 B 14	688		8.91	
18	12 B 14	669		9.91	
19	8 WF 31	1155	5.90	5.85	13.11
20	8 WF 31	1150	6.88	6.29	11.14
21	8 WF 31	1160	9.81	6.88	9.46

downward rather than upward as assumed in Fig. 6 and as strain hardening would lead one to expect. Thus, the point of intersection of these lines, $\left(M_p, \phi_p\right)$; has less significance than anticipated, suggesting that a parabolic or single-line representation of the post-elastic portion that ignores this point might be equally effective. A preliminary trial of a single-line representation showed that it was less effective in following actual test curves for three of the
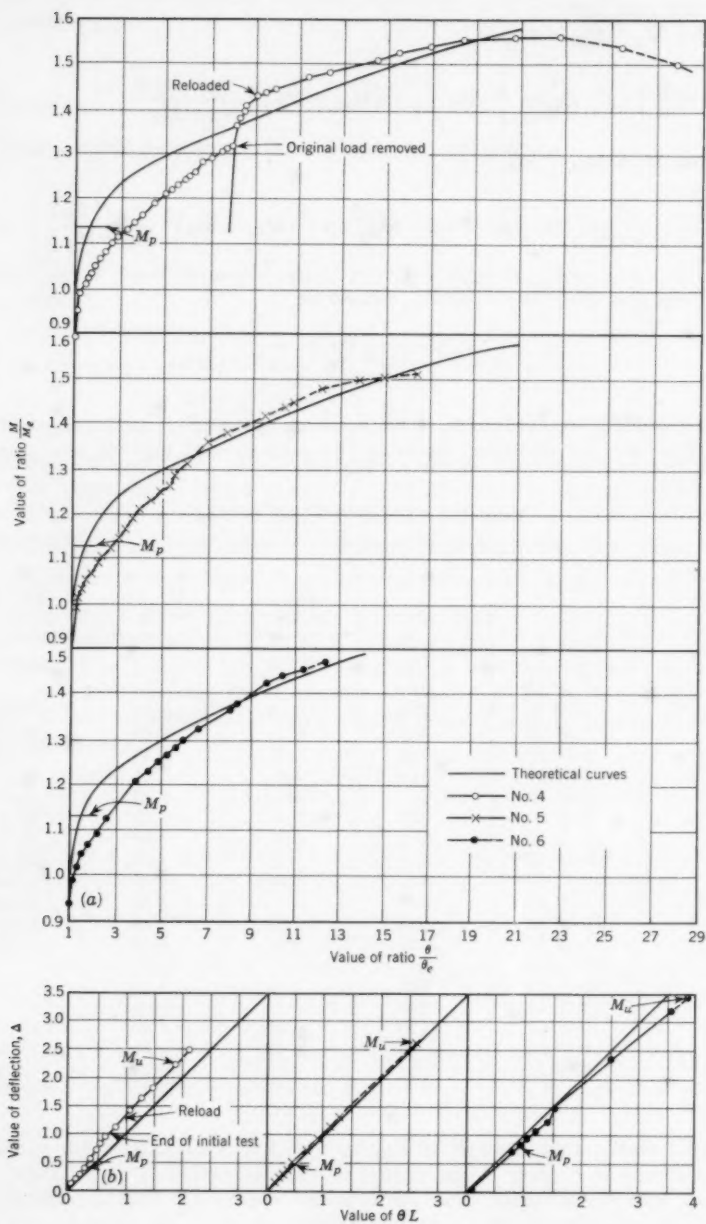
FIG. 8.—TEST RESULTS, BEAMS 4 - 6, 8 W 20
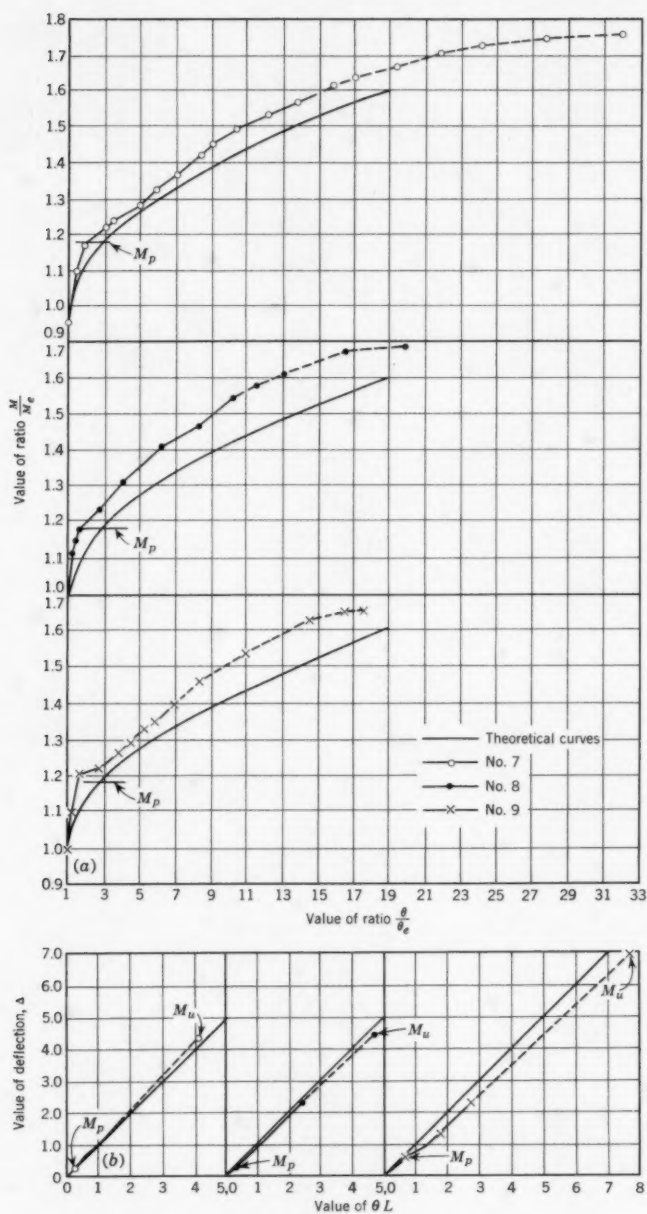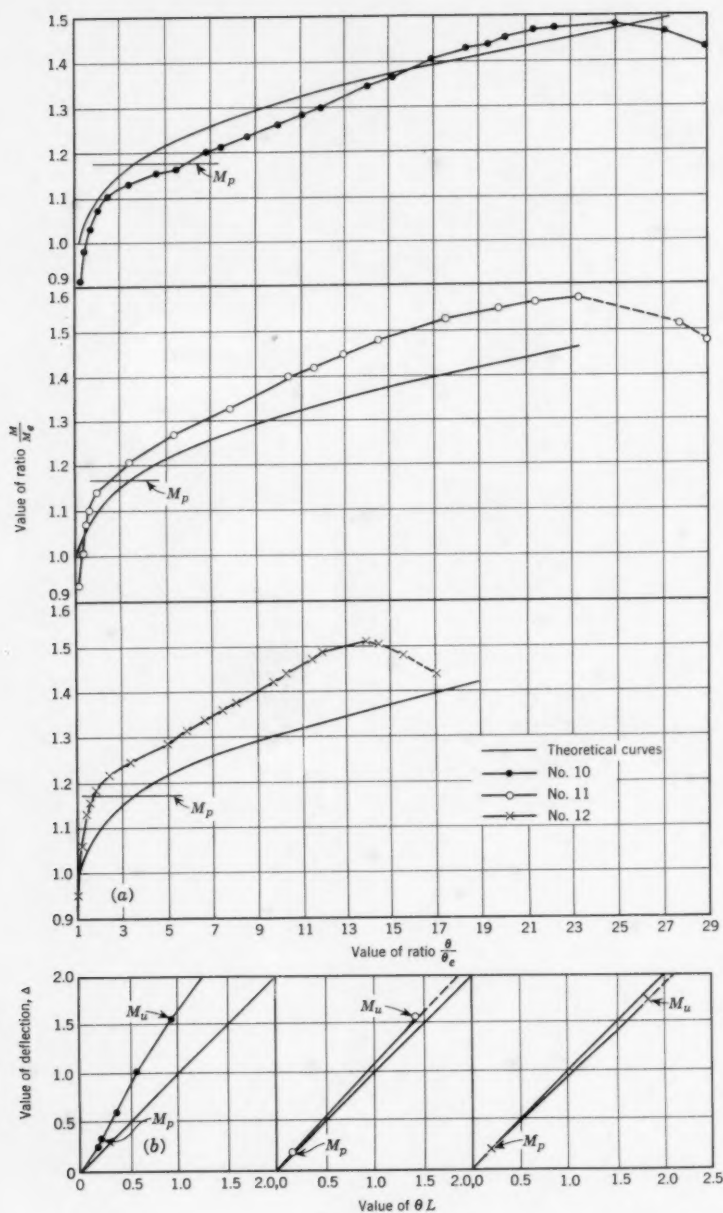
FIG. 9.—TEST RESULTS, BEAMS 7 - 9, 5 B 16

FIG. 10.—TEST RESULTS, BEAMS 10 - 12, 10 B 19
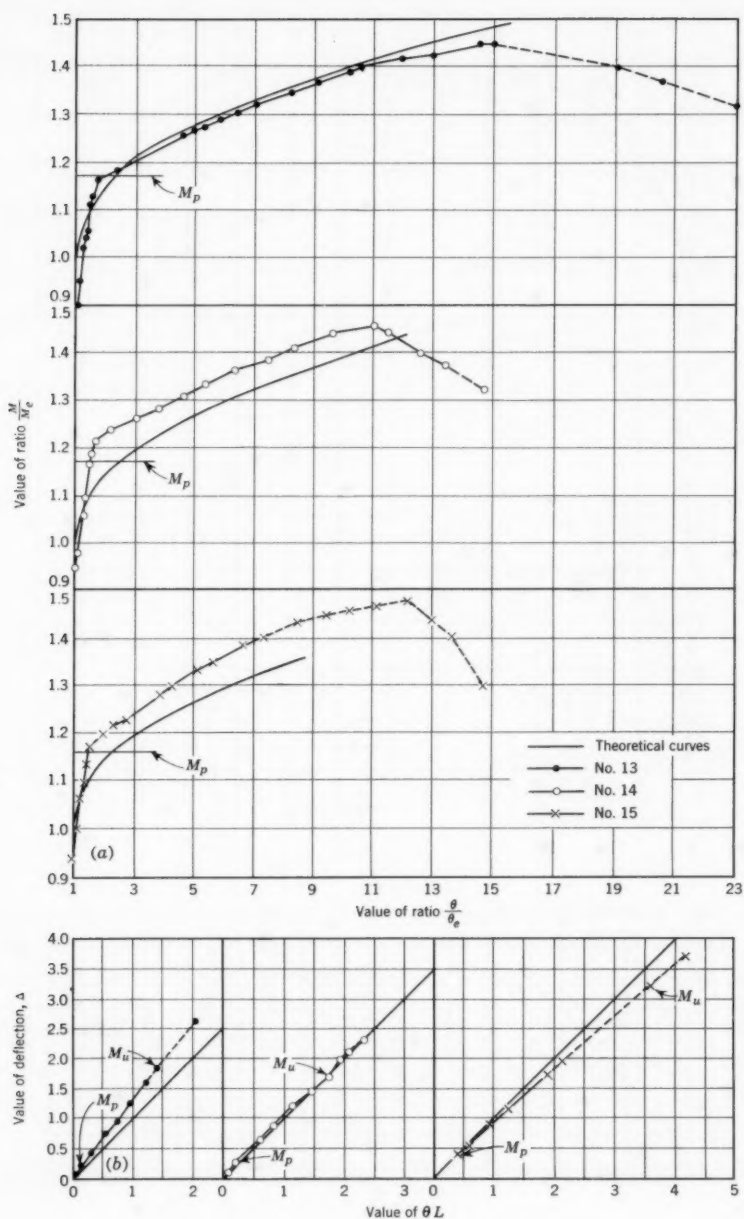
FIG. 11.—TEST RESULTS, BEAMS 13 - 15, 12 W 31
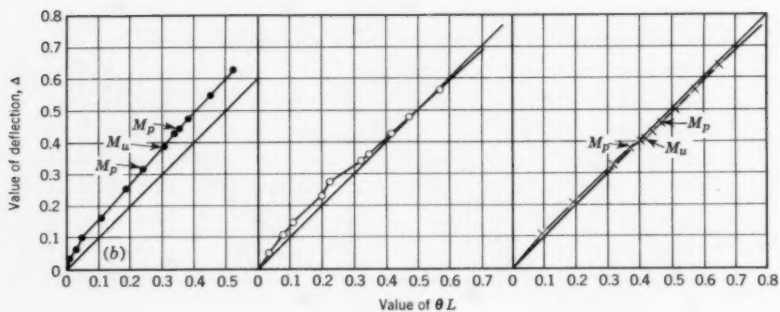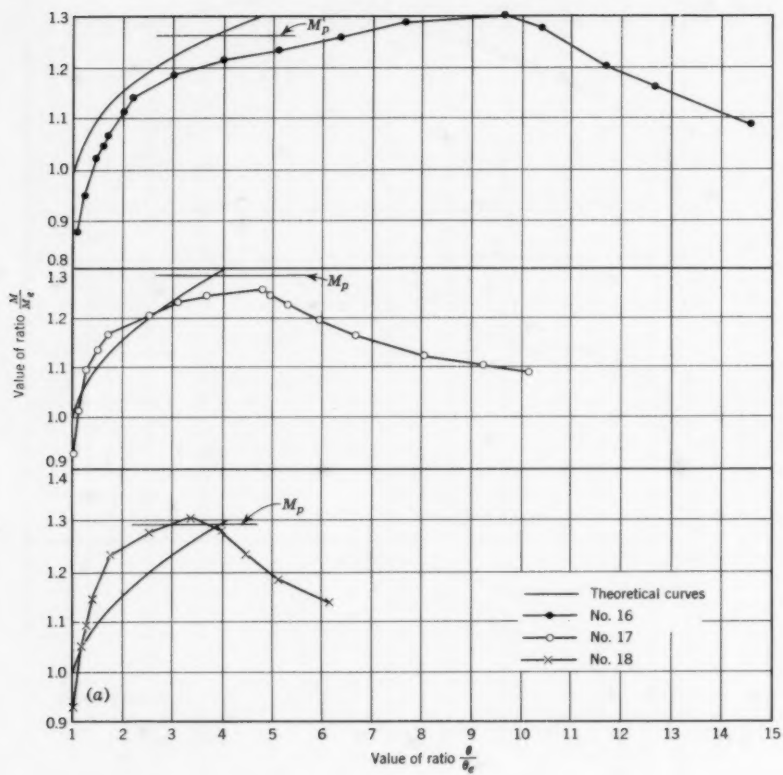
FIG. 12.—TEST RESULTS, BEAMS 16 – 18, 12 B 14
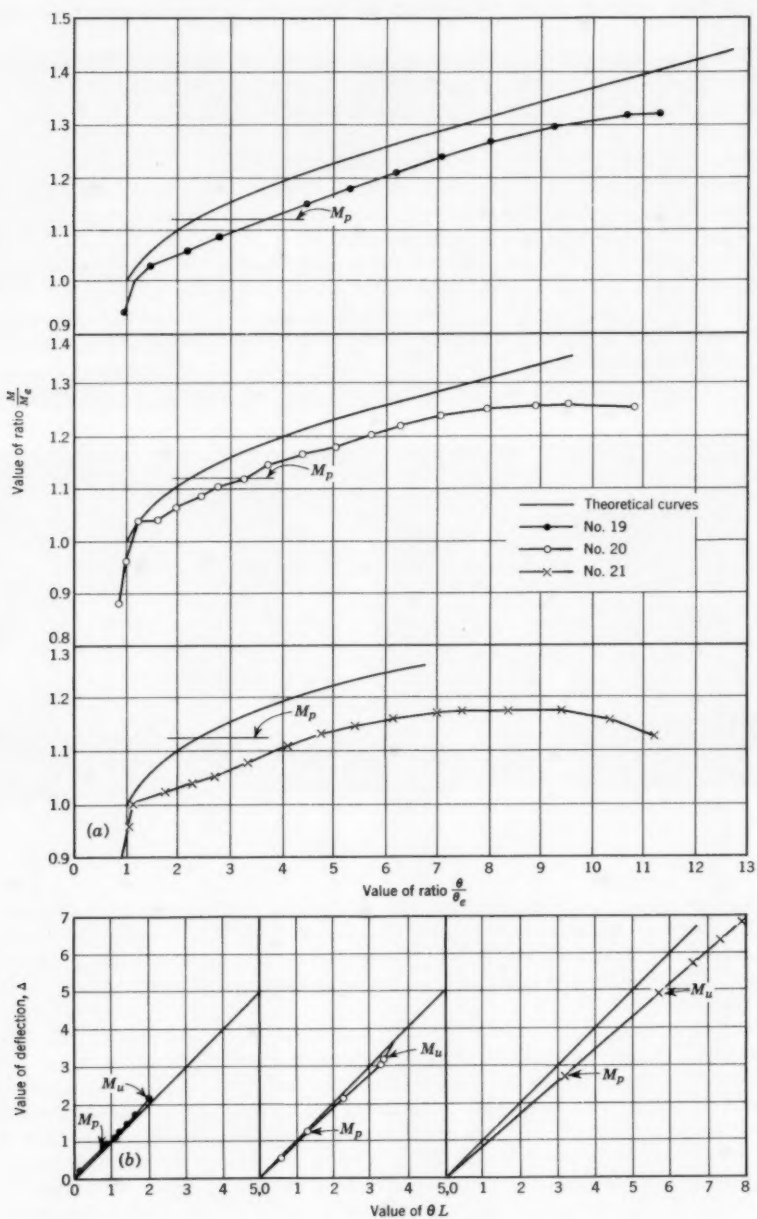
FIG. 13.—TEST RESULTS, BEAMS 19 - 21, 8 WF 31

test groups, approximately equivalent for one group, and more effective for two groups.

One of the test groups, Beams 10, 11, and 12, are shown in post-test condition in Figs. 14 through 17. The decreasing importance of shear deformations with increasing L is apparent from the yield patterns delineated by the white-wash.

Centroid of Bending Angle and Deflection from Shear.—As stated previously, the plots of θ L versus center deflection, Δ, Figs. 8 through 13, were extrapolated as shown by the broken lines to obtain those high values of θ that exceeded the range of the telescope-mirror system.

It is interesting to note that with the simple method to be presented these plots may also be used to obtain two other quantities of potential future importance: K_1, the ratio of $\overline{X}$, the centroidal distance of θ from the near reaction of the beam, to L, and Δ_s, the component of Δ, the total deflection, caused by shearing deformations.
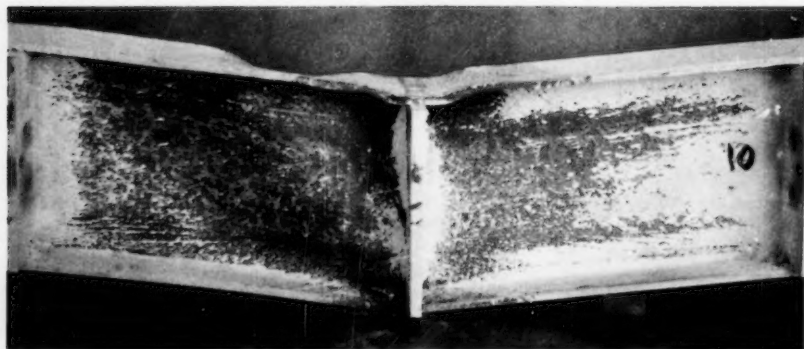
FIG. 14.—BEAM 10 AFTER TEST

Beyond the work by William J. Hall, M. ASCE, and Nathan M. Newmark, F. ASCE, on shear deflection of two continuous beams, little is known about these quantities in the post-elastic range. However, their actual calculation and analysis will be deferred as not being essential to the present investigation of flexural behavior.

It is obvious that if the total bending angle were concentrated at the center point ($K_1 = 1$) and the shear deflection were zero, curves of θ L versus Δ would simply be straight lines through the origin, inclined 45°, and shown on the graphs for reference purposes. Furthermore, values of K_1 less than one will cause the plotted curve to be in a clockwise position with respect to this line, whereas shear deflections would cause it to be in a counter-clockwise position. The position of the curve with shear deflection neglected may be obtained quite accurately for the longest beam of each test group because all shear deflections for this beam are in the elastic range and relatively small, allowing computa-

FIG. 17.—TOP FLANGE OF BEAM 12 AFTER TEST
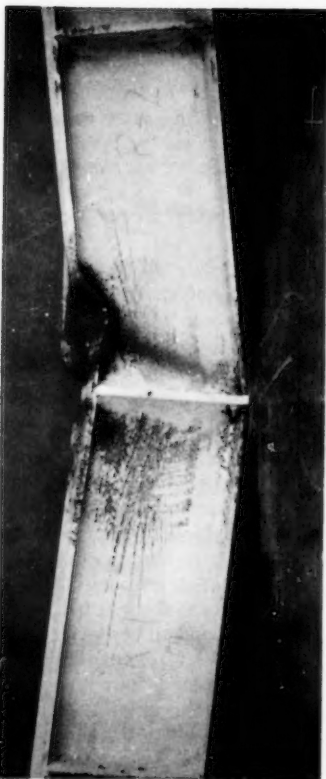
FIG. 15.—BEAM 11 AFTER TEST
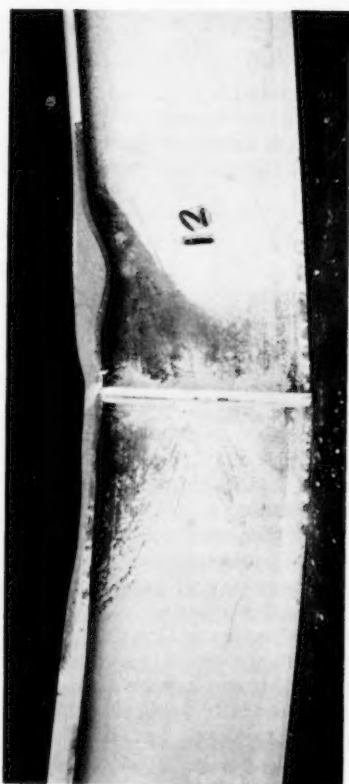
FIG. 16.—ELEVATION, BEAM 12 AFTER TEST

tion of shear deflections with sufficient accuracy by the simple elastic theory

$$\Delta_s = \frac{V L}{A_{web}} G \quad \dots \dots \dots \dots \dots \quad (16)$$

in which A_{web} is the area of the web, and G the shearing modulus of elasticity. For any center moment, M_m, the bending component of deflection for this beam will thus be

$$\Delta_b = \Delta - \Delta_s = \Delta - \frac{M_m}{A_{web} G} \quad \dots \dots \dots \dots \quad (17)$$

Then, because

$$\Delta_b = K_1 L \theta \quad \dots \dots \dots \dots \dots \quad (18)$$

the following expression for K_1 may be written

$$K_1 = \frac{\Delta - \dfrac{M_m}{A_{web} G}}{\theta L} \quad \dots \dots \dots \dots \quad (19)$$

It is reasonable to assume that, for two specimens identical except for length L, loaded so as to produce the same center-line moments M_m, the values of K_1 will be practically equal. With this assumption, using the shorter-beam values of Δ and θL corresponding to M_m, Δ_s may be calculated for the shorter beam

$$\Delta_s = \Delta - K_1 \theta L \quad \dots \dots \dots \dots \dots \quad (20)$$

The results of such a computation for loads corresponding to a maximum moment of 2140 kip-in. on test beams 13 and 15 are shown in Fig. 18.

LIMITATIONS OF TESTS AND RESULTS

The sections chosen for these tests generally had more slender elements and higher b/t and d/w ratios than rolled sections usually used, because investigation of instability was a primary objective. Also, the factors of cost and ease-of-handling encouraged the use of smaller, lighter sections. Although it is believed that the dimensional parameters used for the derived expressions provide the basis for their validity for heavier sections, it is obvious that the degree of accuracy will probably not be as high as for the sections used for the derivation. Contributing to this inaccuracy are the following factors that vary with size: Dimensional variations, residual stresses, yield and ultimate stresses, and carbon content (which is increased with size to prevent excessive lowering of yield and ultimate stresses). Of the six sections tested, four could be used for plastically designed continuous building framing under existing (1961) standards;[2] two are disqualified by b/t ratios exceeding 17 (8 ᵂᶠ 31 and joist 12B14).

All sections tested had laterally unsupported lengths, L_1, equal to L_2, where $L_2 = M_m/V$ (that is, they had lateral supports at points of zero moment and

maximum moment). Where L_1 and L_2 are not equal, obviously an intermediate value of effective length should be used in the derived expressions. Because each of these length has a distinctive effect on the M-ϕ relationship, it must remain for further tests to define, and distinguish between, these effects.

Further tests are also needed for values of L_1 nearer the American Institute of Steel Construction (AISC) limit of $L_1 = 13b$, and for values of L_2, between approximately 10b and infinity. As stated before, the post-elastic behavior of wide flange sections for the limiting case of constant moment $\left(L_2 \text{ equals in-} \right.$ finity$\left.\right)$ has been the subject of many investigations. Almost all investigators have agreed that for such a condition the fully plastic moment is the effective
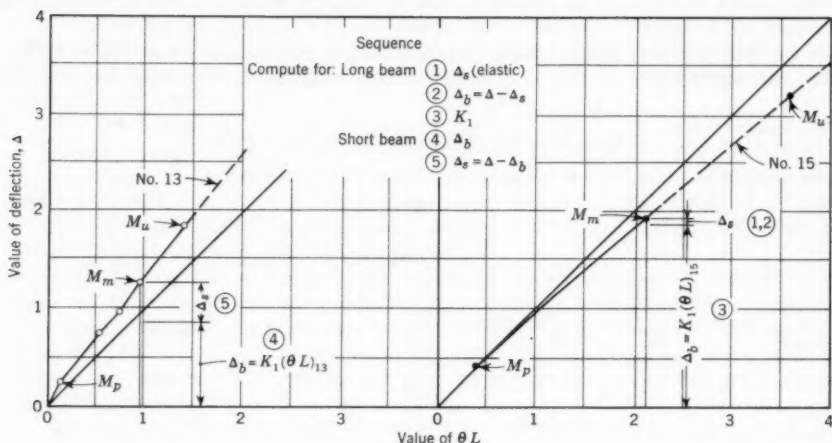
FIG. 18.—TYPICAL COMPUTATION OF SHEAR DEFLECTION

ultimate moment. Although each investigation has provided information on deformations, little is known about the M-ϕ relationship in the strain-hardening range or the limiting values of strain for b/t ratios of less than 15.

COMPARISON WITH OTHER TEST RESULTS

A search was made for published test results by others to which the results of this investigation could be applied. Although there have been many post-elastic tests of rolled steel beams, only two have been discovered for which: (a) web and flange tensile stress-strain curves were given, (b) ultimate moment was not attained first at a length of constant moment, (c) if statically indeterminate, shear deformations were not in the plastic range and thus excessive, and (d) deformations were continued up to and beyond the point of ultimate load, thus determining ultimate load.
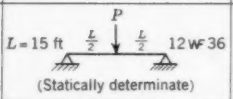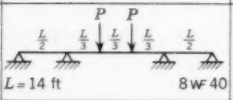
Results for the two tests[4,6] that evidently satisfied these requirements (both performed at the Fritz Laboratory of Lehigh University, Bethlehem, Pa.) are compared in Table 6 with the results obtained using the M-ϕ relationships of this paper. Maximum loads as given by the elastic and fully plastic distribution

of stresses at sections of maximum moment are also given. For the statically indeterminate beam B3 the method used for calculating the distribution of moments is significant and is specified. (For analysis of statically indeterminate structures by use of M-ϕ diagrams, an elasti-plastic method such as those previously presented[16,17] by the writer must be used). The theoretical deflections are purely flexural, whereas the test deflections in total.

For beam T5 the maximum load calculated[4] from the M-ϕ diagram is somewhat lower than the test maximum load, whereas for beam B3 it is somewhat higher. However, the test report[6] for B3 merely states that 56.3 kips was "maximum load carried," and load-deformation data is not given for loads exceeding 49 kips. Because the theoretical flexural deflection at which ultimate load occurs is 14 in., it is probable that this test was not continued to ultimate load.

The deflection values of Table 6 simultaneously signify an important limitation and application of the M-ϕ relationships diagrams presented herein. In

TABLE 6.—APPLICATION TO OTHERS' TESTS

Source[a]	Test beam		Maximum P, in kips, using:				Δ at P, in inches, for maximum P	
			$M_{max} = M_e$	(nominal) $M_{max} = M_p$	M-ϕ diagram	Test	M-ϕ diagram	Test
Driscoll and Beedle[4]	T5	$L = 15$ ft, P, $\frac{L}{2}$, $\frac{L}{2}$, 12 WF 36 (Statically determinate)	42.0	47.2		51.4	55.6	4.2	3.7
Yang, Beedle, and Johnston[6]	B3	$\frac{L}{2}$ $\frac{L}{3}$ $\frac{L}{3}$ $\frac{L}{3}$ $\frac{L}{2}$, P P, $L = 14$ ft, 8 WF 40	47.5	53.2	53.2	61.7	56.3(+?)	14.1	
		Distribution of moments ⟶	Elastic	Elastic	Rigid-plastic	Elasto-plastic	Test	Elasto-plastic	Test

[a] Superscripts refer to corresponding footnotes in text

practice, most structures will probably have lost their effectiveness because of excessive deflection before ultimate load is reached. However, it is only with use of M-ϕ relationships that deflections in the ultimate load range may be calculated. It should be added that deflections of this magnitude cause changes in the shape of the structure which, unless accounted for, lead to gross analytical error, especially for two-and three-dimensional structures.

CONCLUSIONS

For the relatively light-weight sections used in this test program the following conclusions can be made:

16 "Elasti-Plastic Design of Single-Span Beams and Frames," by H. A. Sawyer, Jr., Proc. Paper No. 851, ASCE, Vol. 81, December, 1955, and Proc. Paper No. 1156, ASCE, Vol. 83, No. ST1, January, 1957.

17 "Elasti-Plastic Analysis of Continuous Frames and Beams," by L. P. Johnson, Jr. and H. A. Sawyer, Jr., Proc. Paper No. 1879, ASCE, Vol. 84, No. ST8, December, 1958, p. 114.

1. For twenty-one sections measured, the variation in "I" with respect to nominal handbook values ranged up to 7.4% with a standard deviation of 3.3%. The variation in first moment "Z" with respect to nominal handbook values ranged up to 5.3% with a standard deviation of 2.7%.

2. The excess of σ_{yf} over the American Society for Testing Materials (ASTM) minimum of 33 ksi ranged from 4.7 to 14.6 ksi, the average excess being 8.3 ksi, or 25%. This excess causes a similar excess of fully plastic moment, M_{p1}, over the nominal fully plastic moment, M_{po}, calculated using $\sigma_y = 33$ ksi and the nominal dimensions. The excess of σ_{yw} over the ASTM minimum of 33 ksi ranged from 7.5 to 26.8 ksi, the average being 16.8 ksi, or 51%. There was some indication that these excesses tend to decrease as the thickness of the element increases.

3. The excess of σ_{yw} over σ_{yf} was always positive, ranging from 8.3% to 36%, with an average excess of 20.6%. This excess caused an increase in fully plastic moment with respect to M_{p1} of from 0.9% to 13.7%, the average increase being 5.1%.

4. Combining the excesses of conclusions 2 and 3, the actual calculated M_p exceeded M_{po} by from 12.5% to 58%, the average excess being 34.2%.

5. The initial modulus of strain-hardening for the tensile coupons tested ranged from 440 to 830 ksi., with an average of 640 ksi. The rate of change of the strain-hardening modulus with respect to strain ranged from -8000 to -25,000 ksi, with an average of -17,300 ksi.

6. For eighteen test beams, the actual M_u exceeded M_{p1} by from 6.0% to 53%, the average excess being 28.5%. Actual M_u exceeded M_{p1} for the twelve test beams which would be acceptable for plastic design by AISC standards by from 28.5% to 53%, the average excess being 37.3%. Actual M_u exceeded M_{po}, based on the nominal dimensions and 33 ksi, by from 36.3% to 96%, the average excess being 59%.

7. For these tests of flexural strength, the strengthening effects of an increasing shear and moment-gradient outweighed the weakening effects, contrary to some theoretical predictions.[14] Thus, there are corresponding increases in actual ultimate flexural strength and rotation capacity of those "plastic hinges" in a rigid-plastically designed structure that have the least theoretical plastic-rotation capacity.[16] This fact is strongly reassuring to users of rigid-plastic design methods.

8. The ultimate moment, M_u, may be calcualted from the cross-sectional dimensions and the tensile stress-strain curves for the eighteen specimens tested, using Eqs. 4 and 5, to an accuracy represented by a standard deviation of 4.7%.

9. M-ϕ relationships based on Eqs. 5, 6, and 12, and Fig. 6 represented the relationship between moment and total bending angle for the specimens tested fairly closely for all values of moment up to M_u.

10. These M-ϕ relationships predicted ultimate loads and ultimate-load deflection in fair agreement with the results of one test of a simple beam and one of a continuous beam, both performed by others.[4,6]

11. Excessive deflection at ultimate load will probably prevent the utilization of the ultimate strength for many steel structures. However, M-ϕ relationships must be used to evaluate such deflections.

12. The ratio of plastic bending angle to elastic bending angle for constant-gradient moments varying from zero to M_u ranged from 1.50 to 16.7, with an average ratio of 8.47. For the twelve test beams that would be acceptable for

plastic design by AISC standards this ratio ranged from 6.36 to 16.7, with an average ratio of 10.2.

ACKNOWLEDGMENTS

This project was made possible by the joint sponsorship of the Department of Civil Engineering of the University of Connecticut, Storrs, Conn. the American Institute of Steel Construction, and the Structural Steel Fabricators of Connecticut. The encouragement and contributions to the direction of the program by K. C. Tippy, F. ASCE, Head of the Department, T. R. Higgins, F. ASCE, Director of Engineering and Research of the AISC, and Edward R. Estes, F. ASCE, Research Engineer of the AISC, and specially acknowledged, as well as the extensive contributions of Yechiel Weitsman, graduate assistant, to the planning and execution of the program. John F. Drehen, A. M. ASCE, Thomas F. Zimmie, A. M. ASCE, Ross D. Robison, A. M. ASCE, Henry D. Granger, and Richard W. Sullivan, A. M. ASCE, also made important contributions to the execution of the program.

APPENDIX.—NOTATION

The following symbols, adopted for use in the paper and for the guidance of discussers, conform essentially with "American Standard Letter Symbols for Structural Analysis" (ASA Z10.8-1949), prepared by a committee of the American Standards Association with Society representation, and approved by the Association in 1949:

A   = Area;

A_m = abscissal area of M-ϕ diagram (Fig. 5), or $\int_0^{M_u} \phi \, dM$;

A_{web} = cross-sectional area of web;

b   = breadth of flange;

d   = depth of beams (out-to-out of flanges);

E   = modulus of Elasticity;

E_{sh} = initial strain hardening modulus;

G   = shearing modulus of elasticity;

K_1 = $\dfrac{\overline{X}}{L}$;

L   = length from either reaction to the single load on the test beam, Fig. 1;

L_1 = length between lateral supports;

L_2 = $\dfrac{M_m}{V}$;

M   = bending Moment;

M_e =   elastic-limit bending moment;

M_m =   maximum bending moment for any load;

M_p =   fully-plastic bending moment, Eq. 2, using σ_{yf} and σ_{yw};

M_{po} =   fully-Plastic moment using nominal dimensions and $\sigma_y = 33$ ksi;

M_{p1} =   fully-plastic bending moment, Eq. 1, using σ_{yf};

M_u =   ultimate bending moment;

t   =   thickness of flange at $\frac{b}{4}$ from its edge;

V   =   vertical Shear;

v   = $\epsilon_u / \epsilon_{avg}$. (Eq. 7);

w   =   thickness of web;

$\overline{X}$ =   distance from centroid of θ (centroid of area of ϕ-L diagram) to near reaction;

y   =   vertical distance from centroid of cross-sectional area;

Z   =   first moment of area of cross-section about centroidal axis, designating all moment-arms as positive;

Δ =   center deflection;

Δ = Δ followed by a quantity indicates deviation of the quantity (for example Δ d is deviation in d);

Δ_b =   component of Δ caused by bending deformations;

Δ_s =   component of Δ caused by shearing deformations;

ϵ_{avg} =   average outer-fiber strain in length L at attainment of M_u;

ϵ_e = $\frac{\sigma_y}{E}$;

ϵ_p =   strain from stress-strain curve at onset of strain-hardening (Fig. 2);

ϵ_u = $\frac{\phi_u d}{2}$;

θ =   angle of rotation of stiffener at end reaction with respect to stiffener at center of test beam;

$\theta_{f5\epsilon}$ =   stress from flange stress-strain curve for a strain of $5\epsilon_{avg}$;

θ_u =   value of θ at attainment of M_u;

σ_{yf} =   tensile yield stress of flange steel;

σ_{yw} =   tensile yield stress of web steel;

ϕ =   curvature $\frac{d\theta}{ds}$;

ϕ_e =   elastic-limit curvature;

ϕ_p =   curvature at onset of strain-hardening in outer fiber (Fig. 6); and

ϕ_u =   effective curvature for $M = M_u$ on M-ϕ diagram (Fig. 6).

Journal of the

STRUCTURAL DIVISION

Proceedings of the American Society of Civil Engineers

ELASTOMERIC PADS AS BEARINGS FOR STEEL BEAMS

By Hardy E. Fairbanks,[1] A. M. ASCE

SYNOPSIS

Elastomeric bearings have been proven satisfactory and economical for use with bridges with girders of prestressed concrete. The primary objective of the research reported herein was to determine whether or not elastomeric bearings could be used equally well with bridges having steel girders. The research consists of two phases. A survey of published and unpublished literature was made, and correspondence was conducted with a great number of highway and research agencies, to determine the extent of use and the current development of neoprene bridge bearings. Laboratory tests were performed to determine the effects of load on steel girders seated on solid neoprene pads.

The results of the survey and the tests are described in detail in this paper. These results show clearly that there is a good deal of interest in neoprene bearings, primarily because they offer several advantages over conventional rocker bearings. Further, it appears from the limited tests performed that neoprene bearings can be used satisfactorily with steel beams.

INTRODUCTION

A bridge bearing may be defined as a seat for a girder or truss that provides the necessary reaction to prevent vertical movements of the structure through a uniform transfer of load to the foundation. An acceptable bearing

---

device, however, must at the same time allow certain other movements of the bridge. Expansion and contraction of the bridge girder is permitted by the bearing to prevent the development of thermal stresses in the beam. Also, the girder must be allowed to rotate at the bearing to prevent stress concentrations at the connection of the beam to the bearing.

There are many types of bearings that will perform satisfactorily. For steel girders, a machined steel shoe is usually used. However, since the addition, in 1958, of specification T2-58 to the American Assn. of State Highway Officials (AASHO) Standard Specifications for Highway Bridges[2] (1), elastomeric bearings have been used in a number of bridges. In the AASHO specifications, only neoprene is allowed at the present time (1961). Therefore, this research is restricted to tests of steel beams on neoprene bearings. Fig. 1 shows a typical arrangement of a steel beam on an elastomeric bearing and illustrates the functions that a bearing is expected to perform.
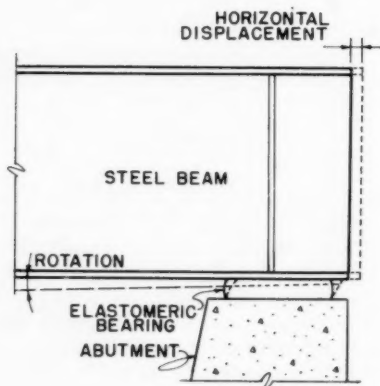
FIG. 1 —STEEL BEAM SEATED ON AN
ELASTOMERIC BEARING

The reason for using neoprene bearings in preference to conventional bearings is primarily a matter of economy. Neoprene bearings are considerably cheaper, initially, than steel shoes and have a life expectancy estimated at between 30 yr and 50 yr. This seems to be an adequate life for most bridges. The primary factors affecting the overall cost of a bridge bearing are as follows: (1) Cost of the material; (2) complexity of fabrication; (3) installation; and (4) maintenance.

Initial cost of neoprene bearings is low; fabrication and installation is quite easy. Furthermore, results of research have shown that neoprene requires little maintenance, whereas it is well known that steel bearings require continued maintenance to prevent deterioration and malfunction due to corrosion.

---

[2] Numerals in parentheses refer to corresponding items in the Appendix.

To illustrate the trend toward the use of neoprene bearings, Fig. 2 was drawn from data received from many highway agencies in the United States. Approximately 40% of these agencies are now using neoprene bearings. A majority has used them only with concrete girders. It seems significant, also, that most of the objections to the use of neoprene bearings were concerned with the adequacy of neoprene itself, and not with the basic functions of the bearing unit. Therefore, it seems reasonable to expect that neoprene bearings will be equally as acceptable for use with steel beams as with concrete beams.

CURRENT DEVELOPMENT OF ELASTOMERIC BEARINGS

Rubber has been used for many years in shock absorbing devices. The French National Railway was apparently the first agency to use rubber pads
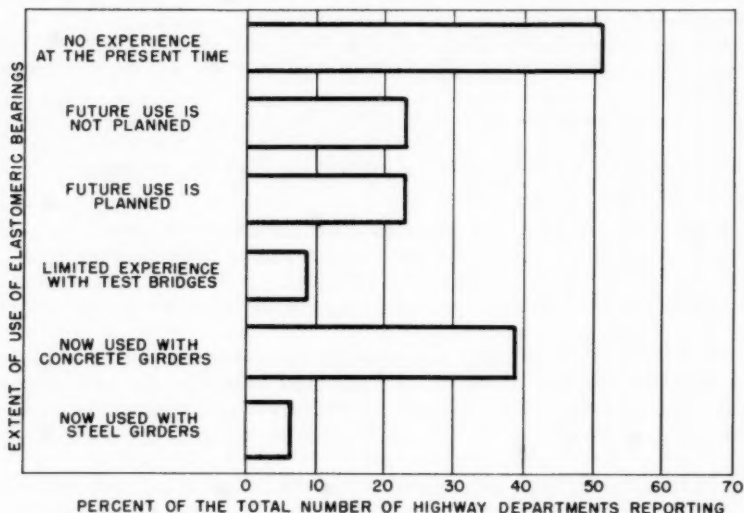
FIG. 2.—CURRENT USE OF ELASTOMERIC BEARING PADS

for bearings in bridge construction. In 1932 they used rubber pads under metal bearings in several railway bridges (2). Much later, in 1948, after a series of mechanical laboratory tests, the French National Railway constructed a bridge at Bourget, France, using only rubber plates for bearings (2). Since then they have built numerous bridges in France and Algeria using this type of bearing. From the references available describing the work done in France, it is not clear what types of bridge girders were used.

In 1955, British engineers used elastomeric bearings on the Pelham bridge, a prominent concrete structure, in Lincoln, England (3). In 1959, in Rio de Janeiro, Brazil, a large concrete bridge was mounted on "Freyssi" bearings

(4). The Freyssi bearing is a laminated pad consisting of rubber plates sandwiched between thin steel stiffening plates.

AASHO adopted neoprene rubber for bridge bearings in its specifications in 1958 (1). The Texas Highway Department was among the first to use neoprene bridge bearings, and has also published specifications concerning their use (5). These specifications differ somewhat from the AASHO specifications.

Charles A. Maguire and Associates (6) made important contributions to the field of elastomeric bearings by conducting extensive tests on molded neoprene pads. The pads were obtained from several manufacturers. In these tests, they determined the physical properties of neoprene and in the report recommended criteria for the design of neoprene bearings. The results and conclusions from the Maguire report are summarized as follows:

1. The tests of elastomer properties were a starting point but were not considered sufficient for determining the adequacy of elastomers to be used in bridge construction. The report did, however, contain recommendations for bearing design.

2. Curves relating the shape effects, hardness effects, time and creep effects, vertical deformation, shear deformation, and loads were included in the report.

3. The initial cost of a bearing is insignificant in comparison with the cost of replacing the bearing, if replacement should become necessary. For elastomeric bearings to be feasible, they should outlast the estimated economic life of the structure they support.

In 1958, A. M. Ozell and J. F. Diniz (7) reported on the fatigue properties of neoprene bearings under repeated shear loads. They concluded that the critical factors in bearing design are the amount of shear deformation that occur in a bearing. They recommended a maximum allowable shear deformation of 25% of the thickness.

In 1959 the E. I. Du Pont De Nemours Company Inc. (8) published a design manual for elastomeric bearings. The purpose of the manual was to present the physical properties of neoprene and to establish criteria for designing neoprene bridge bearings. In this publication several design examples were given.

The California Highway Department, in its Materials and Research Department, (9) has conducted further research into the physical properties of neoprene bearing pads. This research has indicated that laminated pads such as the "Freyssi" bearing offer advantages over the solid pad. Some of these advantages are as follows:

1. Reduces the area that may bulge;
2. reduces the total vertical deformation for a given bearing thickness;
3. permits the use of softer elastomers; and
4. allows bearing units of greater total thickness, thus permitting the use of neoprene bearings on longer bridge spans.

Most of the published literature has attempted to establish the suitability of neoprene as a material for bridge bearings. There are still some questions that remain unanswered in this area. On the other hand, very little information has been found regarding the effects of elastomeric bearings on the design

of the bridge girder itself. Other articles both published and unpublished are listed in the Appendix.

OBJECTIVES OF THE RESEARCH

As a result of the various factors mentioned in the preceding examination, the following objectives were established for the research reported in this paper.

The primary objective was to determine the stresses produced in the steel beams, to observe the pad behavior, including slippage, and to determine the effects of stiffeners in beams on the stresses produced in the steel.

TESTS OF ELASTOMERIC BEARINGS

In the tests, the primary objective was to determine the effects of bridge loads on both the bearing and the steel girder. Therefore, the tests were designed to duplicate as closely as possible actual bridge conditions for several beam and bearing pad combinations. To accomplish this vertical reaction, representative end slope of the beam, and horizontal movement of the beam were prescribed at the bearing. These values are measured ones; that is, they are independent variables. Fig. 3 shows a schematic drawing of the test beam and loading frame positioned in the universal testing machine. The vertical reaction was provided, primarily, by a 120 kip, hydraulic, universal testing machine. Center point loading was utilized in all tests, and the load determined by a Tate-Emery weighing system. For each beam tested, a representative design reaction was determined by considering published bridge designs of the United States Department of Commerce (15). This design reaction was exceeded in each test.

A representative maximum end slope was calculated for each beam and was duplicated quite closely by placing the ends of the beam at different elevations. It should be noted (refer to Fig. 3 and Fig. 4) that the end slope relative to the concrete block is the sum of three components: (1) The difference in elevation of the ends of the test beam. (2) the deflection of the test beam; and (3) the deflection of the loading frame. Items 2 and 3 were found to be quite small. Thus, a preconceived end slope was used, and this was practically invariant. The total beam rotation relative to the concrete bearing block, which represented the bridge bent, was measured with 0.001 in. dial gages.

The horizontal movement of the beam was produced by jacking against the test frame and the test beam. A 30 ton hydraulic jack was used. The total jacking force was measured, using a pressure cell made of a high strength steel bar with SR-4 strain gages, Type A-7. The cell was calibrated against the hydraulic machine, and the results were reproducible.

The value of the jacking force was required primarily to determine the total vertical reaction. It can readily be seen from the force diagram (Fig. 5) that the total vertical reaction can be easily determined from the quantities measured.

The dependent variables in the tests were the resulting stresses in the steel girder and the horizontal deformation of the pad, including slippage. The stresses were determined by Baldwin SR-4, Type A-7 strain gages. These
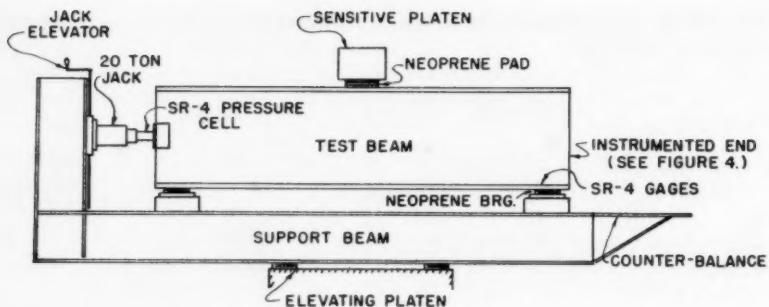
FIG. 3.—SCHEMATIC DIAGRAM OF A TEST BEAM AND THE LOADING FRAME
IN THE UNIVERSAL TESTING MACHINE
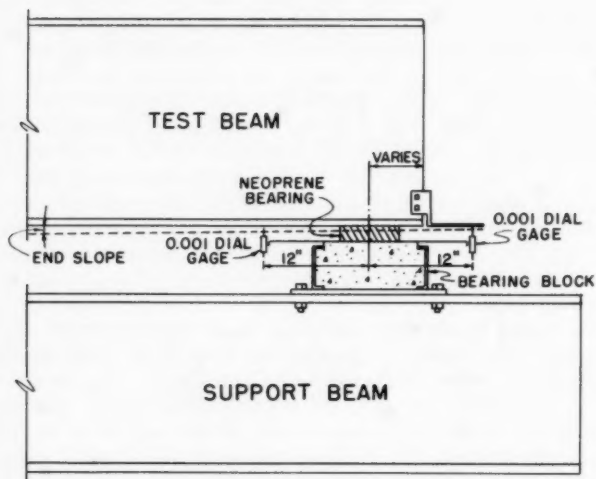
FIG. 4.—SCHEMATIC DIAGRAM SHOWING METHOD OF
END SLOPE MEASUREMENT
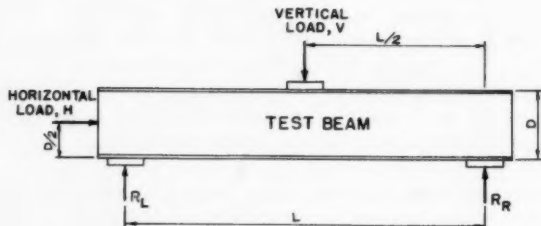
FIG. 5.—FORCE DIAGRAM FOR A TEST BEAM

gages were positioned to determine both the longitudinal and transverse stresses on the top surface of the bearing flange. Longitudinal stresses are those parallel to the beam web. Likewise, a transverse stress is perpendicular to the beam web. By several preliminary tests using rosette gages, it was determined that these are nearly the maximum stresses that occur in the beam flange. The stresses were calculated from the measured strains, using an assumed modulus of elasticity of 30 psi x 10^6 psi. The horizontal displacement of the test beam and the unit shearing strain in the bearing were measured by taking sequence photographs of the beam and bearing pad under constant vertical load and varying horizontal loads. Due to the non-uniform deformation of the pad, this method seemed to be the only satisfactory one. The results, however, should only be considered as approximately correct, and many more future tests are advisable.

TABLE 1.—TEST OF STEEL BEAMS ON NEOPRENE BEARINGS

Beam No.	Size	Stiffeners	Pad Dimensions		
			Length in inches	Width in inches	Thickness in inches
(1)	(2)	(3)	(4)	(5)	(6)
1.	18 WF 50	NO	7.50	5.00	0.25
			7.50	5.00	0.50
			7.50	5.00	0.75
			7.50	5.00	1.00
2.	24 WF 76	NO	9.00	6.00	0.75
			9.00	6.00	1.00
3.	30 WF 108	NO	10.50	6.50	0.75
			10.50	6.50	1.00
4.	18 WF 50	YES	7.50	5.00	0.75
			7.50	5.00	1.00

Other physical details of the testing program are given in Table 1. It should be noted that with the four beams, ten series of tests were run. Thus, the tests were limited; in order that a design procedure can be published and used with confidence, more tests should be performed.

ANALYSIS AND INTERPRETATION OF RESULTS

The stresses in a steel beam near a reaction are influenced by the type of bearing that is used. In order to determine the effects of the thickness of an elastomeric bearing on these stresses, test beam No. 1, a beam with no stiffeners, was tested using four neoprene bearings of different thicknesses. Fig. 6 shows typical curves of vertical reaction as a function of the transverse

stress. Curve A was drawn from the test of a 1 in. thick pad, curve B from a 3/4 in. pad, curve C from a 1/2 in. pad, and curve D from a 1/4 in. pad. From these curves it was deduced that varying only the pad thickness, the maximum beam stress increases as the pad thickness increases.

The maximum transverse stress in the flange was found to be about 34,000 psi when a 30,000 lb reaction was applied through a 1 in. neoprene pad. When a 1/4 in. pad was used, the maximum stress was only 23,000 psi for the same reaction. In every case the longitudinal stresses were found to be appreciably smaller than the transverse stresses. The maximum longitudinal stress was 14,000 psi when a 30,000 lb reaction was applied through a 1 in. bearing pad. The longitudinal stresses were also higher when thicker bearing pads were used.
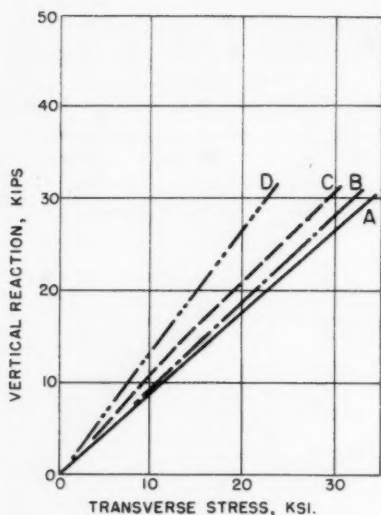
FIG. 6.—TYPICAL CURVE OF TRANS-
VERSE STRESS VERSUS VER-
TICAL REACTION
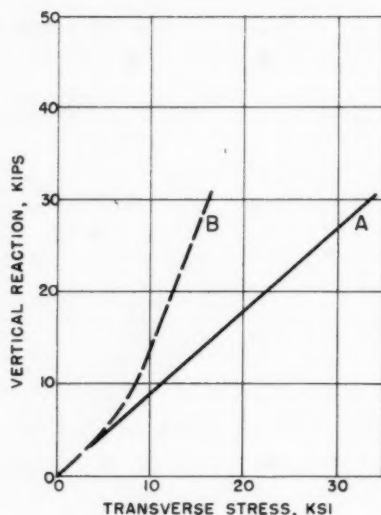
FIG. 7.—TYPICAL CURVE SHOWING THE
EFFECT OF STIFFENERS

The explanation for higher stresses when relatively thick pads are used lies in the distribution of pressure on the bearing flange. The reactive loads are distributed more uniformly when thick neoprene pads are used, causing the flange to transfer more load to the web. If a stiffer material were used, such as steel, the pressure diagram would be concentrated more directly under the web. Although no tests were performed using laminated pads, it seems unlikely that the thin stiffening plates in the laminated pad would much change this distribution. Thus, it is apparent that high local stresses will develop when elastomeric bridge bearings are used, unless stiffeners or some other corrective measures are used.

Test Beam No. 4 showed that stiffeners are an effective means of reducing the beam stresses. This test showed that the maximum transverse stress in the beam was only 18,000 psi when the vertical reaction was 30,000 lbs and the pad thickness was 1 in. The longitudinal stresses were also reduced when stiffeners were used. Fig. 7 shows a comparison between the stresses in a beam without stiffeners and the stresses in a beam with stiffeners. Curve A shows the results of the test of an 18 Wᶠ 50 beam with no stiffeners, and curve B shows the results of the test of the same beam with stiffeners.

Test Beams No. 2 and 3 were tested with 3/4 in. and 1 in. bearing pads only. The maximum reactions applied were in the range that would be expected if these beams were used in a highway bridge. (15) The maximum transverse stresses exceeded the usual design allowable of 20,000 psi for both of these
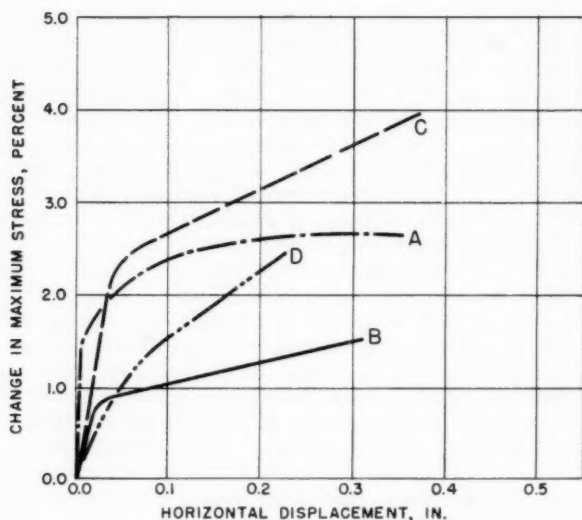
FIG. 8.—TYPICAL CURVE SHOWING THE EFFECT OF
HORIZONTAL DISPLACEMENT ON STRESS

beams. The longitudinal stresses that occurred were not critical. Because a 3/4 in. bearing pad is probably the minimum thickness that will be used for bearings, it is apparent that stresses exceeding the allowable unit stresses will occur in the beam flanges unless stiffeners are used.

The horizontal displacement of the beam had little effect on the beam stresses. The stresses changed from 5% to 10%, due to the friction force between the steel and neoprene. The maximum change is limited by slippage, because the forces involved do not increase after slippage starts. The tests show that slippage occurs when the shearing strain in the neoprene pad is between 0.28 in. per in. and 0.32 in. per in., provided no attempt has been made to bond the neoprene bearing to the steel beam. In order to prevent slippage, it appears that a conservative value of 0.25 in. per in. for allowable shear

strain should be used. Fig. 8 shows the effect of horizontal diaplacement on beam stresses. All the curves in this figure are drawn from data from tests of a 24 W 76 beam with no stiffeners (refer to Table 1, Beam No. 2). The bearing pad thickness was 1 in. in each case. Curve A represents the change in transverse stress as a function of horizontal beam displacement, when the vertical reaction was 20,000 lbs. Curve B gives the same information when the vertical reaction was 40,000 lb. Curve C gives the same information as curve A, except that the change in longitudinal stress is plotted. Likewise, curve D is the same as curve B, except that again the change in longitudinal stress is plotted.

The end rotation was not varied in the tests, it was held constant for each beam at a representative value. The tests showed that the location of the maximum stress is shifted toward the span side of the center of the bearing by the end rotation.

Also, due to the rotation of the end of the beam, the bearing pressure was not uniformly distributed on the pad. The rotation used in the tests with Beam No. 1 was a representative value determined from a bridge design in which an 18 W 50 beam was used. (15) In the tests, it was noted that when the pad thickness was small, that is, 1/4 in. to 1/2 in., the pad was not compressed over its entire area. When thicker pads were tested, this did not occur. It seems reasonable to expect the bearing to operate better, with less tendency for the beam to slip, if this concentration of bearing pressure on one side is not permitted. Therefore, a minimum pad thickness of 3/4 in. neoprene should be used for elastomeric bearings.

As described previously, the shear strain in the bearing pad and the displacement of the beam were determined by sequence photographs for each beam tested. Slippage of the steel beam on the neoprene bearing occurred when the shearing strain in the bearing exceeded approximately 0.30 in. per in. It appears that the 0.50 in. per in. shear strain value recommended in the Du Pont Manual (8) is too high for steel beams on elastomeric bearings. Slippage of the beam relative to the bearing pad should not be allowed. If slippage should occur, two undesirable effects may result: (1) The beam would tend to crawl out of place; and (2) the pad might roll under the beam. No tests were performed in this research to determine whether the pad would be damaged if it rolled slightly under the beam.

CONCLUSIONS

1. Neoprene bearings may be used on bridges using the sizes of beams tested in this research.

2. The use of neoprene bearings with steel beam bridges would result in a substantial savings in cost, compared with that of conventional steel shoes, provided that current estimates of 35 yr to 50 yr for the life of the neoprene are accurate.

3. Permanent deformations in the flange of a steel girder were found to occur when thick bearing pads were used and the girder had no stiffeners.

4. When stiffeners were used, neoprene bearings did not cause excessive stresses in the steel beams. Therefore, bearing stiffeners should always be used.

5. Horizontal beam displacements change somewhat the stresses in the steel beams. For the sizes tested, the maximum change in stress was about 10%.

6. Steel beams will slip on the neoprene pad if the shearing strain in the pad exceeds about 0.30 in. per in.

RECOMMENDATIONS FOR FUTURE RESEARCH

During the conduct of this research, several problems and questions were found to be unanswered by published literature. Some of these came as an outgrowth of the research, and others were suggested by various individuals and agencies. Research that may answer some of these questions is being conducted (as of 1961) by several organizations. Still further research appears to be needed.

Properties of Neoprene Rubber. —Two important properties of neoprene need to be investigated more fully in order that neoprene bearing pads be generally accepted:

1. The properties of neoprene rubber under bridge loads at low temperatures.

2. The effects of saline vapors on the life of neoprene rubber. Several states in colder climates, where temperatures reach 0°F to 40°F below zero, expressed reluctance to use elastomeric bearings until some research of this kind has been published. In atmospheres where saline vapors are present, one state highway department expressed concern about the life of the neoprene when used as a bearing.

Effects of Stress Concentrations on Neoprene Bearings. —It was pointed out in this research that high stress concentrations are likely to occur in the neoprene bearing when used with steel beams. This is due to the bending of the beam flange in both a lateral and a longitudinal direction. Stiffeners definitely will help to distribute the pressure by reducing the amount of bending that occurs. It seems advisable, however, that some research be conducted on the effects of high concentrations of pressure on neoprene.

Laminated Bearings. —For most bridges on elastomeric bearings, the solid neoprene pad has been used. The thickness of the solid pad must be designed so that excessive vertical deformation will not occur. One of the factors influencing the amount of vertical deformation that will occur in a bearing is the shape factor of the neoprene pad.

The shape factor is a property of the pad dimensions and is defined as the ratio of the loaded surface area to the area which is free to bulge. The shape factor decreases as the pad thickness increases. Also, the vertical deformation for a given load increases as the shape factor decreases. Thus, the pad thickness is limited and, therefore, bridge spans on bearing pads are restricted to relatively short lengths. On the other hand, laminated pads have the advantage of greatly increasing the shape factor for a given total thickness. This allows elastomeric bearings to be used on longer bridge spans. More information is needed, however, on the properties and behavior of laminated bearing units so that specifications for their design may be prepared.

Steel Beams and Neoprene Bearings as a Unit. —Steel, when placed on neoprene bearings, will tend to crawl or change its relative position on the pad if

the steel slips on the bearing pad. This may occur when thermal movements take place with one or a combination of several factors: (1) Light dead loads; (2) bridges with skewed girders; or (3) Relatively long bridge spans; or both. In order to use neoprene bearings with confidence some information on methods of preventing crawling of the steel beam is necessary.

Design of End Diaphrams on Steel Girder Bridges. — The stresses that occur in the end diaphrams of steel bridges are not precisely known. Even when conventional bearings are used, there is some question as to the amount of lateral distribution that should be attributed to the diaphram and the amount that should be attributed to the slab. Because the vertical deformation of the elastomeric pads is greater than that of steel shoes, it appears that the design of the diaphram may be more critical than when conventional bearings are used. Therefore, a theoretical study and an experimental determination of the stresses in end diaphrams should prove useful.

ACKNOWLEDGMENTS

APPENDIX—BIBLIOGRAPHY ON USE OF ELASTOMERIC PADS AS BEARINGS FOR STEEL BEAMS

---

1. "Standard Specifications for Highway Bridges," Amer. Assn. of State Highway Officials, Washington, D. C., Item 1.6.47, 1957, p.76.

2. "Rubber Bearing Plates for Girders," Société Téchnique Pour L'Utilisation de la Precontrainte, unpublished research, Paris, France.

3. "The Use of Rubber in Bridge Bearings," Washington, D. C., Vol. 10, No. 2, Summer, 1957, p. 34.

4. "Growing Scope for Rubber Bridge Bearings," Rubber Developments, Washington, D. C., Vol. 12, No. 4, Winter, 1959, p. 113.

5. "Special Provision No. 67 to Items 402, 406, and 422," Texas Highway Dept., Austin, Tex.

6. "Elastomeric Bridge Bearings, Report on Tests and Design Procedure," by Charles A. Maguire and Assocs., Engrs., Providence, R. I., March, 1958.

7. "Report on Tests of Neoprene Pads Under Repeated Shear Loads," by A. M. Ozell and J. F. Diniz, Engrg. and Industrial Experiment Sta., College of Engrg., Univ. of Florida, Gainesville, Fla., November, 1958.

8. "Design of Neoprene Bridge Bearing Pads," E. I. du Pont de Nemours and Co. (Inc.), Wilmington 98, Del., April, 1959.

9. "Memo to Designers," Elastomeric Bearing Pads, California State Highway Dept., Sacramento, Calif., April 4, 1960.

10. "Gummilager für Brüken," by Beton and Stahlbetonbau, Verschiedenes, September, 1959, p. 229.

11. "Rubber Supports," by Christiani and Nielson, unpublished research for la Société Téchnique Pour L'Utilisation de la Precontrainte, Paris, France.

12. "Elastomeric Bearing Pads in Bridge Construction," E. I. du Pont de Nemours and Co. (Inc.), Wilmington 98, Del.

13. "Rubber Seats for Prestressed Beams," by James R. Graves, Engineering News-Record, McGraw-Hill Publishing Co., New York, May 16, 1957, p. 67.

14. "Report on Neoprene Rubber Bridge Bearing Pads," by Moffart, Nichol, and Taylor, Engrs., Portland, Oreg., 1957.

15. "Standard Plans for Highway Bridge Superstructures," U. S. Dept. of Commerce, Bur. of Pub. Roads, Washington, D. C., 1956.

Journal of the
STRUCTURAL DIVISION
Proceedings of the American Society of Civil Engineers

REINFORCED MASONRY DESIGN AND PRACTICE

Progress Report

Task Committee on Reinforced Masonry Design and Practice

Committee on Masonry and Reinforced Concrete

TABLE OF CONTENTS

Note.—Discussion open until May 1, 1962. To extend the closing date one month, a written request must be filed with the Executive Secretary, ASCE. This paper is part of the copyrighted Journal of the Structural Division, Proceedings of the American Society of Civil Engineers, Vol. 87, No. ST 8, December, 1961.

CHAPTER 4 - DESIGN

CHAPTER 5 - TEST PROCEDURES

CHAPTER 1 – INTRODUCTION

SECTION 101 – OBJECT

The purpose of this report is to set forth a Recommended Practice for the design and construction of Reinforced Masonry Structures. It is not a building code. It is an attempt to place in the hands of engineers an evaluation and correlation of present knowledge so that they may more readily design masonry structures and to guide builders in masonry construction. The serviceability of a masonry structure depends to a large degree on the intelligence and care with which it is designed and built. With the advent of reinforced masonry and higher allowable working stresses, every step in design and construction becomes more important.

SECTION 102 – SCOPE

This report in general is limited to masonry units of a size which can be handled manually. The use of larger precast units, such as precast lintels, is considered only where they are used in connection with the smaller units.

In so far as possible, it deals in particular with only those materials specifically mentioned in the report but states "Basic Principles" so as not to exclude any type of material.

There is no intent to cover the requirements of local building codes. Therefore it is recommended that these be studied, particularly when building in earthquake areas.

In making this report it is recognized that there are still many unknowns in the factors which determine the serviceability of masonry structures. This report is therefore intended to provide a basis for correlating new knowledge as well as disseminating that already known.

SECTION 103 – GLOSSARY OF TERMS

ABSORPTION—The amount of water the unit will absorb when immersed in either cold or boiling water for a stated length of time. See ASTM C 104- for concrete units and C 67- for clay products.

ASHLAR MASONRY—Masonry composed of rectangular units of burned clay, concrete, shale, or stone, generally larger in size than brick and properly bonded, having sawed, dressed or squared beds, and joints laid in mortar.

BACKUP—That part of a masonry wall behind the exterior facing.

BAT—A piece of a broken masonry unit.

BATTER—Recessing or sloping a wall back in successive courses; the opposite of corbel.

BED JOINT—The horizontal layer of mortar on or in which a masonry unit is laid.

BELT COURSE—A narrow course of masonry, sometimes slightly projected such as window sills, which is made continuous.

BLIND HEADER—A concealed header in the interior of a wall, not showing on the faces.

BOND—Tying the various parts of a masonry wall together.

Grout Bond—The adhesion to, and/or the interlocking of grout with the masonry units.

Mechanical Bond—Tying masonry units together with metal ties or reinforcing steel or keys.

Mortar Bond—The adhesion of mortar to masonry units.

Running Bond—Units laid so that the vertical mortar joints are centered over the unit below. Sometimes called center bond, or half bond.

Stacked Bond—A bonding pattern where no unit overlaps either the one above or below, all head joints form a continuous vertical line. Also called plumb joint bond, straight stack, jack bond, jack on jack, and checkerboard bond.

BOND BEAM—The course or courses of masonry units reinforced with longitudinal bars and designed to take the stresses resulting from lateral forces. It usually occurs at floor and roof levels.

BOND COURSE—The course consisting of units which overlap those below.

BREAKING JOINTS—The arrangement of masonry units so as to prevent continuous vertical joints in adjacent courses.

BRICK:

Abode Brick—A large clay brick, of varying size, roughly molded, and oven or sun dried.

Common Brick—A solid masonry unit made from clay or shale, dried and burned or fired at about 1850°F., usually without special attention to color, with smooth, textured or designed surfaces, and made in Standard Size, Oversize and Modular Size. Also called Building Brick.

Dry-Press Brick—Brick produced by a process of forming relatively dry clay (5-7% moisture content) in molds at pressures of from 550 to 1500 psi.

Facing Brick—Brick made from a scientifically controlled mixture of natural clays or shales only, and specially processed during manufacture to produce desired colors and textures, regularity in shape and uniformity.

Fire Brick—Brick made of refractory clay material which will resist high temperatures, and heat shock.

Norman Brick—A brick whose actual dimensions are 2-3/16 in. x 3-1/2 in. x 11-1/2 in. laying up three courses to 8 in. in height using 1/2 in. mortar joints.

Roman Brick—A brick whose actual dimensions are 1-1/2 in. x 3-1/2 in. x 11-1/2 in. laying up two courses to 4 in. in height. These brick are sometimes made 15-1/2 in. or more in length.

Salmon Brick—A relatively soft, underburned brick, so-called because of its color.

Soft-Mud Brick—Brick produced by forming relatively wet clay, (20-30% water content) in molds. When the inside of the molds are sanded, the product is called "sand-struck brick." When the molds are wetted to prevent sticking, the product is referred to as "water-struck."

Stiff-Mud Brick—Brick produced by extruding through a die a plastic clay, (12-15% water content).

BUTTERING—Placing mortar on masonry units with a trowel before laying.

CAVITY WALL—A wall built of masonry units so arranged as to provide a continuous air space within the wall. The facing and backing (outer wythes) are tied together with rigid non-corrosive metal ties.

CHASE—A continuous recess built into a wall to receive pipes, ducts, etc.

CLOSER—The last unit laid in a course. A closer may be a whole unit or one that is shorter and usually appears in the field of the wall.

CLOSURE—A supplementary unit with closed ends, used adjacent to corners or at jambs.

CONCRETE MASONRY UNIT:

Concrete Block—A hollow or solid concrete masonry unit made from portland cement and suitable aggregates such as sand, gravel, crushed stone, bituminous or anthracite cinders, burned clay or shale, pumice, volcanic scoria, air-cooled or expanded blast furnace slags, with or without the inclusion of other materials. Sometimes called Concrete Tile.

Concrete Brick—A solid concrete masonry unit made from portland cement and suitable aggregates, with or without the inclusion of other materials.

A-block—A hollow unit with one end closed and the opposite end open forming 2-cells when laid in the wall.

Bond Beam Block—A hollow unit with portions depressed $1\frac{1}{4}$ inches or more to form a continuous channel, or channels for reinforcing steel and grout. U-blocks are sometimes used to form Bond Beams.

Channel Block—A hollow unit with portions depressed less than $1\frac{1}{4}$ inches to form a continuous channel for reinforcing steel and grout.

H-block—A hollow unit with both ends open in the form of one-half of a cell.

Offset Block—A unit which is not rectangular in shape. Usually made as a corner block to keep the construction modular.

Open-end Block—A term applied to both H-blocks and A-blocks. Sometimes applied to standard units with end webs recessed.

Solid Unit—Refers to masonry units in which the vertical cores are less than 25% of the cross-section area. (See definition SOLID MASONRY UNIT).

U-block or Lintel Block—A masonry unit consisting of one core with one side open. (Usually placed with the open side up to form a continuous beam).

COLUMN—A vertical compression member whose ratio of unsupported height to least width is greater than four.

COPING—The material or units used to form a cap or finish on top of a wall, pier or pilaster.

CORBEL—A shelf or ledge formed by projecting successive courses of masonry out from the face of the wall.

COURSE—A continuous horizontal layer of masonry units.

DRY PACK—A mixture of cement and fine aggregate with enought moisture for hydration but dry enough to be rammed into place.

EFFLORESCENCE—A whitish powder resulting from the deposition of soluble salts on the surface of masonry.

EXFOLIATION—Scaling or flaking off of the surface.

FACING—Any masonry, forming an integral part of a wall, used as a finished surface. (As contrasted to Veneer, see definition).

FACED WALL—A wall in which the facing and backing are so bonded together that they act as a composite element.

FAT MORTAR—A mortar that tends to be sticky and adheres to the trowel.

FIRE CLAY—A finely ground clay used as a plasticizer for masonry mortars. (Varies widely in physical properties.)

FIRE WALL—Any wall which subdivides a building so as to resist the spread of fire, by starting at the foundation and extending continuously through all stories to, or above, the roof.

FLOW OF MORTAR—Measure of mortar consistency (sometimes termed the initial flow) determined on the flow table described in ASTM C 230. Use of the flow table and method of calculating the flow is described in Section 9 of ASTM C109-.

FLOW AFTER SUCTION—Flow of mortar measured after subjecting it to a vacuum produced by a head of 2 inches of mercury. The suction apparatus and its use is described in Sections 27 and 28 of ASTM C91-.

FROG—A depression in the bed surface of a masonry unit. Sometimes called a Panel.

FURROWING—The practice of striking a "V" shaped trough in a bed of mortar.

GROUT—A fluid mixture of portland cement, aggregate, and water which is poured into hollow cells, or joints of the masonry walls, to encase steel and bond units together.

HACKING—Laying masonry units so that the bottom edge is set back from the plane surface of the wall. Also the procedure of stacking brick in a kiln.

HARD BURNED—A term applied to clay products which have been fired at high temperatures to near vitrification, producing relatively low absorptions and high compressive strengths.

HARSH MORTAR—A mortar that, due to an improper mixture of materials, is difficult to spread (not workable).

HEAD JOINT—The vertical mortar joint between ends of masonry units; sometimes called the Cross Joint.

HEADER—A masonry unit laid flat with its greatest dimension at a right angle to the face of the wall.

HOG (in a wall)—A wall that is hogged is one in which for any given height at both ends, there is a different height in the field, necessitating adjustment of mortar bed joints of the use of supplementary height units.

HOLLOW MASONRY UNIT—A masonry unit whose net cross-sectional area in any plane parallel to the bearing surface is less than 75% of its gross cross-sectional area measured in the same plane.

JOINTING—The process of finishing mortar joints with a trowel, jointer, rubber ball, etc.

LATERAL SUPPORT-- (of walls) Means whereby walls are braced either by columns, pilasters or crosswalls, or by girt beams, floor or roof construction.

LEAD—The section of a wall built up and racked back on successive courses at the corner of a building. The line is attached to the leads and the wall then built up between them.

LEAN MORTAR—A mortar that, due to a deficiency of cementitious material, is harsh and difficult to spread.

LIME:

Quick Lime—A hot or unslaked lime. A calcined material, the major part of which is calcium oxide, or calcium oxide in natural association with lesser amounts of magnesium oxide, capable of slaking with water.

Hydrated Lime—A dry powder obtained by treating quicklime with water enough to satisfy its chemical affinity for water under the conditions of its hydration. The term may be modified by the use of the prefix high calcium, magnesium, pressure, etc., depending on the exact chemical content and method of manufacture. Hydraulic Hydrated Lime is a different material and is not generally used in masonry construction.

Lime Putty—Quick lime to which sufficient water has been added to make a plastic paste ready for use in mortar.

Processed Lime—Pulverized quick lime.

LINTEL—A beam placed over an opening to carry the superimposed weight above.

MASONRY UNIT—Brick, block, tile, stone or other similar building units, or combination thereof, made to be bonded together by a cementitious agent.

MODULAR MASONRY UNIT—A masonry unit whose nominal dimensions are based on the 4 in. module.

MORTAR—A plastic mixture of cementitious materials, fine aggregate and water.

NOMINAL DIMENSION—A dimension which may vary from the actual dimension by not more than the thickness of a mortar joint.

PARAPET WALL—That part of any wall entirely above the roof line.

PARGING—The process of applying a coat of cement mortar to the back of the facing material or the face of the backing material; sometimes referred to as Pargeting.

PICK AND DIP—A method of laying masonry in which the mason simultaneously picks up a unit and enough mortar to lay one unit in the wall.

PIER—An isolated compression member whose ratio of unsupported length to least width is four or less.

PILASTER—A portion of the wall which projects on one or both sides and acts as a vertical beam, a column, or both.

POINTING—Filling mortar into a joint after the masonry unit is laid.

RACKING—A method of building the end of a wall by stepping back each course, so that it can be built onto and against without toothers; also used in corner leads.

RAGGLE—A groove or channel in a mortar joint, or in a special masonry unit, to receive roofing, flashing or other material which is to be sealed in the masonry.

REINFORCED MASONRY—Masonry in which reinforcement is embedded in such a manner that the component materials act together in resisting forces. Reinforced Grouted Masonry and Reinforced Hollow Unit Masonry are sub-heads that are sometimes used in building codes.

REVEAL—That portion of a recess which is visible from the face of a wall back to the frame placed between the sides of the recess.

ROWLOCK—A unit laid on its face edge. Usually laid in the wall with its long dimension at a right angle to the wall face. Frequently spelled "Rolok." Sometimes called Bull-headers.

SHOVED JOINTS—Produced by placing a unit on a mortar bed and then immediately shoving it a fraction of an inch horizontally against the mortar in the head joint to effect a solid, tight joint.

SLUSHED JOINTS—Head joints filled after units are laid by "throwing" mortar in with edge of trowel.

SOFFIT—The underside of a beam, lintel or reveal.

SOFT BURNED—A term applied to clay products which have been fired at low temperature ranges so as to have relatively high absorptions and low compressive strengths.

SOLDIER—A unit laid on its end so that its greatest dimension is vertical, and its edge exposed.

SOLID MASONRY UNIT—A unit whose net cross-sectional area in every plane parallel to the bearing surface is 75% or more of its gross cross-sectional area measured in the same plane.

SPALL—A small fragment removed from the face of a masonry unit by a blow or by the action of the elements.

SPANDREL WALL—That part of an exterior wall above the top of window in one story and below the sill of the window in the story above.

STORY POLE—A marked pole used to establish vertical heights during the construction of the wall.

STRETCHER—A masonry unit laid with its longest dimension horizontal and parallel to the face of the wall.

STRINGING MORTAR—The procedure of spreading enough mortar on the bed joint to lay several masonry units.

STRUCK JOINT—Any mortar joint which has been finished with the trowel.

TEMPER—To moisten mortar and re-mix to the proper consistency for use. Also called re-tempering.

TIER—Each vertical section of masonry a single unit in thickness; also called withe or wythe.

TOOLING—Compressing and shaping the face of a mortar joint with a special tool other than a trowel. Also called jointing.

TOOTHER—A masonry unit projecting from the end of a wall against which another wall is to be built.

TOOTHING—The temporary ending of a wall wherein the units in alternate courses project.

TUCK POINTING—The filling in with fresh mortar of cut-out or defective mortar joints in masonry.

VENEER—A masonry facing which is attached to the wall but not in a manner to provide composite action under load. (See definition of Faced Wall.)

WATER RETENTIVITY—That property of mortar which prevents the rapid loss of water by absorption to masonry units. Water retention is calculated as described in Section 29 of ASTM C91-.

WEEP HOLES—Suitably formed holes or openings placed in the masonry to permit the escape of moisture from the interior of the wall. In retaining walls, a hole through the wall to permit water to flow through the wall.

WYTHE (or Withe)—Each continuous vertical section of single unit width of masonry; also called a Tier, or Leaf.

CHAPTER 2 - MATERIALS

SECTION 201 - INTRODUCTION

201.1   GENERAL

Reinforced Masonry is composed of masonry units, mortar, grout, and reinforcing steel. Each of these materials is itself a combination of elements. Each element contributes toward the serviceability of the whole and should be selected in reference to the properties desired in the completed structure. Some materials may bear the same name and yet may vary in different localities, and these variations must be considered. Materials not mentioned in this section should be carefully tested and appraised in accordance with the applicable standards, not only as separate items but also combined. Factors which affect the tensile and compressive strength and the bond characteristics of the units require particular attention.

201.2 QUALITY CONTROL

Quality control of materials is maintained through conformance to standard specifications of the American Society for Testing Materials. For this purpose, masonry units are generally divided into two different major categories: (1) units made of baked clay or shale and (2) units made of portland cement mixed with suitable aggregates. Units in both of these categories may be solid or hollow.

Methods of sampling and testing clay or shale brick, are indicated in ASTM Designations C 67-. These tests consist of Modulus of Rupture, Compressive Strength, Absorption by immersion and by boiling, Freezing and Thawing, Suction, Efflorescence, Size and Warpage.

Methods of sampling and testing concrete masonry units are indicated in ASTM Designation C 140-, C 341-, C 426- and C 427-. These tests consist of Compressive Strength, Absorption by immersion, Moisture Content by drying and by relative humidity, and Shrinkage.

Methods of sampling and testing mortar and grout aggregates are mentioned in ASTM Designation C 270- and C 404-. These include controls for the cementitious materials, lime, aggregates, water, and admixtures. Tests for water retentivity and compressive strength are cross-referenced to masonry cement tests, ASTM Designation C 91-. Some field sampling and tests which have not been published in ASTM standards are recommended in Chapter 5 of this report.

The real significance of any test lies in the extent to which it enables us to predict the performance of a material in service. The properties of masonry units in the world probably vary as much as the properties of mortar, grout, or steel, because of the wide variation in the clays, shales, and aggregates used for their manufacture and because of the divergence in manufacturing processes. It is clear that the resulting products demand reliable testing for effective quality control.

Masonry properties which have been found desirable in the completed structure are, compressive, tensile, and shear strength; size, uniformity, and dimensional stability; fire resistance, weather tightness and texture; and ability to adhere to the mortar and grout. These interrelated properties must work together to give a structure the required permanence and serviceability.

Compression is the standard test required of masonry units. The principal value of this test is to control manufacturing processes, but it is limited as a means of determining serviceability of the structure. In clay masonry units an absorption test is often more important than compressive strength. It is important that all of the properties of the units be considered when designing a structure. Where there is doubt concerning quality, a direct tensile test may be required, as outlined under the Section on Testing Procedures, or a Modulus of Rupture Test may be required as specified under ASTM C 67.

Anticipated shrinkage and expansion of units in the wall should be considered. It is recommended that units used in a reinforced masonry wall should have a maximum linear shrinkage of not more than .06 percent when tested in accordance to ASTM C 426 and a maximum linear shrinkage of .08 percent from the saturated to oven dry condition as outlined in the Section on Testing Procedures. Structural clay products have little shrinkage and generally tests are not required.

SECTION 202 - SOLID MASONRY UNITS

202.1 GENERAL

Solid Masonry Units are those units which have less than 25% voids in every horizontal cross section.

202.2 STRUCTURAL CLAY PRODUCTS

a. Clay or Shale Brick should conform to the requirements of Standard Specifications for Building Brick, ASTM C 62-.
b. Facing Brick should conform to the applicable requirements of ASTM C 216- and Ceramic Glazed Units to the requirements of ASTM C 126-.

202.3 CONCRETE PRODUCTS

a. Concrete brick should conform to the requirements of Standard Specifications for Concrete Building Brick ASTM Designation C 55-.
b. Concrete masonry units should conform to the requirements of Standard Specifications for Solid Load-Bearing Concrete Masonry Units ASTM Designation C 145-.

SECTION 203 - HOLLOW MASONRY UNITS

203.1 GENERAL

Hollow Masonry Units are those units which have more than 25% voids in every horizontal cross section.

203.2 CONCRETE PRODUCTS

Hollow concrete masonry units should conform to the requirements of Standard Specifications for Hollow Load-Bearing Concrete Masonry Units ASTM Designation C 90-.

203.3 STRUCTURAL CLAY PRODUCTS

Structural clay tile should conform to the requirements of Standard Specifications for Structural Clay Load-Bearing Wall Tile ASTM Designation C 34-.

SECTION 204 - MISCELLANEOUS UNITS

204.1 GENERAL

Miscellaneous units and units which do not come under the definition of hollow or solid units are considered in this section.

204.2 SAND LIME BRICK

Sand Lime Brick should conform to the requirements of Standard Specifications for Sand-Lime Building Brick ASTM C 73-.

204.3 MORTARLESS UNITS

Hollow units which are manufactured with interlocking faces and laid up without mortar should comply with the requirements for Grade A units in Standard Specifications for Hollow Load-Bearing Concrete Masonry Units ASTM Designation C 90- except that no requirement should be made on shell thickness where only the core filled with concrete is used in design.

204.4 IRREGULAR UNITS

Many manufacturers have special types and shapes of units which they promote as their specialty. Considerable engineering judgment must be used in deciding their best use in construction.

If the units are made of concrete, then the quality of material should be at least comparable to that designated for Hollow Load-Bearing Concrete Masonry Units, ASTM C 90-. If the units are made from burned clay or shale, then the quality should be at least comparable to that designated for Building Brick ASTM C 62-. In addition, all units should meet the shrinkage requirements suggested under Section 201.2 and be subjected to either a Modulus of Rupture test as required in ASTM C 67 or a direct tension test.

204.5 RECLAIMED MASONRY UNITS

Masonry units may be reused when cleaned, and in conformity with the appropriate specification for the type of unit. The ability of mortar and grout to adhere to the units should be checked.

204.6 PRECAST LINTELS

Precast lintels shall conform to the requirements of Building Code requirements for Reinforced Concrete ACI Standard 318-.

SECTION 205 - MORTAR

205.1 GENERAL

Since mortar is itself a mixture of materials put together at the construction site, one should be concerned very closely with both the ingredients as well as the finished product. The same mortar will not give the same results when used with different masonry units. The purpose of mortar is to keep the units apart as well as to hold them together. The measure of a good mortar is one which provides an adequate bond between units, is workably plastic over a period long enough to permit the workmen to position the units, has a relatively low shrinkage value, a high degree of extensibility, is resistant to moisture penetration, and has sufficient durability and strength to resist the stresses to which it is subjected. At the time of use mortar should be as soft (this is in a plastic condition) as a mason can use it without smearing the face of the units.

205.2 SPECIFICATIONS

Mortar should conform to the requirements for Mortar Type M or S of Specifications for Mortar for Unit Masonry ASTM C 270-. It should be noted that under ASTM C 270- Mortar is not required to meet both the property and the proportion specification. The ASTM property specification test must be prepared in the laboratory.

205.3 FIELD TESTS

Mortar as used should have a minimum compressive strength not less than 1500 psi at 28 days. This specification is one that should always be met where field tests are required and when they are conducted as specified under the Section on Testing Procedures.

205.4 FLOW OF MORTAR

When tested in the laboratory under ASTM Specification Designation C 109 masonry mortar should have a flow of 110 percent minimum. Under field conditions this flow should be between 125 percent and 135 percent for 25 drops of the flow table. Flow after suction as defined in the Glossary of Terms of this report is a more definite and important measure and should be not less than 75 percent.

SECTION 206 - GROUT

206.1 GENERAL

Grout is that material used to fill up the interstices in masonry and generally provide bond between reinforcing steel, the mortar and the

units. It should contain enough water to flow freely without segregation of the aggregate. Mortar should not be used as grout.

206.2 SPECIFICATIONS

Grout should be composed by volume of one part portland cement and three parts sand, to which may be added not more than one-tenth part lime putty. In grout spaces in solid unit masonry two inches or more in minimum horizontal dimension, and in grout spaces in hollow unit masonry four inches or more in minimum horizontal dimension, the grout should contain two parts of pea gravel in addition to the above mentioned proportions of cement, sand, or lime putty. Grout should test 2000 pounds per square inch in compression at 28 days of age, as determine ' by the field test.

206.3 FIELD TEST

Grout should be sampled and tested in accordance with the procedures recommended in Chapter 5 of this report.

206.4 AGGREGATE FOR GROUT

Aggregates for grout should meet the requirements of Specifications for Aggregates for Masonry Grout ASTM Designation C 404-.

SECTION 207 - REINFORCEMENT

207.1

Reinforcement should be free from rust scale or other coatings that will reduce bond and except for bars one-quarter inch or less in diameter should conform to the requirements of Standard Specifications for Minimum Requirements for the Deformations of Deformed Steel Bars for Concrete Reinforcement ASTM Designation A 305-.

207.2

Reinforcing bars should conform to one of the following Standard Specifications: ASTM Designation A 15-, ASTM Designation A 16, or ASTM Designation A 160-.

207.3

Wire reinforcement should conform to one of the following Standard Specifications: ASTM Designation A 82-, or ASTM Designation A 185-.

CHAPTER 3 - CONSTRUCTION PRACTICES

SECTION 301 - GENERAL

301.1 WORKMANSHIP

In masonry construction large members are constructed with small units, and the importance of each unit as part of the whole, each mortar head and bed joint cannot be over emphasized.

Every part of the work should be executed in the best workmanlike manner in accordance with accepted good practice of the trade and in full compliance with the applicable building ordinances.

All masonry work should be plumb, level, straight and true to dimensions shown on the plans. The work should start, where feasible, at a least important corner or wall. The masonry contractor should request an early inspection of the work by the architect or engineer. All pattern work, bonds or special details and reinforcement indicated on the drawings should be accurately and uniformly executed.

301.2 SUPERVISION

It is essential that the engineer meet with the general contractor, the inspector and the masonry contractor at the start of the job and explain the work involved.

For multi-story buildings and where critical structural elements are involved such as beams, columns, pilasters, and shear walls the masonry work should have special inspection.

The inspector should not presume to interpret the differences between the plans and specifications, nor should he assume the prerogative or responsibilities of the designer. In the design, consideration has been given to the nature of the building, its use, the materials in its construction and their lateral force resistance and only the designer knows their relationship.

When special inspection is required, the inspector should remain on the job at all times when work requiring special inspection is in progress. The inspector should be in the employ of the Owner, never the contractor.

The architect or engineer should supervise the work of the inspector and should be responsible for the proper performance of his duties. In view of his responsibility for the activities of the inspector, the architect or engineer should verify carefully the inspector's qualifications before approving the appointment.

The inspector should have all the materials tested as directed by the architect or engineer and in accordance with the specifications. The inspector should make all the field tests as directed by the architects or engineer in accordance with the specifications. Extreme care should be used in making field test specimens using accepted techniques which are not necessarily the same as laboratory procedures. (See chapter on Testing Procedures.)

Due to possible variations in the unit sizes which affect face bonding and mortar joint sizes, the inspector should work out deviations with the mason contractor before start of the work.

The inspector should see to it that all the work is carried out according to the plans and specifications. If the inspector deems the work improper he should report to the foreman and not to the mason. If the work is in flagrant violation of the plans and specifications it should be removed and properly rebuilt.

SECTION 302 - FOUNDATIONS

302.1 SOIL TYPES

Where the adequacy of the soil for a foundation is not established a soil test should be made by a qualified engineer.

Where foundation beams are used, such as between piling or other supports, in expansive soil or unstable ground, provision should be made for differential movement of the soil relative to the beam and the pile or other support.

302.2 REINFORCEMENT

Masonry construction is sensitive to foundation and soil movements. In all soils which are expansive or unstable in character, where there is change in soil structure, or where vibrations may occur in the building, or where there is a question of possible differential settlement, special care should be taken to reinforce footings against such differential movement.

Foundation reinforcement should be kept clean and in proper position and should be fully encased in concrete and should have sufficient coverage from the soil to prevent moisture reaching the steel and causing rusting. Suggested coverages are noted in ACI Standard 318.

302.3 DOWELS

Dowels from the foundation to the wall, columns, and pilasters should be accurately placed so that the reinforcement will be in proper position to be fully encased in grout in accordance with the plans. Dowels should be maintained straight.

Every effort should be made for proper alignment of dowels in hollow masonry units. However, in the few cases when a foundation dowel does not line up with the vertical core to be reinforced it should not be bent over, but should be grouted into a core in direct vertical alignment, even though it is in a cell adjacent to the vertical wall reinforcement. In all masonry the dowels should not be bent more than a slope of 1 in 6.

302.4 DEPTH BELOW GRADE

The depth of the bottom of the foundation should be as shown on plans, but in any event not less than 12 inches into undisturbed natural grade. In frost areas the foundation bed should be below frost line.

302.5 TIME BETWEEN PLACING FOUNDATION AND STARTING MASONRY

The minimum time between placing foundation and starting masonry should be when the concrete has attained reasonable strength, but never less than 48 hours to allow for strength and initial shrinkage of the concrete.

For foundation beams such as between piling, etc., the time lapse before starting masonry should be determined by the architect and the engineer.

302.6 TOP OF CONCRETE FOUNDATION

Horizontal concrete surfaces that are to receive masonry should be clean, damp, with the aggregate of the concrete exposed to assure good bond between mortar and grout and concrete. All laitance should be removed as roughness in itself is not indicative of good bond.

For grouted solid masonry units, the first course on each side of a wall should be laid on the concrete, taking care that the first mortar bed joint does not extend into the grout space. Then this full course should be grouted to a point about 1-1/2 in. below the top of the course. Grout space as here mentioned means the inside lengthwise vertical joint between two or more tiers of brick, also called the grout core or collar joint.

Where single units in the wall thickness are used, the above procedure would be used also. In hollow units the grout space is the space within the cores or cells where grout is to be poured.

302.7 MASONRY FOOTINGS

Footings of masonry should be limited to small structures such as dwellings and one story buildings. Such footings should be cured for not less than 48 hours, before proceeding with construction.

SECTION 303 – MASONRY UNITS

303.1 STORING AND HANDLING

Masonry units should be stored in a dry place and off the ground, so that at time of laying, all units should be sound and clean. Masonry units stored directly on the ground are hard to clean and may absorb salts or other substances which may have a deleterious effect on the masonry.

All units should be handled reasonably to avoid damage.

303.2 WETTING

Clay or Shale Brick or Structural Clay Tile.

At time of laying, all units should have sufficient moisture content so that the rate of absorption will not exceed 0.025 ounces per square inch during a period of one minute when placed in 1/8 in. of water. The interior of the unit should be wet and the surfaces only damp when laid. This is to control the rate of absorption (suction rate) of the units to prevent rapid deletion of the water from the mortar or grout.

Concrete Masonry Units.

Concrete masonry units should not be wetted before laying, except in hot dry weather when the bearing surfaces may be slightly moistened immediately before laying. The wetting of concrete units causes slight expansion and subsequent shrinkage upon drying.

303.3 CUTTING UNITS

Where masonry unit cutting is necessary, all cuts should be neat and accurate. Except for minor cuts units should be cut with a mechanical device.

303.4 COMBINATION OF UNITS

Where units of different physical properties or composition are used in the outer wythes or tiers of grouted masonry, care should be exercised to see that the rates of absorption or suction of the units are comparable so that the grout will bond equally to each wythe or tier, and that other properties which differ do not cause excessive differential movements in the construction.

SECTION 304 - SHORING AND SCAFFOLDING

304.1 VERTICAL LOADS DURING CONSTRUCTION

All horizontal load bearing members should be adequately shored. In no case should shores and forms be removed until it is certain that the masonry has hardened sufficiently to carry its own weight and all other loads that may be placed on it during the construction. The results of suitable control tests may be used as evidence that the masonry has attained such sufficient strength. Plastic flow, incipient damage, and deflection should be considered when determining the time to remove shoring.

In addition to the foregoing strength requirement the following arbitrary elapsed times are recommended. Vertical side forms where used for sides of girders, lintels, etc., should not be removed for 48 hours. Shoring under girders, beams, lintels, floors, etc., should not be removed for 10 days, and then only if the grout or concrete has hardened sufficiently to prevent injury. At least 16 hours should elapse after building masonry columns or walls before constructing a floor or roof which is applied as a uniform load, and at least an additional 48 hours should elapse before applying a concentrated load, such as truss, girder or beam.

304.2 LATERAL LOADS DURING CONSTRUCTION

Generally, about 25 times the thickness is the maximum safe unsupported height for solid unit masonry walls, and about 18 times the thickness for hollow unit masonry walls, without bracing. Walls exceeding these heights should be adequately braced against wind and other forces during construction.

304.3 SCAFFOLDING

All scaffolding should be of safe design in accordance with national and local safety rules and should not be overloaded by concentrations of material. A design of 100 pounds per square foot is considered minimum for the platform on a mason's scaffold.

SECTION 305 – MORTAR

305.1 MIXING

All proportions should be determined by reasonably accurate weight or volume measurements at the time of placing in the mixer, and should be mixed in a mechanical mortar mixer. The mix should never be less than a multiple of sacks of cement. When less than one sack of cement is used, extreme care should be used in accurately measuring all parts. A paddle type mixer is preferred because it produces a more intimate mix and the mortar is invariably maintained in a plastic condition for a longer period of time, thereby reducing the need for re-tempering of the mortar.

Mix water, sand and cement for two minutes; then add the lime putty or hydrated lime, if used, and additional water and mix for not less than ten minutes. Make and maintain as high a flow (water content) as possible, consistent with good workability and freedom for smearing the face of masonry work. One way to control the mortar mix is to measure the slump using a truncated cone 2 in. x 4 in. x 6 in. high. Proper slump can be established at the start of a job and then maintained throughout construction.

305.2 ADMIXTURES

No admixture should be incorporated into mortar unless it has been demonstrated by authoritative tests that it will not decrease the strength of bond to brick or to reinforcing steel, nor should any be used without the approval of the architect or engineer. Generally admixtures for concrete are used to reduce the water content and have a definite effect on the flow after suction of the mortar. Therefore, they should be checked for their effect on bond with masonry.

305.3 MORTAR COLOR

Mortar color should be inert mineral or synthetic composition as approved by the architect or engineer and should be accurately measured for each batch of mortar. Additional mixing time to produce an even color may be necessary.

305.4 PLACEMENT

For bed joints the mortar should be spread in length only to the extent that it will still be plastic when the last unit is placed upon it, thus assuring adequate bond between the mortar and the upper masonry unit. The length of mortar spread on the bed joints depends upon the water retention of the mortar, the rate of absorption of the units at time of laying, and weather conditions.

For concrete masonry units 8 inches or so in height it is very difficult to place head joints on the units and to place them immediately in position because the mortar often does not adhere to the vertical face of the units. It is good practice to set several units on end and apply the mortar in sequence, then lay the units in the same sequence.

305.5 RE-TEMPERING

Re-tempering on mortar boards should be done only by adding water within a basin formed with the mortar and the mortar re-worked into the water. Harsh, non-plastic mortar should not be re-tempered nor used. Any mortar or grout which is unused after one hour of the initial mixing should be removed from the work.

Mortar should be re-tempered with water as required to maintain high plasticity.

SECTION 306 - GROUT

306.1 MIXING

All parts should be determined by accurate volume measurement at the time of placing in the mixer, and should be mixed in a mechanical mortar mixer. Care should be used in accurately measuring all the parts. The mix should never be less than a multiple of sacks of cement. When less than one sack of cement is used, extreme care should be used in accurately measuring all the parts.

The water, sand (and pea gravel if used,) and cement should be thoroughly mixed for not less than ten minutes to a fluid consistency. This means, wet enough to pour without segregation or bleeding.

For large cells, such as may occur in hollow masonry units, standard concrete may be used where tamped or puddled in place and specifically approved by the engineer.

306.2 ADMIXTURES

No admixture should be incorporated into grout unless it has been demonstrated by authoritative tests that it will not decrease the strength of bond to masonry units or to reinforcing steel. No admixture should be used without the approval of the architect or engineer.

306.3 PLACEMENT

Solid Masonry

Grout should be thoroughly agitated and mixed to eliminate segregation before being placed. All interior grout spaces should be filled with grout and immediately puddled or swished with a stick or rod (not a trowel) sufficiently to cause the grout to flow into all interstices between the bricks and to fully encase the reinforcing steel. Wherever possible, grouting should be done from the inside face of exterior masonry. If any grout contacts the finished masonry, it should be removed immediately and the surface cleaned.

In masonry which is more than two (2) tiers in thickness, including pilasters and columns, the interior should be of whole or half bricks placed into grout with not less than three-fourths (3/4) in. of grout surrounding each brick or half brick. All grout should be stopped one and one-half (1-1/2) in. below the top of both outer tiers, except at the finish course. Before placing the next lift of grout the joint should be cleaned. Where necessary to stop off a longitudinal run of masonry, it should be

done only by racking back one-half brick length in each course and stopping the grout four (4) in. back of the rack.

Hollow Unit Masonry.

Mortar "fins" protruding more than 3/8 in. from joints should be removed before pouring grout. The minimum continuous clear dimensions of vertical cores or grout spaces should be 2 in. Where pour heights are in excess of 8 ft the minimum core dimension should be 4 in. Provide cleanouts at the bottom masonry course of each core to be reinforced when the pour height is in excess of 4 ft. When cleanouts are required they should not be closed until after inspection of the core space and the setting of the vertical reinforcement in fixed position.

Where pour heights are in excess of 4 ft, grout should be poured in lifts of 4 ft maximum for the complete length of the continuous wall section under construction allowing at least 30 min for settlement of grout before pouring the next lift. Grout should be rodded or puddled during placement to insure complete filling of the core. When grouting is stopped for one hour or longer, the grout pour should be stopped 1-1/2 in. below the top of a masonry unit.

Horizontal beams may be built of hollow unit masonry, using channelled units to permit horizontal reinforcement to be placed in the desired position. The top of unfilled cores below such horizontal beams should be covered to confine the grout fill to the beam section. No material should be used which destroys the bond between courses. Grouting of beams over openings should be done in a continuous operation. All grout should be puddled in place to insure complete filling of cores and incasement of reinforcement.

306.4 POUR HEIGHT

Solid Masonry

The grouting operation may be done in one or more passes and the height should be from the center of one course to the center of another course. It is advisable to do this in order to prevent rotation of the brick due to suction of the grout on the brick. If the brick rotates, the mortar joint bond may be destroyed.

One outer tier should be carried up not more than twelve inches (12 in.) before grouting, but the other tier should be not more than four inches (4 in.) high before placing the grout.

Higher pour heights may be used where metal ties are used to prevent spreading of the wythes, where grout joints are more than 2 in. in least dimension, and where special construction are used. An example of this method is outlined by the Division of Architecture, State of California.

Hollow Unit Masonry

Grout pour height should not exceed 48 times the minimum net core dimension with a maximum pour height of 12 ft. Pours should be stopped 1-1/2 in. below the top of a course to form a key at pour joints.

306.5 VIBRATION

Grout should be rodded or puddled during placement to insure complete filling of the core. This releases trapped air and insures better bond between the reinforcing steel and the grout.

Grouted Solid Masonry Units

In columns or pilasters fillers of brick should be "floated" or pushed 1-1/2 in. down into the grout space.

Hollow Unit Masonry

When concrete is used in columns or pilasters it should be placed in accordance with the ACI Code.

SECTION 307 - REINFORCEMENT

307.1 CLEANING

Before being placed, all reinforcement should be free from loose rust and other coatings that would destroy or reduce bond.

307.2 BENDING

All reinforcement should be accurately cut to length and bent without injury to the material. All kinks or bends in the bars caused by handling incident to delivery should be straightened before placement and without injury to the material.

307.3 SPLICES

Splices should be made only at such points and in such a manner that the strength of the member will not be reduced. Lapped splices should provide sufficient lap to transfer the working stress of the bars by bond and shear with a minimum lap of 30 bar dimeters. Welded or mechanical connections, if used, should develop the strength of the bar.

307.4 PLACEMENT

The minimum clear distance between parallel bars except in columns should be equal to the nominal diameter of the bar.

In solid unit masonry, vertical reinforcement should be accurately placed and held rigidly in position before work is started. Mechanical devices should be used to maintain correct position. Horizontal reinforcement may be placed as the work progresses.

In hollow unit masonry, vertical reinforcement may be placed after cleaning cores and before inspection of cores occurs. Vertical reinforcement should be accurately placed and should be held in position at top and bottom and at intervals not to exceed 192 diameters of the reinforcement, 6 ft for #3 bars, 8 ft for #4 bars, and 10 ft for #5 bars. Horizontal reinforcement may be placed as the work progresses. Corrosion resistant fabricated welded wire mesh may be used in horizontal joints fully embedded in the mortar bed joints.

When mechanical devices are used to hold reinforcement in place care should be used to see that they do not inhibit the flow of grout.

307.5 CLEARANCE

For wall reinforcement the thickness of grout between masonry units and reinforcement should be not less than 1/4 in. In beams, girders, etc., the clearance around the reinforcement should be not less than one-half of the bar diameter, with a minimum of 1/2 in. or the maximum size of aggregate, whichever is greater. Reinforcement in horizontal joints should be kept back at least 1/2 in. from the face of the masonry. 3/16 in. maximum reinforcement may be used in 3/8 in. mortar joints. 1/4 in. maximum reinforcement may be used in 1/2 in. mortar joints.

SECTION 308 - ALIGNMENT

308.1 CONTROLLING JOINT THICKNESS

Proper use of a story pole with a tight stretched line should be used to provide control of joint thickness. Nylon line is recommended.

308.2 VERTICAL AND HORIZONTAL WALL ALIGNMENT

All masonry work should be plumb, level, straight and true to dimensions shown on the plans. Masonry should not vary more than the thickness of a mortar joint nor more than 1/2 in from plumb in each 12 ft height, nor more than the thickness of a mortar joint in length or 1/2 in. from line in each 36 ft length.

All hollow unit masonry should be built to preserve the unobstructed vertical continuity of the cores which are to be filled.

SECTION 309 - BONDING

309.1 RUNNING

In running bond or 1/2 bond vertical joints occur at center of stretchers in alternate courses.

In grouted masonry, headers should not be used since the bonding is accomplished by means of the grout.

Bond of masonry units in a single wythe should be provided by lapping units in successive vertical courses.

309.2 OFF-SET

Where bonding is not shown on the plans the bond should consist of stretcher courses plus one header at corner in alternate courses which would result in off-set bonding where the length of the brick is more than twice its width.

One-third bond or one-quarter bond is considered off-set bond.

309.3 STACK

Masonry which is laid in stack bond should have the center lines of vertical joints plumb. In addition to this face brick should be laid equidis-

tant from this center line with not more than 1/8 in. variation in the width of joints, and brick in each separate 'stack' should not vary more than 1/8 in. in length, but the separate 'stacks' may vary in width.

For hollow masonry units where stack bond is indicated, bond beams or approved horizontal joint reinforcement should be provided as a mechanical bond.

Joint reinforcement usually consists of running two #9 wires, which are tied together at 16 in. maximum o.c., in alternate horizontal joints (16 in. o.c. vertically). Bond Beams should be placed at 48 in. on center maximum where no joint reinforcement is used. Where open end units are used bond may be provided by solid grouting.

309.4 RACKING

Racking is a method of building the end of a wall by stepping back each course, so that later work can be built on to it and against it without toothers. Racking is also used in corner leads.

When walls are racked, such as at corner leads and temporary construction openings, the grouting procedure should be the same as for continuous walls. In order to dam the grout at the rack, a brick should be laid across the grout space and the grout should be held down 1-1/2 in. from top of each course. This brick should be removed after the grout has solidified.

Racking should be held to a minimum. Care should be taken that leads at corners or openings are not too high (normally not over about 6 courses). Racking should never be permitted in wall sections that are less than 4 ft long.

309.5 TOOTHING

Toothing is the temporary ending of a wall wherein the units in alternate courses project in vertical alignment. Toothing should not be permitted except when approved by the architect or engineer.

In construction of new work against masonry which has been toothed it requires great skill to make certain that the top and bottom mortar joints are solidly filled with mortar when shoving the units into place since the mortar is apt to be scrapped off when this is done. It is well to use a tool to make certain that the mortar is compressed into these connecting joints. In brickwork the toothed wall should be dampened before the new work is laid.

309.6 MECHANICAL

Mechanical bonding should be obtained by use of corrosion resistant metal ties laid in the horizontal mortar joints. Such ties are required when the grout pour is excessive in wall construction of wythes where the width exceeds 2 in. or the height of the grout pour exceeds 12 in. Metal ties bonding wythes together should be placed at 12 in. maximum o.c. horizontally. See Section 309.3 for Stack bond.

SECTION 310 - JOINTS

310.1 BED

Bed joints should have sufficient mortar to provide for solid embedment of the units such that extrusions into the grout space will not exceed three-eighths inch.

Grouted Solid Masonry Units

Mortar in all bed joints should be held back 1/4 in. from edges of brick adjacent to grout space, or should be bevelled back and upward from the grout space. Use extreme care to keep mortar droppings out of grout space. The thickness of bed joint should be as specified or shown. Bed joints should not be furrowed. All brick should be shoved at least one-half inch into place.

Hollow Unit Masonry

All units should be laid plumb with full face shell mortar beds. Cross webs adjacent to vertical cores which are to be filled with grout should be fully bedded in mortar to prevent leakage of grout.

310.2 HEAD

Head joints should have sufficient mortar to fill solidly the joints of the units such that extrusions into the grout space will not exceed three-eighths inch.

In grouted solid masonry units, the thickness of the head joints should be as specified or shown. Head joints specified or shown to be less than 5/8 in. thick should be solidly filled with mortar as brick are laid. Head joints 5/8 in. or more in thickness may have mortar sufficient only to form dams to retain the grout.

In hollow unit masonry, all head (or end) joints should be filled solidly with mortar for a distance in from the face of the unit or wall of not less than the thickness of the longitudinal face shells. In beams and girders, head joints should be solidly filled. This may be done by adding enough mortar to each edge to fill to the center when shoved into position.

310.3 INTERIOR

Interior or wall or collar joints should be filled solidly with grout.

Where walls are of three or more wythes, the two outside wythes are laid and the grout should be poured in the grout space in the customary manner. Immediately brick should be floated into place by pushing the brick an inch to an inch and a half down into the grout.

Where grout space is more than about $2\frac{1}{2}$ in. in width, brick or pieces of brick may be embedded into the grout.

In hollow unit masonry the interior cross joints surrounding cells which are to be filled with grout should be filled solidly with mortar.

310.4 MOVING UNITS AFTER PLACING

Masonry units should not be moved after they have come in intimate contact with the mortar. It is permissible to tap the units downward, but

not to rock or slide, as this breaks the bond. Nothing breaks the bond more certainly than moving the units after laying.

Where units are required to be moved for leveling or alignment they should be removed, cleaned of all mortar and reset in fresh mortar.

310.5 TOOLING

Exterior joints should be tooled with a tool jointer while the mortar is thumb print fresh, compacting the mortar into the joint and against the masonry units with firm pressure. All tooling should be done with a clean, preferably stainless steel, joint tool, with the same size and type used for the whole job as specified.

Joints not exposed to the weather may be either tooled or struck with a trowel.

Joints of masonry to be plastered may be cut flush.

Where joints are raked, the raking should be immediately followed by tooling with a flat jointing tool. Deeply raked joints, weeping, or squeezed or extruded joints are difficult to waterproof and should be used with caution.

Joints should be tooled with a jointing runner 2 ft long, pressing the excess mortar out of the joint rather than dragging it out.

The primary object of tooling is to produce weather tightness of joints.

310.6 JOINING NEW AND OLD WORK

The intersection of new and old work should be adequately bonded and doweled to provide for continuity of the masonry.

310.7 CONSTRUCTION JOINTS

Where fresh masonry joins masonry that is partially set or totally set, the exposed surface of the finished masonry should be cleaned with a wire brush and dampened when necessary to obtain the best possible bond with the new work. All loose masonry units and mortar should be removed. The grout should be poured to a point about $1\frac{1}{2}$ in. below the top of the course. Construction joints should not be permitted in any beam.

SECTION 311 - CORBELLING

The projection for each course in a corbel should not exceed one in. and the maximum projection should not exceed one-third of the total thickness of the wall when used to support structural members, unless specifically designed and detailed, by the engineer, as to method of construction.

SECTION 312 - CHASES AND RECESSES

Chases and recesses in masonry walls should not be constructed so as to reduce the required strength, thickness or fire resistance of the wall.

Chases and recesses should be designed and constructed as openings. Wood nailers should not be inserted into masonry walls. Metal nailing clips may be used.

Wood beams and joists should preferably not be inserted in masonry walls. Where this is required the design of the wall should take the wood into consideration and pockets should be provided with proper clearances.

SECTION 313 - ARCHES AND LINTELS

Lintels over openings should be of reinforced masonry or other incombustible materials.

Masonry arches with sufficient abutments may be used to support masonry.

No wood members or materials that deteriorate with time should be used to support masonry.

SECTION 314 - WALL THICKNESS

The thickness of a wall is made up of wythes of brick and grout or face shells and grout and for arbitrary and nominal dimensions is called to the nearest inch. In design the actual thickness should be used.

Consideration should be given to the reduction of wall thickness such as would be caused by raked joints.

SECTION 315 - ADJOINING CONSTRUCTION

315.1 JOINING CONCRETE AND MASONRY

Wherever feasible the concrete should be poured against masonry and adequately dowelled. Where the masonry must be placed against the concrete extreme care should be used to insure adequate bonding of the masonry to the concrete, by doweling, or bolts or other connections.

315.2 JOINING STRUCTURAL STEEL AND MASONRY

Where structural steel columns are adjacent to masonry, there should be a space of one inch clearance to be filled solidly with mortar to allow for steel tolerances, or with an expansion joint material where a control joint is designed. The structural steel should be connected to the masonry by bolts, extending past vertical reinforcing, and through staggered slotted holes in column flange, or by plates welded to column with holes for horizontal reinforcement, or similar detail.

Imbedding structural steel columns partially in masonry is not recommended, unless special reinforcing is provided, and a construction joint is provided in the masonry at this point.

Structural steel columns entirely within masonry are usually connected by dowels welded to columns for horizontal reinforcing. Where the steel column is larger than the core in hollow unit masonry and is within 3 in. of the face of solid unit masonry walls, construction joints should be provided to control cracking of masonry at this point.

315.3 BOLTS AND ANCHORS

All bolts and anchors, etc., should be accurately set into the masonry as the work progresses and should be thoroughly embedded in mortar or grout. When more than 2 bolts occur in a group templates should be used.

Bolts set vertically in walls, pilasters, or columns should be set inside horizontal reinforcing steel or ties and should not be placed closer than 3 in. from the face of the masonry. All vertical bolts should be solidly grouted in position.

Horizontal bolts should be embedded as shown on plans, but not less than two-thirds of the wall thickness. In hollow units, horizontal bolts should be grouted below and above for solid embedment. Horizontal bolts should be embedded solidly in the mortar bed and into the grout space.

315.4 PIPES AND CONDUITS

No pipe or conduit should be embedded in any structural masonry or required fire protection.

Exceptions

Rigid electric conduits may be embedded in structural masonry when their location has been detailed on the approved plans.

Any pipe or conduit may pass vertically or horizontally through any masonry by means of a sleeve at least large enough to pass any hub or coupling on the pipe line. Such sleeves should be placed not closer than three diameters, center to center, nor should they unduly impair the strength of construction, and their location should be detailed on the plans.

Placement of pipes or conduits in unfilled cores of hollow unit masonry should not be considered as embedment.

315.5 BEARING PLATES

Beams, girders, or other concentrated loads supported by a wall. or pier should have bearing at least three in. in length onto the masonry. Metal bearing plate or a continuous reinforced masonry member may be used to distribute the loads along the wall. Bearing plates larger than required for design stresses are often needed to provide for anchorage. Solid dry pack should be used under bearing plates.

315.6 WINDOWS AND DOORS

The jambs, heads and sills of masonry openings should be protected from damage during construction, especially where workmen, materials or equipment are apt to pass through the openings.

Window and door openings should be braced during construction to prevent movement. Window and door frames should be anchored to masonry at a maximum spacing of 24 in. on center. Anchorage of metal frames often require placing the frame before laying the masonry.

SECTION 316 - WALL CARE

316.1 DURING ERECTION

Care should be exercised to protect the faces of the masonry from being smeared or splattered with mortar, grout, or splashings from scaffolds; should this occur, the faces should be immediately cleaned before the mortar or grout has set.

All sills, ledges, offsets, other materials, etc., should be protected from mortar droppings during construction.

The tops of all unfinished masonry should be protected from rain, snow, or other foreign material.

No construction supports should be attached to the wall except where specifically permitted by the architect or engineer.

All forms should be made tight (special attention is necessary for bottom form of block bond beams) and concrete and grout spilled on the wall should be washed off before it can set up.

316.2 CURING

Masonry walls should not be wetted down after construction is completed, except in extreme hot weather when the walls should have their surfaces dampened with a light fog spray for a curing period of three days such that the water does not run down the surface. There is more than enough water in grouted masonry to completely hydrate the cement if the water is retained.

316.3 FREEZING

Adequate equipment should be provided for heating the masonry materials and protecting the masonry during freezing or near freezing weather. No frozen materials nor materials containing ice should be used.

Sand should be heated in such a manner as to remove frost or ice. Water or sand should not be heated to a temperature above 160°F. When necessary to remove frost, the masonry units should be heated.

Whenever the temperature of the surrounding air is below 40°F., all newly constructed reinforced masonry laid in mortar, in which high-early-strength portland cement is used, should be maintained at a temperature of at least 50°F for not less than 24 hours by means of enclosures, artificial heat, or by other protective methods as will meet the approval of the building official. When any cementing material other than high-early-strength portland cement is used, these temperatures should be maintained for at least 72 hours.

All methods and materials for the protection of the fresh masonry work against freezing should be subject to the approval of the local building official. In general the methods and materials now commonly accepted as suitable for the protection of reinforced concrete construction in freezing weather should be used. Salt or other chemical for lowering the freezing temperature of the mortar should not be used. Calcium chloride in excess of 2 percent by weight of portland cement should not be used to obtain high early strength of grout or mortar.

316.4 FINISH

During construction or immediately after completion of a section of masonry all line pin holes and any defects in masonry jointing and also connections to other materials should be carefully and solidly filled with mortar to match the existing work. A capping unit or 1 in. minimm concrete cap or some other means must be used at the top of a wall to keep water from penetrating down into the interior of the wall.

316.5 POINTING

It is recommended that prehydrated mortar be used for pointing. Open joints should be pointed in two operations. The joints should be half filled solidly and the next day the joints should be completely filled and tooled. Prehydrated mortar is obtained by mixing the materials with one-half of the mixing water, left to stand for one hour and then mixed with the remaining water.

316.6 CLEANING

At the completion of masonry work, the contractor should clean down all masonry work, remove his scaffolding and equipment, clean up all debris, refuse and surplus material and remove them from the premises.

Cleaning of masonry should be done about 10 days after the completion of masonry erection.

Acid Washing

To remove mortar or cement stains, wash with water, then while still wet, scrub with a non-metallic brush with a 10 percent muriatic acid and water solution, then immediately and thoroughly wash again with clean water. Extreme care must be used to prevent this acid solution from contacting dry brickwork, and thus prevent possible permanent stains. Acid washing should only be used on burned clay brick.

Sandblasting

After masonry is thoroughly dry, all exterior brick masonry may be lightly sandblasted sufficiently to remove all mortar, grout or other stains, to produce a uniformly clean surface. Other work should be protected from sandblasting, both directly and from sand re-bound.

316.7 EFFLORESCENCE

Where efflorescence appears on newly constructed masonry no attempt should be made to remove it until the masonry has become reasonably dry. Under certain conditions of temperature and humidity such efflorescence will disappear in the matter of a month or two. Efflorescence has no effect on the strength of masonry.

If the joints are properly tooled such efflorescence can be frequently removed by hosing down with water. The amount of efflorescence may be reduced by using low alkali portland cement, by using water free from salts, by tooling all exterior mortar joints, by not wetting grouted masonry during or immediately after construction, by protecting the tops of unfinished work, and by sealing the tops of uncovered finished work.

Green stains may be removed by washing the stains with a bleaching agent. Manufacturer's recommendation should be obtained.

316.8 PAINTING AND WATERPROOFING

Preparation of Masonry Surfaces

Before any painting or waterproofing is done, the masonry should be inspected by the applicator to determine the condition of the masonry, and steps, as required, should be taken for the best possible application of paint or waterproofing.

All mortar joints should be solidly filled and tooled. All loose mortar and dirt should be removed by light sandblasting or scraping and brushing. Wire-brushes should not be used. All efflorescence should be removed. Masonry surfaces should have a temperature of not less than 55°F. at time of painting or waterproofing.

CHAPTER 4 - DESIGN

SECTION 401 - GENERAL

401.1 THEORY

In presenting recommendations for design, consideration has been given to such recent developments as ultimate strength, limit, and plastic design. It is felt that until reinforced masonry is more generally accepted and used, it is better to use accepted formula with the straight line theory of elastic design. However, tests all indicate that the same general principles of design as are used in reinforced concrete apply to reinforced masonry so that any method of design proven for reinforced concrete can be adapted to reinforced masonry.

In this chapter the principal points of discussion will center around items that may appear to differ from the design of reinforced concrete. This is not a building code and in hurricane and earthquake areas building codes should be checked for more rigid requirements.

401.2 ASSUMPTIONS

1. Except in deep beams plane sections before bending remain plane after bending. Fibre strains are directly proportional to their distance from the neutral axis. (A deep beam is herein defined as one in which the span to depth ratio is less than three to one).

2. Compressive stresses in the masonry, mortar and grout, and tensile and/or compressive stresses in the steel (or in unreinforced masonry) are directly proportional to the strains.

3. The bond between the various elements is such that they will work together as a homogeneous material within the range of working stresses.

4. The modulus of elasticity of the masonry, mortar and grout is constant throughout the member within the working stresses.

5. Stress in a reinforcing bar is assumed uniform over its area.

6. The member is straight and of uniform cross-section, or proper consideration shall be made for curving or haunching.

7. External forces are in equilibrium.

8. In reinforced portions of a member, the masonry carries no tensile stress.

9. Net section is used in design.

401.3 DISCUSSION OF ASSUMPTIONS

It is important to keep in mind that the bond between the various elements in masonry is assumed to act together only in the range of working stresses. As a reinforced masonry structural element reaches its ultimate capacity there is seen quite often the phenomenon of separation of materials. This should be expected since the strengths and moduli of elasticity are quite generally different for the component parts in the upper limits of stress.

The fact that bond is adequate for masonry materials to work together is demonstrated by test and is assured by keeping the allowable working stresses low enough to be safe for the weakest element. Care must also be exercised to see that workmanship complies with that specified.

The assumption that masonry carries no tensile stress is ultra conservative in most cases and may lead to erroneous conclusions. It is recognized that unreinforced masonry can develop some tensile value even in stack bond, and more in running bond. Where the reinforcing steel is located at the center of a wall, for example, the wall would necessarily (on basis of assumption of no tension) crack approximately 3/4 of the way through the wall before the steel would be effective in resisting bending stresses. Therefore, it would seem better design to admit the fact that masonry may take some tensile force and proportion steel accordingly, but for ease of design it is generally not done. Reinforcement is necessary in some portions of plain masonry so that the internal forces do not cause cracks which would destroy the tensile strength that would otherwise exist. Also it is necessary to provide resistance to concentration of force, as around openings in walls.

Very often the span of a reinforced member is not large compared to depth; therefore some distinct consideration must be given to short deep members, or thin deep members (e.g. buckling).

The use of net section in design of reinforced hollow masonry is important in several aspects. Masonry mortar joints are sometimes raked to give a particular architectural appearance, and this results in a greatly reduced effective thickness of wall. This is particularly critical for forces perpendicular to the wall, such as wind. In designing beams and columns the depth of the raked joint is usually all that needs consideration in arriving at net section, since these structural elements should be solid grouted, and in such cases the grout, mortar and masonry units are considered as acting together to resist stresses. In designing lintels only that portion which is solid grouted is considered, therefore, it is the same as a solid masonry beam. In designing walls the applicable net section becomes important. For compression stresses on a wall only the net area of the wall should be considered, including masonry unit

area plus solid grouted portions. For flexural stresses perpendicular to the wall the net section would include the masonry unit area within the wall section considered plus the solid grouted cores. This calculation can generally be reduced considerably when it is noted that for a vertical bar at the center of the wall the neutral axis is approximately at the inside of the face shell and thus can be considered as a T-beam. For shear the net section includes all cross webs within the design area as defined in Section 405.2 plus the grouted core. For shear stresses parallel to a masonry wall the gross area of wall minus the hollow cells which are not grouted is taken as the net section.

SECTION 402 - LOADS

402.1 COMBINATION OF LOADS

The provisions for design herein specified are based on the assumption that all structures shall be designed for all the dead and live loads to which they may reasonably be expected to be subjected. Wind, blast, and earthquake need not be assumed as occurring simultaneously.

For stresses due to wind, quake, or blast combined with dead and with real live load, the allowable stresses may be increased one third. Real live loads here refers to loads which are called live loads in the design but which actually have a degree of permanence, such as storage loads, where it may be assumed that one-half of the load is always present on the structure, and thus probably present when the earthquake occurs. Normal roof live load other than snow need not be considered as occurring with wind, earthquake, or blast.

402.2 DEAD LOADS

In computing the weight of masonry it should be remembered that the masonry unit is only part of the weight and that mortar, grout and reinforcing steel generally weigh the same whether light or heavy masonry units are specified. (A list of dead loads is set forth in American Standards Association Code A 58.1).

402.3 WIND

The wind load should be that recognized by local building code authorities and in accordance with the principles set forth in the American Standards Association Code A 58.1.

402.4 SEISMIC

Earthquake loads must be carefully considered, preferably by a code which includes effect of building frequency such as recommended by the Structural Engineers Association of California Committee Report.

Masonry walls acting as shear walls in the direction of earthquake motion may contribute great stiffness, with associated rapid periods and small permissible deflections. The motion normal to the wall may have slow periods due to mass and also greater permissible deflections. If the period is such that the response factor is high, the loads assumed,

i.e., inertia, must be high due to the generally large masses or weights of masonry.

Specific formulae for determining horizontal forces from earthquake loads are to be found in the local building codes of seismic zones.

402.5 CONCENTRATED LOAD

For calculating wall stresses, vertical concentrated loads may be assumed to be distributed over a length of wall not exceeding the center to center distance between loads nor one-half the height of the wall measured from the floor to the bearing plate.

Concentrated load should not be assumed distributed across a continuous vertical joint, such as in stack bond, unless reinforced elements are designed to distribute the load.

In walls laid in running bond, where there is no distributing member under the load, the length of wall considered as supporting a concentrated load should not exceed the width of bearing plus four times the wall thickness.

402.6 SHOCK AND BLAST

In general the resistance of reinforced masonry is very good, the reinforcing ties it together while inertia and arching add resistance. More research is needed before specific recommendations can be made.

402.7 ECCENTRIC LOADS

The effect of eccentric attachments to reinforced masonry should be considered, such as, supporting a roof or floor on a ledger placed at one face of a masonry wall. This is an example of eccentricity that is often overlooked and a fact that should be considered in design.

SECTION 403 - FORMULAE

403.1 NOMENCLATURE

A = area of wall section, t x d

a = diameter of reinforcing bar

A_g = gross area of masonry section

A_s = area of steel reinforcement

A'_s = area of compressive steel reinforcement in flexural members

A_v = area of web reinforcement

b = width of rectangular beam or width of flange of T-beams

b' = width of web in T-beams (used in flexural computations)

d = effective depth of flexural members

d' = distance from extreme compressive fiber to compressive reinment

e = eccentricity measured from gravity axis

E_m = modulus of elasticity of masonry in compression

E_s = modulus of elasticity of steel

E_v = modulus of elasticity of masonry in shear

f_a = computed axial stress in masonry

f_m = compressive stress in extreme fiber of masonry

f'_m = approved ultimate compressive strength of masonry

f_s = stress in steel reinforcement

f'_s = stress in compressive reinforcement in flexural members

f_v = stress in web reinforcement

F_a = allowable axial unit stress in masonry

F_m = allowable flexural unit stress in masonry

h = unsupported height of wall or column; also width of bond beams

h' = effective clear height

H = horizontal load

I = moment of inertia of the gross section, neglecting reinforcement

j = ratio of distance between centroid of compression and centroid of tension stresses to the effective depth (d)

k = ratio of distance between extreme compressive fiber and neutral axis to effective depth

l = clear span

M = external moment

M_m = moment as governed by masonry

M_s = moment as governed by reinforcing steel

M'_s = moment as governed by compression in reinforcing steel

n = ratio of modulus of elasticity of steel (E_s) to that of masonry (E_m) = E_s/E_m

Σ = sum of perimeters of bars

p = ratio of steel reinforcement

p_g = ratio of effective cross-sectional area of the vertical reinforcement to the gross area of the column

P = total axial load

s = spacing of stirrups, parallel to direction of main reinforcement

t = over-all dimension of columns; also thickness of wall

u = bond stress per unit of surface area of bar

v   = unit shearing stress

v_m = shearing stress in masonry

V   = total shear

w   = uniformly distributed unit load

W   = total uniformly distributed loads

403.2 (a) GENERAL EQUATIONS

Moment may be computed in accordance with elastic principles or for general conditions, where the longer of any two spans does not exceed the shorter by more than twenty percent, the following formulae may be used.

One span -------------------- $\dfrac{w\,l^2}{8}$ @ midspan

Two spans ------------------- $\dfrac{w\,l^2}{8}$ @ interior support

------------------- $\dfrac{w\,l^2}{10}$ @ midspan

More than two spans---------- $\dfrac{w\,l^2}{12}$ @ face of interior support and center of interior spans

------------------- $\dfrac{w\,l^2}{10}$ @ midspans of end spans

Shear, end member at interior support--------- $\dfrac{1.2\,w\,l}{2}$

Shear, at other supports------- $\dfrac{w\,l}{2}$

(b) FLEXURAL FORMULAE

$A_v = V_S/(f_v\,j\,d)\,(\text{stirrups})$

$M_S = A_S\,f_S\,j\,d$

$n = E_S/E_m$

$p = A_S/(b\,d)$

$j = 1 - (k/3)$

$u = V/(\Sigma\,o\,j\,d)$

$f'_S = 2\,f_S\,(k\,d-d')/(d-k\,d)$

$A'_S = \left(M'_S/f'_S\right)(d-d')\left(\dfrac{n-1}{n}\right)$

$M_m = j\,k\,b\,d^2\,f_m/2$

$v = V/(b\,j\,d)$

(c) COMBINED AXIAL AND FLEXURAL

$f_a/F_a + f_m/F_m$ shall not exceed 1.0

(d) DEFLECTION FORMULAE (See Section 406.4)

For concentrated horizontal load at top and full fixity at top and bottom

Moment deflection = $H h^3 / (12 E_m I)$

Shear deflection = $1.2 H h/(A E_v)$

For concentrated horizontal load at top and full fixity at the top and a pinned condition at the bottom, or vice versa

Moment deflection = $H h^3/(3 E_m I)$

Shear deflection = $1.2 H h/(A E_v)$

(e) AXIAL FORMULAE

(See Section 406.)

SECTION 404 - STRESS ALLOWABLE

404.1 DISCUSSION

The actual serviceability of any reinforced masonry structure is a function of the material, the design, the workmanship and the use. It is recognized that the elements which make up masonry and reinforced masonry itself develop high strengths in compression, but this alone does not serve as means of determining allowable stresses.

Material has been discussed under Chapter 2 and Workmanship under Chapter 3 of this report. In setting forth allowable stresses it is assumed that both materials and workmanship will be of very good quality. If for some reason materials or workmanship are to be questioned as to their quality, then proper reduction in allowable stresses must be made, or full scale tests should be carried out. The omission of reinforcing steel, grout, or mortar cannot be provided for by a reduction in stresses. There must be proper inspection to insure good workmanship. It is assumed that the designer is qualified and no reduction is made in allowable stresses for his possible incompetence. It is felt that the owner or lessee may misuse the structure by overloading on occasion; therefore some account of this is necessary in choosing allowable stresses.

There are three ways set forth in this Section to determine the stresses which the designer can use as a guide. The first two methods involve a determination of f'_m (see Section 404.2). The third method assumes a selection of quality specified materials. This is the general approach method used in earthquake zones at the present time (see Section 404.4).

404.2 DETERMINATION OF f'_m

(a) BY TEST OF MASONRY ASSEMBLAGES

Preliminary compression tests may be performed on masonry prisms as specified in Sections 506 and 507 to determine f'_m. When this method is used the designer must be certain that the materials used in the test are of the same quality as those to be used in the completed structure. The design values are obtained from Section 404.3.

(b) BY TEST OF MASONRY UNITS

The value of f'_m may be interpolated from Table 1 when preliminary tests have been made on the masonry units. This table is limited to units testing 6000 psi, with the intention that where higher strengths are desired, the masonry assemblage should have preliminary tests to determine f'_m. These values are also limited by the footnote so that f'_m shall not exceed the compressive strength of the mortar or grout. This limitation is felt necessary since types of mortar and grout are only

TABLE 1

Compressive Strength of Units[*]	Assumed f'_m [**]
1,000	900
1,500	1,150
2,500	1,550
4,000	2,000
6,000	2,400

[*]   Compressive strength is here taken on the gross area of solid masonry units and the net area of hollow masonry units.
[**] In no case shall the assumed f'_m be greater than the compressive strength of the mortar or grout, whichever is lesser.

suggested in this report and where higher values are desired, they should be obtained by actual tests of the masonry assemblage.

404.3 ALLOWABLE STRESSES AS RELATED TO f'_m

Compression - axial	$0.20\,f'_m$
Compression - flexural	$0.33\,f'_m$
Shear (no shear reinforcement)	$0.02\,f'_m$ (maximum 40 psi)
Shear (with reinforcement taking entire shear)	$0.05\,f'_m$ (maximum 100 psi)
Bearing	$0.25\,f'_m$
Modulus of Elasticity	$1,000\,f'_m$
Modulus of Rigidity	$400\,f'_m$
Bond - plain bars	60 psi
Bond - deformed bars	160 psi

404.4 ALLOWABLE STRESSES FOR A SPECIFIED REINFORCED MASONRY CONSTRUCTION

The following allowable stresses may be used where Brick units conform to Grade MW ASTM C62-, or Hollow Concrete units conform to Grade A ASTM C90-; the mortar conforms to Section 205, the grout conforms to Section 206, and the construction practices conform to those recommended in Chapter 3 of this report.

Compression - axial	300
Compression - flexural	500
Shear (no shear reinforcement)	30
Shear (with reinforcement taking entire shear)	75
Bearing	375
Modulus of Elasticity	1,500,000
Modulus of Rigidity	600,000
Bond - plain bars	60
Bond - deformed bars	160

SECTION 405 - STANDARD MINIMUM REQUIREMENTS

405.1 COLUMNS

If the load on the pilaster can be carried by a length of wall equal to 4 times the thickness of the wall, then the pilaster is in essence only constructed for convenience of connections and/or to remove eccentricity from the wall. In this case the pilaster is nominal in size and reinforcing. Otherwise the pilaster must be designed and considered a column.

Masonry columns should have a minimum nominal dimension of 12 in. and a maximum height of 20 times their least dimension. Columns which are stressed to less than 1/2 of their allowable stress may have an 8 in. minimum dimension.

Vertical reinforcement should be a minimum of 1/2 of one percent and a maximum of 4% of the gross cross-sectional area of the column.

Columns which are stressed to less than 1/2 of their allowable stresses may have their reinforcement reduced to not less then 1/5 of one percent.

In all cases the reinforcement of columns should not be less than 4 bars of 3/8 in. minimum diameter.

Lateral ties should be not less than #9 wire and should be spaced apart not over 16 bar diameters, 48 tie diameters, or the least dimension of the column. Ties may be placed in the mortar joint or in contact with the vertical steel.

405.2 WALLS

Reinforced masonry shear and bearing walls should be limited by a ratio of height to thickness of 25, where the word "height" is taken to mean the clear distance between lateral supports. The minimum thickness of bearing walls should be 6 inches.

Reinforced masonry non-bearing walls should be limited by a ratio of height to thickness of 48, for interior walls and 30 for exterior walls.

In computing flexural stresses where reinforcement occurs, the effective width should be not greater than four times the wall thickness, the center to center distance between reinforcement, nor 48 in. Where stack bond is used, the effective width should be not greater than 3 times the unit length nor 24 in. in solid unit masonry, and not greater than 1-1/2 times the unit length nor 24 in. in hollow unit masonry.

The spacing of vertical reinforcement should be not greater than 8 ft nor 12 times the wall thickness. The minimum size of vertical bars should be 3/8 in. diameter. The minimum amount of vertical reinforcement should be one-twentieth of one percent of the gross cross-sectional horizontal area of the masonry portion of the wall. There should be a minimum of one vertical bar continuous between lateral supports and each side each opening and each corner.

The spacing of horizontal reinforcement should be not greater than 8 ft. The minimum amount of horizontal reinforcement should be one-tenth of one percent of the gross cross-sectional vertical area of the wall. There should be continuous horizontal reinforcement at the top of the foundation wall, at each floor level, at the roof level, at the top of the wall, and at the lintel height. Horizontal reinforcement should be distributed in the wall in approximatee conformity with the cross-sectional area of the wall. Wire reinforcement in the horizontal joints may be considered as part of the arbitrarily required horizontal reinforcement where it has trussed cross-wires or cross-wires perpendicular to the longitudinal wires providing not less than one cross-wire in each 16 in. length welded to the two longitudinal wires, but shall not be used to resist design loads, other than shear. Where wire reinforcement is used it should be spaced not more than 24 in. on center vertically.

The percentage of vertical reinforcement recommended here is some less than has been used in building codes since it is felt that design criteria should control the vertical reinforcement. Temperature and shrinkage reinforcement are not required in the vertical direction. Eight feet is the maximum spacing suggested on the basis that wind stresses against an unreinforced masonry wall set this limit and also it is necessary to limit this spacing in order to properly bind the wall together and distribute stresses. The percentage of horizontal reinforcement recommended is twice the vertical reinforcement since here temperature and shrinkage reinforcement are required and these generally are established by arbitrary requirements.

405.3 BEAMS

The longitudinal reinforcement in a reinforced masonry beam should not be less than one-fifth of one percent of the gross cross-sectional area, nor less than four-tenths of one square inch. The minimum depth should be 8 in. and the minimum width should be 6 in. Wall reinforcement may be used as beam reinforcement, for both shear and flexure, when the beam is an integral part of a reinforced masonry wall, except that wire reinforcement should not be considered as resisting design stresses, other than shear.

405.4 CONTRACTION JOINTS

Some has been written and much has been said about contraction joints in masonry. The solution to the problem is one in which the designer must use his best judgment. A few suggestions are made as a guide only. Thermal, moisture and other movements in a wall are related to the boundary condition of restraint, the uniformity of the mass of the masonry, the thermal coefficient and the shrinkage coefficient of the masonry, the extensibility of the masonry, the weather conditions during and after construction, the type of workmanship, the use of the structure, etc. Where there is a large change in the mass of the wall, such as at large truck doors, contraction joints should be provided. The average reinforced masonry building which is less than 100 feet long generally can be designed with sufficient reinforcement to make contraction joints unnecessary. Where contraction joints are provided they should be spaced at 50 ft on center maximum, and their location should be at critical changes in cross section.

SECTION 406 - VERTICAL LOAD DESIGN

406.1 AXIAL STRESSES

Axial load formulae such as $P = A_g F_m + A_s F_s$ are obviously not correct nor precise for the relationship of steel stress and masonry stress.

Since the uncertain effect of workmanship would affect the compression strength of masonry less than the bond and tension values there is probably a greater factor of safety in compression than in other stress values. Also, since bond on the newer type bars, especially with the improved techniques of placing, is a vast improvement over older consideration it seems more reasonable to use values of masonry compression and column steel compression more nearly comparable to the comparable moduli, i.e., stress resulting from strain.

if $f_m = 0.2 f'_m$ and $E_m = 1000 f'_m$ and $n = E_s/E_m$;

then $f_s = 30,000,000 \times 0.2 f_m/1000$ or $= 6000$

However, as in comparable concrete column formulae, the steel may be assumed to contribute more, not 20,000 psi perhaps, but 12,000 psi in the grout. Such compromise is recognized and accepted as in the doubling of allowable compression stress in the flexure formulae for beams with compression reinforcement.

Column formulae have been devised involving the percentage of reinforcement in the ties and are available in the ASA Standard A 41.2, however, here we give a simpler formula which has been found adequate. This type of formula is the one which has been used for many years by Engineers in earthquake areas. Another approach to column design is to design the concrete core in accordance with the requirements for concrete columns and consider the masonry as a form only. If this design is used the stress in the column as a masonry column should be checked and in no case should exceed twice the allowable for a masonry column.

Allowable axial load on columns

$$F = A_g \left(0.18 \, f'_m + 0.65 \, f_s \, p_g \right) \left[1 - (h'/30 \, t)^3 \right]$$

The h' for the above equation is the effective clear height which is re-
lated to the actual clear unsupported height as follows:

h' = 1.0 h for pin ended columns
h' = 0.5 h for fixed ended columns
h' = 0.75 h for column fixed one end pinned at other
h' = 2.00 h for cantilever column
h' = 1.8 h for cantilever column guided at top

Due to the fact that columns are frequently fastened top and bottom
and have loads that put compression across the entire face, the general
value for h' is 0.75 h. It is well for the designer to frequently remind
himself that all eccentricities and moments must be considered in his
design.

For the axial load on walls the steel is not considered as adding to the
compression strength and

$$P = 0.20 \, f'_m \left[1 - (h'/30 \, t)^3 \right]$$

except that when reinforced as columns the stresses may be as for
columns. The area of wall considered to act as column area shall be not
further from the column reinforcing than the least dimension of the
column core.

406.2 FLEXURAL STRESSES

The bending moments may be calculated by the moment coefficients
or by the principles of continuity and elasticity.

The span length of freely supported beams shall be the clear span
plus 1/2 the depth of the beam, but not exceeding the center to center
distance of supports.

In the application of continuity, the center to center distance may be
used for moment distribution (with due consideration for haunching).
Governing moments for the end portions of beams and girders, however,
shall be those at the face of supports.

The clear distance between lateral supports of the compression
flange shall not be greater than 32 times the width of the compression
flange.

The compression value of steel reinforcing may be taken at twice the
value indicated by the elastic ratio, but not to exceed the allowable ten-
sion value.

406.3 SHEAR

True shear seldom occurs in masonry but is rather a term which is
generally used to control diagonal tension. There seems to be a relation-
ship between compression and shear. Certainly at points where there
is no compression such as at points of inflection in continuous beams
reinforcement should be designed to take all of the shear. Since so little

is known of the actual characteristics of shear (diagonal tension) failure it is deemed best to keep the allowable stresses low where no shear reinforcement is used (as shown in Section 404) and when these are exceeded, use reinforcement to take the entire shear. According to tests reviewed by the Committee shear values set forth in the tables are low enough to be applicable to walls as well as beams.

406.4 DEFLECTION

When spans are long relative to the depth they should be checked for deflection. It is recommended that the moment of inertia of the masonry cross section be computed (neglect the effect of the reinforcement) and then use the standard deflection formula. Vertical deflection in reinforced masonry should not exceed 1/600 of the span nor a total of 0.3 inches.

Deflection formulae for wall sections and columns are given in Section 403.2. These formulae are used to determine the distribution of horizontal loads.

406.5 COMBINED STRESSES

All members should be designed to resist the combination of axial and flexural loads to which they are subjected. The bending moments due to eccentric loads and end conditions should be determined as for rigid frames or other forms of continuous structures.

Stresses due to axial and flexural stresses should be combined as set forth in the equation in Section 403.2. Where e/t is less than 1/3, the design may be based on the uncracked section.

SECTION 407 – HORIZONTAL FORCE DESIGN

407.1 GENERAL

This section is not intended to cover completely the requirements for horizontal force design. Such considerations are outlined in detail in other standards and in the various codes having jurisdiction over the local design. This is to be merely a general discussion to guide those individuals from areas in which slight consideration is given to seismic activity.

All reinforced masonry walls need to be designed for the wind and/or seismic loads to which they may be subjected. The same rules apply in horizontal design as are used in vertical load design. Most important to consider are the concentrations of stresses at each side of openings, at floor and roof levels, and where there are cantilever members (such as parapets).

407.2 HISTORICAL

Early masonry is a very different building material than the modern reinforced masonry, which received great impetus in development in Southern California after the Long Beach quake of 1933. The early "brickwork" was laid up with little consideration of bond, either as to material or method. The mortar could be said to keep the brick apart,

rather than to bond them together. The earlier material would be more similar to piles of children's building blocks rather than to concrete.

No special ingredients nor details were incorporated to tie the units together. Hence, after demolition of early type brick buildings, cleaning of the brick for reuse was a simple chore. Dumping onto the ground from the truck removed the bulk of the soft mortar. The rest was easily removed by hosing, brooming or rubbing.

Reinforced masonry is different. It is well bonded by cement and other ingredients and tied by reinforcing and bonding or laying techniques. Although it looks similar, it functions more as a homogeneous material rather than a heterogeneous group.

Modern buildings of reinforced masonry can be designed to be wind and earthquake resistant, just as can buildings of other materials.

407.3 GENERAL DESIGN CONSIDERATIONS

These are general principles which will minimize earthquake damage. The basic principle is to recognize that earthquakes are ground motion, erratic and sharp, which will shake the building up and down and horizontally. This motion will be transmitted from the foundations to the various parts of the structure, requiring force to overcome the inertia of those parts.

The effect of vertical acceleration is usually disregarded since it merely increases or decreases the vertical load already provided for with considerable factor of safety in the original design. The lateral motion induces distortions not normally considered in such vertical load design.

Wind forces may act in a very similar manner to earthquakes and for design purposes differ only in magnitude and point of application.

It is essential that the building be well tied together, both vertically and horizontally. Portions such as cantilever walls or appendages should be very carefully tied, or eliminated. If they are non-existent, they will cause little trouble.

Provide for symmetrical distribution of masses and resisting elements and, in general, verify that there is a continuous path for the transmission of force from the ground to all parts of the structure. The framing "scheme" must be complete, with no links omitted in the chain.

Provide for separation of wings of buildings or portions with quite different stiffness, or towers with varying natural periods of vibration. Differential motion of portions of building causes impact and hammering with resultant damage.

All walls should be anchored to floor and roof framing frequently enough to take the shear and tension stresses involved. This anchorage should be equivalent to 200 lb per lineal ft of contact area and more if calculated forces show greater stress. Long narrow buildings are hard to brace adequately due to high deflections in the central portion.

Stairs and stair wells must be checked as to detail and connections. They must be flexible enough so that the motion of one floor relative to another will not cause distress, or stiff and strong enough to resist that relative motion; i.e., strong enough to transmit the shear from one level to the other.

407.4 DESIGN CALCULATIONS

For earthquake forces the basis of calculations is to assume that there are lateral forces proportional to the building masses, applied at the center of gravity of such masses, and to solve by elastic principles of design similar to other structural design. The force factor to assume is established by local code. Where the horizontal diaphragms are adequate to take rotation the building is designed for rotation and relative rigidities, otherwise it is customary to design the building assuming that bracing elements resist tributary areas.

Horizontal diaphragms are used to distribute the lateral motion of the masonry walls to cross-walls or other bracing system which will transmit the assumed forces to the ground. Diaphragms usually consist of concrete, steel, or wood, floors, roofs, or truss systems. Concrete floors and roofs make a very rigid diaphragm and readily distribute the horizontal forces to the resisting elements. Steel and wood diaphragms are more flexible and it is recommended that in buildings using them their spring should not exceed four times their width between cross-walls, or other bracing system. Steel decks require a designed welding pattern to distribute the loads. Wood floors and roofs generally consist of plywood or diagonal (laid at 45 degrees with the joist) sheathing and require a designed nailing pattern. Straight (laid at right angle to the joist) sheathing gives little resistance since the moment couple between nails in a board is its only calculable resistance. In the design of the foregoing diaphragms the masonry walls are generally considered as flanges of a deep girder with the diaphragm itself acting as the web. The shear between the web and the flange is a factor in determining the connection to the masonry wall. Horizontal truss systems usually consist of tension rod diagonals, and compression struts. This type of bracing is not generally recommended for masonry buildings because the deflection is usually excessive as compared to the aforementioned systems.

407.5 CODE PROVISIONS

The most commonly accepted code is the Uniform Building Code of the International Building Officials Conference. In their 1961 edition they have adopted earthquake regulations similar to those recommended by the Structural Engineers Association of California.

For earthquake design most of the Building Codes use the formula, the Horizontal Force equals a Constant times the building Weight. The constant factor is usually related to the natural frequency of vibration or probable response of the building to a shaking effect, but some use an arbitrary figure. For one and two story buildings an acceptable formula is $H = 0.133G$, where G equals the dead weight of the structure.

CHAPTER 5 - TEST PROCEDURES

SECTION 501 - GENERAL

This chapter describes some tests which are not found in the American Society of Testing Materials Standards and which have been found to

be very useful in controlling quality of Reinforced Masonry Construc-
tion, also some tests which it is felt will help correlate research.

The field tests on mortar and grout have been used for some time in
California and are important where close inspection and control of ma-
sonry construction is desired. The compression tests on masonry prisms
are used to establish design criteria. (See Section 404.2.) The test on
completed structures is used for the evaluation of the strength of exist-
ing structures. It is recommended by ASA Standard A 41.2.

The Rapid Method Linear Change Test is one which has been devel-
oped to give a method for indicating the volume change characteristics
of concrete units. It does not give the experimentally exact amount of
shrinkage but has proven useful in eliminating highly expansive units
and in reducing undesirable cracking in masonry structures. The test
is recommended by the Concrete Masonry Association of California
and approved by the Association of California Testing and Inspection
Laboratories.

The Tension Test is introduced for research purposes at this time.
It is obvious that almost all of the signs of distress in Reinforced Ma-
sonry Structures are due to tension failures. There is a need to learn
more concerning the tensile quality of masonry. This test has been
used at several laboratories with promise of becoming a useful control
of quality. There is also a need for developing tests on small masonry
assemblages in order to learn more about tension failures. Some work
has been done in this area at the University of California at Los Angeles
and at the Structural Clay Products Research Foundation in Geneva,
Illinois. It is hoped that this type of a test will be included in a later
report.

SECTION 502 - FIELD SLUMP TEST FOR MORTAR

Use a truncated metal cone 4 in. to 2 in, 6 in. high, and after dampen-
ing, place on a flat, moist non-absorbent base. Fill cone with two layers
of mortar, rodding each layer 10 times with a 1/4 in bullet-nosed rod, dis-
tributing strokes uniformly over the cross section and penetrating
underlying layer. Lightly tap cone on opposite sides, level off, care-
fully lift cone and measure slump. At time of using, mortar on the
boards should have a slump of approximately 2-3/4 in. The exact
amount of slump should be established at the start of the construction.

SECTION 503 - FIELD COMPRESSIVE TEST SPECIMEN FOR MORTAR

Spread mortar on the masonry units between 1/2 in. and 3/4 in.
thick and allow to stand for one minute, then remove mortar and place
in a 2 in. x 4 in. cylinder in two layers, compressing the mortar into
the cylinder using a flat end stick or fingers. Lightly tap mold on op-
posite sides, level off and immediately cover molds and keep them
damp until taken to the laboratory. After 48 hours set, have the labora-
tory remove molds, cap the specimens, and place them in the fog room
until tested in the damp condition.

SECTION 504 - FIELD SLUMP TEST FOR GROUT

Use a truncated metal cone 4 in. to 2 in, 6 in. high, and after dampening, place on a flat, moist, non-absorbent base. Thoroughly mix or agitate grout before placing in cone to obtain a full representative mix. Fill cone with grout, lightly tap cone on opposite sides, level off, carefully lift cone and measure slump. At time of placing, grout should have a slump approximately 5 in.

SECTION 505 - FIELD COMPRESSIVE TEST SPECIMEN FOR GROUT

On a flat non-absorbent base, form a space approximately 3 in. x 3 in. x 6 in. high, using masonry units having the same moisture condition as those being laid. Line the space with a permeable paper or porous separator so that water may pass through the liner into the masonry units. Thoroughly mix or agitate grout to obtain a fully re sentative mix and place into molds in two layers, and puddle each ᴋayer with a 1 in. x 2 in. puddling stick to eliminate air bubbles. Level off and immediately cover molds and keep them damp until taken to the laboratory. After 48 hr set, have the laboratory carefully remove masonry units, cap the specimens, and place them in the fog room until tested. Test in a vertical position and in a damp condition.

SECTION 506 - SOLID MASONRY PRISM COMPRESSION TEST

When the strength of the solid masonry is to be established by preliminary tests, the tests shall be made in advance of the operations using prisms built of similar materials under the same conditions and, in so far as possible, with the same bonding arrangement as for the structure. In building the prisms, the moisture content of the unit at time of laying, the consistency of the mortar and the workmanship shall be the same as will be used in the structure. The test prisms for beams and slabs shall be built of representative units, with their long dimension horizontal.

Unless permission is otherwise given, all specimens shall have a height-to-thickness ratio (h/d) not less than 2 and shall be not less than 16 in. in height. If h/d differs from 2, the value of f'_m shall be taken as the compressive strength of the specimens multiplied by a correction factor as follows:

Ratio of height to thickness (h/d)	1.5	2.0	2.5	3.0
Correction factor	0.86	1.00	1.11	1.20

Factors between those listed shall be determined by direct interpolation.

Test prisms shall be stored in air at a temperature not less than 65°F. The ends of each prism shall be capped with a suitable material such as calcined gypsum to provide bearing surfaces plane within 0.003 inch and approximately perpendiculr to the axis of the prism. The prism shall then be tested in accordance with the relevant provisions of the Standard Method for Compressive Strength of Molded Concrete Cylinders, ASTM C39-.

Not less than three specimens shall be made for each test series.

The standard age of test specimens shall be 28 days but 7-day tests may be used, provided the relation between the 7- and 28-day strengths of the masonry is established by test for the materials used.

SECTION 507 - HOLLOW MASONRY PRISM COMPRESSION TEST

When the strength of the hollow masonry is to be established by preliminary tests, the tests shall be made in advance of the operations, using prisms built of similar materials, under the same conditions and, in so far as possible, with the same bonding arrangement as for the structure.

Test prisms shall be built in the form of hollow squares 8 in. by 8 in. in plan and 16 in. high or in the form of rectangles 8 in. by 16 in. in plan and 16 in. high. The hollow core shall not be filled with grout.

Masonry strength $\left(f'_m \right)$ shall be computed by dividing the maximum load by the net area of the masonry units used in construction of the prisms.

Test prisms shall be stored in air at a temperature not less than 65°F. The ends of each prism shall be capped with a suitable material such as calcined gypsum to provide bearing surfaces plane within 0.003 in. and approximately perpendicular to the axis of the prism. The prism shall then be tested in accordance with the relevant provisions of the Standard Method for Compressive Strength of Molded Concrete Cylinders, ASTM C39-.

Not less than three specimens shall be made for each test series.

The standard age of test specimens shall be 28 days but 7-day tests may be used, provided the relation between the 7- and 28-day strengths of the masonry is established by test for the materials used.

SECTION 508 - TEST OF COMPLETED STRUCTURE

(a) A load test of an existing structure to determine its adequacy (stiffness and strength) for the intended use shall not be made until the portion subjected to the load is at least 56 days old, unless the owner of the structure agrees to the test being made at an earlier age.

(b) When a load test is required and the whole structure is not to be tested, the portion of the structure thought to provide the least margin of safety shall be selected for loading. Prior to the application of the test load, a load which simulates the effect of that portion of the design dead load which is not already present shall be applied and shall remain in place until after a decision has been made regarding the acceptability of the structure. The test load shall not be applied until the structural members to be tested have borne the full design dead load for at least 48 hr.

(c) Immediately prior to the application of the test load, the necessary initial readings shall be made for the measurements of deflections (and strains, if these are to be determined) caused by the application of the test load. The members selected for loading shall be subjected to a superimposed test load of two times the design live load, but not less than 80 psf for floor construction nor less than 60 psf for roof con-

struction. The superimposed load shall be applied without shock to the structure and in a manner to avoid arching of the loading materials. Unless otherwise directed by the building official, the load shall be distributed to simulate the distribution of the load assumed in the design.

(d) The test load shall be left in position for 24 hr. when readings of the deflections shall again be made. The test load shall be removed and additional readings of deflections shall then be made 24 hr after the removal of the test load. The following criteria shall be used in determining conformity with the load test requirements:

(1) If the structure shows evident failure, the changes or modifications needed to make the structure adequate for the rated capacity shall be made; or a lower rating may be established.

(2) The maximum deflection, D, of a flexural member at the end of the 24-hour period shall not exceed the limit in Table 2 considered by the building official to be appropriate for the construction.

The maximum deflection shall not exceed $L/200$ for a floor construction intended to support or to be attached to partitions or other construction likely to be damaged by large deflections of the floor.

TABLE 2.—MAXIMUM ALLOWABLE DEFLECTION

Construction	Deflection
1. Cantilever beams and slabs	$L^2/1800$ t
2. Simple beams and slabs	$L^2/4000$ t
3. Beams continuous at one support and slabs continuous at one support for the direction of the principal reinforcement	$L^2/9000$ t
4. Flat slabs (L = the longer span)	$L^2/10,000$ t
5. Beams and slabs continuous at the supports for the direction of the principal reinforcement	$L^2/10,000$ t

The recovery of deflection within 24 hr after the removal of the load shall be at least 75% of the maximum deflection. However, if the recovery of deflection is less than 75%, the member may be retested upon approval by the building official. A second test shall not be made until at least 72 hr after the removal of the first test load. The maximum deflection in a retest shall not exceed the limits given in Table 2 and the recovery of deflection shall be at least 75%.

SECTION 509 - LINEAR CHANGE (RAPID METHOD) TEST

Rapid Shrinkage Test shall be made in accordance with ASTM C 341-54T with the omission of Section 5 (e) and with the following control:

(a) <u>Oven:</u>

Drying oven shall be a reasonably air tight, insulated cabinet providing for a minimum storage capacity of five test specimens, and shall provide the following features:

(1) A minimum clearance of 1 in. all around each test specimen.
(2) A constant, uniform temperature between the temperature of 220°F and 235°F throughout the cabinet by means of an electrical heat source.
(3) A vented oven with a forced circulation of air within the oven, over and around all test specimens.

(b) <u>Procedure:</u>

(1) Immerse specimens for the drying shrinkage determination in water at 73.4° ± 2° F for 48 hr.
(2) Obtain the initial length reading on the test specimen. The initial reading of specimen length, at saturation, shall be taken with the unit positioned in the water tank so that its gage line is about $\frac{1}{4}$ in. above the water surface to avoid error due to cooling by evaporation.
(3) Obtain the saturated surface dry weight of the test specimen. A saturated surface dry condition shall be obtained by draining the test specimen for 1 min over a 3/8 in. or larger screen and removing visible surface water with a damp cloth.
(4) Dry specimens in the oven at a temperature between 220° and 235°F. Drying shall continue for 48 hr minimum and continue until the rate in loss of weight is less than 1% in a 24 hr period. (This usually means 73 hr drying time.)
(5) Cool to between 65° and 75°F in a cooling chamber consisting of a steel container equipped with a rubber gasketed type cover. The container should be equipped with a thermometer, the bulb of which is in the proximity of the topmost specimen. In the bottom of the container a flat pan shall be placed containing dry calcium chloride crystals of sufficient quantity to absorb the free moisture in the air.
(6) Obtain the final length and weight measurements and calculate the drying shrinkage.

(c) <u>Calculations:</u>

(1) Calculate the drying shrinkage as a percentage of the length to the nearest one thousandth of one percent.
(2) Make all adjustments necessary to correct length readings to standard temperature.
(3) Give the shrinkage for each unit together with the average for all units.

<u>SECTION 510 - TENSION TEST FOR MASONRY UNITS</u>

(a) <u>Sampling:</u>

The test specimens shall be representative of the whole lot of units from which they are selected.

(b) Test Specimens:

Three units shall be tested as soon as possible after delivery to the laboratory.

(c) Preparation of Test:

(1) Four 1/8 in. steel pull plates to be glued to each unit. One pull plate to be placed on each side and at each end of each unit. The end of the plate extending beyond the unit shall have a means of attachment to an adequate yoke for fastening to the testing apparatus. The lap of the steel plate onto the speciment shall be sufficient that failure shall not occur at the glue joint and shall be a maximum lap of 3 in. (Masonry units need cleaning with a steel brush to obtain a surface for good bonding. Plates usually need etching to remove grease. Epoxy type adhesives have been found satisfactory.)

(2) The pull plates shall be placed so that they are truly symmetrical about the unit and the point of attachment is equidistant on each side so that no eccentric loadings are induced.

(d) Testing Machine:

The specimen shall be tested in a machine conforming to ASTM E 4-57T.

(e) Procedure:

(1) All specimens shall be tested in a position such that the load is applied along the centroid of the unit to be tested. The maximum tolerance from the centroid shall be $\frac{1}{4}$ in.

(2) All metal contact surfaces in the testing apparatus jig shall be machined true to $\pm$ 0.01 in.

(3) The test load up to one half of the expected maximum load may be applied at any convenient rate, after which the controls of the machine shall be adjusted to give a uniform rate of travel of the moving head such that the remaining load is applied in not less than 1 min or more than 2 min.

(f) Calculation and Report:

The tension shall be calculated by taking the ultimate tensile load and dividing it by the minimum cross sectional area of the specimen, perpendicular to the direction of the load.

The results shall be reported separately for each unit, together with the average for the three units.

Respectfully submitted,

Thomas G. Atkinson   Ernst J. Maag

Ross H. Bryan   Hugh C. MacDonald, Jr.

W. S. Cottingham   Edward R. Mangotich

Jean Edens, Jr.   Keith E. McKee

John Morley English   Clarence B. Monk, Jr.

Cyrus C. Fishburn   Harry C. Plummer

Norman W. Kelch   Robert W. Shuldes

Marvin J. Kudroff   Walter L. Dickey, Vice Chairman

                                   Albyn Mackintosh, Chairman

Task Committee on Reinforced Masonry Design and Practice

Journal of the

STRUCTURAL DIVISION

Proceedings of the American Society of Civil Engineers

EXPERIMENTAL AND ANALYTICAL STUDY OF A FOLDED PLATE

By A. C. Scordelis,[1] M. ASCE, E. L. Croy,[2] A. M. ASCE, and I. R. Stubbs[3]

SYNOPSIS

A study of a simple-span, aluminum, folded plate model consisting of three north-light shells is presented. Values of longitudinal stresses, transverse moments, and vertical joint deflections, determined experimentally and alalytically, are given. Analytical results obtained by the ordinary folded plate theory, the theory of elasticity, and the elementary beam theory are compared with experimental results, and the validity of the assumptions used in the analytical methods is examined.

INTRODUCTION

A prismatic folded plate structure is a shell consisting of a series of flat plates, mutually supporting along their longitudinal edges, that frame into transverse end diaphragms. These structures may be made of reinforced concrete, prestressed concrete, metal, or wood. Folded plates have been used extensively in the construction of long-span roof systems because of their economy and their interesting architectural appearance. Many other applications of this type of structure are possible in buildings, bridges, airplanes, and missiles.

Numerous technical papers have been written on methods of analyzing folded plate structures. The design method most commonly used was introduced in

the United States by George Winter, F. ASCE and M. L. Pei,[4] M. ASCE, and was later modified by Ibrahim Gaafar,[5] M. ASCE., to include the effect of joint displacements. Subsequent treatments of this approach have been made by many others, including Howard Simpson,[6] M. ASCE, Eliahu Traum,[7] and D. Yitzhaki.[8] Scordelis[9] has presented a matrix formulation of this method that can be readily programmed for a digital computer. The preceding method is based on several simplifying assumptions regarding structural behavior. These will be subsequently described in detail and, hereafter, in this paper, the method will be termed the "ordinary method."

A formulation of the analysis of folded plate structures, using the theory of elasticity, has been developed by John E. Goldberg F. ASCE, and H. L. Leve,[10] A. M. ASCE. This method develops a solution for the stresses in a folded plate structure by combining the equations of the classical plate theory for loads normal to the plane of the plates together with the elasticity equations defining the plane stress problem for loads in the plane of the plates. The method, which requires extensive computations, becomes practical when programmed for a digital computer. This method of analysis will be designated the "elasticity method" in this paper.

In some cases, designers have used the elementary beam theory of strength of materials to calculate stresses in folded plate structures. In general, an analysis by this method may yield stresses considerably in error from the true stresses in the structure. This type of solution will be defined as a "beam method" solution in this paper.

In contrast to the numerous papers on the analysis of folded plate structures, very little information has been published comparing experimental results with analytical results obtained by the theories being used. Gaafar[5] has compared results from an experimental study of an aluminum model of symmetrical cross section with analytical values obtained by the ordinary method. A few tests[11,12] on reinforced concrete folded plates loaded to failure have been performed, and limited conclusions on this type of construction have been offered.

In the investigation reported in this paper, the longitudinal stresses, transverse moments, and vertical displacements in a simple-span aluminum folded

4 "Hipped Plate Construction," by G. Winter and M. L. Pei, Proceedings, ACI, Vol. 43, January, 1947, p. 505.

5 "Hipped Plate Analysis Considering Joint Displacement," by I. Gaafar, Transactions, ASCE, Vol. 119, 1954.

6 "Design of Folded Plate Roofs," by Howard Simpson, Proceedings, ASCE, Vol. 84, No. ST1, January, 1958.

7 "The Design of Folded Plates," by Eliahu Traum, Proceedings, ASCE, Vol. 85, No. ST8, October, 1959, p. 103.

8 "Prismatic and Cylindrical Shell Roofs," by D. Yitzhaki, Haifa Science Publishers, Haifa, Israel, 1958.

9 "A Matrix Formulation of the Folded Plate Equations," by A. C. Scordelis, Proceedings, ASCE, Vol. 86, No. ST10, October, 1960, p. 1.

10 "Theory of Prismatic Folded Plate Structures," by J. E. Goldberg and H. L. Leve, I. A. B. S. E., (Zurich), No. 87, 1957, p. 59.

11 "Tests of a Reinforced Concrete Folded Plate Structure," by Syracuse Univ. Research Inst., Civ. Engrg., Dept., Report No. CE 335-5910F.

12 "Ultimate Strength of a Folded Plate Structure," by G. P. Chacos and J. B. Scalzi, Proceedings, ACI, Vol. 57, February, 1961, p. 965.

plate model, having an anti-symmetrical cross section, were determined experimentally and analytically, with the purpose of studying the following items:

1. A comparison of the analytical results obtained by the ordinary method and the elasticity method to determine the effect of the simplifying assumptions used in the former;

2. a comparison of experimental results and analytical results, obtained by the ordinary method, elasticity method, and beam method, to determine the validity of the assumptions being used in the analytical methods; and

3. the effects on the comparisons of "a" and "b," when the span length of the shell is changed from long to short.

Notation.—The letter symbols adopted for use in this paper are defined where they first appear in the text, and are arranged alphabetically for convenient reference in the Appendix.

EXPERIMENTAL PROGRAM

The model consisted of three north-light shells supported on end diaphragms as shown in Figs. 1 and 2. It had an over-all length of 4 ft and an over all width of 3 ft. Each shell consisted of a folded plate of five plate elements chosen to simulate a general anti-symmetrical cross section. The model material was 2024 ST 3 sheet aluminum. This material has a modulus of elasticity of 10.6 x 10^6 psi and a Poisson's ratio of 1/3. Each folded plate cross section was bent from a single sheet of 0.063 in. thick material. The end diaphragms were cut from material 0.190 in. thick. The folded plates were welded to one end diaphragm and were fastened to the other by closely spaced machine screws. The latter diaphragm could then be moved to a new location to change the span of the model. In this way, the model could be tested on both a nominal 4-ft span and a nominal 2-ft span.

In all its dimensions except the thickness of the plates, the model was designed to a scale of approximately 1/20 of a prototype reinforced concrete roof. The scale factor for thickness was reduced to 1/64th of a normal prototype roof so that measurable strains could be obtained. Note that the scale factor is an approximate value and actually has little significance, except to give some indication of the proportions of the structure that the aluminum model might represent. The model was used to obtain experimental values that could be compared with theoretical values, obtained by various analytical methods. Therefore, the model may be considered to be a small structure, rather than a representation of a full-sized roof, and, thus, the terms "model" and "prototype" become synonymous, and similitude is not a factor.

The instrumentation was designed to provide data from which experimental values of longitudinal stresses, transverse moments, and vertical joint deflections could be determined at selected sections. Only the center shell was instrumented. A total of 144 SR-4 strain gages was used on this shell. Both type A7 and A5 SR-4 strain gages were used. These were arranged in rosette or tee patterns at a number of locations across sections at mid-span, quarter-span, eighth-span, and near an end diaphragm. Gages were attached to the top and bottom surfaces of the shell. At a specific location, strains could then be determined in a transverse and longitudinal direction on the top and bottom surfaces. Utilizing the generalized Hooke's law and the flexure formula, these
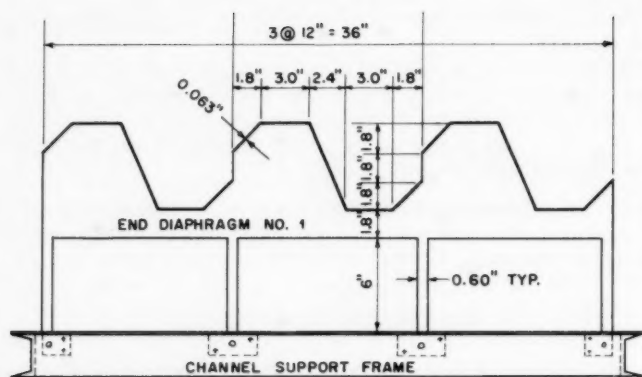
END ELEVATION
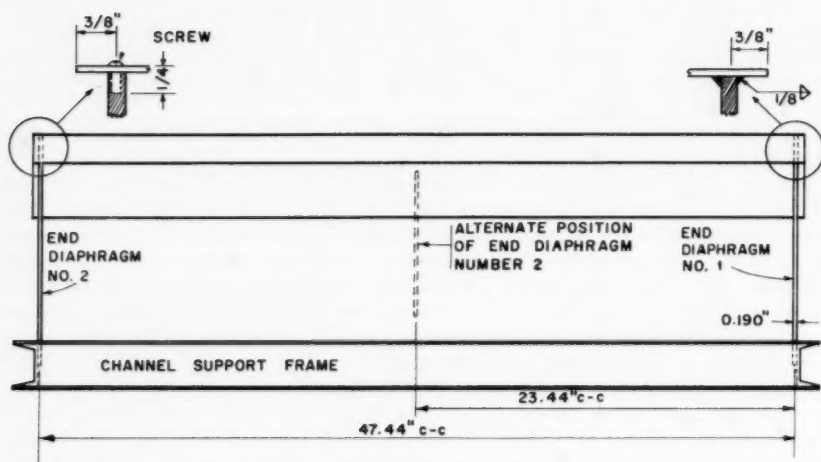
SIDE ELEVATION

FIG. 1.—DIMENSIONS OF THE ALUMINUM MODEL

strains could be converted to longitudinal stresses and transverse moments. Vertical joint deflections were measured by simple dial gages. As the structure was statically indeterminate, the problem of strains due to changes in temperature during the testing program was eliminated by conducting the entire program in a room having a controlled constant temperature of 70°F.

The loading system was designed to produce a uniform line load at each interior joint of the three shells. The ratio of these line loads was determined from the reactions that would be produced at the joints by a load uniformly distributed over the horizontal projection of the structure. The requirements for loading were achieved by means of the "whiffletree" arrangement shown diagrammatically in Fig. 3. This arrangement consists of a series of simple beams, tied and supported by piano wire, whereby a single concentrated load can be distributed successively to a larger and larger number of points as it
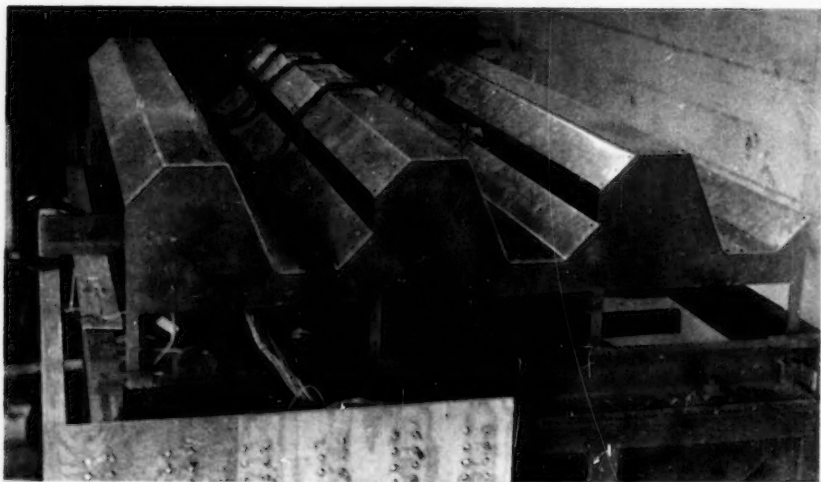
FIG. 2.—MODEL

moves up through the whiffletree. Because the entire system is statically determinate, any desired distribution of loads may be obtained by varying the spans and points of load application on each of the simple beams in the whiffletree.

The uniform line loads were approximated in this case by applying, through the whiffletree, concentrated vertical loads at each interior joint at 6-in. intervals along the span of the model. Two whiffletrees were used so that a separate load could be applied to each half of the 4-ft span. This arrangement also permitted the same system to be used when the span was reduced to 2 ft. The loads were applied to each whiffletree by means of weights using a lever system with a mechanical advantage of 10 to 1. The induced load in the system was checked by means of calibrated dynamometers inserted between the applied loads and the whiffletrees.
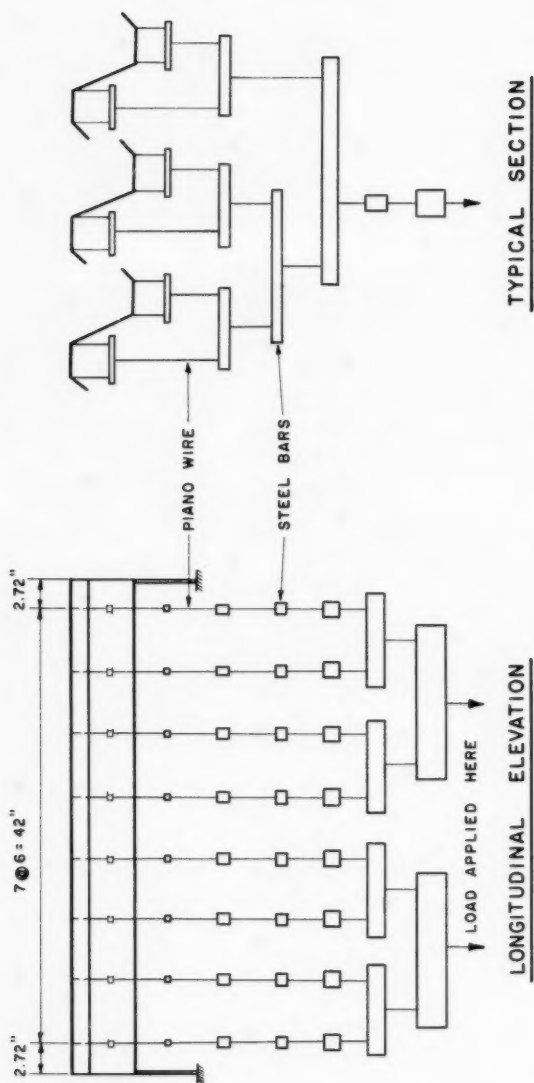
FIG. 3.—WHIFFLETREE LOADING SYSTEM

In testing the model, the linear response to load was first verified at a large number of selected gages. Final values of strain were then obtained from each gage by averaging the values obtained in going from no load to full load three times. Values for each cycle of loading were found to be within a few micro-inches of each other in all cases.

The experimental results for the 4-ft span and the 2-ft span model are given in Tables 5 to 9 and are presented graphically in Figs. 4 to 8. These results will be examined subsequently in connection with those obtained from analytical studies. Tabulated results throughout this paper are for the same common loading shown in Figs. 4 to 8.

ANALYTICAL SOLUTION BY THE ORDINARY METHOD

The "ordinary method" has been thoroughly described and examined in the literature.[5,6,7,8,9] The analysis is based on the following assumptions:

1. The material is elastic, isotropic, and homogeneous;
2. the structure is completely monolithic;
3. slab action is defined by the behavior of transverse one-way slabs spanning between longitudinal joints;
4. longitudinal membrane stresses developed in each plate due to longitudinal plate action may be calculated by the elementary beam theory; therefore, the longitudinal stresses vary linearly over the depth of each plate; and
5. supporting end diaphragms are infinitely stiff parallel to their own plane, but perfectly flexible normal to their own plane.

A matrix formulation of the analysis, described in detail in an earlier paper,[9] was utilized, together with a digital computer, to obtain values of longitudinal stresses σ, transverse moments m, and vertical joint deflections δ. The computer program used is a general one, in which the input data consists of the magnitude and longitudinal distribution of the vertical joint loads, the longitudinal span, and the thickness, vertical projection, and horizontal projection of each plate in the cross-section. The analysis, which consists of a series of matrix algebra operations, is complete and takes into account the effect of relative joint displacements.

In order to directly compare the results found by this method with those obtained by the elasticity method, the uniformly distributed vertical load at each interior joint was replaced by the superposition of harmonic loadings from a Fourier series representation of the actual loading.

$$R_X = \frac{4\,R}{\pi} \sum_{n=1,3,5,7} \frac{1}{n} \sin \frac{n\,\pi\,x}{L} \quad \ldots \ldots \ldots \ldots \quad (1)$$

Solutions were obtained for the first, third, fifth, and seventh harmonics, and the results at midspan are given in Tables 1 and 2. The largest matrix inversion involved in the solution was for a 4-by-4 matrix. Several of these inversions were required. The sign convention used in Tables 1 and 2, and throughout the remainder of the paper, is as follows: longitudinal stresses σ are positive when tensile; transverse moments m are positive when they produce ten-

TABLE 1.—MIDSPAN RESULTS BY ORDINARY METHOD FOR 4-FT NOMINAL SPAN[a,b]

Joint	a	b	c	d	e	f
Harmonic	Longitudinal Stresses σ, in pounds per square inch					
$n = 1$	3545	-2027	-503	503	2027	-3545
$n = 3$	-204	139	-25	25	-139	204
$n = 5$	45	-30	6	-6	30	-45
$n = 7$	-16	11	-2	2	-11	16
Total	3370	-1907	-524	524	1907	-3370
Transverse Moments m, in inch-pounds per inch						
$n = 1$	0	0	-1.459	-1.459	0	0
$n = 3$	0	0	0.012	0.012	0	0
$n = 5$	0	0	-0.00098	-0.00098	0	0
$n = 7$	0	0	0.00018	0.00018	0	0
Total	0	0	-1.448	-1.448	0	0
Vertical Deflections δ, in inches						
$n = 1$	-	0.07754	-0.000856	-0.000856	0.07754	-
$n = 3$	-	-0.00059	0.000080	0.000080	-0.00059	-
$n = 5$	-	0.000046	-0.000006	-0.000006	0.000046	-
$n = 7$	-	-0.000009	0.000001	0.000001	-0.000009	-
Total	-	0.07699	-0.000781	-0.000781	0.07699	-

[a] (L = 47.44 in.)
[b] See Fig. 4 for total uniform load at each joint

TABLE 2.—MIDSPAN RESULTS BY ORDINARY METHOD FOR 2-FT NOMINAL SPAN[a,b]

Joint	a	b	c	d	e	f
Harmonic	Longitudinal Stresses σ, in pounds per square inch					
$n = 1$	1306	-879	137	-137	879	-1306
$n = 3$	-50	34	-6	6	-34	50
$n = 5$	11	-7	1	-1	7	-11
$n = 7$	-4	3	-	-	-3	4
Total	1263	-850	131	-131	850	-1263
Transverse Moments m, in inch-pounds per inch						
$n = 1$	0	0	-0.1715	-0.1715	0	0
$n = 3$	0	0	0.000751	0.000751	0	0
$n = 5$	0	0	-0.000059	-0.000059	0	0
$n = 7$	0	0	0.000011	0.000011	0	0
Total	0	0	-0.1708	-0.1708	0	0
Vertical Deflections δ, in inches						
$n = 1$	-	0.008155	-0.001056	-0.001056	0.008155	-
$n = 3$	-	-0.000035	0.000005	0.000005	-0.000035	-
$n = 5$	-	0.000003	-	-	0.000003	-
$n = 7$	-	0.000001	-	-	-0.000001	-
Total	-	0.008122	-0.001051	-0.001051	0.008122	-

[a] (L = 23.44 in.)
[b] See Fig. 7 for total uniform load at each joint

sion on the bottom fibers; and vertical joint deflections δ are positive downward.

ANALYTICAL SOLUTION BY THE ELASTICITY METHOD

A solution of this type has been presented by Goldberg and Leve.[10] The analysis is based on the following assumptions:

1. The material is elastic, isotropic, and homogeneous;
2. the structure is completely monolithic;
3. the stresses and displacements in each plate due to loads normal to plane of the plate (slab action) are determined by means of the classicial thin plate theory applied to plates supported along all four edges;
4. the stresses and displacements in each plate due to loads in the plane of the plate (membrane action) are determined by means of the elasticity equations defining the plane stress problem; and
5. supporting end diaphragms are infinitely stiff parallel to their own plane, but perfectly flexible normal to their own plane.

A solution by this method requires considerable computational effort. In the case of the aluminum model studied in this paper, a special computer program was developed to minimize the computational problem and the possibilities for error. A computer program applicable to cases involving a general number of plates and a general cross-sectional configuration is being developed at the present time (1961).

The procedure used in the analysis will be outlined briefly. For the aluminum model studied, the external loading consisted solely of vertical harmonic loads at the joints. Each harmonic loading is treated in a similar manner. Isolating a single plate as a free body, the internal forces per unit length existing along each longitudinal edge are a moment m about the longitudinal edge, a shear force V normal to the plane of the plate, a force N in the plane of the plate and normal to its edge, and a longitudinal shear force T in the plane of the plate and parallel to its edge. These internal forces vary longitudinally as harmonics. The possible displacements at each longitudinal edge of a plate are four in number. They are a rotation θ about the axis about which m acts, a displacement w in the direction of V, a displacement v in the direction of N, and a displacement u in the direction of T. These also vary longitudinally as harmonics.

Using classicial, thin-plate theory and the theory of elasticity for plane stress problems, Goldberg and Leve[10] have developed the necessary equations relating the eight force quantities (four at each longitudinal edge) to the eight displacement quantities (four at each longitudinal edge) for each plate. In the present study these equations were programmed for the computer so that the so-called member stiffness matrix k for the entire sturcture could be assembled. The following relationship can then be written:

$$Q = k \Delta \quad \dots \dots \dots \dots \dots \dots \dots \quad (2)$$

in which Q, k, and Δ are, respectively, the matrices representing the plate edge forces, the member stiffnesses, and the plate edge displacements. Once the k

matrix is obtained, the problem can be solved using a displacement type solution (similar to a slope-deflection solution).

The following matrix algebra steps are necessary:

1. Using statics at each joint, the external joint loads R are expressed in terms of the plate edge forces Q

$$R = A Q \quad \ldots\ldots\ldots\ldots\ldots\ldots \quad (3)$$

in which A is a statics or force transformation matrix.

2. Using geometry of displacements, the internal plate edge displacements Δ are related to the external joint displacements δ,

$$\Delta = B \delta \quad \ldots\ldots\ldots\ldots\ldots\ldots \quad (4)$$

in which B is a geometry or displacement transformation matrix. It can be shown that B equals the transpose of A so that one may be obtained from the other.

3. Substituting Eq. 4 into Eq. 2

$$Q = k B \delta = k A^T \delta \quad \ldots\ldots\ldots\ldots\ldots\ldots \quad (5)$$

4. Then Eq. 5 into Eq. 3

$$R = A k A^T \delta = K \delta \quad \ldots\ldots\ldots\ldots\ldots\ldots \quad (6)$$

in which $K = A k A^T$ is the stiffness matrix for the structure that relates external joint loads R to external joint displacements δ.

5. Solving Eq. 6 for δ

$$\delta = K^{-1} R = F R \quad \ldots\ldots\ldots\ldots\ldots\ldots \quad (7)$$

in which $F = K^{-1}$ is the flexibility matrix for the structure. For the aluminum model, which contained a total of five plates and six joints, it was necessary to invert a K matrix having a 24-by-24 size.

6. For the given loading R, joint displacements δ are found by Eq. 7 and then substituted into Eq. 5 so that the plate edge forces Q can be calculated. Once the values of Q are known, longitudinal stresses and transverse moments can be readily obtained.

Midspan results for the aluminum model obtained for the first, third, fifth, and seventh harmonic loadings are given in Tables 3 and 4.

ANALYTICAL SOLUTION BY THE BEAM METHOD

In applying the elementary beam theory to the case of the aluminum model, the general flexure formula for unsymmetrical bending must be used. The general flexure formula can be used to determine longitudinal stresses provided that the following conditions are fulfilled:

1. The material is elastic, isotropic, and homogeneous.
2. The structure is completely monolithic.

TABLE 3.—MIDSPAN RESULTS BY ELASTICITY METHOD FOR 4-FT NOMINAL SPAN[a,b]

Joint	a	b	c	d	e	f
Harmonic	Longitudinal Stresses σ, in pounds per square inch					
n = 1	3267	−1791	−662	662	1791	−3276
n = 3	−202	136	−22	22	−136	202
n = 5	45	−30	5	−5	30	−45
n = 7	−17	11	−2	2	−11	17
Total	3102	−1674	−681	681	1674	−3102
	Transverse Moments m, in inch-pounds per inch					
n = 1	0	0.09380	−1.4510	−1.4510	0.09380	0
n = 3	0	−0.00857	0.01845	0.01845	−0.00857	0
n = 5	0	0.00213	−0.00228	−0.00228	0.00213	0
n = 7	0	−0.00093	0.00067	−0.00093	−0.00093	0
Total	0	0.08643	−1.4342	−1.4342	0.08643	0
	Vertical Deflections δ, in inches					
n = 1	0.1145	0.06969	0.00229	0.00229	0.06969	0.1145
n = 3	−0.00103	−0.00063	0.00006	0.00006	−0.00063	−0.00103
n = 5	0.00009	0.00006	−	−	0.00006	0.00009
n = 7	−0.00002	−0.00001	−	−	−0.00001	−0.00002
Total	0.1136	0.06911	0.00235	0.00235	0.06911	0.1136

[a] (L = 47.44 in.)
[b] See Fig. 4 for total uniform load at each joint

TABLE 4.—MIDSPAN RESULTS BY ELASTICITY METHOD FOR 2-FT NOMINAL SPAN[a,b]

Joint	a	b	c	d	e	f
Harmonic	Longitudinal Stresses σ, in pounds per square inch					
n = 1	1258	−836	107	−107	836	−1258
n = 3	−52	34	5	5	−34	52
n = 5	12	−8	1	−1	8	−12
n = 7	−4	3	−	−	−3	4
Total	1214	−807	103	−103	807	−1214
	Transverse Moments m, in inch-pounds per inch					
n = 1	0	0.05055	−0.2100	−0.2100	0.05055	0
n = 3	0	−0.00264	0.00225	0.00225	−0.00264	0
n = 5	0	0.00094	−0.00037	−0.00037	0.00094	0
n = 7	0	−0.00065	0.00005	0.00005	−0.00065	0
Total	0	0.04820	−0.2080	−0.2080	0.04820	0
	Vertical Deflections δ, in inches					
n = 1	0.01370	0.008077	−0.000843	−0.000843	0.008077	0.01370
n = 3	−0.00007	−0.000051	0.000001	0.000001	−0.000051	−0.00007
n = 5	0.00001	0.000007	0.000001	0.000001	0.000007	0.00001
n = 7	−	−0.000002	−0.000001	−0.000001	−0.000002	−
Total	0.01364	0.008031	−0.000842	−0.000842	0.008031	0.01364

[a] (L = 23.44 in.)
[b] See Fig. 7 for total uniform load at each joint

3. The longitudinal fiber strains and stresses have a planar distribution over the entire cross section.

4. As a result of assumption 3, all points on a given cross section experience the same resultant deflection; therefore, there is no transverse distortion of the cross-section.

5. The resultant of the external loads passes through the shear center of the cross section.

6. Supporting end diaphragms are infinitely stiff parallel to their own plane, but perfectly flexible normal to their own plane.

For the loading on the aluminum model, condition 5 is satisfied because the shear center is located at the centroid of the cross-section, and the external loads are symmetrically applied on either side of this centroid. Thus, the resultant of the external loads passes through the shear center, and, according to the beam theory, there is no tendency for twist.

Condition 4, and, thus, condition 3 are generally not satisfied in a folded plate structure, because the thin plates forming the cross section do not provide a sufficiently stiff transverse slab system to make the transverse distortion of the cross section negligible. If the transverse slab system is made stiffer and stiffer in relation to the longitudinal membrane plate system, condition 4 is gradually approached, and the folded plate structure begins to behave more and more like a beam. Some factors that produce a trend in this direction are an increase in the plate thickness or the longitudinal span, the introduction of transverse stiffening ribs or bulkheads, or the existence of transverse boundary restraints along the longitudinal edges.

The general flexure formula for unsymmetrical bending may be written in the following form:[13]

$$\sigma = \left[\frac{M_{yy}\,I_{xx} - M_{xx}\,I_{xy}}{I_{xx}\,I_{yy} - I^2_{xy}} \right] + \left[\frac{M_{xx}\,I_{yy} - M_{yy}\,I_{xy}}{I_{xx}\,I_{xy} - I^2_{xy}} \right] y \quad \ldots \ldots \quad (8)$$

in which x and y are horizontal and vertical axes passing through the centroid of the cross section. I_{xx}, I_{yy} are moments of inertia, and I_{xy} is the product of inertia, of the entire cross section. M_{xx} and M_{yy} are total bending moments at a section. For the aluminum model I_{xx}, I_{yy}, I_{xy} equaled 4.80 in.,[4] 11.55 in.,[4] and -6.00 in.[4] respectively. Because only vertical loads were applied to the model, M_{yy} equaled zero at all sections.

Values obtained using Eq. 8 are given in Tables 5 to 9 and are shown graphically in Figs. 4 to 8.

EXAMINATION OF EXPERIMENTAL AND ANALYTICAL RESULTS

For purposes of comparison and examination, experimental and analytical results for longitudinal stress σ, transverse moments m, and vertical joint deflections δ are summarized in Tables 5 to 7 and Figs. 4 to 6 for the case of the 4-ft span, and in Tables 8 and 9 and Figs. 7 and 8 for the case of the 2-ft span. All values are for the same common loading condition, shown in Figs. 4 to 8.

---

13 "Indeterminate Structural Analysis," by J. S. Kinney, Addison Wesley Co., Inc., Reading, Mass., 1957, p. 278.

TABLE 5.—MIDSPAN RESULTS FOR 4-FT SPAN (L = 47.44 IN.)

Joint	a	b	c	d	e	f
Method	Longitudinal Stresses σ, in pounds per square inch					
Experi-mental	2500	-1500	-550	600	1500	-2700
Ordinary	3370	-1907	-524	524	1907	-3370
Elasticity	3102	-1674	-681	681	1674	-3102
Beam	1640	-380	-1530	1530	380	-1640
	Transverse Moments m, in inch-pounds per inch					
Experi-mental	0	0.42	-1.19	-1.19	-0.50	0
Ordinary	0	0	-1.448	-1.448	0	0
Elasticity	0	0.086	-1.434	-1.434	0.086	0
	Vertical Deflections δ, in inches					
Experi-mental	–	0.0543	0.0001	-0.0006	0.0544	–
Ordinary	–	0.0770	-0.0008	-0.0008	0.0770	–
Elasticity	0.1136	0.0691	0.0023	0.0023	0.0691	0.1136

TABLE 6.—QUARTER-SPAN RESULTS FOR 4-FT SPAN (L = 47.44 IN.)

Joint	a	b	c	d	e	f
Method	Longitudinal Stresses σ, in pounds per square inch					
Experi-mental	1620	-900	-300	700	950	-1380
Ordinary	2611	-1507	-343	343	1507	-2611
Elasticity	2415	-1336	-457	457	1336	-2415
Beam	1230	-285	-1150	1150	285	-1230
	Transverse Moments m, in inch-pounds per inch					
Experi-mental	0	0.18	-0.88	-0.80	0.22	0
Ordinary	0	0	-1.038	-1.038	0	0
Elasticity	0	0.070	-1.038	-1.038	0.070	0

TABLE 7.—EIGHTH-SPAN RESULTS FOR 4-FT SPAN (L = 47.44 IN.)

Joint	a	b	c	d	e	f
Method	Longitudinal Stresses σ, in pounds per square inch					
Experi-mental	510	-380	-350	450	100	-150
Ordinary	1580	-927	-162	162	927	-1580
Elasticity	1472	-833	-230	230	833	-1472
Beam	720	-166	-670	670	166	-720
	Transverse Moments m, in inch-pounds per inch					
Experi-mental	0	0.10	-0.42	-0.35	0.20	0
Ordinary	0	0	-0.569	-0.569	0	0
Elasticity	0	0.046	-0.574	-0.574	0.046	0

A comparison of the analytical results obtained by the ordinary method and those obtained by the elasticity method indicates relatively good agreement. Longitudinal stresses obtained by the elasticity method were generally lower than those obtained by the ordinary method. The percentage difference in the maximum longitudinal stresses for the 4-ft span was about 8%, whereas for

TABLE 8.—MIDSPAN RESULTS FOR 2-FT SPAN (L = 23.44 IN.)

Joint	a	b	c	d	e	f
Method	Longitudinal Stresses σ, in pounds per square inch					
Experi-mental	950	−530	80	30	480	−900
Ordinary	1263	−850	131	−131	850	−1263
Elasticity	1214	−807	103	−103	807	−1214
Beam	402	−93	−375	375	93	−402
Transverse Moments m, in inch–pounds per inch						
Experi-mental	0	0.11	−0.21	−0.11	0.05	0
Ordinary	0	0	−0.171	−0.171	0	0
Elasticity	0	0.048	−0.208	−0.208	0.048	0
Vertical Deflections δ, in inches						
Experi-mental	–	0.0058	−0.0013	−0.0012	0.0063	–
Ordinary	–	0.0081	−0.0011	−0.0011	0.0081	–
Elasticity	0.0136	0.0080	−0.0008	−0.0008	0.0080	0.0136

TABLE 9.—QUARTER–SPAN RESULTS FOR 2-FT SPAN (L = 23.44 IN.)

Joint	a	b	c	d	e	f
Method	Longitudinal Stresses σ, in pounds per square inch					
Experi-mental	620	−340	−20	20	380	−500
Ordinary	947	−638	100	−100	638	−947
Elasticity	914	−607	79	−79	607	−914
Beam	302	−70	−282	282	70	−302
Transverse Moments m, in inch–pounds per inch						
Experi-mental	0	0.06	−0.15	−0.07	0.10	0
Ordinary	0	0	−0.122	−0.122	0	0
Elasticity	0	0.036	−0.150	−0.150	0.036	0

the 2-ft span it was about 4%. Transverse moments found by the two methods for the 4-ft span were practically the same, whereas for the 2-ft span the elasticity method yielded values somehwat higher than the ordinary method. This trend appears reasonable because as the longitudinal span decreases, the two-way slab action assumed in the elasticity method provides a stiffer slab system than that assumed in the ordinary method. The maximum vertical joint deflections computed by the ordinary method were slightly higher than those found
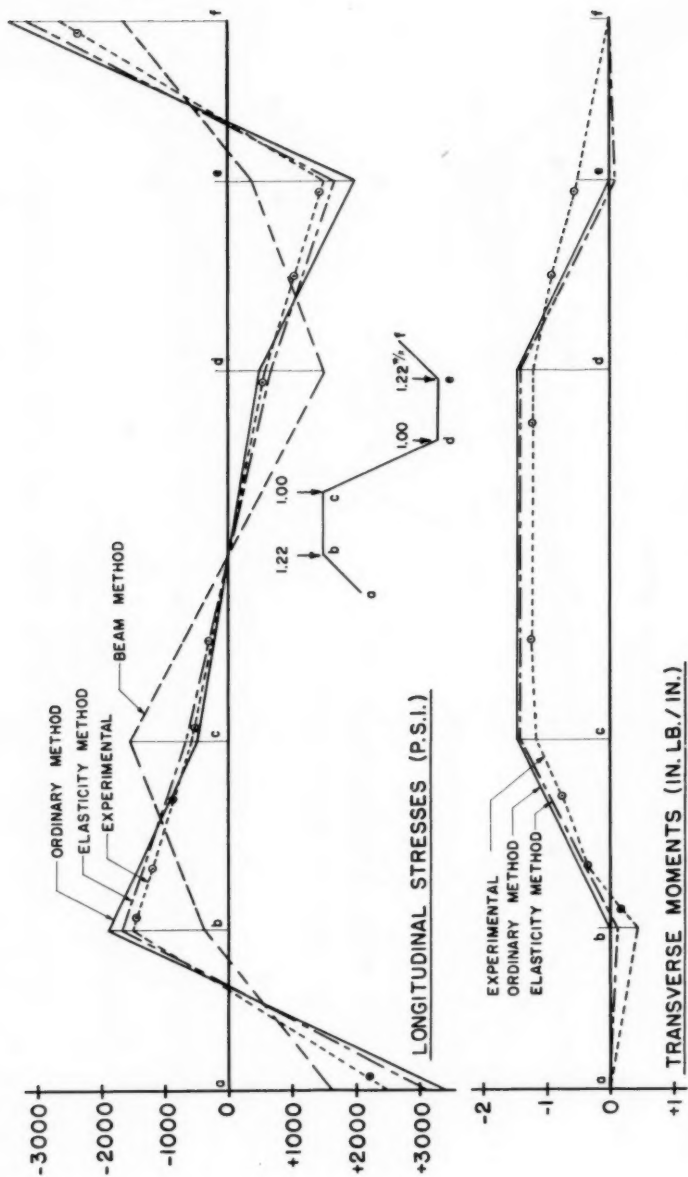
FIG. 4.—4-FT SPAN MODEL — MIDSPAN VALUES OF STRESSES AND MOMENTS
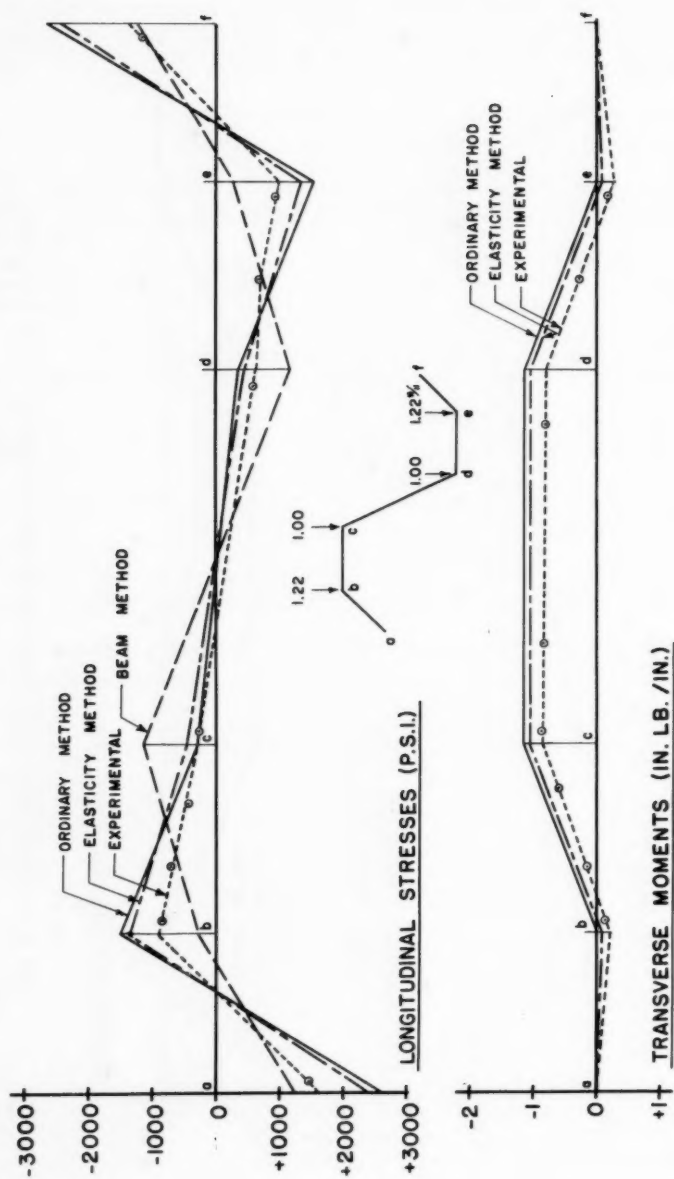
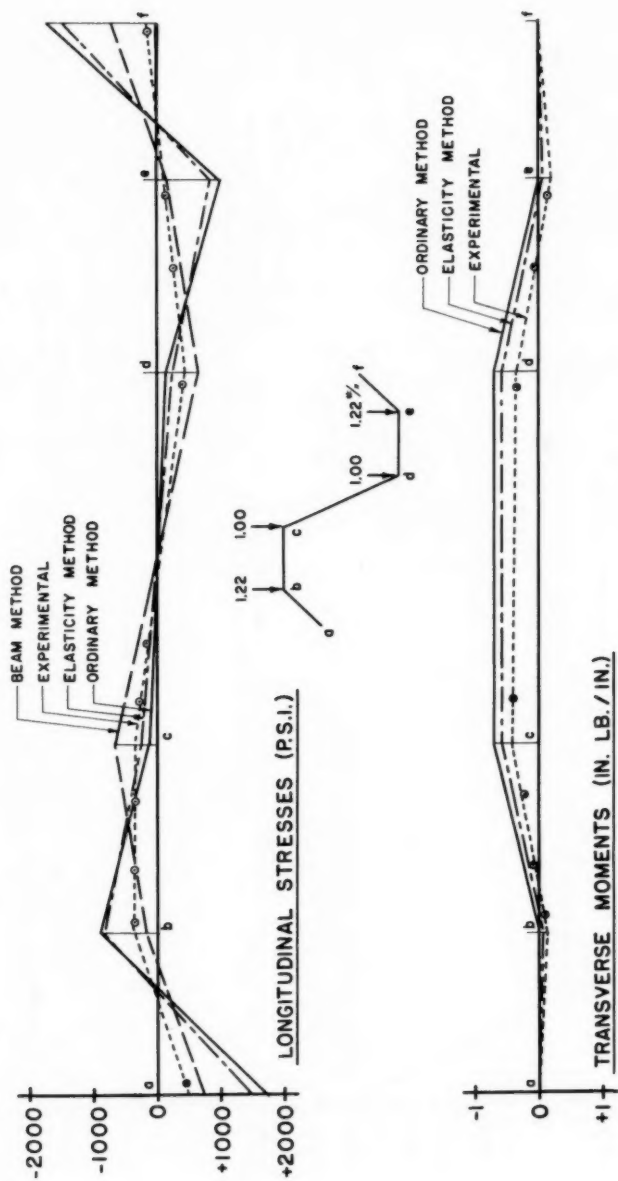FIG. 5.—4-FT SPAN MODEL — QUARTER-SPAN VALUES OF STRESSES AND MOMENTS

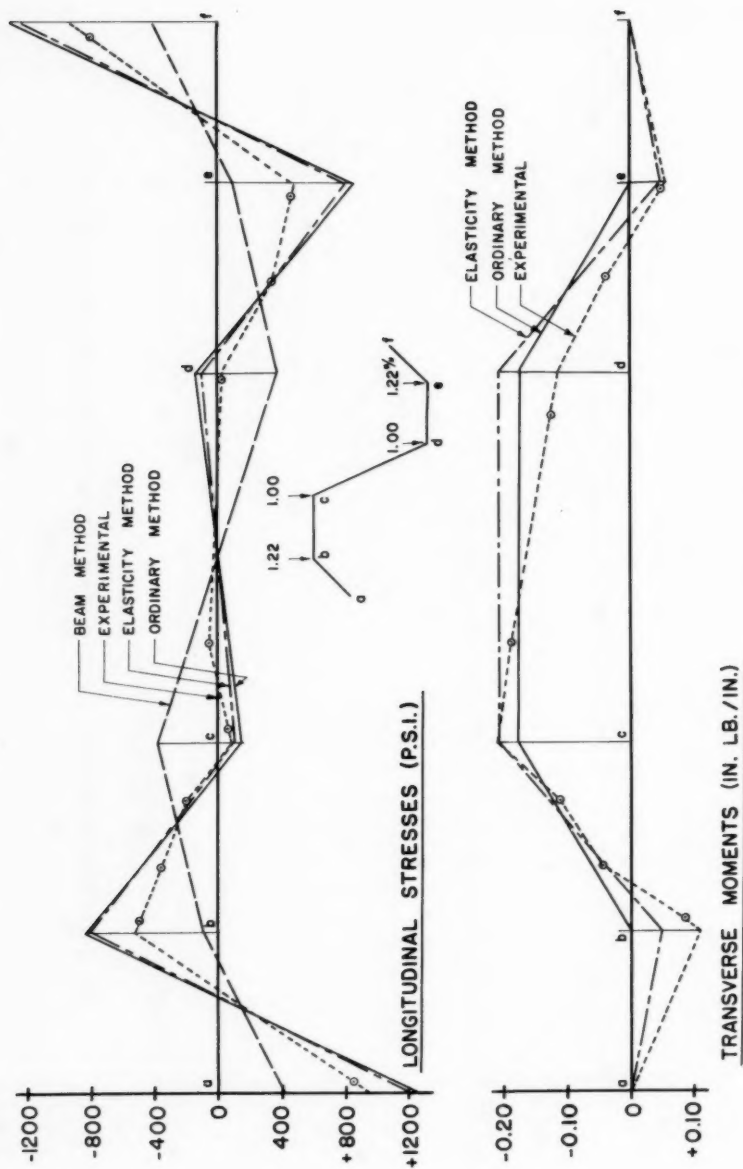FIG. 6.—4-FT SPAN MODEL — EIGHTH-SPAN VALUES OF STRESSES AND MOMENTS

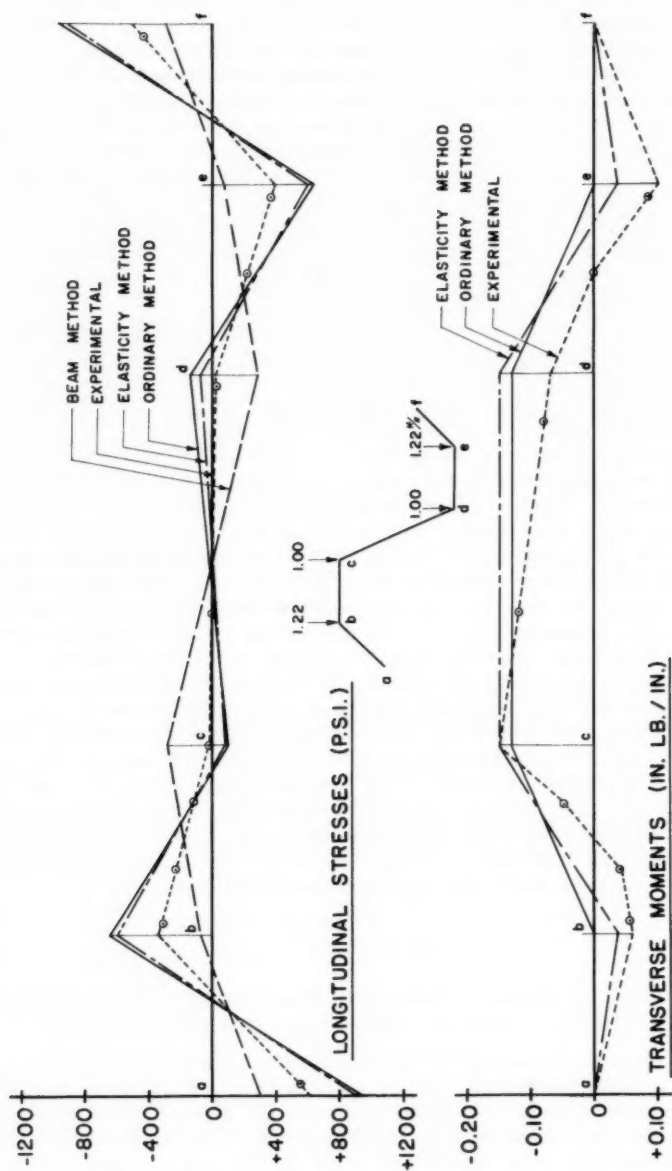FIG. 7.—2-FT SPAN MODEL — MIDSPAN VALUES OF STRESSES AND MOMENTS

FIG. 8.—2-FT SPAN MODEL — QUARTER-SPAN VALUES OF STRESSES AND MOMENTS

by the elasticity method. This difference was expected because the assumptions used in the ordinary method neglect some of the inherent stiffness of the structure. The difference in the maximum deflections was about 11% for the 4-ft span and only about 1% for the 2-ft span.

The experimental results were, in general, significantly lower than those calculated by either the elasticity method or the ordinary method. For example, maximum values of longitudinal stress were about 20% to 30% lower. However, as can be seen in Figs. 4 to 8, the patterns of distribution of both longitudinal stresses and transverse moments across the cross section are similar for the experimental results and the results found analytically by the elasticity method or the ordinary method. From the diagrams (Figs. 4 to 8), it is also immediately apparent that the beam method does not yield analytical values that correctly represent the distribution or the magnitude of the stresses in the model. Values calculated by this method were considerably smaller than the maximum stresses determined experimentally.

The difference in the results obtained experimentally and by the elasticity method must be attributed to an error in one or more of the assumptions made in the latter method. The only one that appears suspect is that which assumes that the supporting end diaphragms are infinitely stiff parallel to their own plane, but perfectly flexible normal to their own plane. This suspicion was checked by evaluating the total axial force P, total moment M_{xx}, and total moment M_{yy} at each section from the stress distributions obatined analytically and experimentally. Each of the three analytical methods yielded values of P, M_{xx}, and M_{yy}, which checked the statical values based on a structure simply supported at the ends. Values of P, M_{xx}, and M_{yy} obtained from the experimental stress distributions, however, indicated that some restraint existed at the end diaphragm and, thus, the diaphragms were not perfectly flexible normal to their own plane. Because the columns supporting the end diaphragms were capable of transmitting only very small moments to the base supports, it is thought that the P, M_{xx}, and M_{yy} produced at the end diaphragm by the middle shell (the only shell instrumented) may have been equilibrated by equal and opposite quantities produced at the end diaphragms by the two outside shells.

The stress distributions in north-light shells of the type used in this study appear to be particularly sensitive to the end restraints mentioned in the preceding paragraph. The problem of end restraint offered by end diaphragms, in cases in which multiple shells are connected to the same end diaphragm, is in need of additional experimental study. Most experimental studies in the past have used only a single shell spanning between end diaphragms.

CONCLUSIONS

On the basis of the study reported herein, the following conclusions may be advanced regarding the behavior and analysis of folded plate structures:

1. In general, the computation of longitudinal stresses, transverse moments, and vertical joint deflections by the "ordinary method" should yield results in relatively good agreement with those found by the more precise "elasticity method." As the longitudinal span is decreased, the differences in longitudinal stresses and vertical joint deflections found by the two methods decrease, whereas the differences in transverse moments (due to joint displacement) increase.

2. An analysis by the "beam method" for longitudinal stresses in a folded plate of unsymmetrical cross section will yield values seriously in error with respect to magnitude and distribution across the cross section.

3. Whereas either the ordinary method or the elasticity method appear to predict accurately the pattern of distribution of stresses, moments, and deflections across a cross section, the magnitudes of these quantities are significantly affected by the restraints imposed by the end diaphragms. These restraints, which are at present commonly neglected in design, require further research, especially in cases of multiple repeating shells of unsymmetrical cross section.

All of the methods of analysis described herein are based on an elastic, isotropic, and homogeneous material. It could be argued, perhaps justifiably, that these methods are not applicable to reinforced concrete. However, the same assumptions are now being followed in the design of curvilinear prismatic shells, and convincing experimental evidence for general cases of reinforced concrete shells would have to be presented before a departure from this approach would be warranted. Perhaps the best approach in the end will be an ultimate strength concept, but considerable analytical and experimental research remains to be done in this area before it is developed into an acceptable general design method for shells.

ACKNOWLEDGMENTS

APPENDIX.—NOTATION

Letter symbols adopted for use in this paper are listed here for convenience of reference and for the aid of discussers:

A   = Statics or force transformation matrix;

B   = geometry or displacement transformation matrix;

F   = flexibility matrix;

I_{xx}, I_{yy} = moment of inertia of cross section about x and y axes respectively;

I_{xy} = product of inertia of cross section;

K   = stiffness matrix;

k   = member stiffness matrix;

L   = longitudinal span;

M_{xx}, M_{yy} = total moment at a section about x and y axes, respectively;

m	=	transverse slab moment at a plate edge;
N	=	plate edge force in the plane of the plate and normal to its edge;
n	=	harmonic number;
P	=	total axial force at a section;
Q	=	plate edge force matrix;
R	=	external joint load;
T	=	plate edge force in the plane of the plate and parallel to its edge;
u	=	displacement at a plate edge in the direction of T;
V	=	plate edge force normal to the plane of the plate;
v	=	displacement at a plate edge in the direction of N;
w	=	displacement at a plate edge in the direction of V;
δ	=	joint displacement;
Δ	=	plate edge displacement matrix;
θ	=	rotation at a plate edge; and
σ	=	longitudinal stress.

Journal of the
STRUCTURAL DIVISION
Proceedings of the American Society of Civil Engineers

STRESSES IN RING STIFFENERS IN CYLINDERS

Wadi S. Rumman,[1] M. ASCE

SYNOPSIS

A semi-empirical approach is presented herein for determining the forces acting on ring stiffeners in long thin-walled cylinders subjected to bending. Included are the results of experimental work and some approximate theoretical investigations. The theoretical work is correlated with the experimental results to establish approximate working formulas to determine the stresses in the ring stiffeners. Both the pure bending of the cylinder and the bending caused by transverse local loading are considered. The transverse loading on the cylinder is limited to a loading of a distributed nature and does not include any concentrated loads applied to either the stiffeners or the shell.

INTRODUCTION

Considerable experimental and theoretical work has been performed by various investigators[2,3,4] on the ultimate capacity of thin-walled cylinders,

both stiffened and unstiffened. However, very little has been done to determine the nature and magnitude of the forces acting on ring stiffeners in thin-walled cylinders subjected to bending.

Ring stiffeners are used in steel chimneys and in many pipe and conduit structures. In such structures, the stresses in the stiffeners are not only caused by the beam bending moments in the structure but also, and, in fact, to a larger extent, by the direct effect of the transverse local loading on the shell. In the case of chimneys, for example, the stiffeners will minimize the distortion of the circular section of the structure. This distortion of the originally circular section is caused by the bending of the chimney as a whole and also by the transverse wind-pressure distribution on the shell.

Although the rigidity of the stiffener is an important factor in its selection, the designer, nevertheless, must determine the nature and magnitude of the forces to which the stiffener is subjected. Therefore, this investigation is primarily concerned with establishing a practical approach for determining the distribution and magnitude of the forces acting on ring stiffeners in cylinders subjected to bending. Only cylinders with constant radius and thickness and with equidistant ring stiffeners are considered.

Notation.—The letter symbols adopted for use in this paper are defined where they first appear, in the illustrations or in the text, and are arranged alphabetically, for convenience of reference, in the Appendix.

SCOPE OF EXPERIMENTAL WORK

The objective of the experimental work was to measure the variations of the stresses in a ring stiffener as a result of the bending of the cylinder. A model (Fig. 1) was therefore built which was essentially a thin-walled long cylinder of constant thickness and radius, reinforced by circular rings uniformly spaced along the cylinder. The material used in the fabrication of the model was aluminum alloy 6061-T6.

The model in Fig. 1 is composed of three circular cylinders (designated in Fig. 1 as End Segment - Center Segment - End Segment) and two end wooden blocks.

Each wooden block is made of a square hollow section except for a length of about 9 in. that fits inside the cylinder and is made of a hollow circular section. The end blocks were used as end supports and to apply the load. One loading basket was attached to each end block, as shown in Fig. 1.

Each of the circular cylinders is 4 ft long and has a mean diameter of 11.28 in. They were rolled from a 0.025 in. thick aluminum sheet. The radius-to-thickness ratio of the model was therefore equal to 225.

The stiffeners were bars that were cut from a 0.25 in. thick plate. The bars were machined to the specified thickness of the stiffeners and were rolled to the required diameter. In each stiffener an allowance was made for a splice.

The end segments of the model were reinforced by 1/4 in. by 1/4 in. ring stiffeners spaced equally at 6 in., center to center. No strain gages were mounted on the end segments and no change in the size or spacing of the end-segment stiffeners was made during the test.

On the center segment, which is the actual test specimen of the model, two different size stiffeners were used during the test, 1/4 in. by 3/16 in. (width x

94 SCREWS (0.1380" O.D.)

142 SCREWS (0.1380" O.D.)

49 SCREWS (0.1120" O.D.) CONNECTING
EACH STIFFENER TO THE CYLINDER

O.D. = OUTSIDE DIAMETER

r = 5.64" $\frac{r}{t}$ = 225
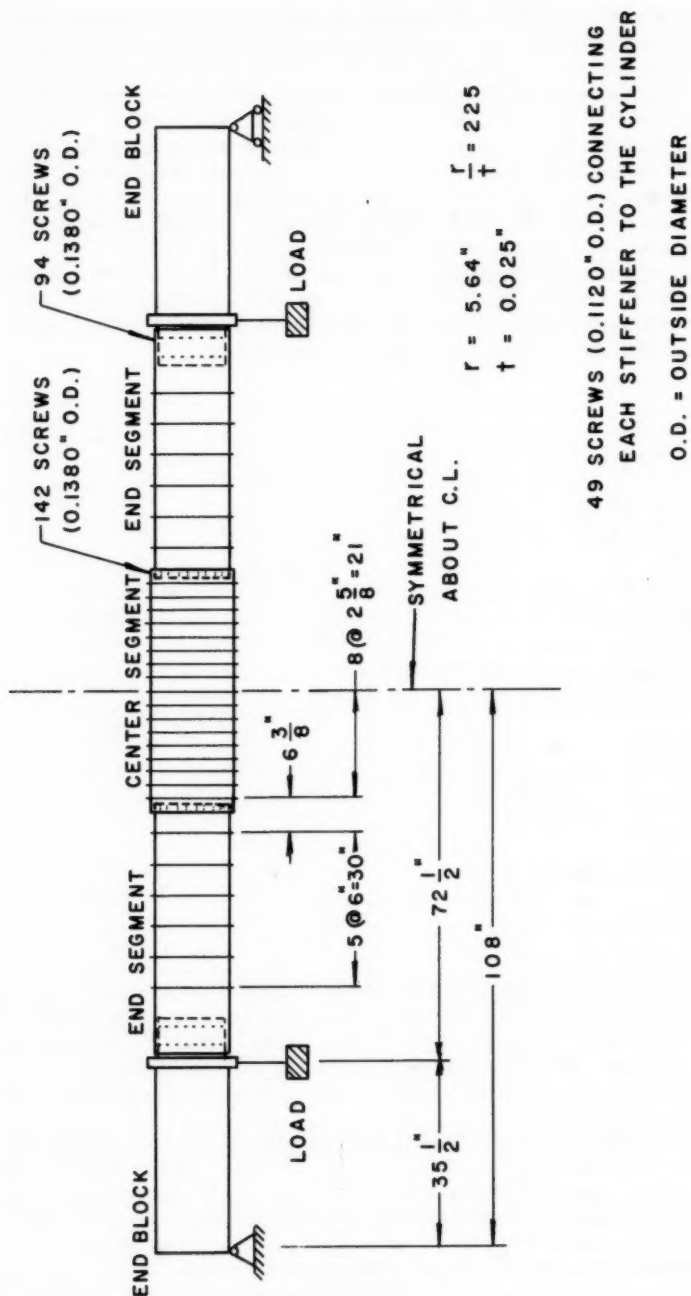
t = 0.025"

FIG. 1.—GENERAL ARRANGEMENT OF MODEL

thickness) and 1/4 in. by 1/8 in. It should be noted that the thickness of the stiffener designates its dimension in the radial direction. For each of the two sizes, the stiffeners were originally spaced at 2 5/8 in., center to center, with provisions to remove some of the stiffeners during the test so that the spacing could be increased to 5 1/4 in, 10 1/2 in., and 21 in.

All the stiffeners were placed on the outside face of the cylinder and were connected to the cylinder by using forty-nine machine screws (with nuts). The distance between the screws was therefore approximately equal to 3/4 in. Machine screws (with nuts) were also used in connecting the circular segments together. The sizes and number of the screws are given in Fig. 1.

As stated previously, the purpose of the test was to measure the stress variations in the stiffeners. Nevertheless, a few AR-1 rectangular rosette gages were mounted on both the inside and outside of the shell for the purpose of detecting any unusual strains in the shell during the test.

(a) GAGE LOCATIONS

(b) LOADING BASKET

(c) PURE BENDING

(d) LOCAL LOADING
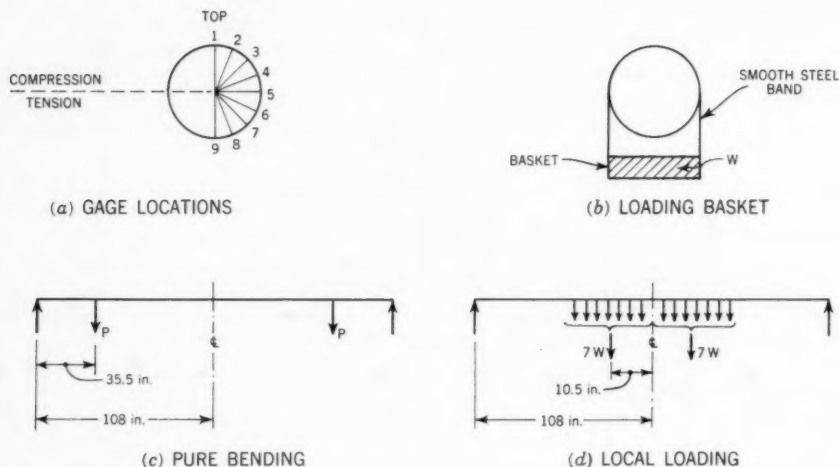
FIG. 2

Nine A-7 gages were placed on the stiffener located at the mid-point of the model; the A-7 gages are relatively short gages and have an active length of 1/4 in. Also A-7 gages were mounted on the inside of the shell opposite to those on the stiffener. These gages were centered between the screws connecting the stiffener to the shell. All the electrical strain gages used were SR-4 gages.

A constant bending moment in the shell was obtained by loading both baskets simultaneously with equal increments of the load (Fig. 1). One type of transverse local loading was investigated, namely a uniformly distributed radial force applied at the top half of the cylinder. This was achieved by using loading baskets at the fourteen locations shown in Fig. 2(d) in which the load from the weights in the basket was applied to the model by bands passing over the upper half of the cylinder (Fig. 2(b)). The bands were very smooth, thus minimizing the effect of the frictional forces.

Typical experimental results are given in Table 1(a) and (b) for the 1/4 in. by 1/8 in. stiffener. The stresses due to the separate effect of the local loading, which are given in Table 1(c), are obtained by subtracting the stresses of Table 1(a) from those of Table 1(b). The bending moment for the pure-bending condition (Fig. 2(c)) is

$$M_C = 3,218 + 35.5 \ P \ \dots\dots\dots\dots\dots\dots \text{(1a)}$$

in which P is the load, in pounds, in each basket, and for the local-loading condition (Fig. 2(d)) the bending moment is

$$M_C = 3,218 + 682.5 \ W \ \dots\dots\dots\dots\dots\dots \text{(1b)}$$

in which W is the load, in pounds, in each basket. From Eq. 1(b)

W, in pounds	M_C, in inch-pounds
0	3,218
5-1/6	6,744
12-1/6	11,522
19-1/6	16,299
26-1/6	21,077

The moment of 3,218 in.-lb which appears in the tables is the beam bending moment at the center of the model due to the weight of the cylinder, the end blocks, and the end loading baskets. It should be noted that the modulus of elasticity, E, used in converting stresses to strains was taken to be equal to 10×10^6 psi. This value for E was the average obtained from four tensile tests.

The strains in the gages on the inside of the shell and opposite to those on the outside face of the stiffener are affected appreciably by any local longitudinal bending and other local conditions, which are difficult to evaluate. For this reason these strains were ignored because it was felt that they could not be used to advantage in the evaluation of the data.

The variation in the stress on the outside face of the 1/4 in. by 1/8 in. stiffener as a function of the applied pure bending moment on the cylinder is shown in Fig. 3. These stresses are plotted for five locations on the stiffener and for a stiffener spacing of 10 1/2 in. As shown in Fig. 3, the maximum applied bending moment used during the tests was equal to 34,000 in.-lb which is approximately 80% of the capacity of the model. The ultimate capacity of the model was checked at the end of the test series by loading the model to failure; the failure occurred by local buckling of the shell.

The nine strain locations on the stiffener start with No. 1 at the top of the stiffener (compressive side of the cylinder) and are spaced at 22.5° around the stiffener with No. 9 located at the bottom of the stiffener (tension half of the cylinder). These locations are shown in Fig. 2(a).

INTERPRETATION OF DATA

A study of the curves in Fig. 3 shows that the variation of the stress at any point in the stiffener is a nonlinear function of the applied pure bending moment

TABLE 1.—STRESSES, IN POUNDS PER SQUARE

Gage	Stiffener Spacing,									
	2 – 5/8					5 – 1/4				
	Bending Moment,									
	3,218	6,744	11,522	16,299	21,077	3,218	6,744	11,522	16,299	21,077
	(a) Pure									
1	150	275	410	475	490	150	280	397	450	435
2	110	205	305	363	390	85	150	210	218	163
3	88	180	310	440	570	55	120	230	350	485
4	35	105	220	355	505	20	65	190	380	615
5	10	35	110	235	395	15	65	185	375	620
6	- 15	- 18	- 5	35	95	3	25	75	165	300
7	- 95	-190	- 325		- 600	- 45	-105	- 205	- 330	- 465
8	-105	-230	- 430	- 655	- 945	-110	-250	- 480	- 760	-1,080
9	-155	-345	- 665	-1,025	-1,435	-180	-400	- 770	-1,160	-1,615
	(b) Local									
1	150	510	990	1,460	1,880	150	730	1,490	2,210	2,850
2	110	320	590	820	1,020	85	345	685	1,015	1,255
3	88	63	- 7	- 127	- 267	55	-165	- 475	- 785	-1,105
4	35	-165	- 445	- 745	-1,035	20	-460	-1,110	-1,750	-2,340
5	10	30	100	200	340	15	45	165	315	525
6	- 15	315	765	1,225	1,715	3	623	1,503	2,413	3,323
7	- 95	- 15	105	205	295	- 45	165	455	715	965
8	-105	-325	- 645	-1,025	-1,425	-110	-420	- 940	-1,500	-2,080
9	-155	-575	-1,185	-1,855	-2,545	-180	-800	-1,710	-2,690	-3,680

(c) Local Loading

Gage	Load W,							
	5 – 1/6	12 – 1/6	19 – 1/6	26 – 1/6	5 – 1/6	12 – 1/6	19 – 1/6	26 – 1/6
1	235	580	985	1,390	450	1,093	1,760	2,415
2	115	285	457	630	195	475	797	1,092
3	-117	-317	- 567	- 837	-285	- 705	-1,135	-1,590
4	-270	-665	-1,100	-1,540	-525	-1,300	-2,130	-2,955
5	- 5	- 10	- 35	- 55	- 20	- 20	- 60	- 95
6	333	770	1,190	1,620	598	1,428	2,248	3,023
7	175	430	670	895	270	660	1,045	1,430
8	- 95	-215	- 370	- 480	-170	- 460	- 740	-1,000
9	-230	-520	- 830	-1,110	-400	- 940	-1,530	-2,065

on the cylinder, especially at Points 1, 5, and 9 (top, center, and bottom of the stiffener). Also, the tensile stress on the outside face of the stiffener at Point 1 increases nonlinearly until the applied bending moment reaches a certain value, after which the tensile stress begins to decrease with the increase of the moment. On the other hand, the stress at Point 9 increases with the increase of the applied moment, with no reversal in the increments of the stress.

The foregoing behavior suggests that the stresses on the stiffener, due to an applied pure bending moment on the cylinder, are caused by more than one type of action. Two types of action are presented to explain the above stress behavior:

1. The flattening of the cylinder; that is an increase in the horizontal diameter and a decrease in the vertical diameter of the cylinder. This is caused

INCH, ON OUTSIDE FACE OF STIFFENER

in Inches									
10 – 1/2					21				
in Inch–Pounds									
3,218	6,744	11,522	16,299	21,077	3,218	6,744	11,522	16,299	21,077
Bending									
135	250	345	325	215	140	250	300	300	200
80	130	150	115	5	– 10	– 20	– 50	– 210	– 780
65	130	220	315	400	40	90	160	260	200
50	135	305	555	840	40	110	270	580	1,180
35	90	240	475	765	40	120	260	540	1,020
– 8	0	45	135	310	20	40	100	190	350
– 55	– 120	– 215	– 320	– 460	– 80	– 130	– 210	– 300	– 540
–120	– 270	– 515	– 820	–1,170	– 70	– 200	– 440	– 720	–1,150
–200	– 435	– 820	–1,285	–1,805	–180	– 400	– 780	–1,240	–1,820
Loading									
135	995	2,115	3,165	4,135	140	1,460	3,000	4,540	6,010
80	460	960	1,400	1,810	– 10	640	1,260	1,850	2,310
65	– 355	– 915	–1,525	–2,105	40	– 600	–1,560	–2,500	–3,470
50	– 780	–1,910	–3,030	–4,080	40	–1,540	–3,360	–5,080	–6,710
35	95	265	475	725	40	290	460	720	1,080
– 8	1,032	2,442	–3,932	5,382	20	1,680	3,750	5,850	7,990
– 55	255	745	1,195	1,615	– 80	520	1,210	1,860	2,450
–120	– 590	–1,290	–2,030	–2,820	– 70	– 720	–1,680	–2,720	–3,780
–200	–1,120	–2,380	–3,680	–5,010	–180	–1,380	–3,040	–4,730	–6,430

Minus Bending

in pounds							
5 – 1/6	12 – 1/6	19 – 1/6	26 – 1/6	5 – 1/6	12 – 1/6	19 – 1/6	26 – 1/6
745	1,770	2,840	3,920	1,210	2,700	4,240	5,810
330	810	1,285	1,805	660	1,310	2,060	3,090
– 485	–1,135	–1,840	–2,505	– 690	–1,720	–2,760	–3,670
– 915	–2,215	–3,585	–4,920	–1,650	–3,630	–5,660	–5,530
5	25	0	– 40	170	200	180	60
1,032	2,397	3,797	5,072	1,640	3,650	5,660	7,640
375	960	1,515	2,075	650	1,420	2,160	2,990
– 320	– 775	–1,210	–1,650	– 520	–1,240	–2,000	–2,630
– 685	–1,560	–2,395	–3,205	– 980	–2,260	–3,490	–4,610

by the curvature of the cylinder when subjected to bending, whereby the longitudinal stresses at both the top and bottom halves of the cylinder will have resultant forces acting towards the center of the cylinder, thus causing it to flatten. (Fig. 5).

2. The increase of the radii of the cylinder on the compression side and their decrease on the tension side due to Poisson's ratio. This action is referred to as the bulging of the cylinder.

Fig. 4 shows the types of stresses on the outside face of the stiffener due to the two types of action - the flattening and the bulging. Both of these two actions have the same sign of stress at Point 9 and opposite signs at Point 1. At Point 5 flattening will be the main contributing factor to the stress, whereas bulging will be the main contributing factor to the stress at Points 3 and 7.

A study of Fig. 4 explains the behavior of the stresses in Fig. 3 and points to the fact that the stresses due to flattening vary at a faster rate than their variation due to bulging.

THEORETICAL INVESTIGATION AND CORRELATION
WITH EXPERIMENTAL RESULTS

Effect of Flattening of Cylinder.—The flattening of the cylinder is illustrated in Fig. 5(a), where both the compressive and tensile longitudinal stresses at
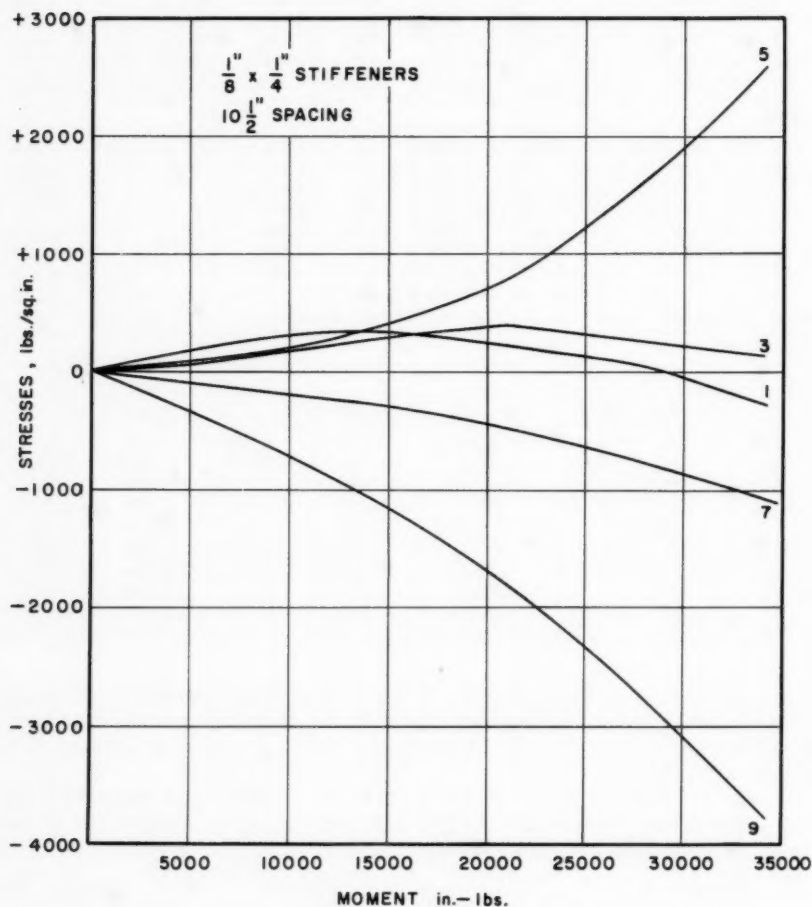

FIG. 3.—STRESSES ON THE OUTSIDE FACE OF THE STIFFENER VERSUS PURE APPLIED BENDING MOMENT
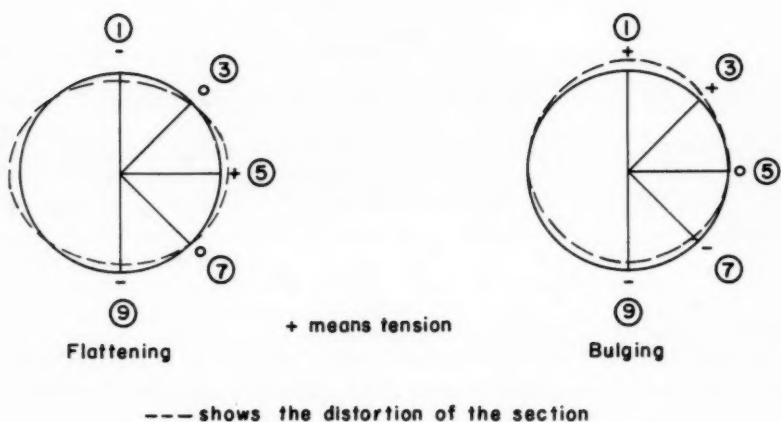
+ means tension

Flattening   Bulging

--- shows the distortion of the section

FIG. 4.—TYPES OF STRESS ON OUTSIDE FACE OF STIFFENER

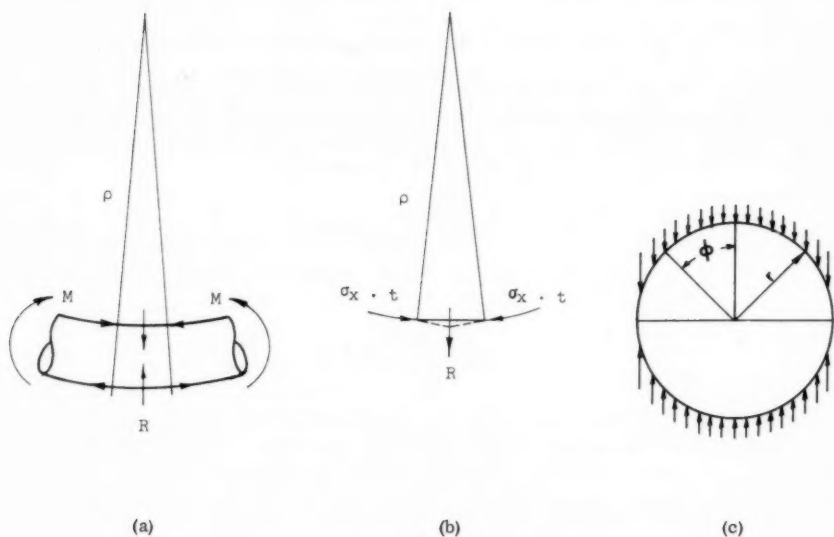(a)   (b)   (c)

FIG. 5.—FLATTENING OF CYLINDER

the top and bottom halves of the cylinder, respectively, have resultant forces, R, parallel to the plane of bending (vertical forces) and acting toward the inside of the cylinder. The longitudinal stress σ_x, at any angle ϕ measured from the vertical, as shown in Fig. 5(c), is equal to

$$\sigma_x = - \frac{E\,r}{\rho} \cos\,\phi \dots\dots\dots\dots\dots\dots (2)$$

in which r is the mean radius of the cylinder and ρ is the curvature of the cylinder.

The resultant of the longitudinal stresses acting toward the inside of the cylinder can be computed at any angle ϕ by considering a unit length both transversely and longitudinally. The value of R per unit of surface (Fig. 5(b)) will be equal to

$$R = \frac{E\,r\,t}{\rho^2} \cos\,\phi \dots\dots\dots\dots\dots\dots (3)$$

in which t is the wall thickness of the cylinder.

The flattening of the cylinder is, therefore, equivalent to subjecting it to vertical pressure whose magnitude is $\dfrac{E\,r\,t}{\rho^2}$ cos ϕ per unit area of surface as

was noted[2] by L. G. Brazier. The distribution of the forces on any stiffener, as a result of flattening of the cylinder, is assumed to vary according to the variation of the pressure on the cylinder. These vertical forces, as shown in Fig. 5(c), are, therefore, taken to be equal to K $\dfrac{E\,r\,t}{\rho^2}$ cos ϕ per unit length of

arc or to K $\dfrac{E\,r\,t}{\rho^2}$ per unit length of horizontal projection. The term K, which

has the unit of length, will be shown to be a complex function varying with the spacing S of the stiffeners and with the other parameters of the problem.

The bending moments, M_r, and the normal forces, N_r, in the stiffener subjected to the flattening forces of Fig. 5(c), are given by

$$M_r = - K \frac{E\,r^3\,t}{4\,\rho^2} \cos(2\,\phi) \dots\dots\dots\dots\dots (4a)$$

and

$$N_r = - K \frac{E\,r^2\,t}{\rho^2} \sin^2\,\phi \dots\dots\dots\dots\dots (4b)$$

Eq. 4a shows that the moments in the stiffener vary in inverse proportion to the square of the curvature of the cylinder. The curvature of a long unstiffened cylinder subjected to pure bending varies nonlinearly with the moment, due to the progressive flattening of the cylinder, as was pointed out by Brazier.[2] The relationship between the moment, M, and the curvature, as derived by Brazier, is

$$M = \frac{E\,\pi\,r^3\,t}{2} \left[\frac{2}{\rho} - \frac{3\,r^4\,(1 - \mu^2)}{\rho^3\,t^2} \right] \dots\dots\dots\dots (5)$$

in which μ is Poisson's ratio.

If no progressive flattening is assumed then the moment is related to the curvature by

$$M = \frac{E \pi r^3 t}{\rho} \dots\dots\dots\dots\dots\dots\dots (6)$$

Both Eqs. 5 and 6 are plotted in Fig. 6 for the model considered herein.

For a stiffened cylinder the true curve, expressing the relationship between the applied bending moment and the curvature, although not quantitatively determinable, should fall between Curves 5 and 6 of Fig. 6. It is reasonable to assume, however, that the curvature, $1/\rho$, varies linearly with the moment as given by Curve 6 especially for the lower values of M, where the divergence between the two curves is negligible. On the other hand the use of an assumed curve falling between 5 and 6 is more justifiable for the higher values of the applied pure bending moment.

Fig. 7 shows a comparative plotting of the stresses on the outside face of the stiffener at Point 5, due to flattening, as a function of the applied bending moment on the cylinder. The experimental stresses at Point 5 obtained from the pure-bending-moment tests on the cylinder are assumed to be caused only by flattening. Both the experimental and theoretical stresses are plotted relative to the stress when $M = 11,522$ in. lb; $M = 11,522$ has been chosen for no reason other than convenience as this moment is one of the experimental moments shown in Table 1(a) and (b); any other base moment, however, could have been used.

It should be noted that the experimental results agree very well with the experimental values, as shown in Fig. 7. Fig. 7 shows that there is a definite flattening action in the cylinder and that the stresses at Point 5 in the stiffener are mainly contributed by this flattening action.

For closely spaced rings, the flattening forces can be assumed to be entirely resisted by the stiffeners in which case K can be taken equal to the stiffener spacing, S. The bending moments in the stiffener will therefore reduce to

$$M_r = - S \frac{E r^3 t}{4 \rho^2} \cos(2 \phi) \dots\dots\dots\dots\dots (7)$$

If ρ, which is the radius of curvature of the cylinder, is taken equal to $E I/M$, then the moments in the stiffener, M_r, will take the form

$$M_r = - \frac{1}{4 \pi^2 r^3 t} \frac{M^2}{E} S \cos(2 \phi) \dots\dots\dots\dots (8)$$

in which I is the moment of inertia of the cylinder, taken equal to $\pi r^3 t$.

Eq. 8 is an approximate formula for determining the bending moments in a ring stiffener due to flattening. A better approximation, however, can be obtained by establishing a more accurate value for the function K. The following paragraphs present the procedure used to establish the major parameters of K:

The vertical pressure acting on the cylinder as a result of its flattening will be resisted in both the transverse and longitudinal directions. This resistance can be closely approximated by assuming that it is similar to a beam subjected to a uniform transverse load and supported on an elastic foundation. The parameters of K can, therefore, be obtained by studying the analogous problem of an infinitely long beam (Fig. 8) loaded by a uniformly distributed load q, and uni-
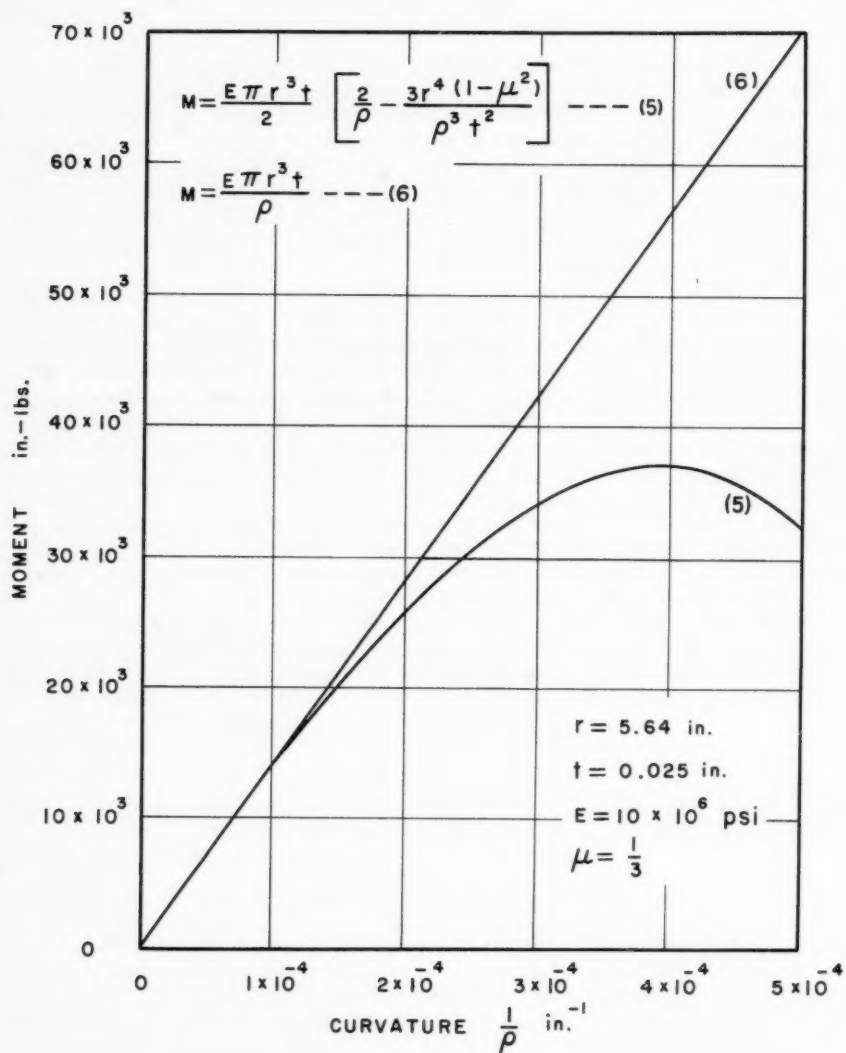
FIG. 6.—MOMENT VERSUS CURVATURE FOR LONG UNSTIFFENED CYLINDER (MOD-
EL)

(a) $\frac{1}{4}'' \times \frac{1}{8}''$ STIFFENER
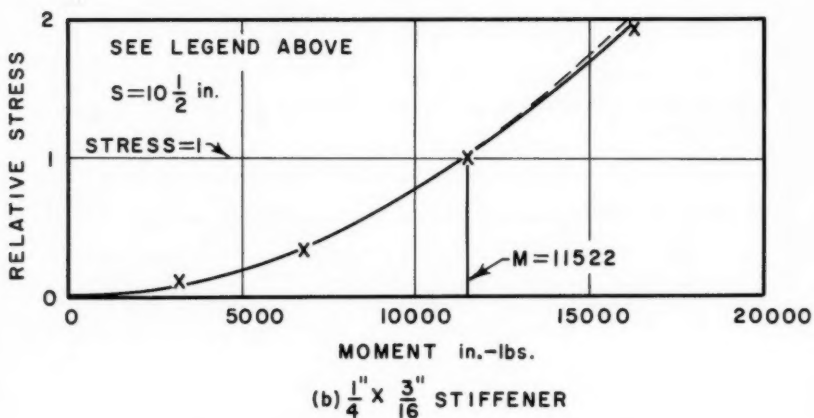
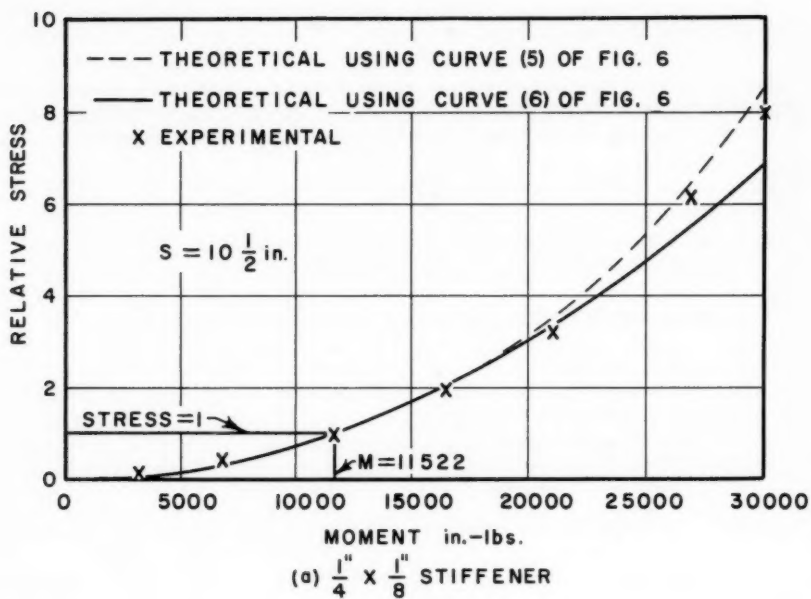(b) $\frac{1}{4}'' \times \frac{3}{16}''$ STIFFENER

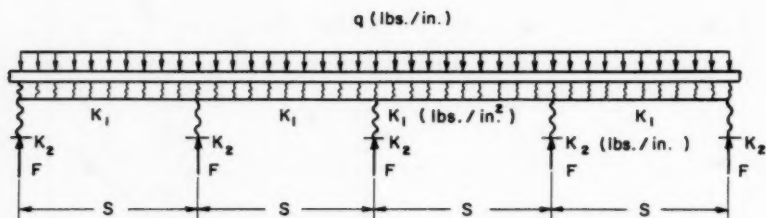FIG. 7.—RELATIVE STRESS VERSUS (FLATTENING)
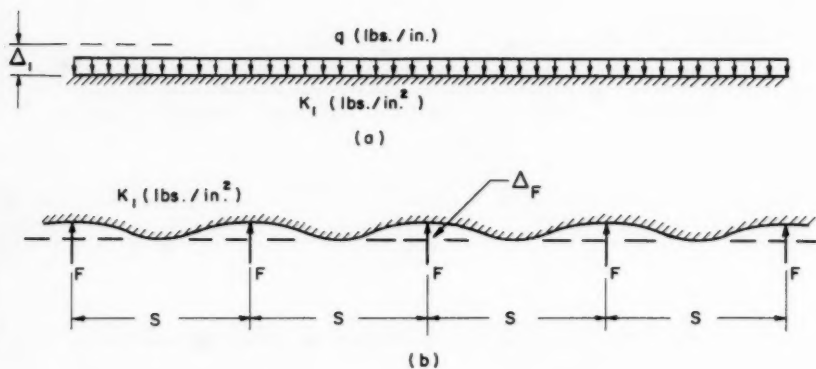
FIG. 8.—INFINITELY LONG BEAM ON ELASTIC SUPPORTS

FIG. 9.—INFINITELY LONG BEAM ON ELASTIC SUPPORTS, METHOD OF SUPER-
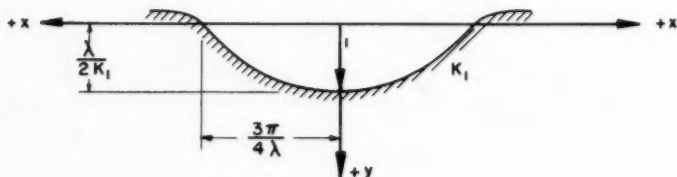POSITION

FIG. 10.—INFINITELY LONG BEAM ON AN ELASTIC SUPPORT LOAD-
ED BY A UNIT CONCENTRATED LOAD

formly supported by an elastic support whose spring constant is K_1. The continuous beam is also supported at different points by concentrated elastic supports whose spacing is equal to S and whose spring constant is K_2.

The magnitude of the force F in any one of the concentrated elastic supports can be obtained by the method of superposition, as illustrated in Fig. 9. Fig. 9(a) shows the elastically supported beam acted on by the uniformly distributed load q and Fig. 9(b) shows the elastically supported beam acted on by the concentrated loads (F-forces). The deflection Δ_1 in Fig. 9(a) is

$$\Delta_1 = \frac{q}{K_1} \quad \dots\dots\dots\dots\dots\dots\dots (9)$$

The deflection Δ_F (Fig. 9(b)) due to the system of concentrated supports should be equal to Δ_1 minus the deformation in the elastic concentrated support. This relationship can be written as

$$\Delta_F = \frac{q}{K_1} - \frac{F}{K_2} \quad \dots\dots\dots\dots\dots\dots (10)$$

The value of Δ_F can be obtained by the use of the reciprocal theorem, making use of the displacement curve of an elastically supported, infinitely long beam, acted on by a unit concentrated load, as shown in Fig. 10. The displacement curve[5] is given by

$$y = \frac{\lambda}{2 K_1} \left\{ e^{-\lambda x} \left[(\cos(\lambda x) + \sin(\lambda x)] \right] \right\} \dots\dots\dots\dots (11)$$

in which

$$\lambda = \sqrt[4]{\frac{K_1}{4 E I}} \quad \dots\dots\dots\dots\dots\dots (12)$$

Using the reciprocal theorem,

$$\Delta_F = F \frac{\lambda}{2 K_1} \left\{ 1 + 2 \sum_{n=1}^{\infty} e^{-n\lambda s} \left[\cos(n \lambda s) + \sin(n \lambda s) \right] \right\} \dots (13)$$

If the value of Δ_F as given in Eq. 13 is substituted into Eq. 10, then F can be written as

$$F = \cfrac{q}{\frac{\lambda}{2} \left\{ 1 + 2 \sum_{n=1}^{\infty} e^{-n\lambda s} \left[\cos(n \lambda s) + \sin(n \lambda s) \right] \right\} + \frac{K_1}{K_2}} \quad \dots (14)$$

If

$$1 + 2 \sum_{n=1}^{\infty} e^{-nx} \left[\cos(n x) + \sin(n x) \right] = \psi(x) \quad \dots\dots\dots (15)$$

---

[5] "Beams on Elastic Foundation," by M. Hetenyi, The Univ. of Michigan Press, Ann Arbor, Mich., 1946.

then the force F of Eq. 14 will be

$$F = \frac{q}{\frac{\lambda}{2}\left[\psi(\lambda\,s)\right] + \frac{K_1}{K_2}} \quad \ldots\ldots\ldots\ldots\ldots\ldots.(16)$$

Values of $\psi(x)$ are given in Table 2.

The resistance of the stiffeners when subjected to the flattening action will be analogous to the resistance of the concentrated elastic supports, whereas the resistance of the shell will be analogous to the resistance of the uniformly distributed elastic supports. Therefore, the forces on the stiffeners $K\,\dfrac{E\,r\,t}{\rho^2}$ (Fig. 5(c)) will be assumed to have the same form as the force F of Eq. 16, in

TABLE 2.—VALUES OF $\psi(x)$ FROM EQ. 15

x	$\psi(x)$	x	$\psi(x)$	x	$\psi(x)$
0.10	20.002	1.40	1.459	3.40	0.921
0.20	10.001	1.50	1.370	3.60	0.929
0.30	6.667	1.60	1.295	3.80	0.938
0.40	5.001	1.70	1.230	4.00	0.949
0.50	4.002	1.80	1.174	4.50	0.973
0.60	3.336	1.90	1.127	5.00	0.991
0.70	2.861	2.00	1.086	5.50	1.000
0.80	2.506	2.20	1.021	6.00	1.003
0.90	2.230	2.40	0.976	6.50	1.004
1.00	2.011	2.60	0.945	7.00	1.003
1.10	1.833	2.80	0.927	7.50	1.001
1.20	1.686	3.00	0.919	8.00	1.001
1.30	1.563	3.20	0.917		

which case $\dfrac{E\,r\,t}{\rho^2}$ will be equivalent to q and K will be equivalent to $\dfrac{1}{\frac{\lambda}{2}\left[\psi(\lambda\,s)\right] + \frac{K_1}{K_2}}$.

The parameters of K can therefore be obtained in the following manner:

$$K_1 \sim \frac{E\,t^3}{r^4} \qquad K_2 \sim \frac{E\,I_r}{r^4} \qquad I \sim t^3$$

therefore,

$$\frac{K_1}{K_2} \sim \frac{t^3}{I_r} \quad \text{or} \quad \frac{K_1}{K_2} = C_1\,\frac{t^3}{I_r}$$

$$\lambda \sim \sqrt[4]{\frac{1}{r^4}} \quad \text{or} \quad \lambda = \frac{C_2}{r}$$

in which C_1 and C_2 are constants. The function K will, therefore, take the form

$$K = \frac{1}{\frac{\lambda}{2}\left[\psi(\lambda\,s)\right] + C_1\,\dfrac{t^3}{I_r}} \quad \ldots\ldots\ldots\ldots\ldots.(17)$$

in which

$$\lambda = \frac{C_2}{r} \dots\dots\dots\dots\dots\dots(18)$$

Experimental results are used to establish average values for the constants C_1 and C_2. The experimental stresses due to flattening were separated from the pure-bending-moment tests by assuming that the stresses at Point 5 are caused only by flattening and that the variation of the stresses around the stiffener due to flattening are proportional to $\cos(2\,\phi)$.

The results of the tests made on both the 1/4 in. by 1/8 in. and the 1/4 in. by 3/16 in. stiffeners were used to determine values for C_1 and C_2 so that the derived equations would agree with the experimental results. The method of determining the coefficients C_1 and C_2 is as follows:

For any stiffener spacing and applied moment, M, the stress at a specified point on the stiffener is computed by using Eqs. 4. This stress, which is expressed in terms of K, is equated to the stress obtained from the experimental results, thus resulting in what one might term the experimental value of K. If for any combination of ring spacing and applied moment, M, one computes the experimental K for the two different size stiffeners, then a set of two simultaneous equations are obtained by substituting these values of K in Eq. 17. These two equations can then be solved for C_1 and C_2.

Different sets of ring spacings and applied moments were used which resulted in different values for C_1 and C_2. The average value for each coefficient was used which resulted in values for $C_1 = 1.0$ and $C_2 = 1.1$. It should be stated that, although values for C_1 and C_2 could have been easily chosen so that one experimental point would coincide with the calculated curve, nevertheless, this agreement would not have been possible for all the experimental points if the general form of Eq. 17 were not correct.

The effective width of the shell acting as an integral part of the stiffener was taken to be equal to 24 times the thickness of the shell. The actual determination of the effective width, which is a problem in itself, was not investigated herein. It might be stated, however, that the effective width is, among other things, dependent on the type of stress, the material, and the method of connecting the stiffener to the shell. The value of 24 t was arbitrarily chosen as an average value used in problems of this type.

Fig. 11 gives the variation of both calculated and experimental stress in the stiffener, due to flattening, at Points 1 and 9 (top and bottom of the stiffener) as a function of the spacing of the stiffeners. The calculated stresses were obtained by using Eqs. 4 and 17.

Effect of Bulging of Cylinder.—The bulging of the cylinder is caused by the increase of the radii in the compression half and a decrease of the radii in the tension half of the cylinder due to Poisson's ratio. The longitudinal stresses in the cylinder due to an applied pure bending moment will be equal to

$$\sigma_x = -\frac{M}{\pi\,r^2\,t}\,\cos\,\phi \dots\dots\dots\dots\dots(19)$$

in which ϕ is measured as shown in Fig. 12. The distortion of the cross-section, δ, from its originally circular shape can be written in the form:

$$\delta = \frac{\mu\,M}{\pi\,r\,t\,E}\,\cos\,\phi \dots\dots\dots\dots\dots(20)$$

(a) $\frac{1}{4}''$ X $\frac{1}{8}''$ STIFFENERS

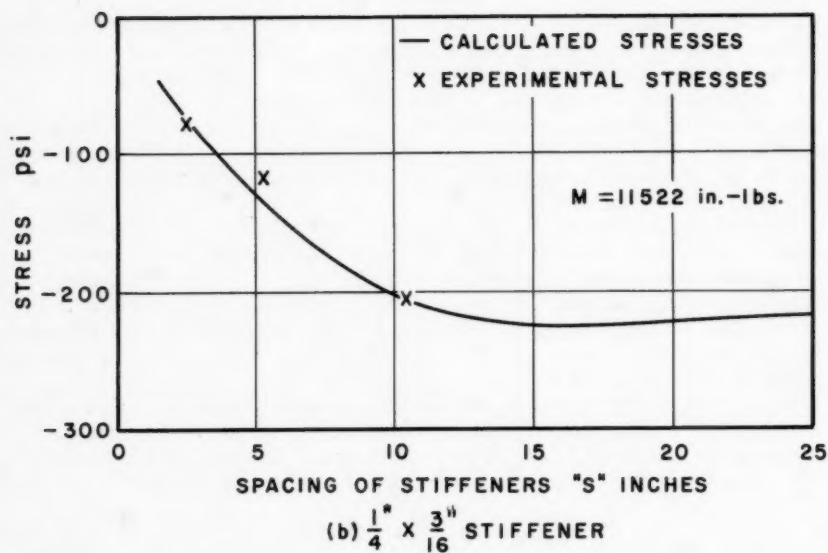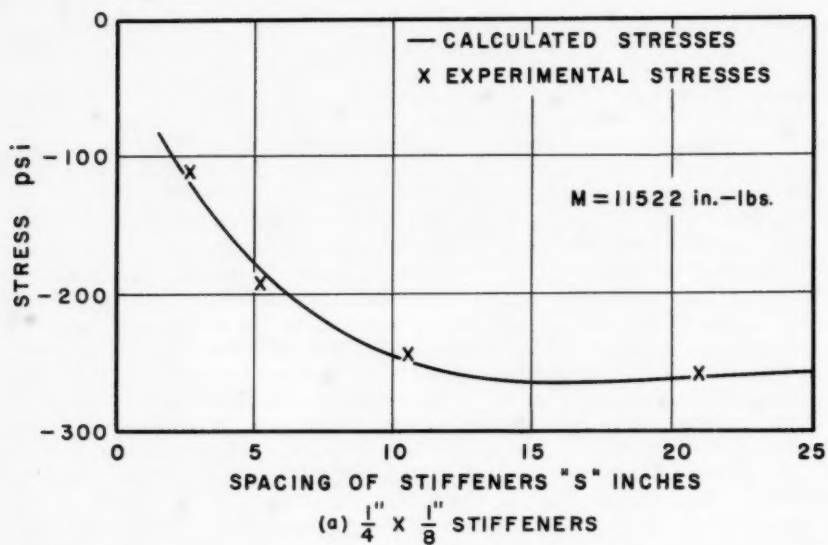(b) $\frac{1}{4}''$ X $\frac{3}{16}''$ STIFFENER

FIG. 11.—STRESSES ON THE OUTSIDE FACE OF STIFFENER AT TOP OR BOTTOM VERSUS SPACING OF STIFFENERS (FLATTENING)

The distribution of the radial forces on the stiffeners will be assumed to be proportional to the radial displacement δ or equal to Z cos φ. The tangential forces will be assumed to be Z sin φ which satisfy the equilibrium conditions (Fig. 13).

If the shear and normal deformations are ignored, then the loading of Fig. 13 produces no bending moments in the ring, a condition which indicates that
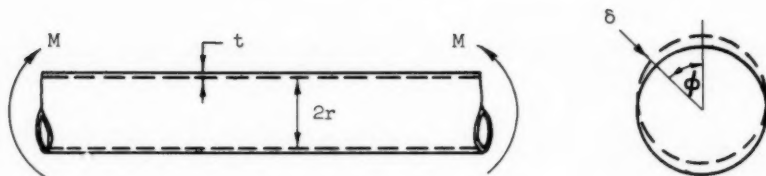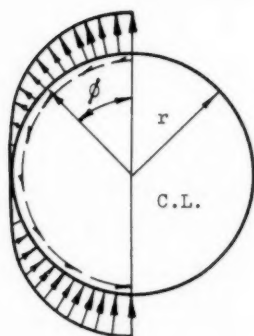

FIG. 12.—ILLUSTRATION OF BULGING OF CYLINDER

Radial Forces = Z cos φ
Tangential Forces = Z sin φ

Symmetrical about C.L.

FIG. 13.—DISTRIBUTION OF FORCES ACTING ON A RING STIFFENER DUE TO BULGING OF CYLINDER

the total strain energy in the ring is approaching a minimum. For this condition of no bending moments, the normal forces in the ring will be given by

$$N_r = Z\ r\ \cos\ \phi \dots\dots\dots\dots\dots\dots(21)$$

As a result of the bulging of the cylinder, the stiffeners are mainly subjected to normal forces as given by Eq. 21. For this reason the major parameters of Z of Fig. 13 can be obtained by utilizing the solution of the following similar problem: Consider an infinitely long cylinder subjected to uniformly distributed line loads, acting along different circular sections and spaced at a distance S (Fig. 14).

The radial displacement of the cylinder under any one of the **F** loads can be obtained by the reciprocal theorem if one uses the solution of an infinitely long cylinder loaded uniformly along one circular section as shown in **Fig. 15**.

The radial displacements of the cylinder in **Fig. 15** are given by[6]

$$y = \frac{F\, r^2\, \beta}{2\, E\, t}\, e^{-\beta x}\Big[\big(\sin(\beta x) + \cos(\beta x)\big] \quad \dots\dots\dots\dots .(22)$$

in which

$$\beta^4 = \frac{3\left(1 - \mu^2\right)}{r^2\, t^2} \quad \dots\dots\dots\dots\dots\dots .(23)$$

Using the reciprocal theorem, the radial displacement, Δ_F, in **Fig. 14** can be written in the form:

$$\Delta_F = \frac{F\, r^2\, \beta}{2\, E\, t}\left\{ 1 + 2 \sum_{n=1}^{\infty} e^{-n\beta s}\,\Big[\sin(n\,\beta\,s) + \cos(n\,\beta\,s)\Big]\right\} \dots .(24)$$

But

$$\left\{1 + 2 \sum_{n=1}^{\infty} e^{-n\beta s}\,\Big[\sin(n\,\beta\,s) + \cos(n\,\beta\,s)\Big]\right\} = \psi(\beta\,s) \dots .(25)$$

as has been defined by **Eq. 15**, therefore

$$\Delta_F = \frac{F\, r^2\, \beta}{2\, E\, t}\,\Big[\psi(\beta\,s)\Big]\dots\dots\dots\dots\dots .(26)$$

The tangential components of the forces **F** (**Fig. 14**) can be written as

$$N = F\, r\dots\dots\dots\dots\dots\dots .(27a)$$

or

$$F = \frac{N}{r}\dots\dots\dots\dots\dots\dots .(27b)$$

The normal forces in the stiffener produced by the bulging of the cylinder are given in **Eq. 21**. Therefore, the parameters governing the radial displacements in the cylinder at any stiffener location, due to the action of the stiffeners on the cylinder can be approximated by substituting N_r of **Eq. 21** for **F** r of **Eq. 26**. These radial displacements should be equal to the displacements in the cylinder due to bulging (given by **Eq. 20**), minus the radial displacements in the stiffener itself. This strain condition can be expressed by

$$\frac{Z\, r(\cos\,\phi)\, r\, \beta}{2\, E\, t}\,\Big[\psi\,(\beta\,s)\Big] = \frac{\mu}{\pi\, r\, t}\,\frac{M}{E}\cos\,\phi - \frac{Z\, r^2}{A\, E}\cos\,\phi\dots .(28)$$

(Note that N_r from **Eq. 21** was substituted for (F r) of **Eq. 26** and that r_r is

---

6 "Theory of Plates and Shells," by S. Timoshenko, McGraw-Hill Book Co., Inc., New York, 1940.

taken equal to r.) Solving for Z of Eq. 28, one obtains

$$Z = \frac{\dfrac{\mu\,M}{\pi\,r^3}}{\dfrac{\beta}{2}\left[\psi(\beta\,s)\right] + \dfrac{t}{A_r}} \quad \dotfill (29)$$

It should be noted that the purpose of using the results of another problem was to establish the major parameters relative to the magnitude of the forces
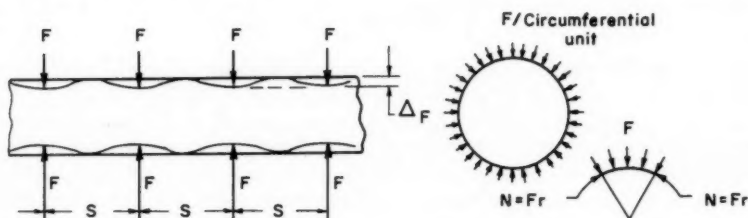

FIG. 14.—INFINITELY LONG CYLINDER SUBJECTED TO EQUALLY SPACED RADIAL LOADS
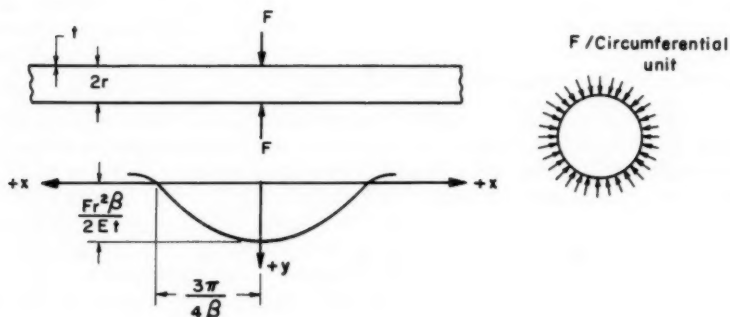
FIG. 15.—INFINITELY LONG CYLINDER SUBJECTED TO UNIFORMLY DISTRIBUTED RADIAL LOADING ALONG A CIRCULAR SECTION

acting on the stiffeners due to the bulging of the cylinder. The value of Z given by Eq. 29 should only be used to establish the parameters rather than the magnitude of the forces acting on the stiffener. Two constants can be introduced to define the magnitude of Z which will make it possible to express the value of Z in the form:

$$Z = \frac{\dfrac{\mu\,M}{\pi\,r^3}}{\dfrac{\beta_1}{2}\left[\psi(\beta_1\,s)\right] + C_3\,\dfrac{t}{A_r}} \quad \dotfill (30)$$

in which

$$\beta_1 = \frac{C_4}{\sqrt{r}\, t} \quad \ldots\ldots\ldots\ldots\ldots\ldots\ldots(31)$$

If the value of Z as given by Eq. 30 is substituted into Eq. 21, then

$$N_r = \frac{\dfrac{\mu\, M}{\pi\, r^2}\cos\phi}{\dfrac{\beta_1}{2}\left[\psi(\beta_1\, s)\right] + C_3\,\dfrac{t}{A_r}} \quad \ldots\ldots\ldots\ldots\ldots(32)$$

in which A_r is the cross-sectional area of the stiffener.

Values of $C_3 = 1.0$ and $C_4 = 0.7$ were established by using the experimental data for the two sizes of stiffeners used. The method of determining C_3 and C_4 is similar to that used in determining C_1 and C_2.

According to Eq. 32 the stresses in the stiffener, due to bulging, will vary linearly with the applied bending moment on the cylinder. This is substantiated by the experimental results as shown in Fig. 16 where both the experimental and theoretical stress at the top of the stiffener (Point 1) are plotted relative to the stress when $M = 11,522$ in. lb. The stress at Point 1 when $M = 11,522$ in. lb is taken to be equal to unity for both the theoretical and experimental values.

The variations of the stresses around the ring stiffener due to bulging should be proportional to $\cos\phi$. The comparison with the experimental results is shown in Fig. 17. The discrepancy between the calculated and the experimental stresses can be attributed to the following:

1. The distribution of the experimental stresses around the stiffener, caused by the flattening effect, was assumed to be identical with the results of the analytical investigation. This means that all the experimental errors are carried over with the experimental stresses due to the bulging of the cylinder.

2. The stresses in the stiffener due to bulging are computed on the basis of a certain distribution of forces acting on a perfectly circular section thus producing no bending moments in the stiffener. Any slight variations in the circular shape of the stiffener or in the distribution of the forces can produce bending moments in the stiffener which will result in appreciable changes in the stress.

The variations of the stresses in the stiffener due to the bulging of the cylinder are given in Fig. 18 as a function of the spacing of the stiffeners. The agreement between the experimental results and the calculated curves is reasonably good.

Separate Effect of Local Loading.—The bending moments in the cylinder resulting from the application of any local loading will cause the cylinder to flatten and to bulge as a result of the general bending action of the cylinder. In addition to the flattening and to the bulging of the cylinder, the local loading will have a separate and an appreciable effect on the ring stiffeners.

If the cylinder is loaded by uniformly distributed radial loading on the top half, then the forces on the stiffeners, due to the separate effect of this loading, can be assumed to follow the distribution shown in Fig. 19, in which w is

(a) $\frac{1}{4}'' \times \frac{1}{8}''$ STIFFENER

(b) $\frac{1}{4}'' \times \frac{3}{16}''$ STIFFENER
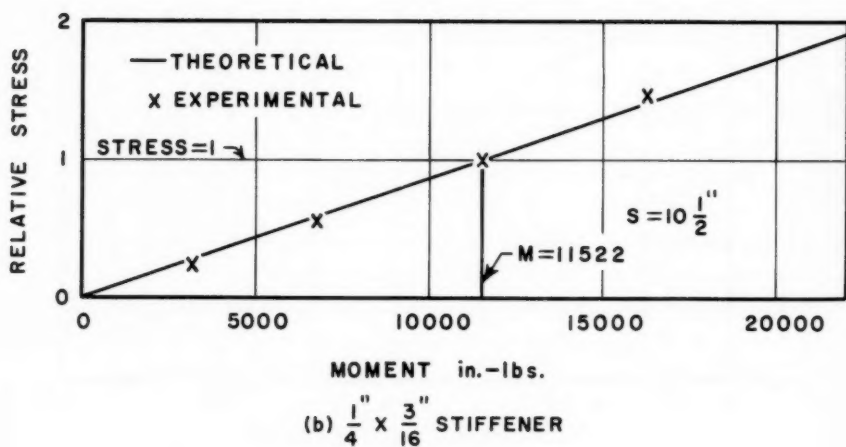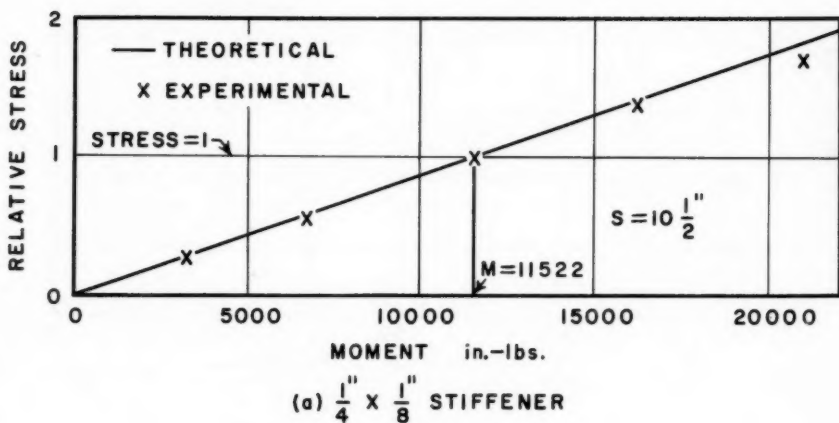
FIG. 16.—RELATIVE STRESS VERSUS MOMENT (BULGING)

(a) $\frac{1}{4}$" X $\frac{1}{8}$" STIFFENER

(b) $\frac{1}{4}$" X $\frac{3}{16}$" STIFFENER
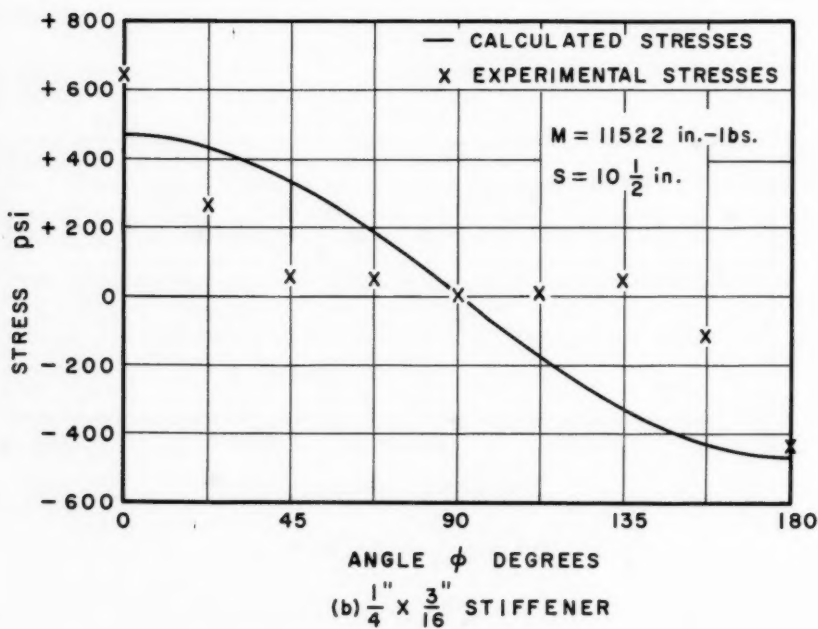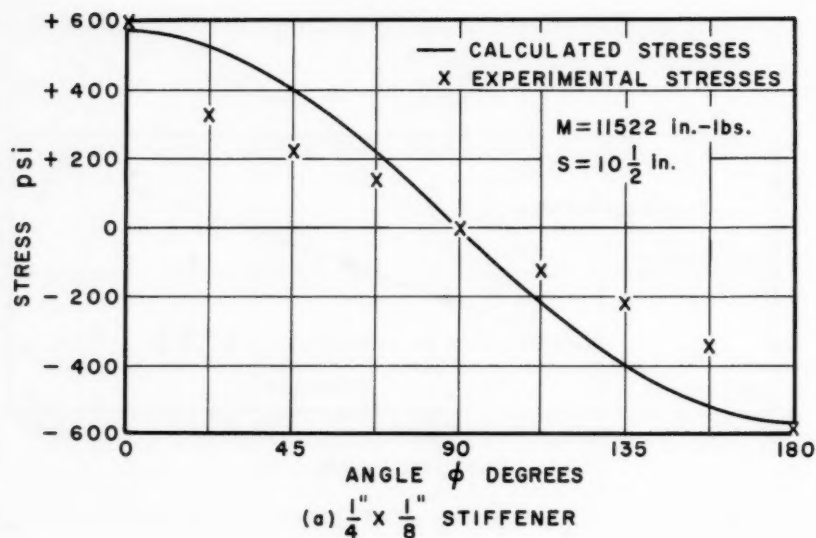
FIG. 17.—VARIATION OF THE STRESSES AROUND STIFFENER (BULGING)

(a) $\frac{1}{4}" \times \frac{1}{8}"$ STIFFENERS

(b) $\frac{1}{4}" \times \frac{3}{16}"$ STIFFENERS
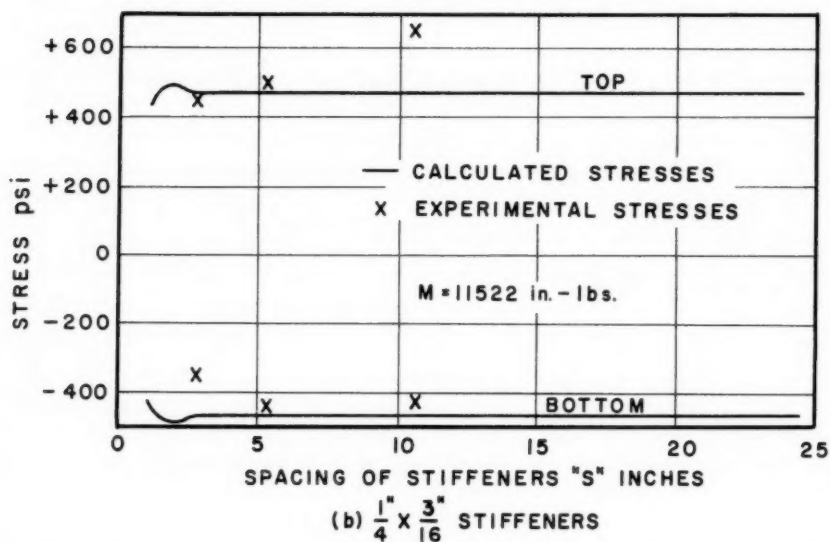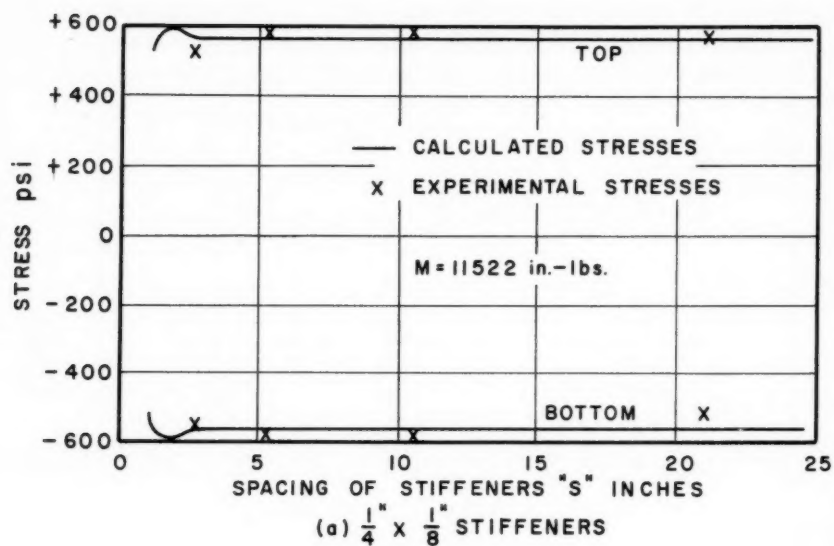
FIG. 18.—STRESSES ON OUTSIDE FACE OF STIFFENER AT TOP AND BOTTOM
VERSUS SPACING OF STIFFENERS (BULGING)

the magnitude of the radial pressure on the cylinder. The tangential forces of $\frac{2}{\pi}$ w' sin ϕ will satisfy the equilibrium condition. This distribution will be shown later to be in agreement with the experimental results.

The bending moments and the normal forces in the ring loaded as shown in Fig. 19 are given by the following equations:

For $0 \lessgtr \phi \lessgtr \frac{\pi}{2}$

$$M_r = \left(\frac{1}{2} - \frac{3}{2\pi} \cos \phi - \frac{1}{\pi} \phi \sin \phi \right) w' \, r^2 \dots \dots \dots \dots (33)$$

For $\frac{\pi}{2} \lessgtr \phi \lessgtr \pi$

$$M_r = \left(\sin \phi - \frac{1}{2} - \frac{3}{2\pi} \cos \phi - \frac{1}{\pi} \phi \sin \phi \right) w' \, r^2 \dots \dots (34)$$

For $0 \lessgtr \phi \lessgtr \frac{\pi}{2}$

$$N_r = \left(- \frac{1}{2\pi} \cos \phi - 1 + \frac{1}{\pi} \phi \sin \phi \right) w' \, r \dots \dots \dots \dots (35)$$

For $\frac{\pi}{2} \lessgtr \phi \lessgtr \pi$

$$N_r = \left(- \frac{1}{2\pi} \cos \phi - \sin \phi + \frac{1}{\pi} \phi \sin \phi \right) w' \, r \dots \dots \dots (36)$$

in which $+M_r$ designates tension on the outside and $+N_r$ designates tension. The term K' (Fig. 19), which has the unit of length, is a function varying with the

Radial loading =
K'w = w'/circumferential unit

Tangential loading =
$(2/\pi)$w' sin ϕ/circumferential unit
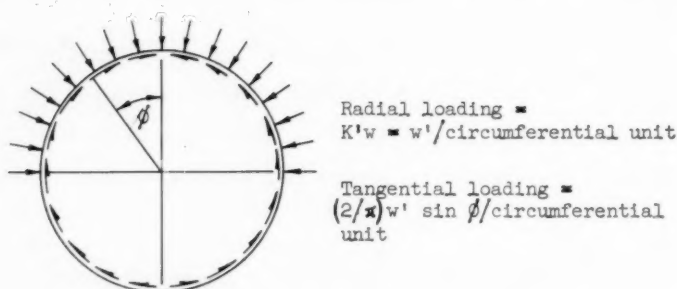
FIG. 19.—FORCES ON STIFFENER DUE TO SEPARATE EFFECT OF LOCAL RADIAL LOADING

spacing of the stiffeners and with the other parameters of the problem. The maximum value that K' can assume is S (spacing of the stiffeners) if the shell is assumed to be completely ineffective in resisting the local forces. A more accurate evaluation of K' can be obtained by assuming that K' has the same
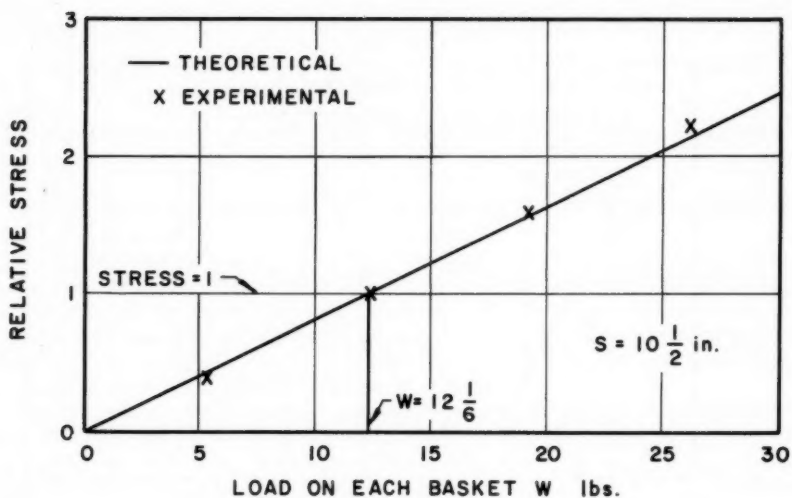
(a) $\frac{1}{4}" \times \frac{1}{8}"$ STIFFENER
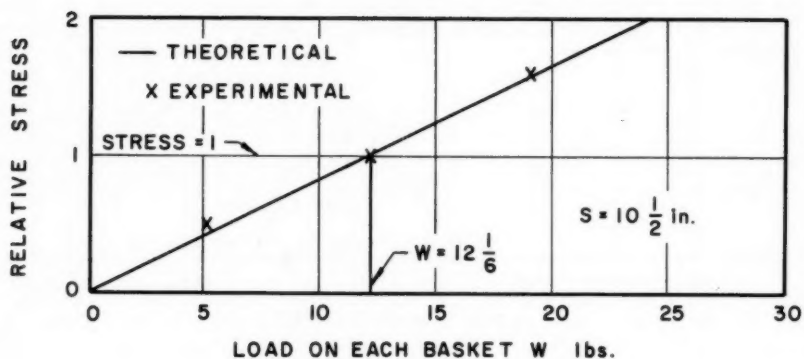
(b) $\frac{1}{4}" \times \frac{3}{16}"$ STIFFENER

FIG. 20.—RELATIVE STRESS VERSUS LOAD (SEPARATE EFFECT OF LOCAL LOADING)
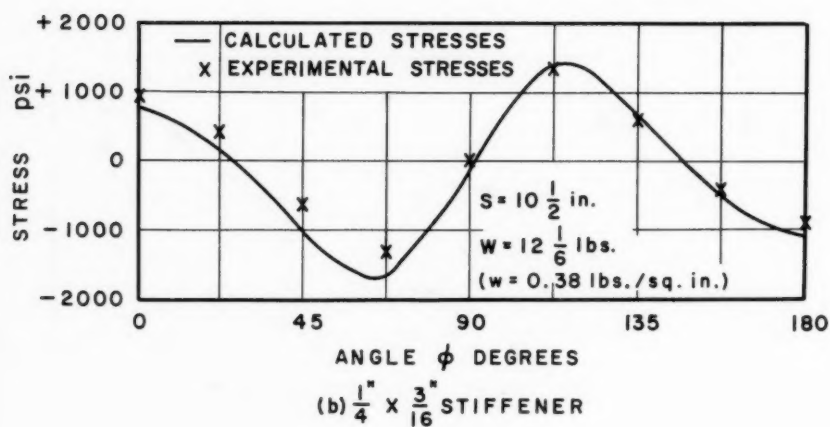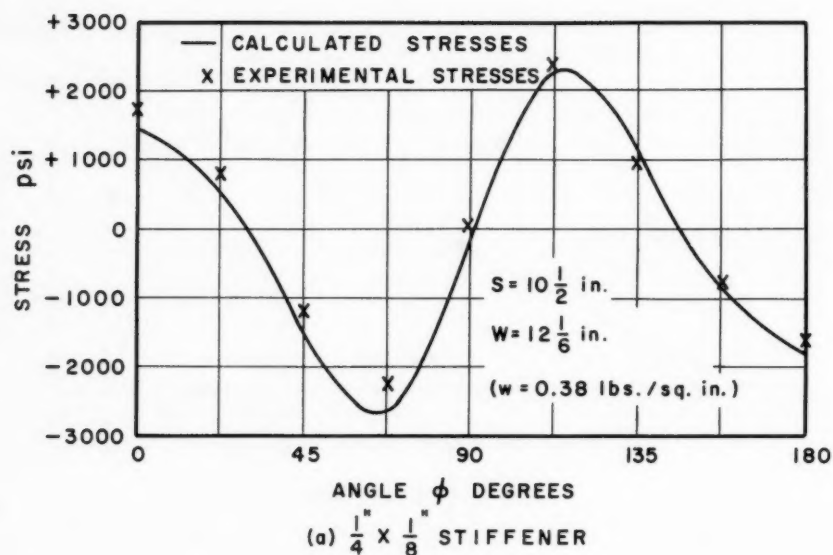
FIG. 21.—VARIATION OF STRESSES AROUND STIFFENER (SEPARATE EFFECT OF
        LOCAL LOADING)

form as K of Eq. 17, or:

$$K' = \cfrac{1}{\frac{\lambda'}{2}\left[\psi(\lambda' \, s)\right] + C_5 \frac{t^3}{I_r}} \quad \dots\dots\dots\dots\dots(37)$$

in which

$$\lambda' = \frac{C_6}{r} \dots\dots\dots\dots\dots\dots\dots\dots(38)$$

The values of C_5 and C_6 that will best satisfy the experimental data were found to be equal to 0.21 and 0.45, respectively.

The stresses in the stiffener due to the separate effect of the local loading should vary linearly with the load according to Eqs. 33 through 36. The comparison with the experimental data is shown in Fig. 20 where both the theoretical and experimental stresses at the top of the stiffener (Point 1) are plotted relative to the stress when $W = 12\text{-}1/6$ lb. Both the theoretical and experimental stress are taken to be equal to unity when $W = 12\text{-}1/6$ lb.

The variations of the stresses around the stiffener as a result of the separate effect of the local radial loading is given in Fig. 21 for both calculated and measured stresses. It is important to note here that the good agreement between calculated and experimental values (Fig. 21) shows that the assumptions used in establishing the forces on the rings due to the separate effect of the local loading are reasonable assumptions.

Fig. 22 shows the variations of the stresses in the stiffener due to the separate effect of the radial local loading, as a function of the spacing of the stiffeners. Both the calculated stresses and the experimental stresses are shown for the 1/4 in. by 1/8 in. stiffener at Points 1 and 9 (top and bottom of the stiffener). It should be noted that the values of C_5 and C_6 were chosen so that the best agreement was obtained between experimental and calculated stresses at both the top and the bottom of the stiffener. It is believed that the discrepancy between calculated and measured stresses is the result of assuming that the baskets transmitting the local loading on the cylinder produce uniform radial pressure on the top half of the shell. This assumption can be in error due, primarily, to the frictional forces between the bands and the shell. It is interesting to observe the better agreement between calculated and measured stresses on the bottom half of the stiffener (Fig. 21).

CONCLUSIONS

The three types of action that are treated herein, (flattening, bulging, and the separate effect of the local loading) are considered to be the major factors in determining the forces acting on ring stiffeners in long thin-walled cylinders subjected to bending.

For each type of action the assumed forces on the stiffener resulted in a distribution of stresses around the stiffener which were shown to agree reasonably well with the experimental results.

It can be stated, therefore, that the stresses in the ring stiffeners can be approximately computed by the formulas developed in this paper. The bending moments and the normal forces due to flattening can be computed by Eqs. 4
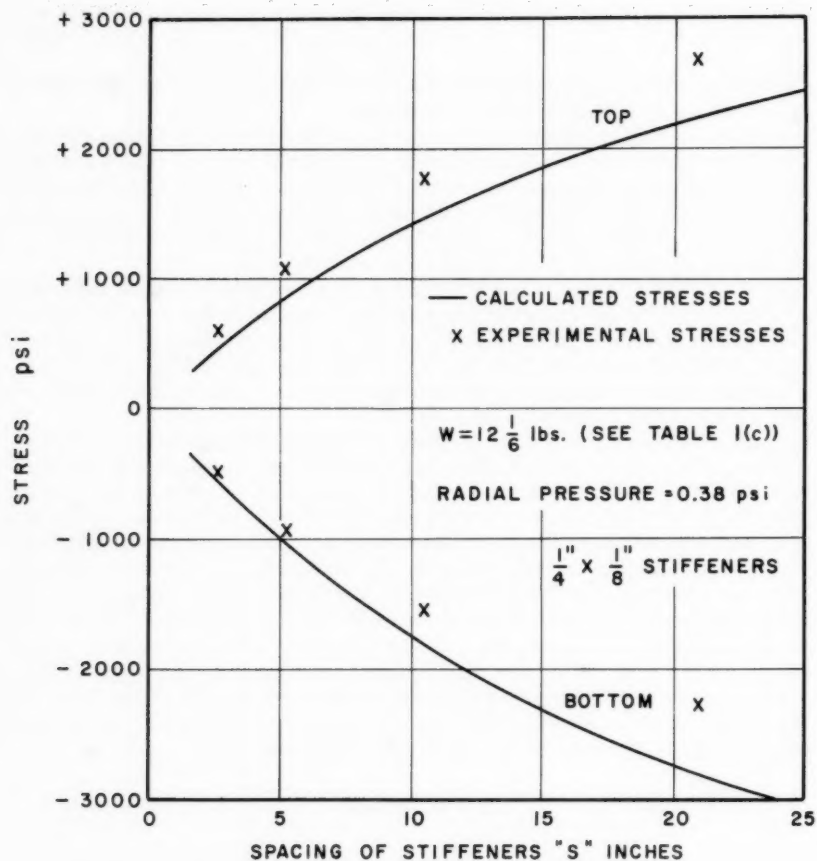
FIG. 22.—STRESSES ON OUTSIDE FACE OF THE STIFFENER AT TOP AND BOTTOM
VERSUS SPACING OF STIFFENERS (SEPARATE EFFECT OF LOCAL
LOADING)

and 17 whereas the normal forces due to bulging can be computed by Eq. 32. From the limited experimental results, values of $C_1 = 1.0$, $C_2 = 1.1$, $C_3 = 1.0$, and $C_4 = 0.7$ are recommended for use in conjunction with the foregoing equations. It should be noted again that these coefficients were obtained from tests on only one cylinder. The stiffeners, however, were changed in size and spacing.

The moments and normal forces in the rings due to the separate effect of the local loading will depend on the distribution of the local forces on the cylinder. To illustrate this type of action, one particular kind of local loading was investigated.

The maximum stresses in the rings can then be obtained by a combination of the foregoing three actions.

ACKNOWLEDGMENTS

This investigation is based on the writer's doctoral thesis[7] at the University of Michigan, submitted to a doctoral committee under the chairmanship of Lawrence C. Maugh, F. ASCE.

APPENDIX.—NOTATION

The following letter symbols, adopted for use in this paper and for the guidance of discussers, conform essentially with "Letter Symbols for Structural Analysis" (ASA Y-10 1961) prepared by a committee of the American Standards Association with the Society representation, and approved by the Association in 1961:

A_r = cross-sectional area;

C_1-C_6 = constants;

E = modulus of elasticity;

F = force;

I = moment of inertia;

I_r = moment of inertia of stiffener;

K = complex function varying with the spacing of the stiffeners and other parameters, defined in Eq. 17;

K_1, K_2 = spring constants;

M = bending moment;

M_r = bending moment in the stiffener;

---

[7] "An Experimental Study of the Stresses in Ring Stiffeners in Long Thin-Walled Cylinders Subjected to Bending." by W. S. Rumman, thesis presented to the Univ. of Michigan, in Ann Arbor, Mich., in 1959, in partial fulfilment of the requirements for the degree of Doctor of Philosophy.

N_r = normal force in the stiffener;

P   = load in basket for pure-bending condition;

q   = uniformly distributed load;

R   = resultant force;

r   = mean radius of cylinder

S   = stiffener spacing;

t   = wall thickness of cylinder;

W   = load in basket for local-loading condition;

w   = radial pressure on the cylinder;

x   = longitudinal direction;

y   = vertical direction;

β = terms defined in Eqs. 23 and 31;

Δ = deflection;

δ = distortion;

λ = terms defined in Eqs. 12 and 18;

μ = Poisson's ratio;

ρ = curvature of the cylinder;

σ_x = longitudinal stress; and

ϕ = angle.

Journal of the

STRUCTURAL DIVISION

Proceedings of the American Society of Civil Engineers

MOMENTS AT SELECTED POINTS IN CONTINUOUS GIRDERS

By George H. Dell,[1] F. ASCE

SYNOPSIS

Formulas for areas under the influence line are presented for use in the computation of maximum moments at any point in girder spans of continuous structures carrying uniform load. The girders are assumed to be of constant cross section. Two cases are treated, namely, beams or girders receiving the uniform loading directly, and girders in which the uniform floor loads are applied in the form of floor beam concentrations.

INTRODUCTION

Continuous beam- or girder-spans in which the uniform loads are applied directly are examined, and equations of the influence line for moment at any point of a particular span are derived, together with formulas expressing the total areas under the influence line. Subsequently, criteria are given for ascertaining whether or not partial-span loading is required in order to obtain maximum moment, and formulas for use in this case are presented for the evaluation of the partial areas under the influence line.

A procedure similar to the preceding one is used in application to girder-spans in which the live loads are applied through floor beams. Numerical examples illustrative of the equations and procedures are presented. Methods for determining the boundaries of the regions of partial loading are examined.

The principal terms employed herein are defined as follows:

Reference section denotes the section to which a particular influence line pertains;

Primary span is the span containing the reference section;

Secondary span describes any span other than the primary span;

Primary region of partial loading denotes a region, in the primary span, within which, for all reference sections contained therein, partial loading of that span is required in order to obtain maximum moment;

Secondary region of partial loading refers to a region, in the primary span, within which, for all reference sections contained therein, partial loading of a particular secondary span is required in order to obtain maximum moment;
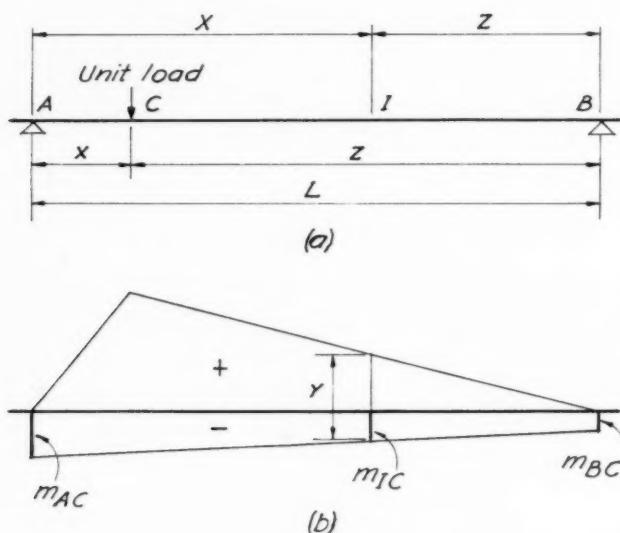
FIG. 1

Partial areas denotes the two areas, one positive and the other negative, occurring in the influence line in a given span when partial loading of that span is involved;

m-moments describes the "indeterminate" moments in any span, resulting from unit load at a specified point of a given span; and

u-moments refers to the indeterminate moments in any span, resulting from a unit negative fixed-end moment at a specified end of a given span.

The m-moments and u-moments are further defined by two subscripts, the first of which designates the location of the moment, and the second, the point of application of the corresponding unit load or fixed-end moment.

Fig. 1(a) represents a primary span, the reference section being at one of the ends of the span or at an intermediate point, I. Fig. 1(b) shows the m-moments produced at points A, B, and I by a unit load at point C [Fig. 1(a)].

The length of the span is designated by L, and the location of point C is given by the abscissae x and z, measured from A and B, respectively. The location of the reference section is given by the distances X and Z, measured from A and B, respectively. Ordinates to the influence line in the primary span are denoted by Y.

Fig. 2 illustrates a secondary span, with a unit load applied at point c. This unit load produces end-moments m_{Ac} and m_{Bc} in the primary span, and a moment m_{Ic} at the reference section, I. The length of the span is designated by l, and point c is located by the abscissae x and z, measured from the end-points, a and b, respectively. Ordinates to the influence line in a secondary span are denoted by y.

In the case of the influence line for moment at an interior support of a series of continuous spans on simple supports, either of the spans adjacent to the support may be taken as the primary span.

The m-moments can be expressed as simple functions of the u-moments. The latter may be conveniently evaluated with the aid of analyses that give the end-moments produced by a unit couple (or unbalanced moment) applied successively at the various joints. Sets of analytical data in this form are shown in Figs. 3 and 4 for use in subsequent numerical examples. Analyses of the three-span series of girders in Fig. 3(a) are given in Figs. 3(b), 3(c) and 3(d).
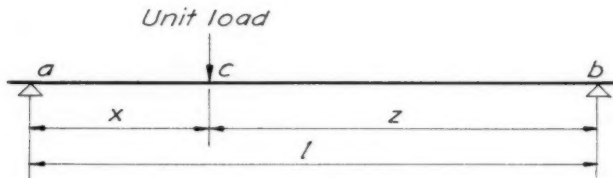
FIG. 2

Similar analyses for a single-story continuous frame are given in Figs. 4(a) to 4(d), inclusive. The quantities enclosed in circles in Figs. 3(a) and 4(a) are the relative stiffnesses of the members, that is, the relative values of the moment of inertia divided by the span length. The modulus of elasticity is assumed to be constant. In numerical examples, a particular span is identified according to span number, counting from left to right.

The signs of all moments follow the so-called "designer's convention," the moment being positive or negative according to whether the upper fibers are in compression or tension, respectively. With this sign-convention, equations developed for one end of a span are readily adapted to the other end by interchange of terms and symbols.

The analyses shown in Figs. 3 and 4 were made by the slope-deflection method, and the signs were then changed wherever necessary to conform to the stated sign-convention. In accordance with Eqs. 3a, 3b, 18a, and 18b, to be presented, the u-moments are obtained by superposition. Therefore, in a given set of slope-deflection equations, the right-hand term of the joint equation for the joint where the unit unbalanced moment is applied is placed equal to unity, and the right-hand terms of the remaining joint equations are zero. When sidesway is involved, as in the single-story frame in Fig. 4 (there being no
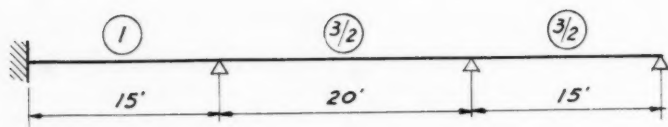
FIG. 3

lateral forces), the necessary additional equation also has a zero right-hand term, consistent with the requirement that the sum of the column shears be zero. The analyses shown in Fig. 3 were carried out concurrently, as were those in Fig. 4.

The determination of the magnitudes and signs of the u-moments from analyses such as shown in Figs. 3 and 4 is explained in detail in Example 1.

Notation.—The letter symbols adopted for use in this paper are defined where they first appear in the text, and are arranged alphabetically, for convenience of reference, in Appendix I.

BEAMS OR GIRDERS WITH DIRECT UNIFORM LOADING

Primary Span.—Referring to Fig. 1, the fixed-end moments resulting from a unit load at C are $-\dfrac{xz^2}{L^2}$ and $-\dfrac{x^2z}{L^2}$, at A and B, respectively. With the joints balanced and any necessary sidesway conditions satisfied, the end-moments, in terms of u-moments, are

$$m_{AC} = \frac{x\,z}{L^2}\left(z\,u_{AA} + x\,u_{AB}\right) \dots \dots \dots \dots (1a)$$

and

$$m_{BC} = \frac{x\,z}{L^2}\left(z\,u_{BA} + x\,u_{BB}\right) \dots \dots \dots \dots (1b)$$

At an interior reference section, I, the indeterminate moment resulting from a unit load at C, obtained by interpolation from Eqs. 1a and 1b, is

$$m_{IC} = \frac{Z}{L}\,m_{AC} + \frac{X}{L}\,m_{BC} \dots \dots \dots \dots (2)$$

The following relations are also obtained by interpolation:

$$u_{IA} = \frac{Z}{L}\,u_{AA} + \frac{X}{L}\,u_{BA} \dots \dots \dots \dots (3a)$$

and

$$u_{IB} = \frac{Z}{L}\,u_{AB} + \frac{X}{L}\,u_{BB} \dots \dots \dots \dots (3b)$$

Substituting Eqs. 3a and 3b into Eq. 2 yields

$$m_{IC} = \frac{x\,z}{L^2}\left(z\,u_{IA} + x\,u_{IB}\right) \dots \dots \dots \dots (4)$$

For a reference section at an intermediate point, I, the influence ordinate is the algebraic sum of m_{IC} and the simple beam moment due to unit load at C. Thus

$$Y = \frac{x\,z}{L^2}\left(z\,u_{IA} + x\,u_{IB}\right) + \frac{x\,Z}{L}, \qquad (x \gtreqless X) \dots \dots \dots (5a)$$

and

$$Y = \frac{x\,z}{L^2}\left(z\,u_{IA} + x\,u_{IB}\right) + \frac{z\,X}{L} \qquad (x > X) \dots \dots \dots (5b)$$
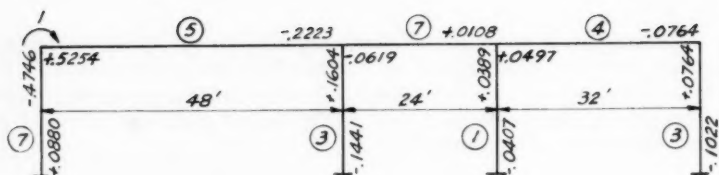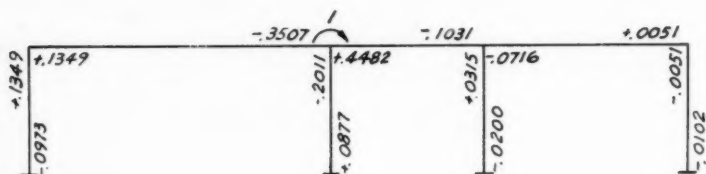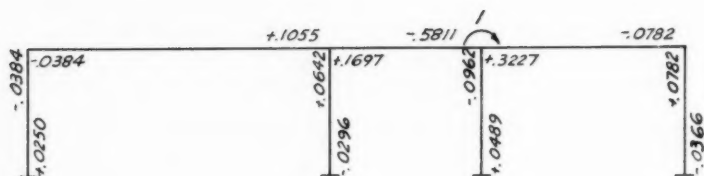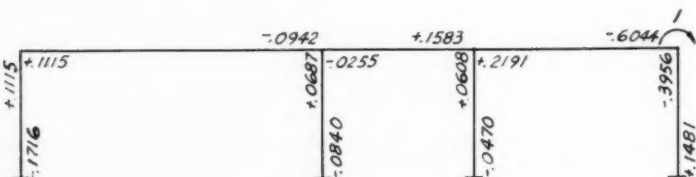
FIG. 4

Eqs. 5a and 5b are also applicable when the reference section is at one of the ends of the span. For example, when the reference section is at B, Eq. 5a applies, with $Z = 0$. Upon replacing the subscribt I with B, the following relation is obtained for the equation of the influence line

$$Y = \frac{x\,z}{L^2} \left(z\,u_{BA} + x\,u_{BB} \right) \ldots \ldots \ldots \ldots \ldots (6)$$

To facilitate integration, the relation $\frac{x}{L} + \frac{z}{L} = 1$ is used in rewriting Eqs. 5a and 5b, as follows

$$Y = \frac{u_{IA} - u_{IB}}{L^2}\,x^3 - \frac{2\,u_{IA} - u_{IB}}{L}\,x^2 + u_{IA}\,x + \frac{Z\,x}{L}, \qquad (x \gtreqless X) \ldots (7a)$$

and

$$Y = \frac{u_{IA} - u_{IB}}{L^2}\,x^3 - \frac{2\,u_{IA} - u_{IB}}{L}\,x^2 + u_{IA}\,x + \frac{X\,z}{L}, \qquad (x > X) \ldots (7b)$$

The area under the influence line represented by Eqs. 7a and 7b is

$$\int_0^L Y\,dx = \int_0^L \left[\frac{u_{IA} - u_{IB}}{L^2}\,x^3 - \frac{2\,u_{IA} - u_{IB}}{L}\,x^2 + u_{IA}\,x \right] dx$$

$$+ \frac{Z}{L} \int_0^X x\,dx + \frac{X}{L} \int_0^Z z\,dz \ldots \ldots \ldots \ldots \ldots (8)$$

Integration of Eq. 8 results in the following formula for the total area

$$\int_0^L Y\,dx = \frac{L^2}{12} \left(u_{IA} + u_{IB} \right) + \frac{X\,Z}{2} \ldots \ldots \ldots \ldots (9)$$

Formulas for the areas under the influence line for moment at A and at B are obtained from Eq. 9 by replacing the subscript I by A and by B, respectively, and omitting the final term.

When the influence line within a given primary span contains both a positive portion and a negative portion, as in Figs. 5(b) and 5(c), the reference section lies within a primary region of partial loading, that is, a region within which it is necessary to use partial-span loading of the primary span in order to obtain maximum moment. Such a region occurs in the neighborhood of every fixed or continuous span-end, and, in beams or girders subjected directly to uniform load, it begins just inside the support and extends to an inner boundary, beyond which point the influence line, in the primary span, becomes wholly positive.

In order to obtain, with certainty, the maximum moment at a selected point in a beam or girder, it is necessary to know whether or not the reference section lies in a region of partial loading. In the following analysis, the span-end that is nearer to the reference section is designated the near end, and the end more remote from the reference section is called the far end. Three cases are to be considered:

1. The reference section is in the neighborhood of a continuous end, the far end of the span being continuous, or simply supported but non-continuous;

2. the reference section is in the neighborhood of a continuous end, the far end of the span being fixed; and

3. the reference section is in the neighborhood of a fixed end, the far end of the span being continuous.

In cases 1 and 2, the length of the primary region of partial loading does not usually exceed $L/4$. Procedures for determining the inner boundaries of primary regions of partial loading will be explained subsequently. If, for any reason, it is preferred to dispense with this step, the need for partial loading in connection with reference sections in the vicinity of a continuous end is readily investigated by means of the derivatives of Y at the ends of the span (or by ascertaining whether a point of zero ordinate occurs in the influence line between the reference section and the far end of the span).

In case 1 the desired derivatives are Y_A', the value of dY/dx at A, and Y_B', the value of dY/dz at B. These quantities are the end-slopes of the influence line, and they are positive when the influence line slopes upward from the end towards the center of the span, as in Fig. 5(a). Figs. 5(b) and 5(c) show typical influence lines representative of case 1, in which partial areas occur. As seen from the figures, when the reference section is in a primary region of partial loading the end-slopes are opposite in sign, and the sign of the partial area adjacent to a given end agrees with that of the end-slope. The slope at the near end of the primary span is positive in all influence lines for moment at reference sections lying within a distance of $L/4$ (or even $L/2$) from that end. Therefore, if the slope at the far end is negative, the influence line contains partial areas, as in Figs. 5(b) and 5(c).

From Eq. 7a

$$\frac{dY}{dx} = \frac{u_{IA} - u_{IB}}{L^2} \, 3 \, x^2 - \frac{2 \, u_{IA} - u_{IB}}{L} \, 2 \, x + u_{IA} + \frac{Z}{L} \quad \ldots \ldots (10)$$

from which the slope of the influence line at A is

$$Y_A' = u_{IA} + \frac{Z}{L} \quad \ldots \ldots \ldots \ldots \ldots \ldots (11a)$$

The slope of the influence line at B may be obtained from Eq. 11a by rewriting from right to left

$$Y_B' = u_{IB} + \frac{X}{L} \quad \ldots \ldots \ldots \ldots \ldots \ldots (11b)$$

The influence lines in case 2 differ from those in Figs. 5(b) and 5(c) to the extent that the slope at the far end is zero. In this case, if the rate of change of slope, Y'', at the far end, is negative, the influence line contains partial areas. Differentiation of Eq. 10 yields

$$\frac{d^2Y}{dx^2} = \frac{u_{IA} - u_{IB}}{L^2} \, 6 \, x - \frac{2}{L} \left(2 \, u_{IA} - u_{IB} \right) \ldots \ldots \ldots (12)$$

from which

$$Y_A'' = \frac{2}{L} \left(u_{IB} - 2 \, u_{IA} \right) \ldots \ldots \ldots \ldots \ldots (13a)$$

Eq. 13a is for use in case 2 when the reference section is near the right end of the span, as in Fig. 5(b). The corresponding relation, for use when the refer-
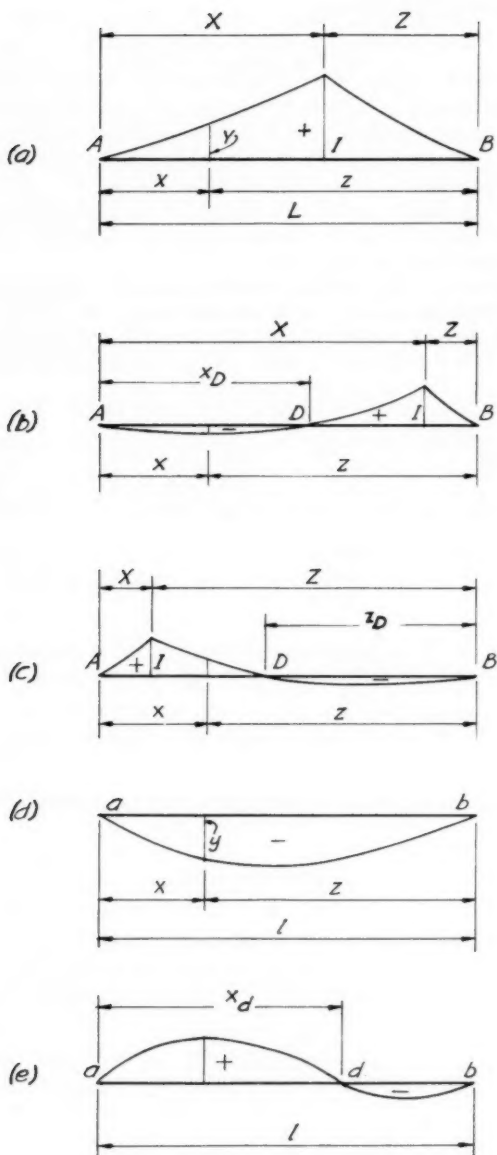
FIG. 5

ence section is near the left end of the span, as in Fig. 5(c), is obtained by reversing the preceding expression

$$Y_B'' = \frac{2}{L} \left(u_{IA} - 2\, u_{IB} \right) \quad \ldots\ldots\ldots\ldots\ldots \quad (13b)$$

In case 3, the length of a primary region of partial loading adjacent to a fixed end of a beam, of constant cross section and subjected directly to uniform load, is $L/3$, and therefore the influence line for moment at any reference section within this range contains partial areas.

When partial loading is required, the negative partial area is first computed, and the positive partial area is then obtained by algebraic subtraction of the negative area from the total area, Eq. 9.

When the reference section lies in the right-hand region of partial loading, as in Fig. 5(b), the upper limit of integration is x_D. In order to obtain an expression for the determination of x_D, the influence ordinate given by Eq. 7a is placed equal to zero, from which, with $x = x_D$, the following quadratic equation is obtained

$$\left(u_{IA} - u_{IB} \right)\left(\frac{x_D}{L} \right)^2 - \left(2\, u_{IA} - u_{IB} \right) \frac{x_D}{L} + Y_A' = 0, \quad \left(Y_A' < 0 \right) \ldots \quad (14a)$$

The area under the negative portion of the influence line is then

$$\int_{O}^{x_D} Y\, dx = \frac{x_D^2}{12} \left[3\, Y_A' - \left(2\, u_{IA} - u_{IB} \right) \frac{x_D}{L} \right] \quad \ldots\ldots\ldots \quad (15a)$$

For reference sections lying in the left-hand region of partial loading, as in Fig. 5(c), the upper limit of integration is z_D. Its value may be obtained from

$$\left(u_{IB} - u_{IA} \right) \left(\frac{z_D}{L} \right)^2 - \left(2\, u_{IB} - u_{IA} \right) \frac{z_D}{L} + Y_B' = 0, \quad \left(Y_B' < 0 \right) \ldots \quad (14b)$$

The area under the negative of the influence line is given by

$$\int_{O}^{z_D} Y\, dz = \frac{z_D^2}{12} \left[3\, Y_B' - \left(2\, u_{IB} - u_{IA} \right) \frac{z_D}{L} \right] \quad \ldots\ldots\ldots \quad (15b)$$

Secondary Span.—In Fig. 2, the fixed-end moments resulting from a unit load at c are $-\left(x\, z^2 \right)/l^2$ and $-\left(x^2\, z \right)/l^2$, at a and b, respectively. At the ends of the primary span the "indeterminate" moments produced by this unit load are

$$m_{Ac} = \frac{x\, z}{l^2} \left(z\, u_{Aa} + x\, u_{Ab} \right) \quad \ldots\ldots\ldots\ldots\ldots \quad (16a)$$

and

$$m_{Bc} = \frac{x\, z}{l^2} \left(z\, u_{Ba} + x\, u_{Bb} \right) \quad \ldots\ldots\ldots\ldots\ldots \quad (16b)$$

The corresponding moment at an interior reference section, I, obtained by in-

load at c are $-\left(\dfrac{x\, z^2}{l^2} \right)$ and $-\left(\dfrac{x^2\, z}{l^2} \right)$, at a and b, respectively. At the ends of the primary span the "indeterminate" moments produced by this unit load are

terpolation from Eqs. 16a and 16b, is

$$m_{Ic} = \frac{Z}{L} \, m_{Ac} + \frac{X}{L} \, m_{Bc} \quad \cdots\cdots\cdots\cdots\cdots \quad (17)$$

The following additional relations are also obtained by interpolation

$$u_{Ia} = \frac{Z}{L} \, u_{Aa} + \frac{X}{L} \, u_{Ba} \quad \cdots\cdots\cdots\cdots\cdots \quad (18a)$$

and

$$u_{Ib} = \frac{Z}{L} \, u_{Ab} + \frac{X}{L} \, u_{Bb} \quad \cdots\cdots\cdots\cdots\cdots \quad (18b)$$

Upon substituting from Eqs. 18a and 18b into Eq. 17 and noting that m_{Ic} is the influence ordinate, y, the following equation is obtained for the influence line in a secondary span

$$y = \frac{x \, z}{l^2} \left(z \, u_{Ia} + x \, u_{Ib} \right) \quad \cdots\cdots\cdots\cdots\cdots \quad (19)$$

When the reference section is located at one of the ends of the primary span, the equation for the portion of the influence line in the secondary span is obtained from Eq. 19 by replacing the subscript I by A or by B, as the case may be.

The total area under the portion of the influence line represented by Eq. 19 is

$$\int_0^l y \, dx = \frac{l^2}{12} \left(u_{Ia} + u_{Ib} \right) \quad \cdots\cdots\cdots\cdots\cdots \quad (20)$$

The end-slopes of the influence line in a secondary span are y_a', the value of dy/dx at a, and y_b', the value of dy/dz at b. From Eq. 19 these end-slopes are found to be

$$y_a' = u_{Ia} \quad \cdots\cdots\cdots\cdots\cdots\cdots \quad (21a)$$

and

$$y_b' = u_{Ib} \quad \cdots\cdots\cdots\cdots\cdots\cdots \quad (21b)$$

Fig. 5(d) illustrates an influence line in a secondary span in which the end-slopes are both negative, the area under the influence line being likewise negative.

In continuous frames subject to sidesway, such as illustrated in Fig. 4, as well as in various other cases, secondary regions of partial loading occur, that is, regions within which it is necessary to use partial loading of one or more secondary spans in order to obtain maximum moment at a given reference section. Secondary regions of partial loading do not occur in the case of continuous beams or girders such as those shown in Fig. 3. When the reference section lies in a secondary region of partial loading, y_a' and y_b' are opposite in sign, and there is a negative partial area at the end having negative slope and a positive partial area at the end having positive slope, as in Fig. 5(e). In such cases, the influence ordinate becomes zero at some point d, the abscissa of

which is x_d. Then, from Eq. 19

$$\left(1 - \frac{x_d}{l}\right) u_{Ia} + \frac{x_d}{l} u_{Ib} = 0 \quad \ldots \ldots \ldots \ldots \quad (22)$$

or

$$\frac{x_d}{l} = \frac{u_{Ia}}{u_{Ia} - u_{Ib}} \quad \ldots \ldots \ldots \ldots \quad (23a)$$

The area from a to d is

$$\int_0^{x_d} y \, dx = u_{Ia} \int_0^{x_d} x \left(1 - \frac{x}{l}\right)^2 dx + \frac{u_{Ib}}{l} \int_0^{x_d} x^2 \left(1 - \frac{x}{l}\right) dx$$

$$= \frac{x_d^2}{12} \left[\left(6 - \frac{8 \, x_d}{l} + \frac{3 \, x_d^2}{l^2}\right) u_{Ia} + \left(\frac{4 \, x_d}{l} - \frac{3 \, x_d^2}{l^2}\right) u_{Ib}\right] \quad \ldots \ldots \quad (24)$$

With the aid of the relations given in Eqs. 22 and 23a, Eq. 24 may be rewritten as

$$\int_0^{x_d} y \, dx = \frac{x_d^3}{12 \, l} \left(u_{Ia} - 2 \, u_{Ib}\right) \quad \ldots \ldots \ldots \ldots \quad (25a)$$

The partial area from b to d, Fig. 5(e), may be found by algebraic subtraction of the area given by Eq. 25a from the total area, Eq. 20, or by rearranging Eq. 25a to read from right to left, as

$$\int_0^{z_d} y \, dz = \frac{z_d^3}{12 \, l} \left(u_{Ib} - 2 \, u_{Ia}\right) \quad \ldots \ldots \ldots \ldots \quad (25b)$$

in which

$$\frac{z_d}{l} = \frac{u_{Ib}}{u_{Ib} - u_{Ia}} \quad \ldots \ldots \ldots \ldots \quad (23b)$$

Summary.—In the primary span, the total area under the influence line is given by Eq. 9, in which the quantities u_{IA} and u_{IB} are computed in accordance with Eqs. 3a and 3b. Reference sections within a distance of $L/3$ from a fixed end lie within a primary region of partial loading. Reference sections in the vicinity of a continuous end are in a primary region of partial loading (1) if, when the far end is continuous, or simply supported but non-continuous, the slope of the influence line at the far end, as given by Eq. 11a or Eq. 11b, is negative; or (2) if, when the far end is fixed, the rate of change of slope of the influence line at that end, as given by Eq. 13a or Eq. 13b, is negative. For reference sections in the right-hand primary region of partial loading, the negative partial area is given by Eq. 15a, where x_D is found from Eq. 14a. For reference sections in the left-hand primary region of partial loading, the negative partial area is given by Eq. 15b, in which the quantity z_D is obtained from Eq. 14b.

In secondary spans, the total area under the influence line is computed from Eq. 20, where the quantities u_{Ia} and u_{Ib} are as given by Eqs. 18a and 18b, respectively. If u_{Ia} and u_{Ib} are opposite in sign, the influence line in a secondary span contains partial areas. In this case, the partial area adjacent to the left end of the span is computed by means of Eq. 25a, in which the quantity x_d is obtained from Eq. 23a.

GIRDERS WITH FLOOR BEAMS

In the following treatment of continuous structures containing one or more girders with floor beams, the panels in a given span are assumed to be of equal length unless otherwise stated. It is assumed that the floor panels act as simple beams in transmitting their loads to the girder at the panel-points, and accordingly the influence line for moment at any reference section is polygonal in shape, the successive ordinates at the panel-points being connected by straight lines. The determination of the influence line, therefore, involves only the evaluation of the panel-point ordinates. Whereas the reference sections may be taken at any point in a span, they would ordinarily be chosen only at the ends of the span, at panel points, and at the boundaries of the primary regions of partial loading. The determination of partial areas in a primary span would then be involved only at such panel-points as may happen to lie in the primary regions of partial loading.

With a unit load acting at a specified panel-point, the fixed-end moments are the same as for spans having no floor beams, and the values of the ordinates at panel-points in a primary span are as given by Eqs. 5a and 5b and, in a secondary span, by Eq. 19, regardless of whether the panels are of equal or unequal length.

Primary Span.—Fig. 6(a) shows the influence line for moment at a reference section, I, located in the central region of the span, in which all of the ordinates are positive. Fig. 6(b) shows the influence line for moment at a reference section near the right end of the span, in which both positive and negative ordinates occur. The length of span is $L = NP$, in which N is the number of equal panels and P is the length per panel. The location of a given panel-point, at which a unit load is applied and the ordinate Y is to be determined, is defined by the abscissae $x = r\,P$ and $z = s\,P$, in which r and s indicate the number of panels from A and from B, respectively. The location of the reference section is defined by the distances X and Z, measured from points A and B, respectively. If the reference section lies between two panel-points, $X = R\,P + J$ and $Z = S\,P + J'$; if at a panel-point, $J = 0$ and $J' = P$. When the reference section lies in a primary region of partial loading, as in Fig. 6(b), the point of zero ordinate, D', will ordinarily fall between two panel-points, E and F, rather than at a panel-point.

In the case of N equal panels, the equations for the ordinates to the influence line at panel-points may be written as

$$Y = \frac{r\,s\,P}{N^2}\left(s\ u_{IA} + r\ u_{IB}\right) + \frac{Z\,r}{N}, \qquad \left(r \gtreqless \frac{X}{P}\right) \quad \ldots \ldots (26a)$$

and

$$Y = \frac{r\,s\,P}{N^2}\left(s\ u_{IA} + r\ u_{IB}\right) + \frac{X\,s}{N}, \qquad \left(r > \frac{X}{P}\right) \quad \ldots \ldots (26b)$$
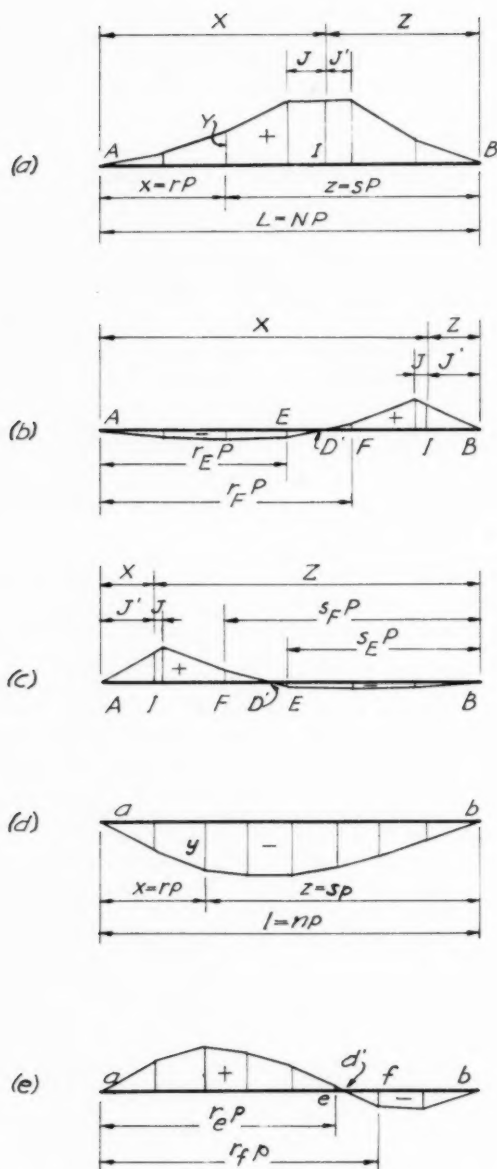
FIG. 6

Two procedures are available for the computation of the areas under the influence line. In the first, the ordinates are computed individually, and the required areas are then determined arithmetically. This procedure is particularly applicable to spans consisting of panels of unequal length, in which case the panel-point ordinates are obtained from Eqs. 5a and 5b, and the required areas are then computed by summation of the areas of the individual triangles in the polygon. When the panels are of equal length, the ordinates at the panel-points may be computed from either Eqs. 5a and 5b or from Eqs. 26a and 26b. The total area is then equal to P (Σ Y). In either case, if the reference section lies in a primary region of partial loading, the location of the point of zero ordinate, D', is determined from similar triangles, after the ordinates have been computed, and the partial areas are then computed.

The second procedure applies only to girder spans in which the panels are of equal length. It uses formulas for the computation of the required areas, but does not involve the computation of individual ordinates. The total area under the influence line in a primary span is denoted by $\sum\limits_{0}^{L} Y \, \Delta x$, and the negative partial area indicated in Fig. 6(b) is denoted by $\sum\limits_{0}^{x_{D'}} Y \, \Delta x$.

For the purpose of deriving a formula for the total area, Eqs. 26a and 26b may be written as

$$Y = P\left[\frac{u_{IA} - u_{IB}}{N^2} r^3 - \frac{2 u_{IA} - u_{IB}}{N} r^2 + u_{IA} r\right]$$

$$+ \frac{P Z}{L} r, \quad \left(r \gtreqless \frac{X}{P}\right) \quad \ldots \ldots \ldots \ldots \ldots \quad (27a)$$

and

$$Y = P\left[\frac{u_{IA} - u_{IB}}{N^2} r^3 - \frac{2 u_{IA} - u_{IB}}{N} r^2 + u_{IA} r\right]$$

$$+ \frac{P X}{L} s, \quad \left(r > \frac{X}{P}\right) \quad \ldots \ldots \ldots \ldots \ldots \quad (27b)$$

The total area under the influence line is

$$\sum\limits_{0}^{L} Y \, \Delta x = P^2\left[\frac{u_{IA} - u_{IB}}{N^2} \sum\limits_{1}^{N} r^3 - \frac{2 u_{IA} - u_{IB}}{N} \sum\limits_{1}^{N} r^2\right.$$

$$\left.+ u_{IA} \sum\limits_{1}^{N} r + \frac{Z}{L} \sum\limits_{1}^{R} r + \frac{X}{L} \sum\limits_{1}^{S} s\right] \quad \ldots \ldots \ldots \ldots \quad (28)$$

The following formulas are applicable in the evaluation of the summations in

the preceding expression:

$$\sum_1^n r = \frac{n\ (n+1)}{2}$$

$$\sum_1^n r^2 = \frac{2\ n+1}{3} \sum_1^n r \Bigg\}\ \dots\dots\dots\dots (29)$$

and

$$\sum_1^n r^3 = \left[\sum_1^n r\right]^2$$

With their use, the expression for the area becomes

$$\sum_0^L Y\ \Delta x = \frac{\left(N^2-1\right)\ P^2}{12}\ \left(u_{IA}+u_{IB}\right)$$

$$+\frac{P^2}{2\ L}\ \left[Z\ R\ (R+1)+X\ S\ (S+1)\right]\ \dots\dots\dots (30)$$

Substitution of the relations $R = \frac{X-J}{P}$ and $S = \frac{Z-J'}{P}$, with subsequent simplifi-

cation, leads to

$$\sum_0^L Y\ \Delta x = \frac{L^2-P^2}{12}\ \left(u_{IA}-u_{IB}\right)+\frac{X\ Z-J\ J'}{2}\ \dots\dots\dots (31)$$

When the reference section lies at a panel-point, the product $J\ J'$ is zero. If the reference section is taken at one of the ends of the span, both $X\ Z$ and $J\ J'$ are zero. For example, the total area under the influence line for moment at A is $\frac{L^2-P^2}{12}\ \left(u_{AA}+u_{AB}\right)$.

The primary regions of partial loading occurring in girders with floor beams differ from those in girders without floor beams in that the former have their inner boundaries somewhat nearer the supports than the latter, and their outer boundaries are located at finite distances inside the supports, rather than at an infinitesimal distance therefrom as in girders without floor beams. When reference sections are taken at (or in the neighborhood of) panel-points located within a distance of approximately $L/4$ or less from the supports, an examination should be made to ascertain whether partial loading is required. In the latter event, the determination of the partial areas involves the following steps: (1) Solution of a quadratic equation for the purpose of determining the panel within which the common boundary of the partial areas is located; (2) use of a formula for computing the negative partial area; and (3) determination of the positive partial area, by subtracting the negative partial area from the total area given by Eq. 31.

The determination of the boundaries of the regions of partial loading will be treated subsequently. If this step is omitted, the possibility that partial loading may be required for maximum moment at a given reference section near the right-hand end of the primary span, as in Fig. 6(b), may be investi-

gated by determining the sign of Y_1, the ordinate at the first interior panel-point on the left end of the span. If Y_1 is negative, the reference section lies in a region of partial loading. The sign of Y_1 may be obtained from the following relation, that is obtained by substituting $r = 1$ and $s = N - 1$ in Eq. 26a

$$\alpha\ Y_1 = (N - 1)\ u_{IA} + u_{IB} + \frac{N^2}{N - 1}\ \frac{Z}{L} \ \dots \dots \dots \ (32a)$$

The factor α in Eq. 32a is a positive constant for given values of N and P.

In Fig. 6(d), D' is the point of zero ordinate in the influence line, and points E and F, with abscissae r_E P and r_F P, are the panel-points at the ends of the panel containing point D'. The panel within which point D' lies may be determined by finding the two consecutive integral values of r, namely r_E and r_F, between which the root occurs in the following quadratic equation

$$G\ r^2 - H\ r + Y_A' = 0 \ \dots \dots \dots \dots \ (33a)$$

in which

$$G = \frac{u_{IA} - u_{IB}}{N^2} \ \dots \dots \dots \dots \ (34a)$$

and

$$H = \frac{2\ u_{IA} - u_{IB}}{N} \ \dots \dots \dots \dots \ (35a)$$

and $Y_A' = u_{IA} + \frac{Z}{L}$, as given by Eq. 11a.

The negative area indicated in Fig. 6(b) may then be found from the following formula, the derivation of which is contained in Appendix II

$$\sum_0^{x_{D'}} Y\ \Delta x = \frac{(r_E\ r_F\ P)^2}{2} \left\{ \frac{3\ G}{2} - \left(\frac{1}{r_E} + \frac{1}{r_F}\right) \frac{H}{3} \right.$$
$$\left. - \frac{\left[(r_E + r_F)\ G - H\right]^2}{\left(r_F^3 - r_E^3\right) G - (r_E + r_F)\ H + Y_A'} \right\} \ \dots \dots \dots \ (36a)$$

In the event that point D' falls at a panel-point, the negative area may be obtained from either Eq. 36a or Eq. 62 (Appendix II) provided that r_F is taken equal to $r_{D'}$, with $r_E = r_F - 1$.

When reference sections are taken near the left end of the primary span, partial areas are involved if Y_{N-1}, the ordinate at the first interior panel-point on the right end of the span, is negative. The sign of Y_{N-1} may be obtained from

$$\alpha\ Y_{N-1} = (N - 1)\ u_{IB} + u_{IA} + \frac{N^2}{N - 1}\ \frac{X}{L} \ \dots \dots \ (32b)$$

In Fig. 6(c), D' is the point of zero ordinate in the influence line, and points E and F, with abscissae s_E P and s_F P, are the panel-points at the ends of the panel containing point D'. The panel within which point D' lies may be determined by finding two consecutive integral values of s, namely s_E and s_F. The

root occurs between these values in

$$G' \, s^2 - H' \, s + Y'_B = 0 \quad \ldots \ldots \ldots \ldots \quad (33b)$$

in which

$$G' = \frac{u_{IB} - u_{IA}}{N^2} \quad \ldots \ldots \ldots \ldots \quad (34b)$$

and

$$H' = \frac{2 \, u_{IB} - u_{IA}}{N} \quad \ldots \ldots \ldots \ldots \quad (35b)$$

and Y'_B is, as given by Eq. 11b. The negative area indicated in Fig. 6(c) may then be found from

$$\sum_0^{z_{D'}} Y \, \Delta x = \frac{(s_E \, s_F \, P)^2}{2} \left\{ \frac{3 \, G'}{2} - \left(\frac{1}{s_E} + \frac{1}{s_F} \right) \frac{H'}{3} \right.$$

$$\left. - \frac{\left[(s_E + s_F) \, G' - H' \right]^2}{\left(s_F^3 - s_E^3 \right) G' - (s_E + s_F) \, H' + Y'_B} \right\} \quad \ldots \ldots \ldots \quad (36b)$$

Secondary Spans.—A typical interior secondary span (see Fig. 2), of length l, is subdivided into n equal panels of length p, with a unit load at some panel-point c, the abscissae of which are $x = r \, p$ and $z = s \, p$, measured from a and from b, respectively. Fig. 6(d) illustrates the portion of an influence line contained in a given secondary span, where the ordinates are all of the same sign. The ordinates at the panel-points of a secondary span are given by Eq. 19, that may be rewritten as

$$y = \frac{r \, s \, p}{n^2} \left(s \, u_{Ia} \, r \, u_{Ib} \right) \quad \ldots \ldots \ldots \ldots \quad (37)$$

The terms u_{Ia} and u_{Ib} are as given in Eqs. 18a and 18b. The total area under the influence line represented by Eq. 37 is

$$\sum_0^l y \, \Delta x = \frac{l^2 - p^2}{12} \left(u_{Ia} + u_{Ib} \right) \quad \ldots \ldots \ldots \ldots \quad (38)$$

Secondary regions of partial loading occur in girders with floor beams under essentially the same conditions as in girders in which the live loads are applied directly. The determination of the boundaries of secondary regions of partial loading will be treated subsequently. In Fig. 6(e), the point of zero ordinate is d'; points e and f, with abscissae $r_e \, p$ and $r_f \, p$, are the panel-points at the ends of the panel containing point d'. When the reference section lies in a secondary region of partial loading, the ordinates y_n and y_{n-1}, at the first interior panel-points on the left and on the right, respectively, are opposite in sign, and the sign of the partial area agrees with that of the corresponding ordinate. These signs may be determined from the relationships

$$\beta \, y_1 = (n - 1) \, u_{Ia} + u_{Ib} \quad \ldots \ldots \ldots \ldots \quad (39a)$$

and

$$\beta \, y_{n-1} = (n-1) \, u_{Ib} + u_{Ia} \quad \ldots \ldots \ldots \ldots \quad (39b)$$

in which β is a positive constant for given values of n and p. It will be noted that when u_{Ia} and u_{Ib} have the same sign, partial areas are not present.

The panel within which point d' lies may be determined by finding the two consecutive integral values of r, namely r_e and r_f, between which r_d occurs in the equation

$$r_d = \frac{n \, u_{Ia}}{u_{Ia} - u_{Ib}} \quad \ldots \ldots \ldots \ldots \ldots \ldots \quad (40)$$

In the event that Eq. 40 results in an integral value of r_d, r_f is taken equal to r_d, with $r_e = r_f - 1$. Eq. 40 is basically the same as Eq. 23a, and the subscript d refers to the point of zero ordinate in the influence line in the analogous case where the live loads are applied directly, as noted in the section "Beams and Girders with Direct Uniform Loading."

The partial area on the left side of the influence line, whether positive or negative, may be computed from a formula that is similar in form and derivation to Eq. 36a, namely

$$\sum_{0}^{x_{d'}} y \, \Delta x = \frac{(r_e \, r_f \, p)^2}{2} \left\{ \frac{3 \, g}{2} - \left(\frac{1}{r_e} + \frac{1}{r_f} \right) \frac{h}{3} \right.$$

$$\left. - \frac{\left[(r_e + r_f) \, g - h \right]^2}{\left(r_f^3 - r_e^3 \right) g - (r_e + r_f) \, h + u_{Ia}} \right\} \quad \ldots \ldots \ldots \ldots \quad (41)$$

in which

$$g = \frac{u_{Ia} - u_{Ib}}{n^2} \quad \ldots \ldots \ldots \ldots \ldots \ldots \quad (42)$$

and

$$h = \frac{2 \, u_{Ia} - u_{Ib}}{n} \quad \ldots \ldots \ldots \ldots \ldots \quad (43)$$

The partial area on the right side of the influence line is obtained by subtracting the area in Eq. 41 from the total area, Eq. 38.

Summary.—In the primary span, the total area under the influence line is given by Eq. 31, in which the quantities u_{IA} and u_{IB} are computed in accordance with Eqs. 3a and 3b. When the reference section is in the vicinity of the right end of the span, the sign of Y_1 is investigated by means of Eq. 32a, and, if negative, the influence line is of the form shown in Fig. 6(b). In this case, the quantities G, H, and Y_A' are computed from Eqs. 34a, 35a, and 11a, respectively. Then, r_E and r_F, the two consecutive integral values of r between which the root occurs in Eq. 33a are determined. The negative partial area adjacent to the left end of the span is then computed in accordance with Eq. 36a.

When the reference section is in the vicinity of the left end of the span, the sign of Y_{N-1} is investigated by means of Eq. 32b, and, if negative, the influ-

ence line is of the form shown in Fig. 6(c). In this case, the quantities G', H', and Y'_B are obtained from Eqs. 34b, 35b, and 11b, respectively. Then s_E and s_F, the two consecutive integral values of s between which the root occurs in Eq. 33b are determined. The negative partial area adjoining the right end of the span is then found by means of Eq. 36b.

In secondary spans, the total area under the influence line is given by Eq. 38, in which the quantities u_{Ia} and u_{Ib} are found from Eqs. 18a and 18b. The influence line in secondary spans does not contain partial areas when u_{Ia} and u_{Ib} are of the same sign. However, when these quantities are of opposite sign, partial areas are present if the signs of y_1 and y_{n-1}, as given by Eqs. 38a and 39b, are opposite. In this case, Eq. 40 is used for finding r_d, from which r_e and r_f are the consecutive integral values that are respectively less than and greater than r_d. The partial area adjacent to the left end of the span is then computed by means of Eq. 41, in which g and h are obtained from Eqs. 42 and 43.

EXAMPLES

The following abbreviations are used in connection with the numerical examples in Tables 1 to 4:

A_t = Total area under the influence line in a given span;

A_+ = positive area in span;

A_- = negative area in span;

w_D = dead load per foot of span;

w_L = live load per foot of span;

M_D = dead load moment at reference section—$w_D A_t$;

M_L = maximum positive or negative live load moment at reference section—$w_L A_+$ or $w_L A_-$;

M_+ = maximum positive (or minimum negative) moment at reference section—$\sum \left(w_D A_t \right) + \sum \left(w_L A_+ \right)$; and

M_- = maximum negative (or minimum positive) moment at reference section—$\sum \left(w_D A_t \right) + \sum \left(w_L A_- \right)$.

Examples 1 and 2 (Tables 1 and 2, respectively) illustrate the application of formulas in the section, "Beams or Girders with Direct Uniform Loading." Examples 3 and 4 (Tables 3 and 4, respectively) deal with the application of formulas in the section "Girders with Floor beams." An alternate solution of Example 4 is also shown in Columns 1 - 6 of Table 4, in which the ordinates to the influence line are computed individually and the areas are determined arithmetically.

Example 1.—The reference section is taken at a distance of 0.60 L from the left end of span No. 1, Fig. 3. Detailed computations of u_{IA} and u_{IB} (for span No. 1) and of u_{Ia} and u_{Ib} for spans Nos. 2 and 3 as well as preliminary data are shown in Table 1. Because the reference section is near the middle of the span

it does not lie in a primary region of partial loading, and because the structure consists of a series of continuous spans over simple intermediate supports, secondary regions of partial loading do not occur. Computations of the required total areas are shown in Column 9. The quantities M_D and M_L are then given, and the solution is completed by recording the extreme values of the moments, M_+ and M_-.

The procedure for determining the u-moments from analyses such as in Figs. 3 and 4 merits particular attention. These have been defined as the indeterminate moments in any span, resulting from a unit negative fixed-end moment at a specified end of a given span. The magnitudes and signs of the u-moments in Table 1 are determined as follows:

(a) Span No. 1 (primary span). As the left end of span No. 1 is fixed, u_{AA} (the indeterminate moment at A resulting from a unit negative fixed-end moment at A) is simply -1, and u_{BA} (the indeterminate moment at B resulting from a unit negative fixed-end moment at A) is zero. In finding u_{AB} and u_{BB} (the indeterminate moments at A and B resulting from a unit negative fixed-end moment at B), it is noted that any load on span No. 1 will result in a counter-clockwise rotation of the right-hand joint of that span. Because this is contrary to the direction of the unit couple shown in Fig. 3(b), the signs of the moments shown there are assumed to be reversed. Hence, $u_{AB} = -7/32$, and $u_{BB} = -1 + 7/16 = -9/16$.

(b) Span No. 2 (secondary span). The quantities u_{Aa} and u_{Ba} are the indeterminate moments at the left and right ends, respectively, of span No. 1 (the primary span), resulting from a unit negative fixed-end moment at the left end of span No. 2. This negative fixed-end moment implies the presence of a load on span No. 2, that will produce a clockwise rotation of the joint at which the unit couple is shown in Fig. 3(b), and the signs of the moments in this figure are now taken as shown. Hence, $u_{Aa} = +7/32$, and $u_{Ba} = -7/16$. The quantities u_{Ab} and u_{Bb} are the indeterminate moments at the left and right ends, respectively, of span No. 1, resulting from a unit negative fixed-end moment at the right end of span No. 2. A load on span No. 2 will produce a counter-clockwise rotation of the joint at which the unit couple is shshown in Fig. 3(c). Because this is contrary to the direction of the unit couple, the signs of the moments are assumed to be reversed. Hence, $u_{Ab} = +1/16$ and $u_{Bb} = -1/8$.

(c) Span No. 3. In accordance with the foregoing explanation, the quantities u_{Aa} and u_{Ba} are taken directly from span No. 1 in Fig. 3(c), and the quantities u_{Ab} and u_{Bb} are taken from span No. 1 in Fig. 3(d) with reversed signs.

Example 2.—The reference section is located at a distance of 0.20 L from the left end of span No. 2, Fig. 4. Preliminary data are listed in Table 2, Columns 2 to 4. Because u_{Ia} and u_{Ib}, in span No. 1, are both negative, the area under the influence line in this span, as computed in Table 2, is wholly negative (see Eqs. 21a and 21b).

Because the reference section is in the left-hand quarter of span No. 2, it is to be suspected that it lies in a primary region of partial loading. Therefore, in Table 2, Column 9, Y_B' is computed and found to be negative. The point of zero ordinate is next determined, and the total and partial areas are then computed.

In the case of span No. 3, since u_{Ia} is positive and u_{Ib} is negative, there is a positive partial area on the left and a negative partial area on the right. Ta-

TABLE 1.—MAXIMUM AND MINIMUM

Span (1)	Length, in feet (2)	w_D, in kips per feet (3)	w_L, in kips per feet (4)	u-Moments (5)			M_D (6)	M_L (7)
1	15	0.6	1.5	u_{AA} -1	u_{BA} 0	u_{IA} -0.400	+6.92	+17.30
				u_{AB} -7/32	u_{BB} -9/16	u_{IB} -0.425		
2	20	0.8	1.5	u_{Aa} +7/32	u_{Ba} -7/16	u_{Ia} -0.175		
				u_{Ab} +1/16	u_{Bb} -1/8	u_{Ib} -0.050	-6.00	-11.25
3	15	0.6	1.5	u_{Aa} -1.16	u_{Ba} +1.8	u_{Ia} +0.050	+0.84	+ 2.11
				u_{Ab} -1.32	u_{Bb} +1.16	u_{Ib} +0.025		
				M_+ = +21.17 ft-kips			+7.76	+19.41
				M_- = - 9.49 ft-kips			-6.00	-11.25
							+1.76	

a Z/L 0.40 X/L 0.60

ble 2, Column 9, shows computations for determining the point of zero ordinate and the total and partial areas. Completing the solution, the quantities M_D, M_L, M_+, and M_- are listed in Table 2, Columns 6 and 7.

Example 3.—The reference section for this example is taken at a distance of 0.14 L from the right end of span No. 2, Fig. 3. From the preliminary data shown in Table 3, Columns 2 to 6, it is seen that each span is subdivided into panels 5 ft long. The total areas for the various spans are computed in Table 3. Partial areas do not occur in secondary spans of strucutres of the type under consideration.

In the case of span No. 2, it is to be anticipated that, because the reference section falls in the outer quarter of the span, it may lie in a primary region of partial loading. Accordingly, αY_1 is computed and found to be negative. As the presence of partial areas is thus confirmed, computations are performed in order to determine the panel within which the zero ordinate occurs and to evaluate the partial areas.

The remainder of the solution consists in the computation of M_D, M_L, M_+, and M_-, as shown in Table 3. In this example, as well as in Example 4, the uniform dead load of the girders is assumed to be concentrated at the panel-points.

Example 4.—As shown in Table 4, the reference section is at the first interior panel-point from the left end of span No. 1, Fig. 4. The panel-length in each span is 8 ft. In Table 4, Column 11, the total area under the influence

MOMENTS,[a] SPAN NO. 1, FIG. 3

Equation	Computation	A_t	A_+	A_-
(8)	(9)	(10)	(11)	(12)
(3a)	$u_{Ia} = 0.40(-1) + 0.60(0) = -0.400$			
(3b)	$u_{IB} = 0.40\left(\frac{-7}{32}\right) + 0.60\left(\frac{-9}{16}\right) = -0.425$			
(9)	$A_t = \frac{225}{12}(0.400 + 0.425) + \frac{9(6)}{2}$	$+11.53$	$+11.53$	
(18a)	$u_{Ia} = 0.40\left(\frac{+7}{32}\right) + 0.60\left(\frac{-7}{16}\right) = -0.175$			
(18b)	$u_{Ib} = 0.40\,\frac{+1}{16} + 0.60\left(\frac{-1}{8}\right) = -0.050$			
(20)	$A_t = -\frac{400}{12}(0.175 + 0.050)$	-7.50		-7.50
(18a)	$u_{Ia} = 0.40\left(\frac{-1}{16}\right) + 0.60\left(\frac{+1}{8}\right) = +0.050$			
(18b)	$u_{Ib} = 0.40\left(\frac{-1}{32}\right) + 0.60\left(\frac{+1}{16}\right) = +0.025$			
(20)	$A_t = \frac{225}{12}(0.050 + 0.025)$	$+1.41$	$+1.41$	

line for span No. 1 is first computed. As the reference section is near the end of the span, the sign of $\alpha\,Y_{N-1}$ is investigated, and, when found to be negative, the computations required for locating the panel that contains the point of zero ordinate and for determining the partial areas are performed.

As the signs of u_{Ia} and u_{Ib} are alike for span No. 2 and also for span No. 3, partial areas are not present in these secondary spans and only the total areas need to be computed. As in previous examples, the solution is completed with the calculations of M_D, M_L, M_+ and M_-, as shown in Table 4, Columns 8 and 9.

An alternate solution of example 4 is also given in Tabel 4, Columns 15 through 22. This alternate solution contains the computation of the panel-point ordinates, in accordance with Eqs. 26b and 37. The various steps in these computations are explained in the respective columns of Table 4 by reference to preceding columns. It will be noted that the u-moments in Column 17 are obtained by linear interpolation between the values of the u-moments at the ends of the various spans. The computation of the total area in each span and of the partial areas in span No. 1 is shown in Table 4, Column 22.

BOUNDARIES OF REGIONS OF PARTIAL LOADING

Beams or Girders with Direct Uniform Loading.—As noted previously, a primary region of partial loading occurs in the neighborhood of each continu-

TABLE 2.—MAXIMUM AND MINIMUM

Span (1)	Length, in feet (2)	w_D, in kips per feet (3)	w_L, in kips per feet (4)	u-Moments (5)			M_D (6)	M_L (7)
1	48	1.5	2.0	$u_{Aa}-0.0619$	$u_{Ba}+0.0108$	$u_{Ia}-0.0473$		
				$u_{Ab}-0.4482$	$u_{Bb}+0.1031$	$u_{Ib}-0.3379$	-110.94	-147.92
2	24	0.8	2.0	$u_{AA}-0.5518$	$u_{BA}-0.1031$	$u_{IA}-0.4620$	$+10.69$	$+27.44$
				$u_{AB}-0.1697$	$u_{BB}-0.4189$	$u_{IB}-0.2196$		-0.72
3	32	1.0	2.0	$u_{Aa}+0.1697$	$u_{Ba}-0.5811$	$u_{Ia}+0.0196$	$+0.71$	$+1.84$
				$u_{Ab}+0.0255$	$u_{Bb}-0.1583$	$u_{Ib}-0.0113$		-0.42
				$M_+ = -70.26$ ft–kips			$+11.40$	$+29.28$
				$M_- = -248.60$ ft–kips			-110.94	-149.06
							-99.54	

[a] $Z/L = 0.80$ $X/L = 0.20$

ous or fixed end, beginning just inside the support and extending to some limiting reference section for which the influence line in the primary span becomes wholly positive. In case 1, in which the reference section is in the neighborhood of a continuous end and the far end of the span is continuous, or simply supported by non-continuous, the influence line in the primary span contains partial areas if the slope of the influence line, Y', at the far end is negative. In case 2, in which the reference section is in the neighborhood of a continuous end and the far end of the span is fixed, the influence line in the primary span contains partial areas if the second derivative, Y'', at the far end of the span is negative. As the reference section moves towards the center of the span, the negative partial area on the far end approaches zero. Therefore, the inner boundary of a primary region of partial loading may be determined by placing Y', in the former case, and Y'', in the latter case, equal to zero at the far end of the span and solving for the location of the corresponding reference section.

MOMENTS,[a] SPAN NO. 2, FIG. 4

Equation	Computation	A_t	A_+	A_-
(8)	(9)	(10)	(11)	(12)
(20)	$A_t = -\dfrac{48^2}{12}(0.0473 + 0.3379)$	-73.96		-73.96
(9)	$A_t = -\dfrac{24^2}{12}(0.4620 + 0.2196) + \dfrac{4.8(19.2)}{2}$	$+13.36$		
(11b)	$Y'_B = -0.2196 + 0.20 = -0.0196$			
(14b)	$0.2424\left(\dfrac{z_D^2}{L}\right) - 0.0228\dfrac{z_D}{L} - 0.0196 = 0;$ $\dfrac{z_D}{L} = 0.335,\ z_D = 8.05'$			
(15b)	$A_- = \dfrac{8.05^2}{12}\left[3(-0.0196) - 0.0228(0.335)\right]$		$+13.72$	-0.36
(20)	$A_t = \dfrac{32^2}{12}(0.0196 - 0.0113)$	$+0.71$		
(23a)	$\dfrac{x_d}{1} = \dfrac{0.0196}{0.0196 + 0.0113} = 0.634;\ x_d = 20.3'$			
(25a)	$A_+ = \dfrac{0.634(20.3)^2}{12}(0.0196 + 0.0226)$		$+0.92$	-0.21

In case 1, Eq. 11a may be written as

$$Y'_A = \frac{Z}{L}\left(1 + u_{AA} - u_{BA}\right) + u_{BA} \quad \cdots\cdots\cdots\cdots (44)$$

from which, with $Y'_A = 0$, the inner boundary of the right-hand primary region of partial loading is given by

$$\frac{Z_i}{L} = \frac{-u_{BA}}{1 + u_{AA} - u_{BA}} \quad \cdots\cdots\cdots\cdots (45a)$$

In a similar way, the inner limit of the primary region of partial loading on the left end of the span is found from the relation

$$\frac{X_i}{L} = \frac{-u_{AB}}{1 + u_{BB} - u_{AB}} \quad \cdots\cdots\cdots\cdots (45b)$$

In case 2, if the reference section is in the neighborhood of the right end and the left end of the span is fixed, $u_{AA} = -1$ and $u_{BA} = 0$. Accordingly, eval-

TABLE 3.—MAXIMUM AND MINIMUM

Span (1)	Length, in feet (2)	N or n (3)	P or p, in foot (4)	w_D, in kips per foot (5)	w_L, in kips per foot (6)	u-Moments (7)			M_D (8)
1	15	3	5	0.6	1.5	u_{Aa} 0 $\quad$ u_{Ab} -9/16	u_{Ba} 0 $\quad$ u_{Bb} +9/64	u_{Ia} 0 $\quad$ u_{Ib} +0.042	+0.42
2	20	4	5	0.8	1.5	u_{AA} -7/16 $\quad$ u_{AB} -1/8	u_{BA} -9/64 $\quad$ u_{BB} -15/32	u_{IA} -0.182 $\quad$ u_{IB} -0.421	+1.73
3	15	3	5	0.6	1.5	u_{Aa} +1/8 $\quad$ u_{Ab} +1/16	u_{Ba} -17/32 $\quad$ u_{Bb} -17/64	u_{Ia} -0.438 $\quad$ u_{Ib} -0.219	-6.57
						$M_+ = +1.85$ ft-kips			+2.15
						$M_- = -22.82$ ft-kips			-6.57
									-4.42

a Z/L 0.14 X/L 0.86

uation of u_{IA} and u_{IB} in Eq. 13a yields

$$Y_A'' = \frac{2}{L} \left[\frac{Z}{L} \left(2 + u_{AB} - u_{BB} \right) + u_{BB} \right] \quad \ldots\ldots\ldots\ldots (46)$$

When Y_A'' is placed equal to zero in this expression, the following relation is obtained for determining the location of the inner boundary of the right-hand primary region of partial loading

$$\frac{Z_i}{L} = \frac{- u_{BB}}{2 + u_{AB} - u_{BB}} \quad \ldots\ldots\ldots\ldots\ldots (47a)$$

A similar equation, for use in determining the location of the inner boundary of the left-hand primary region of partial loading when the right end of the span is fixed, may be obtained by rearranging Eq. 47a to read from right to

MOMENTS,[a] SPAN NO. 2, FIG. 3

M_L	Equation	Computation	A_t	A_+	A_-
(9)	(10)	(11)	(12)	(13)	(14)
+ 1.05	(38)	$A_t = \frac{255-25}{12}(0 + 0.042)$	+ 0.70	+0.70	
+ 5.22 - 1.98	(31)	$A_t = \frac{400-25}{12}(-0.182 - 0.421)$ $+ \frac{17.2(2.8) - 2.2(2.8)}{2}$	+ 2.16		
	(32a)	$\alpha Y_1 = 3(-0.182) - 0.421 + \frac{16}{3}(0.14)$ $= -0.220$			
	(34a)	$G = \frac{-0.182 + 0.421}{16} = +0.0149$			
	(35a)	$H = \frac{-0.364 + 0.421}{4} = +0.0142$			
	(11a)	$Y'_A = -0.182 + 0.14 = -0.042$			
	(33a)	$0.0149r^2 - 0.0142r - 0.042 = 0;$ $r_E = 2, r_F = 3$			
	(36a)	$A_- = \frac{900}{2}\left\{\frac{0.0447}{2} - \frac{5(0.0142)}{6(3)}\right.$ $\left. - \frac{[5(0.0149) - 0.0142]^2}{19(0.0149) - 5(0.0142) - 0.042}\right\}$		+3.48	- 1.32
-16.42	(38)	$A_t = -\frac{225-25}{12}(0.438 + 0.219)$	-10.95		-10.95
+ 6.27 -18.40					

left, as follows

$$\frac{X_i}{L} = \frac{-u_{AA}}{2 + u_{BA} - u_{AA}} \quad \ldots \ldots \ldots \ldots \ldots (47b)$$

Eqs. 45a and 45b may also be applied in case 3, in which the primary region of partial loading is adjacent to the fixed end of the span and the far end is fixed. For example, when the left end of the span is fixed, as in the first span in Fig. 3, the quantity $-u_{AB}$ in Eq. 45b is equal to $\frac{1}{2}(1 + u_{BB})$. Therefore, the length of the region of partial loading is $L/3$, as stated in the section "Beams and Girders with Direct Uniform Loadings."

In application to continuous beams and girders, such as in Fig. 3, subjected directly to uniform loading, the inner boundaries of the primary regions of partial loading are the "fixed points."

TABLE 4.—MAXIMUM AND MINIMUM

Span (1)	Length, in feet (2)	N or n (3)	P or p, in feet (4)	w_D, in kips per foot (5)	w_L, in kips per foot (6)	u-Moments (7)			M_D (8)
1	48	6	8	1.5	2.0	u_{AA}-.4746	u_{BA}-.2223	u_{IA}-.4326	+57.10
						u_{AB}-.1349	u_{BB}-.6493	u_{IB}-.2206	
2	24	3	8	0.8	2.0	u_{Aa}+.1349	u_{Ba}-.3507	u_{Ia}+.0540	+ 2.34
						u_{Ab}+.0384	u_{Bb}-.1055	u_{Ib}+.0144	
3	32	4	8	1.0	2.0	u_{Aa}-.0384	u_{Ba}+.1055	u_{Ia}-.0144	
						u_{Ab}-.1115	u_{Bb}+.0942	u_{Ib}-.0772	- 7.33

$M_+ = +146.55$ ft-kips $+59.44$
$M_- = + 24.99$ ft-kips $- 7.33$
                                $+52.11$

Span (15)	Point (16)	u-Moment (17)	rsP/N (18a)	rsp/n (18b)	Product (19) Col. 19 = Col. 17 x Col. 18	Xs/N (20a)	Zr/N (20b)
1	A	-0.4326					
	1	-0.3973	20/3		-2.6487	20/3	
	2	-0.3619	32/3		-3.8603	16/3	
	3	-0.3266	12		-3.9192	4	
	4	-0.2913	32/3		-3.1072	8/3	
	5	-0.2559	20/3		-1.7060	4/3	
	B	-0.2206					
2	a	+0.0540					
	1	+0.0408		16/3	+0.2176	-	-
	2	+0.0276		16/3	+0.1472	-	-
	b	+0.0144					
3	a	-0.0144					
	1	-0.0301		6	-0.1806	-	-
	2	-0.0458		8	-0.3664	-	-
	3	-0.0615		6	-0.3690	-	-
	b	-0.0772					

[a] $Z/L = 5/6$, $X/L = 1/6$

MOMENTS,[a] SPAN NO. 1, FIG. 4

M_L (9)	Equation (10)	Computation (11)	A_t (12)	A_+ (13)	A_- (14)
+88.60	(31)	$A_t = \dfrac{40(56)}{12}(-.6532) + \dfrac{40(8)}{2}$	+38.07		
-12.46	(32b)	$\alpha Y_{N-1} = 5(-.2206) - .4326 + \dfrac{36}{5}\left(\dfrac{1}{6}\right)$ $= -.335$			
	(34b)	$G' = \dfrac{-.2206 + .4326}{36} = +.00589$			
	(35b)	$H' = \dfrac{-.4412 + .4326}{6} = -.00143$			
	(11b)	$Y'_B = -.2206 + .1667 = -.0539$			
	(33b)	$.0059s^2 + .0014s - .0539 = 0;$ $s_E = 2,\ s_F = 3$			
	(36b)	$A_- = \dfrac{48^2}{12}\left\{\dfrac{.01767}{2} + \dfrac{5(.00143)}{6(3)} - \dfrac{[5(.00589)+.00143]^2}{19(.00589)+5(.00143)-.0539}\right\}$		+44.30	-6.23
+ 5.84	(38)	$A_t = \dfrac{16(32)}{12}(.0540 + .0144)$	+ 2.92	+ 2.92	
-14.66	(38)	$A_t = \dfrac{25(40)}{12}(-.0144 - .0772)$	- 7.33		-7.33
+94.44 -27.12					

Ordinate (21) Col. 21 = Col. 19 x Col. 20	Computation (22)
+4.0180 +1.4730 +0.0808 -0.4405 -0.3727	Location of point D' : $\dfrac{0.0808(8)}{0.0808 + 0.4405} = 1.24'$ right of point 3 $A_+ = 8(4.0180 + 1.4730) + 4.62(0.0808) = +44.30$ $A_- = 8(-0.3727) + 7.38(-0.4405) = -6.23;\ A_t = +38.07$
+0.2176 +0.1472	$A_t = 8(0.2176 + 0.1472) = +2.92$
-0.1806 -0.3664 -0.3690	$A_t = -8(0.1806 + 0.3664 + 0.3690) = -7.33$

In structures having secondary regions of partial loading, a given primary span contains, in general, one such region for each secondary span. For a given secondary span the region of partial loading is on that end of the primary span that is the more remote from the secondary span. Its boundaries are determined by locating the reference sections for which zero end-slopes occur in the influence line in the secondary span, that is, by making y'_a and y'_b equal to zero. Two cases occur: In the first case, two reference sections can be found, for one of which $y'_a = 0$ and, for the other, $y'_b = 0$, and the secondary region of partial loading lies between these two reference sections; in the second case, only one reference section occurs for which y'_a or $y'_b = 0$, and the secondary region of partial loading extends from this reference section to that end of the primary span that is farther removed from the secondary span. The secondary regions of partial loading in the strucutre shown in Fig. 4 all come under the former case.

From Eq. 21a, when $y'_a = 0$, the location of the reference section is found from

$$\frac{X_a}{L} = \frac{u_{Aa}}{u_{Aa} - u_{Ba}} \quad \ldots \ldots \ldots \ldots \ldots (48a)$$

Similarly, from Eq. 21b, when $y'_b = 0$, the reference section may be found from

$$\frac{X_b}{L} = \frac{u_{Ab}}{u_{Ab} - u_{Bb}} \quad \ldots \ldots \ldots \ldots \ldots (48b)$$

The inner boundaries of the primary regions of partial loading in case 1 may be found directly from analyses such as shown in Figs. 3 and 4. For example, when the second span in Fig. 3 is taken as the primary span, the values of $1 + u_{AA}$ and u_{BA}, shown in Fig. 3(b), are $+9/16$ and $-9/64$, respectively. The zero point on the closing line connecting these moments occur at a distance of $L/5$ from the right end of the span, the result being in agreement with Eq. 45a. Likewise, in the same span, the values of $1 + u_{BB}$ and u_{AB}, shown in Fig. 3(c), are $+17/32$ and $-1/8$, respectively, from which X_i/L is found to be equal to $4/21$, which is also in agreement with Eq. 45b.

The boundaries of the secondary regions of partial loading may likewise be determined directly from moments such as shown in Fig. 4. For example, when span No. 2 is the primary span and span No. 3 is the secondary span, the quantities u_{Aa} and u_{Ba} in Eq. 48a, as shown in Fig. 4(c), are $+0.1697$ and -0.5811, and the quantities u_{Ab} and u_{Bb} in Eq. 48b, shown in Fig. 4(d), are $+0.0255$ and -0.1583. It is readily seen that a zero ordinate occurs in each of the closing lines drawn between these two pairs of end-moments, and the secondary region of partial loading lies between these points.

Girders with Floor Beams.—Fig. 7(a) represents a span of several panels of equal length, continuous at both ends, or continuous at one end and fixed at the other. Fig. 7(b) shows the form of the moment diagram resulting from a unit load at the first interior panel-point on the left, the points of inflection, No. 1 and No. 2, having the abscissae X_O and Z_i, respectively. Likewise, Fig. 7(c) shows the form of the moment diagram resulting from a unit load at the first interior panel-point on the right, with points of inflection Nos. 3 and 4, whose abscissae are X_i and Z_O, respectively. If moment diagrams are drawn for a unit load at the remaining interior panel-points, the resulting points of inflection on the left portion of the span will be found to lie between points 1 and 3, and those on the right portion of the span will lie between points 2 and 4.

It will be noted that the span contains three types of regions: (a) between the left support and point 1 and between the right support and point 4, where the moments caused by live loads on the span are always negative; (b) between points 2 and 3, where the moments caused by live loads on the span are always positive; and (c) between points 1 and 3 and between points 2 and 4, where the moments caused by live loads on the span may be either positive or negative, depending upon the location of the live loads. The latter regions are the
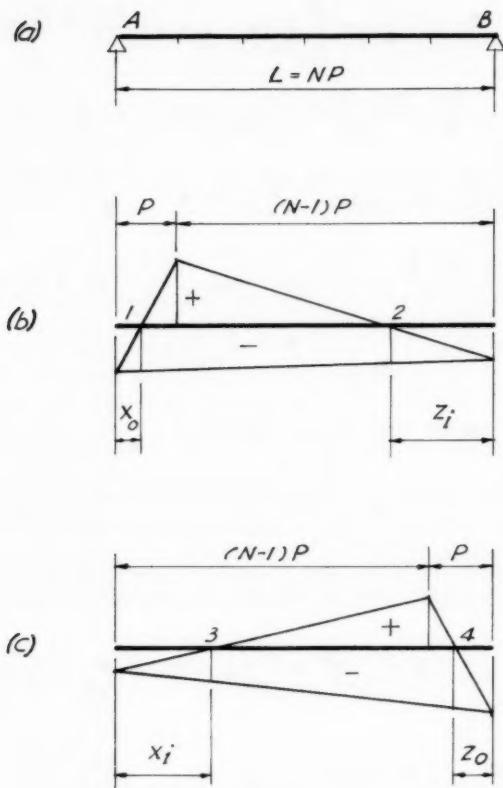
FIG. 7

primary regions of partial loading, because, in order to obtain maximum live load moment at a given reference section therein, a particular portion of the span must be loaded.

As shown in Figs. 7(b) and 7(c), the outer and inner boundaries of the left-hand region of partial loading have the abscissae X_O and X_i, respectively; and the corresponding boundaries of the right-hand region of partial loading have the abscissae Z_O and Z_i, respectively.

The outer boundary of a primary region of partial loading on a given end of a span is a reference section for which the influence line has a zero ordinate at the first interior panel-point on that end. The inner boundary of this region is a reference section for which the influence line has a zero ordinate at the first interior panel-point on the opposite end of the span.

For the determination of Z_o, the ordinate Y_{N-1} is to be placed equal to zero. From Eq. 27a, with $r = N-1$ and $s = 1$

$$Y_{N-1} = (N-1)\ P\left[\left(\frac{N-1}{N}\right)^2 (u_{IA} - u_{IB}) - \frac{N-1}{N}\left(2\ u_{IA} - u_{IB}\right)\right.$$

$$\left. + u_{IA}\right] + (N-1)\ \frac{Z_o}{N} = \frac{(N-1)\ P}{N^2}\left[u_{IA} + (N-1)\ u_{IB} + N^2\ \frac{Z_o}{L}\right] \quad .. (49)$$

Upon substituting the values of u_{IA} and u_{IB} from Eqs. 3a and 3b and placing $X_o/L = 1 - Z_o/L$, Eq. 49 becomes

$$Y_{N-1} = \frac{(N-1)\ P}{N^2}\left\{(N-1)\ u_{BB} + u_{BA} + \frac{Z_o}{L}\left[(N-1)\left(u_{AB} - u_{BB}\right)\right.\right.$$

$$\left.\left. + u_{AA} - u_{BA} + N^2\right]\right\} \dots\dots\dots\dots\dots (50)$$

which, with Y_{N-1} placed equal to zero, becomes

$$\frac{Z_o}{L} = \frac{(N-1)\ u_{BB} + u_{BA}}{(N-1)\left(u_{BB} - u_{AB}\right) + u_{BA} - u_{AA} - N^2} \quad \dots\dots (51a)$$

For the determination of Z_i, the ordinate at the first interior panel-point on the left end of the span is to be placed equal to zero. From Eq. 27a, with $r = 1$ and $s = N-1$:

$$Y_1 = P\left[\frac{u_{IA} - u_{IB}}{N^2} - \frac{2\ u_{IA} - u_{IB}}{N} + u_{IA} + \frac{Z_i}{L}\right]$$

$$= \frac{(N-1)\ P}{N^2}\left[(N-1)\ u_{IA} + u_{IB} + \frac{N^2}{N-1}\ \frac{Z_i}{L}\right] \dots\dots (52)$$

Upon substituting from Eqs. 3a and 3b, Eq. 52 becomes

$$Y_1 = (N-1)\ P\left\{(N-1)\ u_{BA} + u_{BB} + \frac{Z_i}{L}\left[(N-1)\left(u_{AA}\right.\right.\right.$$

$$\left.\left.\left. - u_{BA}\right) + u_{AB} - u_{BB} + \frac{N^2}{N-1}\right]\right\} \dots\dots\dots\dots (53)$$

from which, with $Y_1 = 0$

$$\frac{Z_i}{L} = \frac{u_{BB} + (N - 1)\, u_{BA}}{u_{BB} - u_{AB} + (N - 1)\left(u_{BA} - u_{AA}\right) - \dfrac{N^2}{N - 1}} \qquad \dots\, (54a)$$

Similar formulas for the boundaries of the left-hand region of partial loading may be obtained from Eqs. 51a and 54a, respectively, by a rearrangement reading from right to left

$$\frac{X_o}{L} = \frac{(N - 1)\, u_{AA} + u_{AB}}{(N - 1)\left(u_{AA} - u_{BA}\right) + u_{AB} - u_{BB} - N^2} \qquad \dots\, (51b)$$

and

$$\frac{X_i}{L} = \frac{u_{AA} + (N - 1)\, u_{AB}}{\left(u_{AA} - u_{BA}\right) + (N - 1)\left(u_{AB} - u_{BB}\right) - \dfrac{N^2}{N - 1}} \qquad \dots\, (54b)$$

The boundaries of a secondary region of partial loading may be determined by a procedure similar to that used in the case of girders with direct uniform loading, except that the investigation is based on the values of y_1 and y_{n-1}, the ordinates of the influence line in the secondary span at the first interior panel-points at the left and right ends, respectively. As in beams or girders with direct uniform loading, two cases occur. In the first case, two reference sections can be found, for one of which $y_1 = 0$ and, for the other, $y_{n-1} = 0$, and the secondary region of partial loading lies between these two reference sections. In the second case, only one reference section occurs for which y_1 or y_{n-1} becomes equal to zero, and the secondary region of partial loading extends from this reference section to that end of the primary span that is farther removed from the secondary span.

Substituting the values of u_{Ia} and u_{Ib} in Eqs. 18a and 18b into Eqs. 39a and 39b yields

$$\beta\, y_1 = (n - 1)\, u_{Aa} + u_{Ab} - \frac{X}{L}\left[(n - 1)\left(u_{Aa} - u_{Ba}\right)\right.$$

$$\left. + u_{Ab} - u_{Bb}\right] \qquad \dots\dots\dots\dots\dots\, (55a)$$

and

$$\beta\, y_{n-1} = u_{Aa} + (n - 1)\, u_{Ab} - \frac{X}{L}\left[u_{Aa} - u_{Ba}\right.$$

$$\left. + (n - 1)\left(u_{Ab} - u_{Bb}\right)\right] \qquad \dots\dots\dots\dots\, (55b)$$

From Eq. 55a, when $y_1 = 0$

$$\frac{X_a}{L} = \frac{(n - 1)\, u_{Aa} + u_{Ab}}{(n - 1)\left(u_{Aa} - u_{Ba}\right) + u_{Ab} - u_{Bb}} \qquad \dots\dots\dots\, (56a)$$

Likewise, from Eq. 55b, when $y_{n-1} = 0$

$$\frac{X_b}{L} = \frac{u_{Aa} + (n - 1)\ u_{Ab}}{u_{Aa} - u_{Ba} + (n - 1)\left(u_{Ab} - u_{Bb}\right)} \quad \ldots \ldots \ldots \text{(56b)}$$

In the foregoing expressions, X_a and X_b denote the values of X corresponding to zero values for the ordinates y_1 and y_{n-1}, that is, the ordinates at the interior panel-points nearest to a and to b, respectively.

CONCLUSIONS

Equations and criteria have been presented for use in computing the ordinates and the areas under the influence lines for moment at any point in uniformly loaded prismatic girders of continuous structures. The treatment has included beams or girders subject directly to uniform loading, and girders with floor beams arranged, primarily, at equal intervals.

The procedure for determining the total and partial areas in the various cases has been described in detail in the summaries at the end of the first two sections of this paper and the appropriate equations were enumerated.

Numerical examples of the determination of maximum and minimum moments were presented with the aid of Tables 1 through 4, in which the required computations were identified by equation number.

APPENDIX I. — NOTATION

The following symbols have been adopted for use in this paper:

Primary Span:

G,G' = see Eqs. 34a and 34b;

H,   = see Eqs. 35a and 35b;

J,J' = distances from reference section to adjacent panel-points. $0 \gtreqless J < P$, $0 < J' \gtreqless P$ (see Fig. 6);

L   = span length;

N   = number of panels of equal length;

P   = length of panel;

r   = abscissa of ordinate to influence line from point A, in panel-lengths;

s   = abscissa of ordinate to influence line from point B, in panel-lengths;

u_{IA} = indeterminate moment at reference section, I, resulting from unit negative fixed-end moment at point A;

u_{IB} = indeterminate moment at reference section, I, resulting from unit negative fixed-end moment at point B;

x   = abscissa of ordinate to influence line measured from point A;

X   = distance from point A to reference section;

Y   = ordinate to influence line;

Y_A' = slope of influence line at point A;

Y_A'' = value of d^2Y/dx^2 at point A;

Y_B' = slope of influence line at point B;

Y_B'' = value of d^2Y/dz^2 at point B;

Y_1 = ordinate to influence line at panel-point nearest to point A;

Y_{N-1} = ordinate to influence line at panel-point nearest to point B;

Z   = distance from point B to reference section;

z   = abscissa of ordinate to influence line measured from point B; and

α = a positive constant for given values of N and P.

Secondary Span:

g   = see Eq. 42;

h   = see Eq. 43;

l   = span length;

n   = number of panels of equal length;

p   = length of panel;

r   = abscissa of ordinate to influence line from point a, in panel-lengths;

s   = abscissa of ordinate to influence line from point b, in panel-lengths;

u_{Ia} = indeterminate moment at reference section, I, resulting from unit negative fixed-end moment at point a;

u_{Ib} = indeterminate moment at reference section, I, resulting from unit negative fixed-end moment at point b;

x   = abscissa of ordinate to influence line measured from point a;

y   = ordinate to influence line;

y_a' = slope of influence line at point a;

y_b' = slope of influence line at point b;

y_1 = ordinate to influence line at panel-point nearest to point a;

y_{n-1} = ordinate to influence line at panel-point nearest to point b;

z   = abscissa of ordinate to influence line measured from point b; and

β = a positive constant for given values of n and p.

APPENDIX II.–DERIVATION OF EQ. 36a

In Fig. 6(b), let Q denote the length of the fractional panel from point D' to panel-point F. The negative partial area is

$$\sum_0^{x_{D'}} Y \, \Delta x = P \sum_1^{Y_E} Y - \frac{Q \, Y_E}{2} \quad \dots \dots \dots \dots \dots (57)$$

From similar triangles

$$Q = \frac{P \, Y_F}{Y_F - Y_E} \quad \dots \dots \dots \dots \dots \dots (58)$$

From Eq. 27a, the ordinates at points E and F are

$$Y_E = P \left(r_E^3 \, G - r_E^2 \, H + r_E \, Y_A' \right) \quad \dots \dots \dots \dots (59)$$

and

$$Y_F = P \left(r_F^3 \, G - r_F^2 \, H + r_F \, Y_A' \right) \quad \dots \dots \dots \dots (60)$$

Upon substituting the foregoing values of Y_E and Y_F into Eq. 58 and noting that $r_F - r_E = 1$, the following expression for Q is obtained

$$Q = r_F \, P \left[\frac{r_F^2 \, G - r_F \, H + Y_A'}{\left(r_F^3 - r_E^3 \right) G - \left(r_E + r_F \right) H + Y_A'} \right] \quad \dots \dots (61)$$

The quantity $P \sum_1^{Y_E} Y$ in Eq. 57 is evaluated by the method used in the derivation of Eq. 31, yielding

$$P \sum_1^{Y_E} Y = \frac{r_E \, r_F \, P^2}{2} \left[\frac{r_E \, r_F \, G}{2} - \frac{\left(r_E + r_F \right) H}{3} + Y_A' \right] \quad \dots (62)$$

The quantity $Q \, Y_E / 2$, as found from Eqs. 59 and 61, is

$$\frac{Q \, Y_E}{2} = \frac{r_E \, r_F \, P^2}{2} \left[\frac{\left(r_E^2 \, G - r_E \, H + Y_A' \right) \left(r_F^2 \, G - r_F \, H + Y_A' \right)}{\left(r_F^3 - r_E^3 \right) G - \left(r_E + r_F \right) H + Y_A'} \right] \quad \dots (63)$$

Substituting from Eqs. 62 and 63 into Eq. 57 and subsequent simplification result in the formula given by Eq. 36a.

Journal of the

STRUCTURAL DIVISION

Proceedings of the American Society of Civil Engineers

DISCUSSION

BAR-CHAIN METHOD FOR ANALYZING TRUSS DEFORMATION[a]

Closure by S. L. Lee and P. C. Patel

S. L. LEE,[18] M. ASCE, and P. C. PATEL.[19]—Appreciation is expressed for the suggestion by Liu that the conjugate bar chain for the horizontal deflection components be viewed from the right-hand side of the computation sheet, that Eq. 16 be replaced by Eq. 28, and that the directions of θ_{ax}, θ_{cx}, δ_{ax}, and δ_{cx} be reversed, thus allowing the application of the usual beam convention for shear and moment. The choice of sign convention is a matter of convenience and the use of a more familiar one does have merit. In accordance with Liu's suggestion, however, the signs of one side of Eq. 19 and 20 must be reversed.

The comparison between the proposed method and the Scordelis-Smith method[17] discussed by Chinn is interesting. The analogy between the actual structure and the conjugate structure established in the latter is in principle more direct, but it seems that the sign convention is comparatively more involved. Here again the choice between one method and the other is a matter of preference.

Errata.—On p. 74, in the 16th line from the top, "θ_{cy}" should read "δ_{cy}" and, in the bottom line, "p. 55" should read "p. 60." In the bottom line of p. 76, "p. 337" should read "p. 340" and in the 15th line from the bottom of p. 82, "$\delta\beta_1$" should read "$\delta\beta,$."

DESIGN OF WELDED ALUMINUM STRUCTURES[a]

Closure by H. N. Hill, J. W. Clark, and R. J. Brungraber

H. N. HILL,[15] F. ASCE, J. W. CLARK,[16] M. ASCE, and R. J. BRUNGRA-BER,[17] A. M. ASCE.—The use of aluminum alloys in bridges has been discussed by Eduard Luss, who considers the paper important and timely because it will promote the use of welding in aluminum structures. He feels, however, that "the presented design rules will have only limited value for this special field" because they reflect a "steel approach" to the problem. There is, however, nothing in the paper that restricts the application of the design rules to any particular shapes or design configurations. The writers tried to express the design procedures in general terms in order to make them applicable to most types of welded aluminum alloy structures. It is recognized that these design rules will not be entirely adequate for all design problems; this is an area of continuing research.

It is agreed that "the problem of shape or form is most important" in design and that optimum shape or form is influenced by the characteristics of the material used. When Luss states that this fact "has been grossly overlooked," he must mean by some bridge designers. Certainly the aluminum industry has long preached this "gospel" in promoting the advantage of the extrusion process in providing members of optimum shape for their intended use. The fact that special extruded sections are used in two of the aluminum bridges (24)[b] that Luss cites, indicates that at least some bridge engineers are not overlooking the shape problem. Many designers in other structural fields are also fully cognizant of this situation. Structural design has probably reached its highest stage of refinement in the aero-space field; these designers are entirely uninhibited by preconceived notions of the availability of "standard" shapes or products.

That the aluminum industry has not promoted a set of "standard structural shapes" different from steel shapes, does not indicate a lack of recognition of the influence of material properties on optimum shape. Rather, it reflects the further knowledge that the optimum shape is equally influenced by the function the structure or member is to perform. The designer is encouraged to seek his optimum design unhampered by limitations of "standard shapes." At the same time, one should not overlook the successful and economical use designers have made of conventional structural shapes in a variety of aluminum alloy

---

structures, such as transmission towers, electrical substations, and roof trusses.

Apparently in his desire to advocate welded aluminum alloy construction, Luss has questioned the reliability of rivetedand bolted aluminum structures. Although this subject is not completely germane to the content of the paper, the comments appear to be based on such limited information and, in some cases, apparent misinformation, that they cannot go unanswered.

Luss questions the ability of unpainted riveted aluminum alloy structures to maintain satisfactory resistance to corrosion for an expected lifetime of 50 yr. He arrives at this attitude from a consideration of the so-called "mobility theory" of susceptibility to corrosion. This theory, wherein a metal was thought to corrode at a rate proportional to its "internal mobility," was an early attempt to understand the corrosion mechanism. According to the theory, steel, having less internal mobility than aluminum, should exhibit higher resistance to corrosion; this is, of course, not the case. In the light of modern understanding of corrosion mechanisms, it is generally accepted that the "mobility" theory is an unfortunate over-simplification. It neglects the important contributions of surface films and polarization characteristics and does not account for the great influence of alloying elements.

The important commercial forms of aluminum are obtained by alloying with other elements. The highest strength alloys are generally not the ones that are the most resistant to corrosion; however, alloys at the same strength level may vary in their resistance to corrosion. In choosing an alloy for a given structural application, one must consider such factors as corrosion resistance and cost. One cannot blindly choose "the most suitable alloy for the required stress." For riveted and bolted structures such as bridges, in which freedom from maintenance is desired, the recommended alloy (1) is 6061-T6, with a typical yield strength of 40,000 psi. This alloy is used in all types of structures without paint protection. If a higher strength material is required for a heavy-duty riveted and bolted structure, alloy 2014-T6, with a typical yield strength of 60,000 psi, is recommended (25). Paint protection is usually required for such structures.

Luss's reported experience with corrosion of aluminum bridge railing demonstrates the importance of alloy selection. The case in question (which was identified during correspondence) involved the use of nuts of alloy 2011-T3, even though 6061-T6 alloy nuts had been specified. Use of the 2011-T3 nuts, that would not be recommended for such an application, resulted in stress cracking and thread corrosion. Opposed to a few isolated instances of poor corrosion behavior, such as that cited by Luss (which can be traced to some form of misuse) there are many installations throughout the world of items such as aluminum bridge railings, hand rails, stanchions, and light standards, on bridges and highways that have exhibited excellent resistance to corrosion in all types of weather. For example, the unpainted aluminum alloy railings on the Loop Parkway Bascule Bridge at Jones Beach, N. Y., have a maximum depth of attack of only 0.0039 in. after 25 yr of service over a salt-water inlet.

In Table 4 Luss mentions alloy 7176-T6. According to the recent listing there is no such alloy registered with the Aluminum Association. It could be that what is meant is 7076-T6, or, more likely, 7178-T6. In either case these are high strength alloys developed for the aircraft industry and the writers would not recommend them for unpainted structures such as bridges.

The statement that "crevices and indentations caused by over-driven rivet heads . . . micro-fissures at punched holes and scratches . . . will result in electrolytic corrosion when moisture is present" seems to indicate a lack of knowledge of the mechanism of corrosion resistance in aluminum alloys. The natural oxide film, that largely provides the excellent resistance to corrosion of aluminum, repairs itself almost instantaneously if ruptured by mechanical abuse. Also, contrary to Luss's statement, differences in stress between a rivet and adjacent material do not introduce a significant susceptibility to electrolytic corrosion.

Luss's comments on the Arvida bridge are in error. According to D. G. Elliot, F. ASCE (who was closely associated with the design and construction of the Arvida bridge)

"the shade temperatures at the site vary from well below -30°F in winter to somewhere between +90°F and +100°F in summer."

Concerning the rivets which Mr. Luss says were virtually without heads, Elliot says,

"All shop rivets had standard heads. Purely to facilitate the cold field-driving of heat-treated aluminum rivets, a new type of head was evolved for the field-driven rivets (26). This head bears little resemblance to the caricature of Fig. 17 which Mr. Luss presents as descriptive of it. This new type of head was proved by exhaustive tests to be capable of invariably breaking the rivet shank. In no case were rivets virtually without heads used on the Arvida bridge."

When Luss states that rivets bigger than 5/8 in.

"require much more pressure to drive and so the chances of harming the parent metal are increased. This is probably one of the reasons for the 5/8-in. rivets used on the bridges under construction in New York State."

he must be referring to the riveted plate girder bridges on the Long Island Expressway (24). The shear connectors on these bridges were attached with 7/8-in. diameter rivets and the flange angles were connected to the webs with 3/4-in. rivets. All rivets were of aluminum alloy 6061-T6, driven cold.

Luss is, of course, entitled to his opinion concerning the structural merits of composite concrete and metal bridges. His fears that "the service life of such riveted aluminum structures can become very short indeed," however, are unfounded. As he notes, all of the recent developments in aluminum alloy highway bridges have used composite action. One can be sure that the designers of these structures explored thoroughly this question of the compatibility of aluminum and concrete before making this important decision. According to one of these designers (27)

"The problem of the corrosion of aluminum in contact with wet concrete has loomed largely in engineers' minds for many years. Elaborate tests made by the aluminum companies leave no doubt as to the compatibility of structural aluminum with concrete. Extensive investigation of this problem indicates that wet concrete has only a mild surface etching effect, with no impairment of the structural qualities of the aluminum alloy in contact with it."

Tests show that after many years of service, the attack depth rarely exceeds that observed after the first few hours of embedment (28). To minimize even this superficial corrosion, aluminum alloy parts in contact with concrete are sometimes given a coat of zinc chromate primer. Extensive testing and service experience has also shown that suitable paint coatings on faying surfaces provide adequate protection against possible galvanic corrosion between aluminum and other metals.

If by his statement that "the industry admits that it does not have enough experience" (to prove adequate corrosion resistance of riveted and bolted aluminum bridge structures for 50 yr), he means that one cannot point to bridge structures with 50 yr service experience, he is correct. Considering that aluminum became commercially available only slightly more than 60 yr ago, and considering further the continuing alloy and application development required to bring the metal to its present state of widespread use, this is not surprising. There exists, however, a vast body of knowledge in the form of service experience with many kinds of riveted and bolted structures under all types of environments, and accelerated laboratory corrosion tests. The industry has found this information adequate to give the user or potential user of aluminum for bridges complete confidence that, with reasonable attention to design and fabrication, he can obtain an unpainted riveted or bolted structure that will retain its integrity for the expected lifetime.

The following is a list of riveted and bolted aluminum alloy bridge structures with more than 10 yr service. This list does not include aluminum bridges erected since 1950, or bridges in European countries:

1. Floor System, Smithfield Street Bridge (29), Pittsburgh, Pa. (1933).—This is in a duralumin type alloy, no longer commercial. The structure was painted and has had reasonable paint maintenance. The performance of this bridge has been satisfactory, despite a corrosive industrial atmosphere.

2. Grasse River Bridge (30), Massena, N. Y. (1946).—This is an aluminum plate girder span of a railroad bridge. It is of aluminum alloy 2014-T6, with 7/8-in. diameter aluminum alloy rivets. One panel has been left unpainted. There has been no significant corrosion.

3. Huey Long Bridge (31), New Orleans, La. (1950).—This is a bolted protective cover over the wooden ties of a railroad bridge. Its function is to prevent the ties from catching fire and to protect the steel structure below the deck from the highly corrosive attack of brine drippings and sewage from passing cars. After extensive service testing, aluminum was chosen as the most suitable material. The alloy used is Alclad 3004, chosen primarily on the basis of its excellent corrosion resistance. Service experience has been good.

4. Arvida Bridge, Arvida, Quebec, Canada, (1950).—This is a highway bridge over the Saguenay River. It is of the same alloy as the Grasse River Bridge, with rivets of a slightly different alloy. The bridge is unpainted. No significant corrosion has developed.

Luss advocates the use of resin adhesives for joints in bridge structures. This method of joining is attractive, but widespread use in such structures is being delayed by lack of service experience. Experience in this field is indeed meager compared with that for riveted aluminum structures.

Errata.—p. 104, line 3, change "F. H. Howell" to "F. M. Howell"; line 33, insert the word "a" before the words "10-in. gage length."

p. 110, Fig. 6, insert "(Eq. 1)" after the words "ultimate strength" and "(Eq. 2)" after the words "yield strength."

p. 113, sixth line from bottom, change "equals" sign to "minus" sign.

ADDITIONAL REFERENCES

24. "Two Bridge Designs Contrast but Both of Them Call for Aluminum," Engineering News-Record, January 21, 1960, p. 58.

25. "Specifications for Structures of Aluminum Alloy 2014-T6," by the Committee of the Structural Division on Design in Lightweight Structural Alloys, Proc. Paper No. 971, ASCE, Vol. 82, No. ST3, May, 1956, p. 35.

26. "Fabrication and Erection of the Arvida Aluminum Bridge," by E. Anders and D. G. Elliot, Engineering Journal, Engrg. Inst. of Canada, June, 1950.

27. "Problems Involved in the Developing and Designing of the Aluminum Bridges for the Long Island Expressway," Andrews & Clark, Consulting Engrs., New York, N. Y. (Presented at the March, 1959 Annual Convention of New York Assoc. of Highway Engrs., New York, N. Y.

28. "The Compatibility of Aluminum with Alkaline Building Products," by C. J. Walton, F. G. McGeary, and E. T. Englehart, Corrosion, September, 1957.

29. "The Structural Aluminum Floor System of the Smithfield Street Bridge - Pittsburgh, Pa.," Engineering News-Record, November 9 and 23, and December 28, 1933.

30. "All Aluminum Span Carries Rail Traffic Over Grasse River Bridge," Civil Engineering, December, 1946.

31. "Huey Long Bridge Gets Aluminum Deck," Railway Age, December 9, 1950.

32. "Canadians Build World's First Aluminum Arch Bridge," Civil Engineering, August, 1950.

CONCEPTS OF STRUCTURAL SAFETY[a]

Closure by C. B. Brown

C. B. BROWN.[33]—The remarks made by Jack R. Benjamin, M. ASCE, fall into two groups, those regarding the responsibility of the individual engineer, and those involving the place of statistical and probability theory in design.

If it is admitted that the engineer's final professional responsibility is to society, it would appear reasonable for society to demand competency in the judgments involved. To ensure this the committee approach has often been used, if for no other reason than to provide standards by which judgments may be made. These committees, of which Benjamin disapproves as restrictions on scientific progress, are, in fact, seldom occupied with the science of engineering but only with the art. In this respect they place no curb on science if they cease to have authority in matters in which scientific reasoning, as opposed to judgments, is effective.

The place of statistical and probability theory in the design problem is exactly the same as that of any other mathematical theory that may be used. In essence, a mathematical model has no engineering significance unless it allows the reasonably accurate prediction of interesting phenomona. This is the only criterion on which the admissibility of a mathematical theory may be judged. In the usual case, a whole array of material and loading constants are required. These may be furnished by a statistical approach if the model used gives physically significant results. Certainly, the engineer should have available as wide a range of mathematical techniques as possible, but he must make the ultimate decisions concerning the reasonability of the models used and the interpretation of the results that they give.

The concepts of a definite life-span assumption as opposed to design on a monumental basis is discussed by George B. Begg, Jr., M. ASCE, with special reference to the vertical extension of existing structures. Although, to the client, the idea of a definite life span being associated with his structure may be horrifying, in the final analysis this may be the ultimate result. The extensive redevelopment of the centers of many cities has resulted in the complete removal of buildings that were undoubtedly originally envisaged on a monumental basis. The idea of limited time usage has become acceptable with regard to much of our personal hardware and it would appear reasonable to anticipate such ideas spreading to property utilization. Whether the engineer or architect should be the moderator in a discussion of structural life span requires consideration as to whether the basis of each profession is established on a static or vacillating foundation. Having in mind the contemporary scorn

---

a December 1960, by C. B. Brown (Proc. Paper 2678).

33 Research Fellow, Dept. of Aeronautics and Engrg. Mechanics, Univ. of Minnesota, Minneapolis, Minn.

poured on buildings that were considered elegant in their day, one is driven to the conclusion that only the engineer's opinion will be based on sound and permanent precepts.

Vertical extensions may be considered under two headings. In the case of the extension of existing structures the designer is obligated to build as light a superstructure as possible. It is unlikely that this arrangement will be too durable and is, in part, an admission of the need for some definite life-span planning. The new structure, in which the possibility of vertical extension is envisaged, requires provision of safety planning for the alterations probable in its later life. One cannot bewail the absence of life-span designing in existing constructions but it would appear a necessary and valid consideration in contemporary structures.

STRENGTH AND DESIGN OF METAL BEAM-COLUMNS[a]

Discussion by T. V. Galambos

T. V. GALAMBOS,[4] M. ASCE.—In the first part of the paper Walter J. Austin, F. ASCE, presents two practical methods for the design of beam-columns that fail by excessive bending in the plane of the applied moments. These methods are: (1) the limiting stress criterion, and (2) the interaction equation. Because of the approximate nature of these two methods it is desirable to compare them with analytically exact methods. For this comparison the interaction curves developed in References 39 and 47 are used in the following presentation. These "exact" interaction curves were computed by numerical integration for the 8 W 31 steel rolled shape containing linearly varying cooling residual stresses. The maximum compressive residual stress was assumed to be $0.3 \sigma_y$ (in which σ_y is the yield stress of the steel). A yield stress of 33 ksi and a modulus of elasticity of 30,000 ksi were used as the basis for the computations. Bending was assumed to be about the strong axis, and failure by lateral-torsional buckling was excluded. It was shown (39) that the interaction curves were applicable to all rolled wide-flange shapes. Good correlation between the theory and experimental results obtained from full-scale beam-column tests was observed (39), (48).

The comparisons between the approximate design methods and the "exact" solution are shown in Figs. 8, 9, and 10. The theoretical solution is indicated in these figures by the solid curves; the curves made up of long and short dashes are obtained by the interaction equation (Eq. 13), and the dashed curves represent the initial yield solution.

Comparisons are made for three loading cases: (1) Equal end moments causing single curvature deformation (Fig. 8), (2) bending moment applied at one end of the beam-column only (Fig. 9), and (3) equal end moments causing double curvature deformations (Fig. 10). The coordinates of these curves are the same as in Fig. 1, with the exception that the non-dimensionalized load P/P_y (in which P is the axial load supported by the member and P_y is the area times the yield stress) was used as the ordinate instead of the average stress.

The initial yield solutions are based on the premise that failure will occur when the yield stress is reached at the most stressed fiber in the beam-column. The curves for this comparison were computed by the equations given by S. Timoshenko (5), with the assumption that the initial eccentricities given in Table 1 are present.

---

a April 1961, by Walter J. Austin (Proc. Paper 2802).

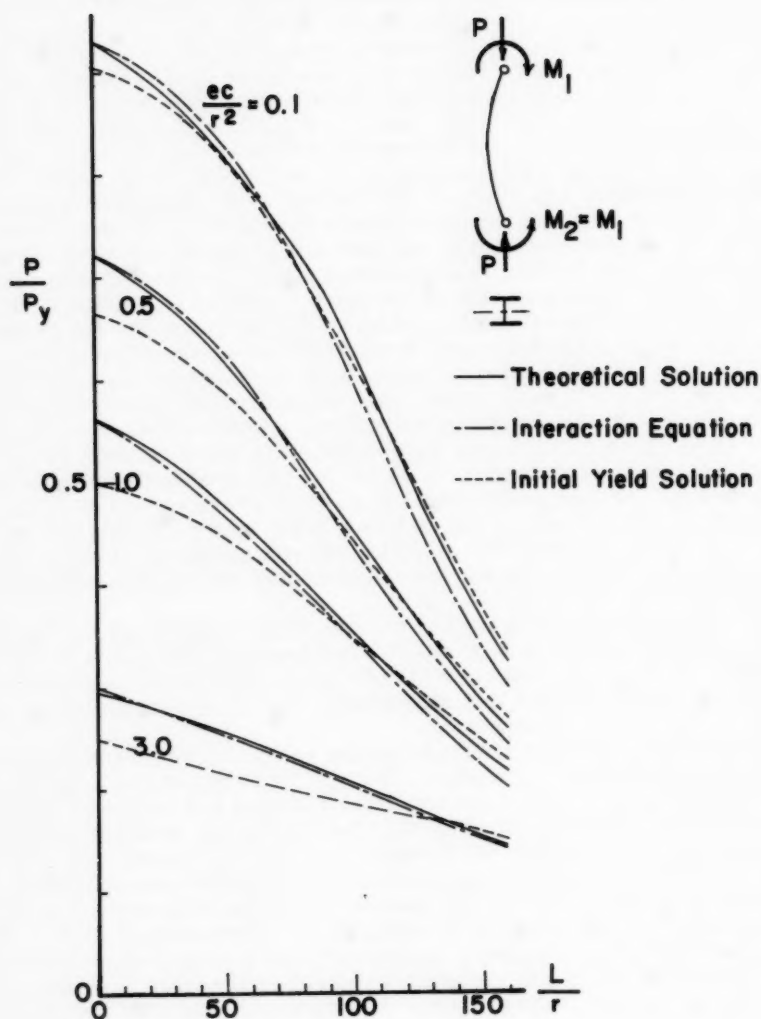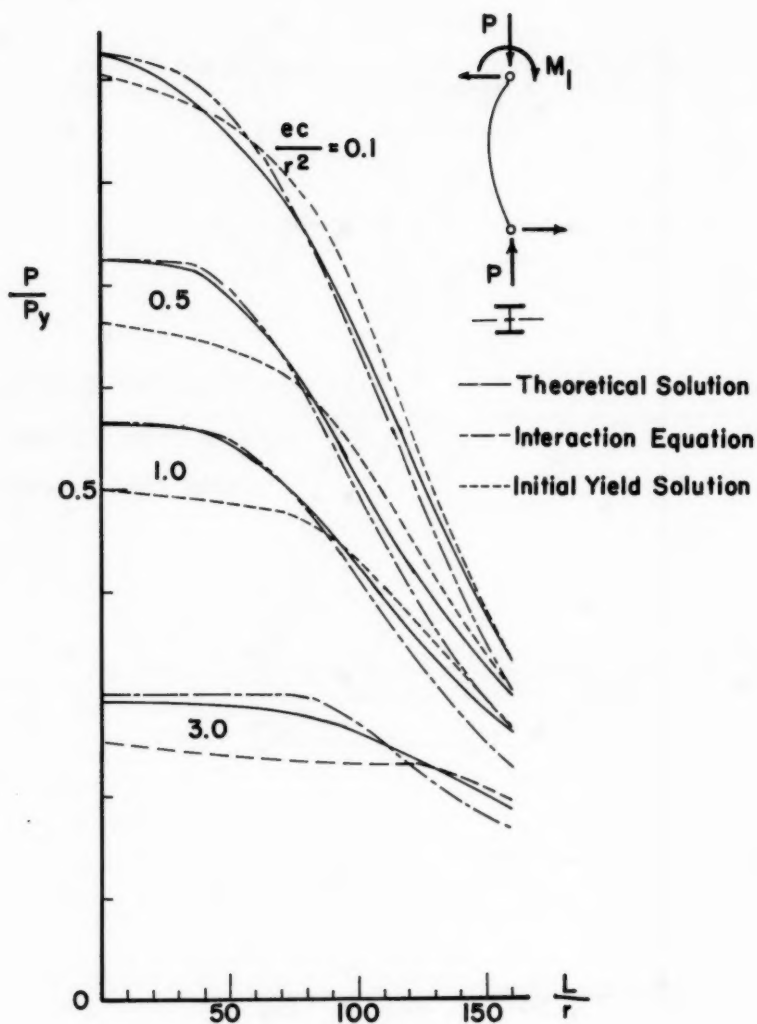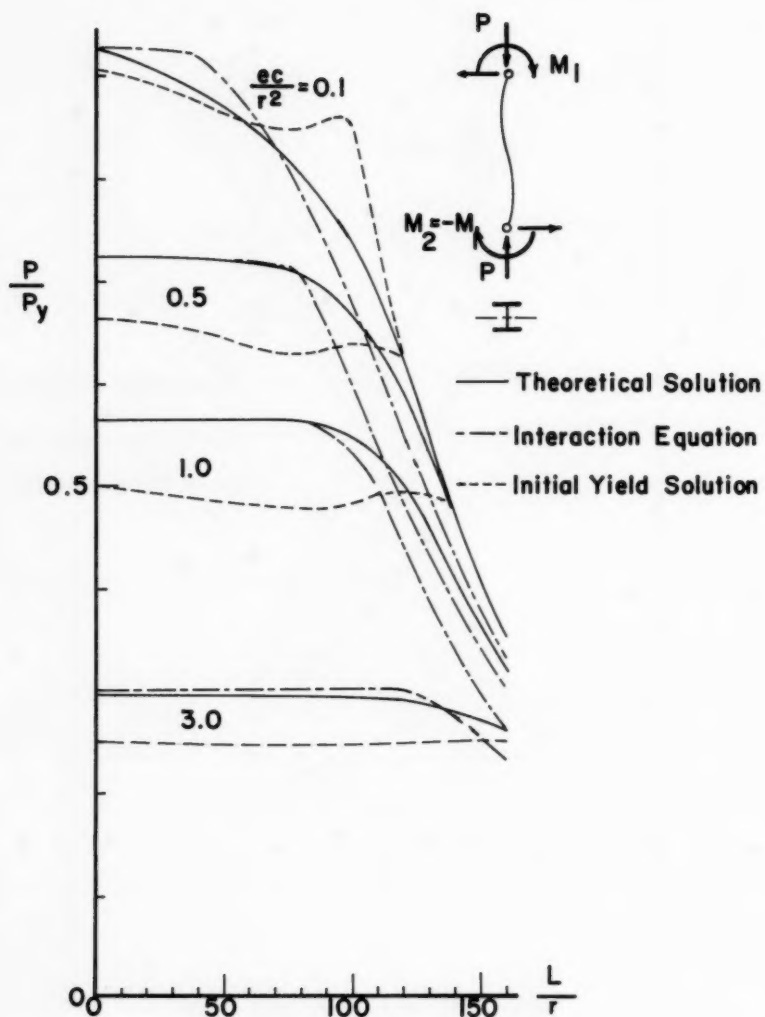4 Research Asst. Prof., Civ. Engrg. Dept., Lehigh Univ., Bethlehem, Pa.

FIG. 8

FIG. 9

FIG. 10

The following form of the interaction equation (Eq. 13) was used:

$$\frac{P}{P_O} + \frac{M_{eq}}{M_p} \; \frac{1}{1 - \dfrac{P}{P_e}} = 1.0 \; \ldots \ldots \ldots \ldots \; (31)$$

Eq. 31 was obtained by multiplying the stresses σ_a, σ_c, and σ_e by the area, and the stresses σ_b and σ_y by the section modulus in Eq. 13. In Eq. 31 P is the
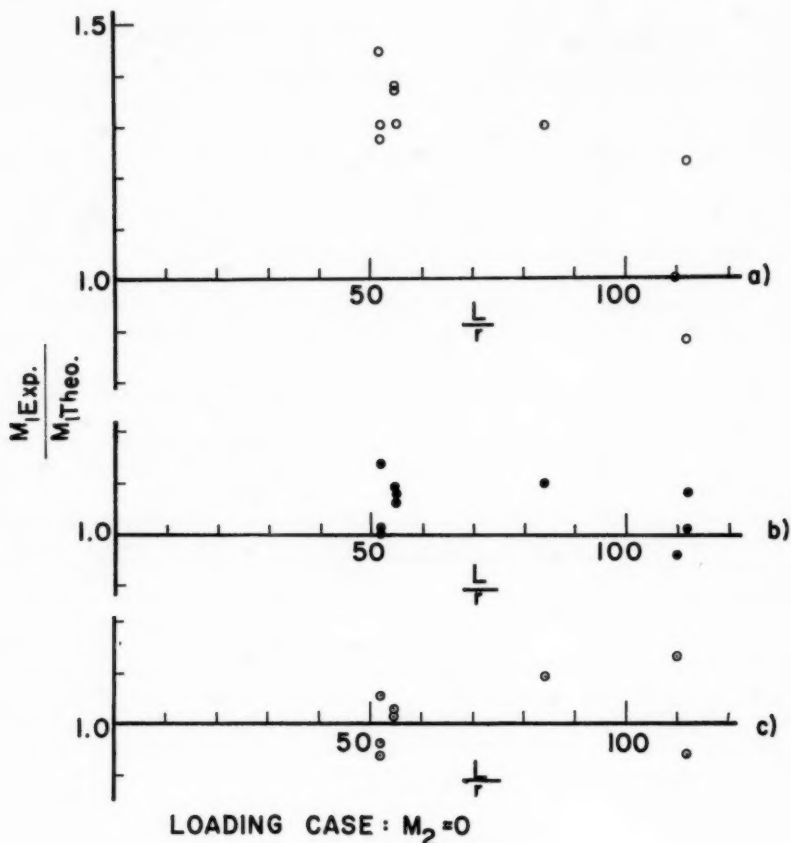
FIG. 11

applied axial load, P_O is the axial load that the column could carry in the absence of bending moments, P_e is the Euler load, M_{eq} is the equivalent moment, and M_p is the plastic moment of the section if bending only is present. The
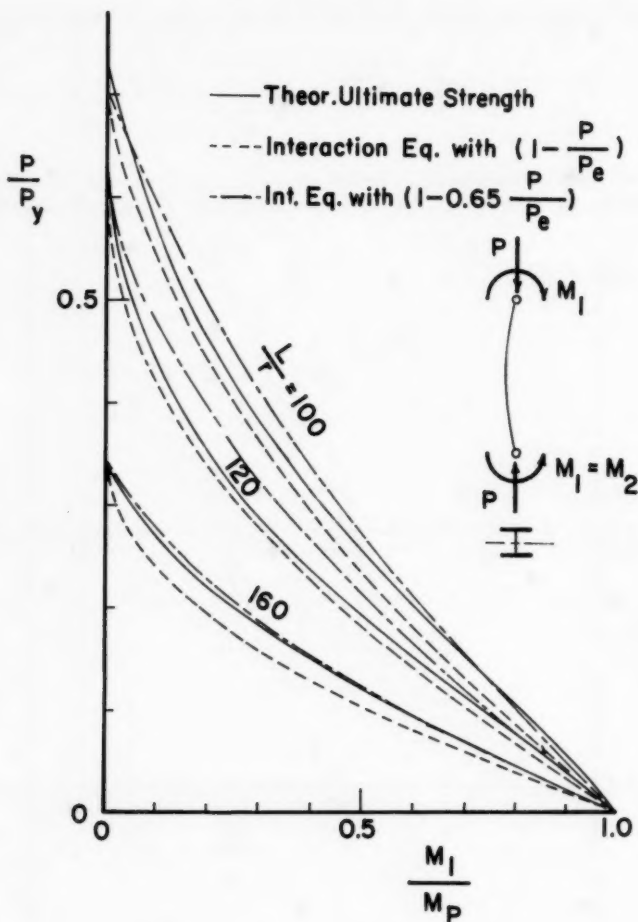
FIG. 12

following expression (45) was used for P_O:

$$\frac{P_O}{P_y} = 1 - \frac{\sigma_y}{4\pi^2 E}\left(\frac{L}{r}\right)^2 \quad \ldots\ldots\ldots\ldots\ldots.(32)$$

The equivalent bending moment was computed by Eq. 12(a) for the full range $+1.0 \geq \dfrac{M_2}{M_1} \geq -1.0$. In addition to Eq. 31, the equation for the maximum bending moment at the end (Eqs. 16(a) and 16(b)) were used where applicable.

The following conclusions may be reached from the comparison shown in Figs. 8, 9, and 10:

1. The initial yield solution, as modified by the initial eccentricities given in Table 1, is conservative for all loading cases in the range where most beam-columns in civil engineering structures would fall (that is for slenderness ratios less than 100). For higher eccentricity ratios the initial yield solution may be as much as 30% conservative (see curves for e c/r^2 = 3.0 in Figs. 9 and 10). Because the tangent modulus procedure (Fig. 1) gives approximately the same results as the initial yield method, the same conclusion applies for that method.

2. The curves computed by the interaction equation compare well with the exact solution, especially in the region of practical slenderness ratios. This method is conservative for higher slenderness ratios (over 100) and for double curvature bending.

3. The results of the comparison show that the formula for the equivalent end moment (Eq. 12a) may be applied with confidence over the whole range

$+ 1.0 \geq \dfrac{M_2}{M_1} \geq -1.0$. Thus for double curvature bending $\left(M_2/M_1 = -1.0\right)$ a value

of M_{eq} = 0.2 M_1 may be used instead of the value of M_{eq} = 0.4M_1 as suggested by Austin.

4. Because of the greater reliability and simplicity of the interaction equation, it would serve better as a basis for design rules than the initial yield method.

Additional comparisons with experimental results are shown in Fig. 11. These experiments were performed on laterally braced wide-flange beam-columns bent about the strong axis by one end moment (48). The sections were 8 WF 31, 8B13 and 4 WF 13 members. In Fig. 11 the ordinates are the ratio of the maximum experimentally obtained moment to the maximum theoretical end moment; the abscissa represent the slenderness ratios. The test results are compared with the initial yield solution in Fig. 11(a); the comparison with the exact solution is given in Fig. 11(b), and Fig. 11(c) shows correlation obtained by using the interaction equation. The comparisons in Fig. 11 show that the interaction equation predicted the strength of the test columns with more accuracy than the initial yield solution.

In conclusion it should be noted that the replacement of the term $\left(1 - P/P_e\right)$ in the interaction equation by the term $\left(1 - 0.65 \; P/P_e\right)$ would, (Eq. 4), in addition to making the formula more complicated, result in an unconservative design. This is shown in Fig. 12, in which the effect of the change in the reduction term is shown by the interaction curves for slenderness ratios of 100, 120, and 160.

ADDITIONAL REFERENCES

47. "Further Studies of the Strength of Beam-Columns," by Robert L. Ketter, Proceedings, ASCE, Vol. 87, No. ST6, August, 1961, P. 135.

48. "Beam-Column Experiments," by R. C. Van Kuren and T. V. Galambos, Report No. 205A.30, Fritz Lab., Lehigh Univ., Bethlehem, Pa., June, 1961.

PHILOSOPHICAL ASPECTS OF STRUCTURAL DESIGN[a]

Discussion by A. H. Metcalfe

A. H. METCALFE,[6] F. ASCE.—In reading the paper, the writer was reminded of the admonition received as a young man from a prominent architect, long since gone to his reward, that a good engineer is one who designs structures that are just a little-bit weak. Reflection over the years has corroborated the fact that weakness in design stems from perfect accuracy that is never attainable, but perfection may be closely approached by the top-flight engineer.

The generally accepted theory of design today (1961), has been proven to be sound by observation and study, and it has been verified by tests. Correctness of design has been substantiated in structures satisfactorily serving the purposes for which they were intended.

Working stresses have been long established by usage, except for the newest construction materials, and maximum allowable stresses have been prescribed by law into various building codes. To the public, these codes represent definite, as well as the best, rules of design.

In the writer's opinion, they do not necessarily reflect the ultimate in good engineering. They simply apply a minimum standard to comply with the law and with public safety. Assumed data is of primary consideration, and is valuable to supplement the knowledge and experience of the designer; but completion of the computations is not the full answer. Assumed data, statistics, and computations are only the tools to be used by the structural engineer in applying his best judgment in the determination of his design.

---

[a] June 1961, by Hsuan Loh Su (Proc. Paper 2843).
[6] Cons. Engr., Rochester, N. Y.

STEEL FRAME FOLDED PLATE ROOF[a]

Discussion by G. G. Goble, Jacob Eldar, and Abraham Woolf

G. G. GOBLE,[3] A. M. ASCE.—In presenting folded plates constructed of steel space trusses Oliver A. Baer, M. ASCE, has rendered a great service to those engineers interested in the design of a variety of commercial and industrial buildings. As presently conceived, the roofs of these buildings are frequently supported by trusses spanning between supporting columns. Considerable secondary bracing is necessary for erection and stability. The resulting structures are highly indeterminate and are analyzed by assuming the inaction of convenient members. The reduction of these structures to a statically determinate system, as indicated by the author, greatly increases the accuracy and reliability of the analysis. From a constructional standpoint most of the members required in the folded-plate system are used in the traditional roof as secondary bracing. A considerable saving of material is possible because many of the secondary members are designed by code limitations on their slenderness ratio. The secondary bracing of the conventional structure will probably require only minor increases in size to perform satisfactorily as main members in the folded plate. Considerable cost savings should result due to both decreased material costs and simplified fabrication.

The author outlines the basic requirements for the elements of a folded plate as

"(1) the ability of the webs of the plates to carry the roof loads between the chords and to carry the shear from the beam action of the plates; (2) chords at the intersection of the plates; (3) plane plates with straight chords; and (4) rigid diaphragm end walls to absorb the web shears from the plates."

In the structure outlined by Baer, condition 1 is satisfied by designing the purlins and roofing to transfer the loads to the rafters and hence into the truss system. The writer would like to point out a system in which, as in folded plates of concrete or wood, condition 1 is satisfied by a single element. By using one of the commercially available steel deckings with a cross section of the general type shown in Fig. 12(a), placed to span between the chords, the load normal to the plate (slab load) is carried to the adjacent plate intersections. The flat plate will carry the shear due to beam action. The corrugated plate gives the section sufficient depth to be effective in bending and, in addition, stiffens the flat web plate against buckling.

Many connection details must be developed based on economic considerations. Slab shear forces at the plate intersections must be transferred be-

---

3 Assistant Professor of Structures, Case Institute of Technology, Cleveland, Ohio.

tween the connecting plates. These forces are usually small and, perhaps, could be carried by coping the ends of the section in such a manner as to allow the intersecting webs of the corrugated sections to be bolted together. The transverse edges, a and b in Fig. 12(b), of the prefabricated section could be either welded or bolted, or a combination of shop welding and field bolting could be used as dictated by economic conditions. Thus, a variation of plate thickness along the span could be used to satisfy the shear requirements. A transverse section through a typical structure of this type is shown in Fig. 12(a). It is possible that for short spans the chord plates may be unnecessary.

The analysis of structures of this type would have to follow folded-plate theory. For a system with transverse connections as outlined, the elementary analysis would give satisfactory results. For long-span roofs of this type the buckling characteristics should be studied.
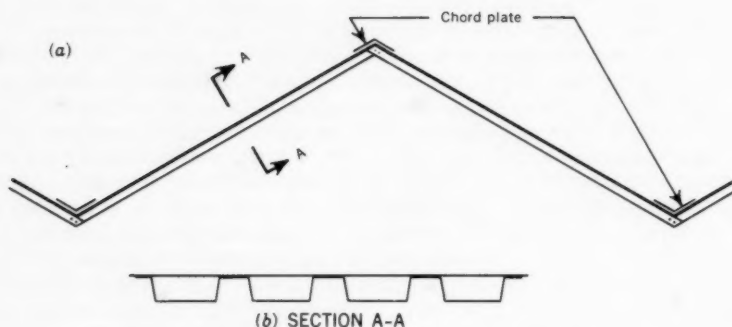
FIG. 12.—TYPICAL FOLDED PLATE CROSS SECTION

Folded plates constructed as outlined previously would give a clean, un-cluttered appearance that would be satisfactory for a wide variety of commercial structures. It seems that structures of this type and as more generally outlined by the author offer many advantages both from the economic and constructional standpoint.

JACOB ELDAR,[4] M. ASCE.—This interesting paper attempts to shed some light on a type of structure that, in reinforced concrete, received long and well-deserved attention. The problems of the design of steel frame folded plate roofs were, until now, largely neglected; the writer knows only two sources of more than passing remarks on this subject.[5,6]

Actually, there is no significant difference between the concrete and steel folded plates, and therefore anything said and written about the statics of concrete folded plates can be utilized in design of steel roofs. The "slab stiffness"

---

[4] Structural Engr., Ammann and Whitney, New York, N. Y.

[5] "Steel Designers' Manual," by Charles S. Gray, Crosby Lockwood, London, England, 1959.

[6] "Design of Structures," by Edelman and Harel, Engineering Handbook, Vol. II, Part 3, Massada, Tel-Aviv, Israel, 1958.

of a steel roof is discontinuous (except in the case of a steel skin) and therefore its influence can be entirely neglected, making the design procedure much simpler.

In the writer's opinion, the procedure outline by Baer is too simplified, in that it disregards the interaction between the separate trusses. This simplification does not come into play in case of structures made of two plates only (Figs. 1 and 8), but its influence can be quite large in the structure in Fig. 9. To follow through this simplification would mean to provide a special kind of connection between the adjacent chords, a connection which would not transfer any shear forces between them; though it is entirely feasible to work out a proper detail, the resulting structure will be heavier than required. When both
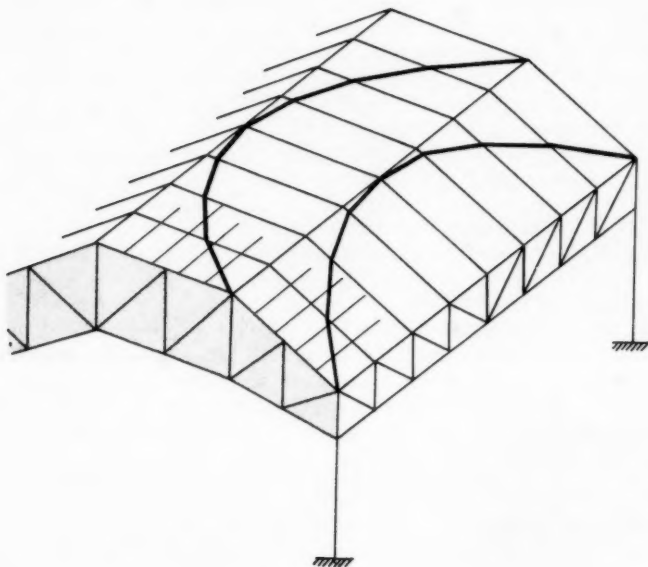
FIG. 13.—USE OF A CATENARY

chords are combined into one, the resulting one can be designed to withstand the resulting force only, which usually will be much smaller than the separate forces. To provide a combined chord does not necessarily mean a continuity in the rafters; they can be pin-connected to the chord, thus avoiding the problem of indeterminacy in the design of the rafters.

Quite often, and especially when the distance between the chords is large, the rafters can be made of open-web joists or trussed beams instead of rolled section. This substitution can result in considerable saving in steel; for example, the 8 W 17 shown in Fig. 6 could be replaced by an open-web joint 16 in. high weighing 10 lb per ft.

Instead of inclined trusses the writer utilized a catenary (inverted arch) as shown in Fig. 13. This arrangement is especially suitable in the construction of continuous structures, as it does away with the problem of continuity of the trusses over the intermediate support and enables full utilization of the material. An additional aspect of steel folded plates, not mentioned in the paper, is the possibility of doing away with columns at the sides of the building. This can be easily done by an additional truss, similar to the edge beam of a shell or concrete folded plate (Fig. 2). The load acting on this truss will consist of half the load of the first inclined plane, in addition to the dead load of the truss itself.

ABRAHAM WOOLF,[7] F. ASCE.—This paper is most refreshing; Baer's approach to the folded-plate-roof problem from the structural designer's point of view makes for comfortable reading and comprehension. The consideration of the steel frame and the conventional truss as basic parts of the structural system of folded plates emphasizes the simplicity of such frame structures. To comprehend the basic principles of any complex structure allows for the considered use of such structures with facility and understanding.

It may be, however, that the problem was over-simplified. The author's analysis is generally based on pin-end connected elements. This, in itself, eliminates the provoking questions that arise when a rigid-frame structure is considered.

In concrete construction, the folded-plate roof behaves as a series of plates integrated into a space structure. In the steel frame, the individual elements can act as beams and at the same time be integrated into the space structure. In concrete, the "crack" has forced many designers to develop the concrete structure into a monolith with resulting internal moments and shears of controversial character. In steel, the so-called pin connection rotates, moves, twists, and so forth, but these controversial moments and shears that were put into the concrete structure by the designer are now non-existent in the steel structure; it is strange what the so-called pin connection will do to the designer, let alone the structure!!

The writer, with a sympathetic attitude, respects the boldness of Baer for taking his stand on a problem of deep controversial character and presenting his case on folded plates in such a simple, logical, and refreshing manner.

The writer's first experience with steel folded plates was in the design of a saw-tooth type monitored roof for a factory. Placing long trusses in the plane of the roof eliminated the supporting columns. This pleased the client and made the project designer proud. The steel fabricator, however, had his problems. That design was based on a simple pin end-connected system, yet the riveted connections were far from simple.

In 1938, the writer was introduced to the diagonal system of framing steel and concrete.[8] This system consists of a frame formed with a monolithic grid of elements in a diagonal pattern either in a plane or folded spatially.

When the opportunity presented itself, the design of a steel-frame folded-plate roof was proposed and accepted for the Club House of Bay State Racing Association in Foxboro, Mass. (Fig. 14). Economy precluded concrete construction for the folded plate. The architect required that if steel were used

---

a June 1961, by Oliver A. Baer (Proc. Paper 2845).

7 Consulting Engineers, Abraham Woolf & Assoc., Inc., Boston, Mass.

8 "Electric Welding," Diagrid Structures, Vol. VI, No. 36, London, England.

it present a uniform pattern, and that the connections of the elements be clean and uniform in appearance. A welded structure was developed, but the fabricator favored a high-strength bolted connection to which suggestion the engineer yielded, with the requirement that the connection be simple and practical. This requirement made the smaller connections larger so that there would be

(a) STEEL ERECTION

(b) COMPLETED

FIG. 14.—FOXBORO RACE TRACK CLUB HOUSE

uniformity to the appearance of exposed roof. The steel was painted a carbon black against an off-white gray roof deck. This gave the structure expression, purpose, and texture.

The entire system of the integrated members may be looked on as a series of inclined trusses connected together at the ridge and valleys and kept from

spreading by end gable ties. These trusses span longitudinally and cantilever over the supporting columns. The web members of the sloping trusses are the diagonals of the truss and are connected to the ridge and valley members that form the top and bottom chords of the trusses. The roof load is carried by these truss diagonals that span between the ridge and valleys and are made to be continuous at the chord nodes because of the heavy gusset plates. These grid node points lying along the chords locate the supporting points of forces in the continuous cranked grid beams.

The design of this folded plate roof was based on the following procedure:

Step 1.—The basic frame was divided into a system of sloping woven trusses to carry the total roof load.

Step 2.—The truss members were designed for bending, $w\, l^2/10$, and direct load tension or compression.

Step 3.—The interaction of truss chords were then analyzed assuming the web members as rigidly connected at the joints and the chord member sizes adjusted accordingly.

Step 4.—Buckling, local at the joints and spatial in the plane of the truss, was investigated and the sizes of the basic diagonal truss members were adjusted accordingly.

Step 5.—Distortion and stiffness analysis was made to determine vertical deflections and horizontal spread of the folds.

Steps 1 and 2 presented no problems because the static conditions based on a pin-connected system develop stresses that may be computed by the elementary theory of the polygon of forces. The simple-beam theory for the bending was applied to determine the bending stresses. The final stresses for these two conditions were found by the superposition of both the direct and bending stresses.

Step 3 was analyzed on the basis of the diagonal grid, consisting of the cranked beams that are fully continuous at the cranking points and are capable of transmitting moments and shear from one side of the crank to the other side, notwithstanding the fact that these beams cranked (or folded) are, by reason of their slope, subjected to the direct forces (compression or tension) as a result of being the diagonal in the truss action.

Furthermore, at each node, there are two cranked beams intersecting with the top or bottom chord of the fold. Because each node in the cranked beam is at different positions in the truss, the vertical deflection along the cranked beam varies. Because the same node offers different moments in each beam, it is clear that bending and torsion is introduced into the truss chord. The final distortion of the node will produce, in addition to the assumed basic primary stresses, a stress pattern of secondary character.

With a few reasonable assumptions for the deflections and with unit-load equations for beams divided into nodes, the computations can be made to determine such moments. There is a marked degree of symmetry in the frame; with uniform loading and the well-known theories of slopes and deflections, the final equations reduce to a workable minimum. As to the correctness of the obtainable moment and shear values, one can only judge the range that these stresses develop as compared to the basic direct and bending stresses and make additional assumptions to establish the trend. Before plastic design, the secondary values would be of serious magnitude, but with plastic considerations together with the phenomena of elastic relief, where the moments fall off

as a result of the distortion of the member itself or the rotation of the joint, it is conceivable to have computed stresses with the range of 25% above the allowable - 25,000 psi for the steel. Under the circumstances, these stresses can be reasonably accepted if they do not affect the buckling stability.

The buckling of the structure as a whole as a space structure and then analyzing it as one with individual members offers some mathematical difficulty. Concrete shell structures have been analyzed for buckling. The three-dimensional aspects applied to the form develop stiffness beyond that anticipated. The buckling phenomena in a steel frame consisting of parts integrated to form a whole does not generate the same structural stability that exists in a homogeneous monolith such as a concrete shell or folded plate. The integrated parts must be considered individually. To this end, serious consideration must be given to the ratio of the end moments of each member, its torsional rigidity, and its warping rigidity.

Where the roof deck can supply lateral stability, the structure assumes the rigidity of a concrete plate. It would, therefore, appear consistent to consider this fact and analyze the structure accordingly. Yet with the structural elements providing concentrated strengths at localized points, one cannot neglect the independent buckling phenomena as applied to an I-beam thrust and unequal end moments. To this end, the investigation was purely academic and more serious consideration was given to the stability offered by the decking.

The determination of the deflections and distortions (Step 5) for a folded plate is not a simple problem if all the contributing stresses that either add to or detract from the final values are to be considered. The method recommended is the simple energy method for trusses. Deflection due to shear, moment, and torsion were neglected. In the cantilever ends of the folds, it was found that the spread at the cantilever end could be serious if the end wing was not provided for. In the analysis, the end wings developed two important and necessary conditions in addition to the architect's aesthetic requirements:

1. Lateral stiffness to minimize the spread at the cantilever ends.
2. End moments in the diagonal members of the first sloping truss.

After the complete design was made, it was found that there was a slight variation in the member sizes chosen from the stress conditions as a result of the investigation under Steps 3, 4, and 5.

This design confirms Baer's contention that a steel-framed folded plate roof is subject to a conventional analysis. The design also shows that structural steel can be adapted to the folded-plate concept with reasonable economy as an aesthetic architectural element beyond its structural function.
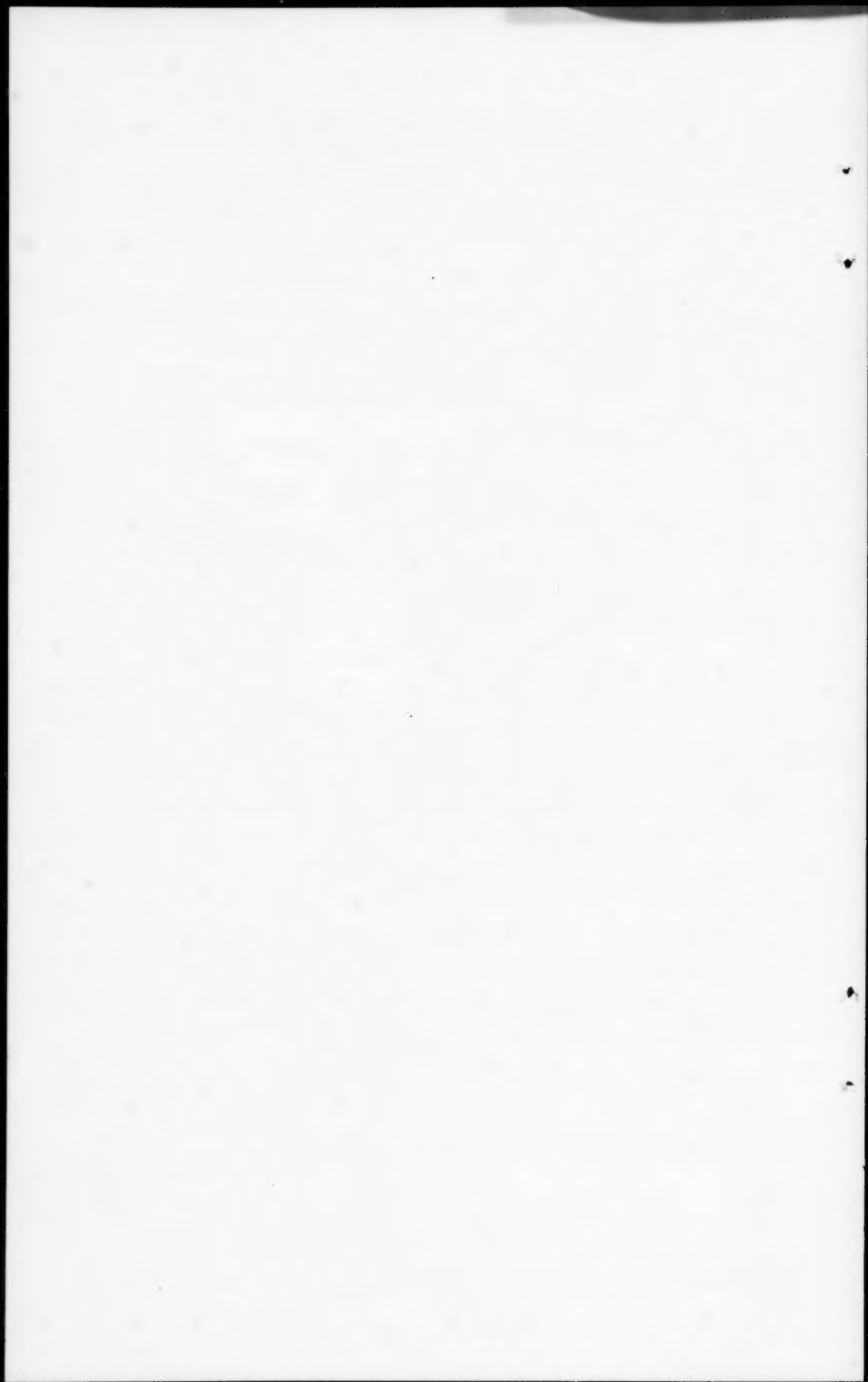
TORSIONAL BEHAVIOR OF SUSPENSION BRIDGE TOWERS[a]

Discussion by Thomas R. Kuesel

THOMAS R. KUESEL,[13] M. ASCE.—The literature of suspension bridges contains many papers useful to the analyst trying to determine stresses and deformations of a structure physical dimensions and properties of which are known or assumed. There are few papers that offer much help to the designer trying to establish these dimensions and properties, or trying to compare and evaluate alternate possibilities in various preliminary designs. Among the contributors to this select group have been Shortridge Hardesty and Harold A. Wessman,[14] H. A. Miklofsky, F. ASCE,[15] K. K. Chu,[16] and I. K. Silverman, M. ASCE,[17]. Frank Baron, F. ASCE, and Anthony G. Arioto, A. M. ASCE, have made a notable addition in their comparative studies of the behavior of suspension bridge towers subject to torsion.

The authors have confined their presentation generally to the torsional behavior of the tower by itself. The writer would like to extend the discussion to the implications given in this paper as to the effects of the towers on the torsional behavior of the bridge as a whole.

It has been well established that the towers offer little resistance to symmetrical longitudinal motions of the cables, or to vertical deflections and stresses resulting from such motions. In fact, it is customary to neglect the longitudinal tower stiffness entirely in the analysis of cables and trusses for vertical loads. Chu demonstrated[16] that the error involved in this approximation for the Mackinac Straits Bridge is approximately 0.8%.

In a tower without struts (Case D), subject to torsion resulting from unsymmetrical cable pulls, each column would be free to deflect longitudinally, independent of the other column. In such a case, the tower columns would offer the same (negligible) resistance to torsion that they offer to symmetrical cable pulls. The addition of a single strut at the top of the tower (Case C) causes the columns to restrain each other. The amount of restraint depends on the transverse stiffness of the strut and the torsional stiffness of the columns, as well as on the ratio of tower height to width.

---

a August 1961, by Frank Baron and Anthony G. Arioto (Proc. Paper 2879).

13 Assoc., Parsons, Brinckerhoff, Quade, and Douglas, New York, N. Y.

14 "Preliminary Design of Suspension Bridges," by Shortridge Hardesty and Harold A. Wessman, Transactions, ASCE, Vol. 104, 1939, p. 579.

15 "Bending Interaction in Suspension Bridges," by H. A. Miklofsky, Proc.-Sep. No. 652, ASCE, Vol. 81, March, 1955.

16 "The Design of the Main Towers of the Mackinac Bridge," by K. H. Chu, Proc. Paper No. 1565, ASCE, Vol. 84, No. ST 2, March, 1958.

17 "The Lateral Rigidity of Suspension Bridges," by I. K. Silverman, Proc. Paper No. 1292, ASCE, Vol. 83, No. EM3, July, 1957.

For the actual towers included in their investigation, the authors found that the addition of a single top strut increased the torsional stiffness of the tower from 3.5 to 22.5 times, compared to the stiffness of the unstrutted columns (Table 6, Cases C and D). For their hypothetical towers, Baron and Arioto found the increase to range up to 100 times (Group F). The greatest increase is for tall, narrow towers (long, narrow spans), and the smallest for short, wide ones.

Evidently, an increase of 4 times in a negligible resistance will not make it a major resistance. However, an increase of 20 or 100 times may be important. This is significant when one considers that a decrease in relative width of span drastically decreases the torsional stiffness of the suspended structure, resulting in greater torsional loads on the cables and towers. In a narrow span, the towers may furnish, and may have to furnish, a substantial part of the resistance to torsion.

Considering each independent column of an unstrutted tower as a vertical cantilever, it is evident that a restraint to horizontal deflection of the tower top will be much more effective if applied at the end of the cantilever than if it is applied somewhere down the column. Thus it should not be surprising (in the clear reflection of hindsight) that the authors found that adding intermediate struts had little additional effect on the torsional stiffness of the tower (the effect on lateral stiffness is, of course, substantial).

The writer is not entirely in agreement with the authors' statement that "Table 8 shows . . . the influence of the vertical saddle reactions on the torsional behavior of the actual towers is practically negligible." Table 8 is based on $P = 0.4\ P_e$, whereas the actual P_{DL} for the First Tacoma Bridge is given in the same table as $0.964\ P_e$. (It is not stated whether this includes the tower weight, which may be appreciable.) It would be instructive to have Table 8 amplified to show relative values for $P = 0.8\ P_e$ and $P = 1.0\ P_e$.

For the case of $P_{DL} = P_e$, the tower columns have no longitudinal flexural stiffness. At this point, the towers begin to lean on the cables for support, instead of the other way around. For this same case, the unstrutted tower (Case D) has no torsional stiffness. The strutted tower derives all of its torsional stiffness from bending the struts and twisting the tower columns.

As the ratio P_{DL}/P_e decreases, the flexural stiffness of the columns increases, and begins to contribute to the torsional stiffness of the strutted tower as a whole. For tall, narrow towers the relative increase will be small; for short, wide towers it may be substantial.

Torsional forces on the towers may originate, as stated by the authors, from unsymmetrical live loading or from torsional aerodynamic oscillations. The live load torsion is usually not of great concern for highway bridges, though the matter is certainly of interest for railway bridges, and perhaps for bridges carrying urban transit loadings, as evidenced by experiences with New York's Manhattan Bridge.

The aerodynamic torsional oscillations, however, may be of primary interest. The writer believes that all of the severe aerodynamic oscillations observed in truss-stiffened suspension bridges have been either purely torsional, or a coupled form combining torsional and vertical oscillations. Pure vertical oscillations have reached alarming proportions in some girder stiffened bridges, but they have generally not been large enough in truss-stiffened spans to cause concern.

Torsional oscillation in the fundamental mode, with one loop in the main span and the cables $180°$ out of phase, requires an alternate lengthening and shortening of the main span length between tower tops, which is resisted by the torsional rigidity of the tower (as well as by the cables and trusses).

It is sometimes stated that the towers offer no resistance to torsional oscillation in the first asymmetric mode, with one node at the center of the main span, because such oscillations can occur without change in the span length between towers. However, this mode requires a longitudinal oscillation of the center node point, in order to permit a sag in one half of the cable with a corresponding rise in the other half. The most effective preventive for this disease is to attach the cables at mid-span to the trusses, or preferably, to a rigid "torsion box" such as was devised by L. Chadenson for the Tancarville Bridge in France. If this remedy is adopted, each half of the cable will tend to oscillate between the tower top and the fixed center point, and the towers will be called on to furnish torsional resistance to this mode of oscillation as well.

Higher torsional modes, with two or more nodes in the main span, are usually not of great concern, because their higher frequencies are less likely to be excited by the natural wind, and their amplitudes are generally smaller than those associated with the lower modes.

A statement by the authors in a previous paper[5] bears repetition:

> "The damage that can occur in a tower due to torsional oscillation of a bridge is strikingly illustrated by the towers of the first Tacoma Narrows Bridge. Concerning these towers, each Board reporting on damage to the bridge stressed the great damage that was done to the cells, anchorages, splices, and top struts of the towers as a result of the torsional oscillations and the subsequent failure of the bridge. It is reported that the towers were near collapse when the roadway peeled off the suspenders."

The first Tacoma Narrows Bridge had no torsional stiffness in its suspended structure. Thus, all torsional forces were carried by the cables, that attempted to transfer them to the towers. The towers were unusually narrow, the top struts unusually thin, and the columns both flexurally and torsionally flexible. In addition, the dead load on the tower was almost equal to the Euler buckling load, thus destroying whatever flexural stiffness the columns might have had. The combination of maximum torsional forces and motions with minimum torsional strength and stiffness was too much for this bridge. (It may be appropriate to observe that it is frequently easier to see 20 years backward than one year forward.)

This does not, however, indicate how much torsional stiffness was required for the Tacoma Bridge (or for any other bridge), nor the best way to provide it. The first question depends in large degree on how skillful the designer is in minimizing the torsional forces to which the bridge is subjected. For live load effects, some control can be exercised in bridges carrying mixed traffic by arranging the cross section to concentrate the heaviest live loads near the center of the bridge. For aerodynamic effects, the highest skill of the designer is needed. Suggestions made by D. B. Steinman,[18] F. ASCE, F. B. Farquhar-

___

18 "Mackinac Bridge Designed for Complete Aerodynamic Stability," by D. B. Steinman, Civil Engineering, Vol. 26, May, 1956, p. 37.

son,[19] F. ASCE, and George B. Vincent[20] merit careful attention; nonetheless, this remains an area offering opportunities for fruitful investigation.

The vertical stiffness of a suspension bridge depends primarily on the interaction of two elements—cable and truss. The torsional stiffness depends on three interacting elements—cable, truss, and tower. The relative contribution of each of these elements depends on the proportions of the structure. In some cases, it will be hopeless to attempt to modify the torsional stiffness of the bridge as a whole through changes in tower proportions. In such cases, the towers should preferably be designed to be torsionally flexible, to limit the participation stresses to which they will be subjected. In other cases, the tower design may have an appreciable influence on the torsional properties of the bridge as a whole. Such cases require more careful investigation. The authors' paper makes a valuable contribution to techniques whereby the influence of the towers may be assessed in preliminary design.

19 "The Investigation of Models of the New Tacoma Narrows Bridge Under the Action of Wind," by F. B. Farquharson, Bulletin No. 116, Univ. of Washington Engrg. Experiment Sta., Seattle, Wash.

20 "Aerodynamic Stability of Suspension Bridges," Progress Report of the Advisory Board on the Investigation of Suspension Bridges," Transactions, ASCE, Vol. 120, 1955, p. 721.

BENDING OF RECTANGULAR PLATES[a]

Discussion by Mario G. Salvadori

MARIO G. SALVADORI,[14] F. ASCE.—The author has clearly presented another ingenious method for the evaluation of bending stresses in rectangular plates.

His procedure presents the following advantages:

1. The use of a physical model allows a good understanding of plate behavior.

2. The approximations obtainable by the procedure seems to be better for moments than for deflections.

3. The procedure can easily be extended to a variety of boundary conditions and to the solution of non-isotropic plates.

On the other hand in comparison with the standard application of finite differences the procedure presents the following disadvantages:

1. The number of equations to be solved is equal to that used in the finite differences method, but the writing of the equations is preceded by substantially more work. It would seem easier to apply a finite difference operator mechanically than to set up the equations as the author does.

2. Although the convergence of the procedure seems to be greater than that of the finite difference method it is slow enough to require the use of h^2 - extrapolations.

Wherever elementary computers are not available the author's procedure may present definite merits. Wherever computers are available a straight forward application of finite differences would be easier and faster.

---

[a] August 1961, by Mounir Badir (Proc. Paper 2908).
[14] Prof., Civ. Engrg. Dept., Columbia Univ., New York 17, N. Y.

FURTHER STUDIES OF THE STRENGTH OF BEAM-COLUMNS[a]

Discussion by Phillip L. Gould and Morris Ojalvo

PHILLIP L. GOULD,[17] A. M. ASCE.— The solution presented for the strength of a beam-column represents a logical approach to the problem that may be easily understood. The writer believes that solutions which consider the actual load-deformational response of a member are preferable to and longer lived than so-called "curve fitting" formulas that have little physical meaning. Of course, the practicing designer does not always have time to make these computations; however, curves, such as those presented, together with an explanation of how they are obtained, give the designer a reliable method of determining the strength of a beam-column. Consideration must also be given to the possible changes in the $\dfrac{M_0}{M_p} / \dfrac{P_0}{P_y}$ ratio ("eccentricity") in going from design loading to ultimate capacity.

It should be noted that the method considered in the ultimate capacity solution also may be applied to determine the total stress in the elastic range due to combined bending and axial load. This is conveniently done by the use of Newmark's numerical procedure.[16]

For both the elastic and ultimate analyses by the load-deformational response method, a good estimate of the deflection values at any point along the member will reduce the number of trials required to establish the correct configuration. Timoshenko has shown[18] that the relationship

$$Y_1 = \frac{\alpha}{1 - \alpha} \, a \sin \frac{\pi x}{L} = \frac{\alpha}{1 - \alpha} \, Y_0 \ldots \ldots \ldots \ldots (22)$$

holds in the elastic range, in which Y_1 are the additional deflections due to axial load, Y_0 is the deflection due to lateral load only, Y_T is the total deflection $= Y_0 + Y_1$, and

$$\alpha = K^2 \frac{L^2}{\pi^2} = \frac{P}{EI} \frac{L^2}{\pi^2} = \frac{P}{P_e} \ldots \ldots \ldots \ldots \ldots (23)$$

---

a August 1961, by Robert L. Ketter (Proc. Paper 2910).

17 Structural Engr., Skidmore, Owings & Merrill, Chicago, Ill.

18 "Theory of Elastic Stability," by S. Timoshenko, McGraw-Hill Book Co., Inc., New York, N. Y., 1936, p. 32, Eq. 47.

Substitution of $\alpha = \dfrac{P}{P_e}$ into Eq. 22 gives

$$Y_1 = \frac{1}{\dfrac{P_e}{P} - 1} \quad\ldots\ldots\ldots\ldots\ldots\ldots\ldots (24)$$

The assumed total deflection will then be $Y_T = Y_0 + Y_1$. When using New-mark's procedure, the value of Y_T is estimated at each panel point and used for the first cycle. The results of the first cycle are used as the input to the second cycle. The value of Y_1 and Y_T obtained by this method will probably be somewhat inaccurate in the inelastic range but will serve as a first esti-mate until a number of solutions have been made and a more accurate esti-mating procedure may be developed.[19]

MORRIS OJALVO.[20]—Reference will be made herein to the column-deflection curve corresponding to a beam-column. This column-deflection curve is the full wave that would be developed if the beam-column extends beyond its sup-ports and if the reactive forces and moment at the supports are replaced by the equivalent thrust (Fig. 19). The $M - P - \phi$ relationship, together with
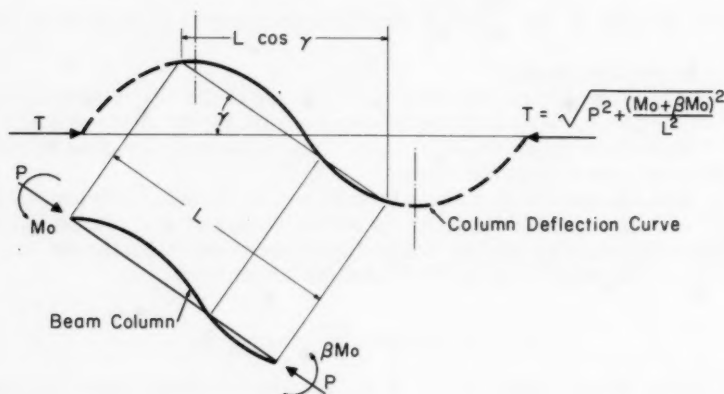
FIG. 19

the slope, moment, shear, and axial load at either end of the beam-column, uniquely determines the shape of the beam-column's column deflection curve. Subsequently, Ketter's criteria for unwinding will be examined to determine whether it adequately predicts the limiting moments consistent with stable beam-columns.

---

19 Discussion by P. L. Gould of "Design Criteria for Reinforced Columns Under Axial Load and Biaxial Bending," by Boris Bressler, Journal, ACI, Vol. 32, No. 5, November, 1960, p. 481.
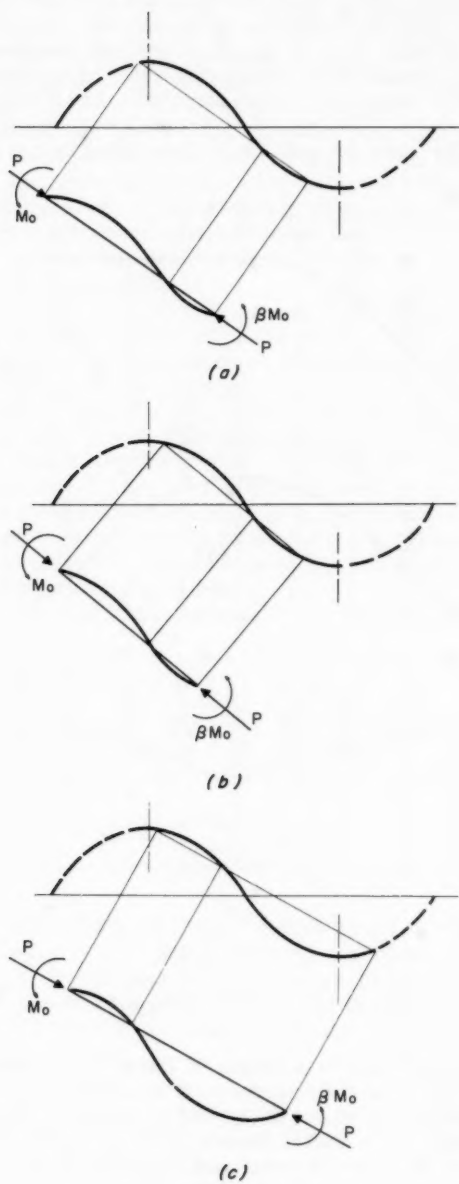20 Assoc. Prof. of Civ. Engrg., Ohio State Univ., Columbus, Ohio.

FIG. 20

For the present (a proof follows), the assumption is made that the length of a stable beam column must be smaller than the half wave length of its column deflection curve for all values of β in the interval $-1 < \beta \leq 1$. If the preceding statement is true, then the length of a stable beam-column can only exceed the half wave length of its column deflection curve when $\beta = -1$. But β can only be exactly equal to -1 in an ideal case, and it follows that no real stable beam column can be longer than the half wave length of its column-deflection curve. Because the criteria for unwinding that is proposed makes
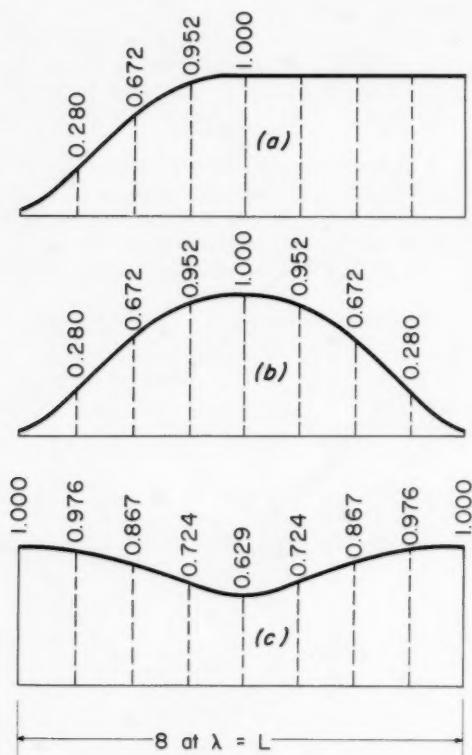
FIG. 21.—RATIOS OF $(E\ I)_{EFF}/(E\ I)$

no provision to insure against a length of beam-column larger than its half wave length, it follows that the criteria must be inadequate.

This section contains a proof of the preceding statement regarding the maximum possible length for a stable beam-column in which β is different than -1. Consider the three cases of beam-columns and column-deflection curves that may arise for negative values of β (Fig. 20).

Two basic assumptions (with which the writer is in complete accord) made by Ketter in his computations are that the slopes of the beam-column are every-

where small and that the shear is small in comparison with P. This is implied because the axial load for the moment-thrust-curvature relation is taken as equal to P at all sections of the beam column. It follows from the approximation that γ, as shown in Fig. 19, must also be small and L cos γ may be taken as equal to L. Because $|M_0| > |\beta M_0|$, it is obvious that only the beam-column of Fig. 20(c) is longer than the half wave length of its column-deflection curve. It is also obvious that for this case the beam column deflections are predominantly in the direction of the smaller applied end moment. This equilibrium shape of the beam column cannot be achieved by gradually increasing end moments. It can only be achieved by forcing the column into that configuration and then removing the restraints. It is for this reason that the configuration of Fig. 20(c) may not be considered among the group of stable equilibrium configurations of the beam-column.

Ketter's criteria seek to determine when a bifurcation of an equilibrium configuration is possible. More complete criteria should also ask whether it is reasonable to expect the beam column to achieve the initial equilibrium shape under gradually increasing end moments.

It is interesting to compare Mr. Ketter's criteria with other criteria that may arise from the same line of thinking and with a third group of criteria that are equivalent to those that have been adopted by the writer.[21] Fig. 21(a) shows the variation of $(E I)_{EFF}$ adopted in Fig. 18. Fig. 21(b) would be the $(E I)_{EFF}$ that might be adopted, using the same reasoning together with the Engesser tangent modulus concept of inelastic buckling. The use of the $(E I)_{EFF}$ variation of Fig. 21(c) in the computations of Fig. 18 results in criteria equivalent to those obtained[21] by the writer.

The values of $(E I)_{EFF}/(E I)$ shown in Fig. 21(c) were obtained as follows:

At x = 0 and L,

$$\frac{(E I)_{EFF}}{E I} = \frac{M/M_y}{\phi/\phi_y} \quad \dots \dots \dots \dots \dots (25)$$

at station $x = \frac{1}{2} L$ in Fig. 17. At $x = \frac{1}{8} L$ and $\frac{7}{8} L$,

$$\frac{(E I)_{EFF}}{E I} = \frac{M/M_y}{\phi/\phi_y} \quad \dots \dots \dots \dots \dots (26)$$

at station $X = 3/(8 L)$ in Fig. 17. Other values in Fig. 21(c) are determined from Fig. 17 according to the pattern indicated previously.

The criteria that are adopted for unwinding will affect the results. The writer's analysis shows that a column for which $M_0/M_y = 0.440$, $P/P_y = 0.6$, $L/r = 110$, and $\beta = -1$ is not in stable equilibrium.

---

[21] Discussion by Morris Ojalvo of "The Plastic Method of Designing Steel Structures," by John G. Baker, Proceedings, ASCE, Vol. 85, No. ST9, November, 1959.

PROCEEDINGS PAPERS

The technical papers published in the past year are identified by number below. Technical-division sponsorship is indicated by an abbreviation at the end of each Paper Number, the symbols referring to: Aero-Space Transport (AT), City Planning (CP), Construction (CO), Engineering Mechanics (EM), Highway (HW), Hydraulics (HY), Irrigation and Drainage (IR), Pipeline (PL), Power (PO), Sanitary Engineering (SA), Soil Mechanics and Foundations (SM), Structural (ST), Surveying and Mapping (SU); and Waterways and Harbors (WW), divisions. Papers sponsored by the Department of Conditions of Practice are identified by the symbols (PP). For titles and order coupons, refer to the appropriate issue of "Civil Engineering." Beginning with Volume 82 (January 1956) papers were published in Journals of the various Technical Divisions. To locate papers in the Journals, the symbols after the paper number are followed by a numeral designating the issue of a particular Journal in which the paper appeared. For example, Paper 3029 is identified as 3029(ST8) which indicates that the paper is contained in the eighth issue of the Journal of the Structural Division during 1961.

VOLUME 86 (1960)

DECEMBER: 2668(ST12), 2669(IR4), 2670(SM6), 2671(IR4), 2672(IR4), 2673(IR4), 2674(ST12), 2675(EM6), 2676(IR4), 2677(HW4), 2678(ST12), 2679(EM6), 2680(ST12), 2681(SM6), 2682(IR4), 2683(SM6), 2684(SM6), 2685(IR4), 2686(EM6), 2687(EM6), 2688(EM6), 2689(EM6), 2690(EM6), 2691(EM6)^C, 2692(ST12), 2693 (ST12), 2694(HW4)^C, 2695(IR4)^C, 2696(SM6)^C, 2697(ST12)^C.

VOLUME 87 (1961)

JANUARY: 2698(PP1), 2699(PP1), 2700(HY1), 2701(SA1), 2702(SU1), 2703(ST1), 2704(ST1), 2705(SU1), 2706 (HY1), 2707(HY1), 2708(HY1), 2709(PO1), 2710(HY1), 2711(HY1), 2712(ST1), 2713(HY1), 2714(PO1), 2715 (ST1), 2716(HY1), 2717(SA1), 2718(SA1), 2719(SU1)^C, 2720(SA1)^C, 2721(ST1), 2722(PP1)^C, 2723(PO1)^C, 2724(HY1)^C, 2725(ST1)^C.

FEBRUARY: 2726(WW1), 2727(EM1), 2728(EM1), 2729(WW1), 2730(WW1), 2731(EM1), 2732(SM1), 2733(WW1), 2734(SM1), 2735(EM1), 2736(EM1), 2737(PL1), 2738(PL1), 2739(PL1), 2740(PL1), 2741(EM1), 2742(ST2), 2743(EM1), 2744(WW1), 2745(WW1), 2746(SM1), 2747(WW1), 2748(EM1), 2749(WW1), 2750(WW1)^C, 2751 (EM1)^C, 2752(SM1)^C, 2753(PL1)^C, 2754(ST2)^C, 2755(PL1).

MARCH: 2756(HY2), 2757(IR1), 2758(AT1), 2759(CO1), 2760(HY2), 2761(IR1), 2762(IR1), 2763(HY2), 2764 (ST3), 2765(HY2), 2766(HW1), 2767(SA2), 2768(CO1), 2769(IR1), 2770(HY2), 2771(SA2), 2772(HY2), 2773 (CO1), 2774(AT1), 2775(IR1), 2776(HY2), 2777(HY2), 2778(SA2), 2779(ST3), 2780(HY2), 2781(HY2)^C, 2782 (HW1)^C, 2783(SA2)^C, 2784(CO1), 2785(CO1)^C, 2786(IR1)^C, 2787(ST3)^C, 2788(AT1)^C, 2789(HW1).

APRIL: 2790(EM2), 2791(SM2), 2792(SM2), 2793(SM2), 2794(SM2), 2795(SM2), 2796(SM2), 2797(SM2), 2798 (EM2), 2799(EM2), 2800(EM2), 2801(EM2), 2802(ST4), 2803(EM2)^C, 2804(SM2)^C, 2805(ST4)^C.

MAY: 2806(SA3), 2807(WW2), 2808(HY3), 2809(WW2), 2810(HY3), 2811(WW2), 2812(HY3), 2813(WW2), 2814 (HY3), 2815(WW2), 2816(HY3), 2817(HY3), 2818(SA3), 2819(WW2), 2820(SA3), 2821(WW2), 2822(WW2)^C, 2823(HY3), 2824(SA3), 2825(HY3), 2826(SA3)^C, 2827(HY3)^C.

JUNE: 2828(SM3), 2829(EM3), 2830(EM3), 2831(IR2), 2832(SM3), 2833(HW2), 2834(IR2), 2835(EM3), 2836 (IR2), 2837(IR2), 2838(SM3), 2839(SM3)^C, 2840(IR2)^C, 2841(HW2)^C, 2842(EM3)^C, 2843(ST5), 2844(ST5), 2845(ST5), 2846(ST5)^C.

JULY: 2847(PO2), 2848(SU2), 2849(HY4), 2850(PO2), 2851(HY4), 2852(PO2), 2853(SU2), 2854(HY4), 2855 (PO2), 2856(PO2), 2857(PO2), 2858(SA4), 2859(SU2), 2860(SA4), 2861(PO2), 2862(SA4), 2863(HY4), 2864 (HY4), 2865(HY4), 2866(HY4), 2867(HY4), 2868(PO2)^C, 2869(SA4)^C, 2870(SU2)^C, 2871(HY4), 2872(HY4)^C, 2873(SU2), 2874(SA4).

AUGUST: 2875(WW3), 2876(WW3), 2877(WW3), 2878(SM4), 2879(ST6), 2880(EM4), 2881(SM4), 2882(EM4), 2883(WW3), 2884(EM4), 2885(SM4), 2886(WW3), 2887(EM4), 2888(WW3), 2889(AT2), 2890(AT2), 2891 (AT2), 2892(AT2), 2893(AT2), 2894(AT2), 2895(AT2), 2896(AT2), 2897(AT2), 2898(AT2), 2899(AT2), 2900 (AT2), 2901(AT2), 2902(SM4), 2903(ST6), 2904(ST6), 2905(SM4), 2906(ST6), 2907(EM4), 2908(ST6), 2909 (EM4), 2910(ST6), 2911(EM4), 2912(SM4), 2913(ST6), 2914(WW3)^C, 2915(ST6)^C, 2916(EM4)^C, 2917(SM4)^C.

SEPTEMBER: 2918(SA5)^C, 2919(HW3)^C, 2920(HY5)^C, 2921(SA5), 2922(PL2), 2923(IR3), 2924(HY5), 2925 (HY5), 2926(CP1), 2927(HY5), 2928(IR3), 2929(IR3), 2930(HY5), 2931(CP1), 2932(PL2), 2933(HY5), 2934 (HY5), 2935(HY5), 2936(HY5), 2937(HW3), 2938(CP1), 2939(PL2), 2940(SA5), 2941(SA5), 2942(SA5), 2943 (HY5), 2944(PL2)^C, 2945(CP1)^C, 2946(IR3), 2947(HW3), 2948(IR3), 2949(IR3)^C.

OCTOBER: 2950(PP2), 2951(PP2), 2952(PP2), 2953(ST7), 2954(SM5), 2955(ST7), 2956(ST7), 2957(ST7), 2958 (ST7), 2959(SM5), 2960(EM5), 2961(EM5), 2962(ST7), 2963(ST7), 2964(EM5), 2965(SM5), 2966(SM5), 2967 (ST7), 2968(ST7), 2969(ST7), 2970(ST7), 2971(SM5), 2972(SM5)^C, 2973(EM5)^C, 2974(ST7)^C, 2975(PP2).

NOVEMBER: 2976(HY6), 2977(HY6), 2978(HY6), 2979(PO3), 2980(WW4), 2981(HY6), 2982(HY6), 2983 (HY6), 2984(HY6), 2985(SA6), 2986(SA6), 2987(WW4), 2988(WW4), 2989(WW4), 2990(HY6), 2991 (WW4), 2992(HY6), 2993(PO3), 2994(WW4), 2995(PO3), 2996(HY6), 2997(SA6), 2998(PO3), 2999 (PO3)^C, 3000(HY6)^C, 3001(SA6), 3002(SA6), 3003(SA6)^C, 3004(WW4)^C.

DECEMBER: 3005(IR4), 3006(RI4), 3007(IR4), 3008(SM6), 3009(EM6), 3010(ST8), 3011(IR4), 3012(SM6), 3013(EM6), 3014(ST8), 3015(IR4), 3016(ST8), 3017(EM6), 3018(EM6), 3019(EM6), 3020(SM6), 3021(ST8), 3022(ST8), 3023(ST8), 3024(ST8), 3025(ST8), 3026(EM6), 3027(EM6), 3028(EM6), 3029(ST8)^C, 3030(EM6)^C, 3031(IR4)^C, 3032(SM6)^C.

c. Discussion of several papers, grouped by divisions.